MULTI-STOREY BUILDING FRAMES STIFFENED WITH DISSIPATIVE SHEAR WALLS

Teză destinată obţinerii
titlului ştiinţific de doctor inginer
la
Universitatea "Politehnica" din Timişoara
în domeniul INGINERIE CIVILĂ
de către

Ing. Călin NEAGU

Conducător ştiinţific:

Prof.Dr.Ing.Dr.H.C. Dan Dubină	Universitatea Politehnica Timişoara

Referenţi ştiinţifici:

Prof.univ.Dr. Ioannis Vayas	Universitatea Tehnică Atena
Prof.Univ.Dr.Ing. Dan Creţu	Universitatea Tehnică Bucureşti
Conf.Univ.Dr.Ing. Florea Dinu	Universitatea Politehnica Timişoara

Ziua susţinerii tezei: 12 martie 2011

Seriile Teze de doctorat ale UPT sunt:

1. Automatică
2. Chimie
3. Energetică
4. Ingineria Chimică
5. Inginerie Civilă
6. Inginerie Electrică
7. Inginerie Electronică şi Telecomunicaţii
8. Inginerie Industrială
9. Inginerie Mecanică
10. Ştiinţa Calculatoarelor
11. Ştiinţa şi Ingineria Materialelor
12. Ingineria sistemelor
13. Inginerie energetică
14. Calculatoare şi tehnologia informaţiei

Universitatea „Politehnica” din Timişoara a iniţiat seriile de mai sus în scopul diseminării expertizei, cunoştinţelor şi rezultatelor cercetărilor întreprinse în cadrul şcolii doctorale a universităţii. Seriile conţin, potrivit H.B.Ex.S Nr. 14 / 14.07.2006, tezele de doctorat susţinute în universitate începând cu 1 octombrie 2006.

România, 300159 Timişoara, Bd. Republicii 9,
tel. 0256 403823, fax 0256 403221
e-mail: editura@edipol.upt.ro

Acknowledgements

To my parents

The thesis was developed during my activity (2007 – 2011) within the Department of Steel Structures and Structural Mechanics CMMC, the Center of Excellence in the Mechanics of Materials and Safety of Structures CEMSIG, from the "Politehnica" University of Timişoara.
I would like to offer my sincere gratitude to some very special people who helped me in the process of my education, my parents, I offer my heartfelt thanks for all of their support throughout my life, confidence in my abilities and patience throughout these 4 years of PHD studies.
I would like to express my sincere appreciation to my advisor, Prof. Dr. Ing. Dr. H.C. Dan Dubină, for sharing a great deal of his knowledge and experience and for his patience, support and guidance throughout this research project.
My deep gratitude to Assoc. Prof. Dr. Ing. Florea Dinu for providing support when i needed it most during my work, and for taking such an interest in my overall personal growth and success.
My special thanks go to my Colleagues, PhD Student Filip Vacarescu Norin, PhD Student Gelu Danku and PhD Student Nicolae Muntean for the team work showed during the experimental tests. My thanks to Mr. Dan Scarlat whose professional experience and involvement helped me in the laboratory work.
Special thanks also to Lecturer Dr. Ing. Sorin Herban for his good collaboration and patience during the experimental tests.
My thanks to Prof. Dr. Ing. Daniel Grecea, Assoc. Prof. Dr. Ing. Aurel Stratan, Assoc. Prof. Dr. Ing. Viorel Ungureanu, Assoc. Prof. Dr. Ing. Adrian Ciutina, Senior Lecturer Dr. Ing. Adrian Dogariu, PhD Student Andrei Crisan and Dr. Ing. Sorin Bordea for their observations and suggestions.
Thanks also to Ing. Popa Viorel, for helping me in the management of the research contracts.

Timişoara, Martie 2011 Ing. Neagu Călin

Neagu, Călin

Title of thesis: Multi-storey Building Frames Stiffened with Dissipative Shear Walls

Teze de doctorat ale UPT, Seria 5, Nr. 66, Editura Politehnica, 2011, 193 pagini, 210 figuri, 36 tabele.

ISSN:1842-581X

ISBN: 978-606-554-270-9

Keywords:

Steel plate shear walls, experimental tests, behavior factor q, modeling of SPSW, acceptance criteria, numerical analysis, incremental dynamic analysis, energy dissipation, overstrength factor.

Abstract:

The thesis investigates the behavior of steel frames with dissipative steel shear walls.
Both numerical analyses and experimental tests have been conducted in order to asses the performance of steel plate shear wall systems. The main objective of the thesis is the evaluation of the behavior factor q used for design of such structures. The tests have been conducted for two series of three-bay-two-storey frames, with rigid and semi-rigid MR joints, respectively, two bays stiffened with Shear Walls. Specimens have been half scaled (½), and tested under monotonic and cyclic loading.
A numerical model has been calibrated via test results. Parametric studies have been conducted on different frame typologies in order to obtain the q factor.
The value of the q factor, around 6, obtained in the numerical analysis is in good agreement with the values obtained in the experimental program. These values indicate SPSW structures exhibit a good dissipative behavior, similar to other dissipative structures, like for example moment resisting frames.

Cuprins

Table of content

Notations, abbreviations and acronyms

Notations

Chapter 2

α	Inclination of the tension field according to vertical
t	Thickness of infill plate
A_c	Area of VBE
A_b	Area of HBE
A	Area of the equivalent brace
ϕ	The acute angle of the brace with respect to the column;
h	Distance between HBE centerlines
L	Distance between VBE centerlines
δ_y	Yield displacement (CAN/CSA S16-01)
M_{pc} or M_p	Plastic resistance of beam
V_s	Storey shear
Ω_s	System overstrength factor
F_y	Yielding resistance of infill plates

Chapter 3

t_w	Thickness of infill plate
I_c	Moment of inertia of VBE
q	Behavior factor (Europe)
R	Reduction factor (America)
e_y	Yield displacement (ECCS)
F_y	Corresponding yielding force (ECCS)
F_u	Ultimate resistance
Δ_{yield}	Yield displacement (ATC 24)
Δ_m	Targeted maximum deformation amplitude (FEMA 461)
Δ_0	Targeted smallest deformation amplitude (FEMA 461)
n	Number of increments
a_i	Amplitude at ith cycle (FEMA 461)
Δ_b	Deformation (AISC 2005)
Δ_{by}	Yield deformation (AISC 2005)
Δ_{bm}	Design storey drift (AISC 2005)
f_y	Yield resistance
T_c	Corner period
a_g	Ground motion intensity
γ_{ov}	Factor with accounts for supplied material
Ω	Accounts for the strength reserve in main dissipative elements
L_{cf}	Clear distance between VBE
V_n	Nominal shear strength
ϕ	Equal with 0.9 (equation 3.1)
$M_{j,Rd}$	Joint resistance
$M_{b,Rd}$	Beam resistance
E	Young modulus
I	Moment of inertia
S_j	Stiffness (EN)

A_s	Area of a strip
N	Number of trips per plate
P	Axial force
P_y	Yielding axial force
Δ	Displacement
Δ_y	Yield displacement
A_u	Specific elongation
e_{ow}	Initial imperfection (EN1993-1-5)
a	Length of the plate (EN1993-1-5)
b	Height of the plate (EN1993-1-5)
K_α	Initial stiffness (CEN)
K_β	Second stiffness line (CEN)
e_w	Out of plane deformation (EN1993-1-5)
K_w	Stiffness of the plate
G	Shear modulus of the brace
a	Clear width of plate between columns
h	Clear height of wall between beams
$K_{brace,tension}$	Echivalent braqce stiffness
L_{brace}	Length of the diagonal brace
K_{frame}	Stiffness of the frame
K_1	Stiffness of the frame surrounding the infill plates
K_2	Stiffness of the internal coupling beam
$I_{c.\ beam}$	Moment of inertia of coupling beam
$L_{c.\ beam}$	Length of the coupling beam
K_{SPSW}	Stiffness of the SPSW system
q_u	Ductility reduction factor (EN)
q_Ω	Overstrength factor (EN)
R_s	Overstrength factor (AISC)
V_d	Design strength
V_y	Actual strength
V_e	Elastic strength
μ	Displacement ductility factor
Δ_u	Maximum plastic displacement

Chapter 4

H_e	Total height
$W_{pl(beam)}$	Plastic modulus of the beam
f_{ym}	Beam yielding resistance
f_{yw}	Steel plate yielding resistance
$M_{j,Sd}$	Static bending moment
$M_{c,Rd}$	Column resistance
M_w	Earthquake magnitude on Richter scale
θ_y	Beam yield rotation
F_i	normalized lateral forces
m_i	mass in the *i*-th storey
Φ_i	normalized displacements
Φ_n	normalized top displacements equal with 1
m^*	mass of an equivalent SDOF system

F^*	Force of equivalent SDOF system
d^*	Displacement of equivalent SDOF system
F_b	Base shear force of MDOF system
d_n	Control node displacement of MDOF system
$E_m{}^*$	Actual deformation energy up to the formation of the plastic mechanism.
d^*_y	Yield displacement of the idealized SDOF system
T^*	Period of the idealized equivalent SDOF system
D^*_{et}	STarget displacement of the structure with period T^* and unlimited elastic behavior
$S_e(T^*)$	Elastic acceleration response spectrum at the period T^*
$d_t{}^*=D_t$	Target displacement of MDOF system
q_u	Ratio between the acceleration in the structure with unlimited elastic behavior $S_e(T^*)$ and in the structure with limited strength $F_y{}^*/m^*$
q_{max}	Maximum over all storeys peak interstorey drift ratio
λ	Ground motion intensity factor
S_a	Spectral accelera
a_{gu}	Peak ground acceleration leading to collapse
a_{gy}	Peak ground acceleration corresponding to first yielding

Chapter 5

N_{Ed}	Design axial force
M_{Ed}	Design bending moment
V_{Ed}	Design shear force
$N_{pl,Rd}$	Column plastic strength
k_v	Plate buckling coefficient
$1.1\gamma_{ov}R_{fy}$	Shear corresponding to moments at each end
I_E	Moment of inertia
F_a	An acceleration-based site coefficient

Abbreviations

SPSW	Steel plate shear walls
MRF	Moment resisting frame
PBSE	Performance base seismic evaluation
IO	Immediate occupancy
LS	Life safety
CP	Collapse prevention
SLS	Serviceability limit state
ULS	Ultimate limit state
CPLS	Collapse prevention limit state
PGA	Peak ground acceleration
EPA	Effective peak ground acceleration
HBE	Horizontal boundary element
VBE	Vertical boundary element
PBSD	Performance base seismic design
SDOF	Single degree of freedom system

MDOF	Multi degree of freedom system
IDA	Incremental dynamic analysis
EDP	Engineering demand parameters
IM	Seismological intensity measures
DM	Damage Measure
MRF+SPSW	Moment resisting frame stiffened with steel plate shear walls
EBF	Eccentrically braced frames
BRB	Frames with buckling restrained braces
FEM	Finite element method
DCH	Ductility class high
DCM	Ductility class medium
CBF	Centrically braced frames

Abbreviations

M-PFI	Modified Plate Frame Interaction
LYP	Low Yield Point
AISC	American Institute of Steel Constructions (http://www.aisc.org/)
CAN	Canadian Standard Association
ASCE	American Society of Civil Engineers (http://www.asce.org/)
ATC	
CEMSIG	Research Center for Mechanics of Materials and Structural Safety -CEMSIG is a RTD (Research and Technical Development) unit of the "Politehnica" University of Timisoara, at the Faculty of Civil Engineering, Department of Steel Structures and Structural Mechanics (http://cemsig.ct.upt.ro/cemsig/index.php)
COST C26	Urban Habitat Constructions under Catastrophic Events; an European Action in order to increase the knowledge of the behavior of constructions in urban habitat under catastrophic events, when exposed to extreme events (http://www.cost.esf.org/)
EC8	Eurocode 8
ECCS	European Convention for Constructional Steelwork (http://www.steelconstruct.com/)
FEMA	Federal Emergency Management Agency is an agency of the United States Department of Homeland Security (http://www.fema.gov/)
NEHRP	National Earthquake Hazards Reduction Program (http://www.nehrp.gov/)
NBCC	Uniform Building Code of Canada
SEAOC	Structural Engineering Association of California
SIMQKE-1	Statistically independent accelerograms software generator

List of figures

List of tables

Rezumat

Teza de doctorat are ca obiect studiul comportării structurilor din oţel în cadre multietajate echipate cu sisteme de panouri metalice disipative, supuse la acţiuni seismice. Autorul şi-a propus ca, pe baza studiilor experimentale şi numerice şi pornind de la stadiului de cunoaştere actual cu privire la tema tezei, să caracterizeze şi să cuantifice parametrii care controlează comportarea acestor sisteme structurale, să propună valori pentru factorii de comportarea şi de suprarezistenţă care intervin în proiectarea antiseismică.
Obiectivul principal al tezei îl reprezintă evaluarea factorului de comportare q si a criteriilor de acceptare a structurilor cu panouri disipative din oţel. Scopul final este acela de a dezvolta o metodologie de proiectare bazată pe performanţă PBSE/PBSD pentru acest tip de structuri.
Teza este împărţită în 6 capitole şi demonstrează eficacitatea sistemului SPSW prin încercari experimentale (teste pe cadre cu trei deschideri două nivele, scara 1/2) şi prin analize numerice (analize structurale pe diferite tipologii de cadre).

Capitolul 1: Introducere
Se prezintă cadrul în care s-a realizat lucrarea, scopul şi obiectivele tezei. Sunt prezentate pe scurt ideile principale şi rezumatul fiecărui capitol.

Capitolul 2: Stadiul actual de cunoaştere
Capitolul prezintă o sistematizare a lucrărilor de cercetare care au contribuit la dezvoltarea sistemelor cu panouri din oţel. Sunt descrise studii teoretice, programe experimentale şi analize numerice desfăşurate în ultimii 30 de ani pe plan mondial şi aplicaţii importante ale acestor sisteme la cladiri multietajate. Se pune de asemenea în evidenţă evoluţia prevederilor şi a recomandărilor de calcul pe plan mondial. În încheierea capitolului sunt prezentate principalele probleme aflate în discuţie şi se face legătura cu programul experimental din capitolul urmator.

Capitolul 3: Program experimental
Capitolul prezintă în deschidere obiectivele principale ale programului experimental. Se prezintă protocoalele de încărcare în cazul acţiunilor ciclice aplicate pe cadre din oţel cu elemente care disipează energia printr-o comportare histeretică. În a doua parte sunt descrise încercările experimentale efectuate. Se urmăreste în principal evaluarea factorului de comportare q şi a parametrilor care contribuie la evaluarea lui. Un alt obiectiv îl constituie definirea parametrilor de intrare în analiza preliminară (rigiditatea iniţială şi capacitatea elastică a panourilor) şi contribuţia elementelor structurale la comportarea globală a structurii. Sunt evidenţiate contribuţiile îmbinărilor grindă-stâlp şi ale grinzilor de legătură dintre zonele cu panouri. Capitolul se încheie cu concluziile programului experimental.

Capitolul 4: Program numeric
În introducere se descrie conţinutul programului de simulări numerice, încluzand tipurile de structuri analizate şi se prezintă apoi dimensionarea lor pe baza prevederilor din norme, luand în considerare şi rezultatele obţinute la capitolul 3 (direcţia tensiunilor principale, aria echivalentă a panourilor, factorul de comportare q). Structurile studiate sunt structuri duale obţinute prin combinarea a două substructuri cu proprietăţi de rigiditate, rezistenţă şi ductilitate diferite şi anume cadrele contravântuite cu panouri din oţel şi cadre necontravântuite. S-au avut în

vedere îmbinări articulate şi îmbinări rigide grindă-stâlp (aferente panourilor) cât şi 3 regimuri diferite de înălţime si anume 6, 12 şi respectiv 18 etaje. Pentru evaluarea performanţelor seismice, s-a utilizat o metodologie pe bază de performanţă. Sunt descrise nivelele de performanţă (cu criteriile de acceptare aferente), nivelele de hazard şi metodele de analiză neliniară (statică şi dinamică). Modelele numerice pentru panouri utilizate în analiza neliniară au fost calibrate pe baza rezultatelor încercărilor experimentale din capitolul 3. Se prezintă detaliat rezultatele obţinute din analiza statică neliniară (metoda N2) şi analiza dinamică incrementală (IDA). În final sunt prezentaţi indicii de performanţă seismică, cum ar fi mecanismele plastice, nivelul de degradere din elemente (deformaţii plastice) şi factorul de comportare q.

Capitolul 5: Metodologie de proiectare a sistemelor duale cu panouri disipative din oţel

Acest capitol prezintă elaborarea conceptului de structură cu pereţi de forfecare prin similitudinea cu structuri contravantuite centrice în X şi modul de predimensionare a panourilor din oţel în conformitate cu normele actuale. Se prezintă descrierea sumară a evaluării bazată pe performanţă şi verificarea finală a structurilor. Capitolul se încheie cu prezentarea unei scheme logice pentru proiectare şi pentru analiza avansată a sistemelor cu panouri disipative din oţel.

Capitolul 6: Concluzii finale, contribuţiile autorului şi diseminarea rezultatelor

Sunt prezentate concluziile finale obţinute în urma programului experimental şi a analizelor parametrice efectuate, împreună cu principalele contribuţii personale ale autorului. Se pune în evidenţă modul de diseminare şi de valorificare a tezei prin proiecte de cercetare, publicaţii şi prezentări la conferinţe de specialitate.

Summary

The thesis investigates the behavior of multi-storey steel structures with dissipative steel plate shear walls SPSW in seismic areas. On the basis of experimental and numerical studies, and starting from the state of art results, the author characterized and quantified the parameters used for the control of this type of systems. He also proposed values for the behavior factor q and overstrength factor Ω, which are used in seismic design.
The main objective of the thesis is the evaluation of the behavior factor q and of acceptance criteria for structures with dissipative SPSW. The final scope is to develop a coherent methodology for performance based design PBSD of structures using dissipative steel shear walls.
The thesis is divided in 6 chapters and demonstrates the efficiency of the SPSW systems by means of experimental investigations (experimental tests on SPSW three bay two storey frames, half scaled) and numerical analysis (structural analysis on different typologies of frames).

Chapter 1: Introduction
It is presented the scope and main objectives of the thesis. The main ideas and the summary of each chapter are described.

Chapter 2: State-of-art
The chapter presents a summary of the research literature that contributed to the development of structural systems with steel plate shear walls SPSW. Theoretical studies, experimental programs and numerical analysis done worldwide in the past 30 years, together with important applications to buildings are reported. This chapter highlights, also, the development of the code provisions and regulations in time. The chapter ends with the main aspects regarding the research needs for the development of SPSW systems.

Chapter 3: Experimental program
At the beginning, the main objectives of the experimental programs are stated and compared to available test results. The test set-up and monotonic and cyclic loading protocols are presented. Second part describes the experimental tests on SPSW systems. The performance of the experimental frames is assessed, presenting the evaluation of the behavior factor q and frames dissipation capacity. The contribution of connections and coupling beams between steel shear walls is investigated. At the end, the conclusions based on the experimental tests are presented.

Chapter 4: Numerical program
In the firs part of this chapter, the modeling of the SPSW for static and dynamic analysis, together with the calibration and validation of the numerical model based on experimental results is presented. The modeling parameters are used in a numerical evaluation of contribution of structural elements to global behavior. Structures selected for the analysis are similar to those tested in chapter 3 and combines two sub-subsystems, one stiffened with SPSW and one unbraced. Dual frame structures with coupling beams were selected based on their favorable seismic behavior. The beam to column connections (in the plate area) and the height of the frames were considered the main parameters. For the evaluation of the systems performance, a performance base seismic evaluation was used.

Performance levels with associated hazard levels and identified acceptance criteria (i.e. drifts, plastic rotations) are described. The preliminary numerical models were calibrated based on the results of the experimental tests. Are presented in detail the results (drifts, plastic rotations, plastic mechanisms) of the static procedure (N2 method) and nonlinear incremental dynamic analysis (IDA). The chapter ends with the conclusions of the numerical program.

Chapter 5: Design approach for multi-storey frames of dissipative shear walls

This chapter presents in detail the elaboration of the structural concept of a SPSW, starting with a simplified procedure based on equivalent X type centrically braced frame and the pre-design of the steel plate shear walls according to current codes. It is presented also the verification according to performance base seismic evaluation and the final design. The chapter ends with presentation of a flowchart for the design and for advanced analysis of structures using SPSW systems.

Chapter 6: Final conclusions, contributions of the author and dissemination of results

In this chapter are presented the final conclusions of the thesis, as well as the main contributions of the author. It is presented the dissemination of the results through research programs, publications and presentations at national and international conferences.

1. Introduction

1.1. Scope

Earthquake is generally considered one of the most destructive natural hazards. In the last three years only, there were many powerfull quakes that affected many parts of the world, developed countries and least developed countries: China, 12 May 2009, Sichuan, the earthquake had a magnitude 7.9 Mw, a total of approximately 69 000 victims; Italy, the earthquake from Abuzzo area, with 6.3 Mw magnitude, which practically destroyed the Aquila city, 108 victims and 50000 remaining homeless; the catastrophic earthquake in Haiti, in January 2010, with more than 300 000 fatalities and more than 1 000 000 remaining homeless; one of the strongest gound motion in history, Chile 2010 earthquake, with a magnitude of 8.8 Mw, and at the time of writing, the catastrophic 6.3-magnitude quake that shooked New Zealand's South Island and its largest city of Christchurch, causing more than 100 fatalities and 12 billion in damages.
In essence, the earthquake problem was defined by F. Press at the opening of the 7th world conference of seismic engineering (1984, 'The Role of Science and Engineering in Natural Hazards'): "Earthquakes are a very special type of natural hazards according in the sense that they are very rare, low-probability events, whose consequences, when they do occur, are very large in terms of destruction and suffering".
In his report "Codification, Design and Application", presented at the 2nd international conference on Behavior of steel structures in seismic areas – STESSA'97 (Kyoto, 3-8 August, 1997), Vitelmo Bertero defined the seismic event as follows:

"EQs are natural disasters whose feature is that most of the human and economic losses are not due to the the EQ mechanism, but to failure of human-made facilities (buildings, dams, bridges, transportation systems, etc.) which supposedly were design and constructed for the comfort of human beings".

The seismologist and structural engineers try to respond to these threats, and as a consequence there is a continuous development in this field, including the following topics:
Adequacy of antiseimic design in relationship with the type and nature of the seismic hazard and the site characteristics;
Construction material behavior modeling and evaluation under extreme conditions;
Prediction of the failure mode, ductility criteria and oversterngth (collapse control design) with alternative types of stress distribution in post-elastic state;
Efficient exploration of:
base isolation systems, of structural systems equipped with dampers and/or passive, with controlled response, active or semi active energy dissipation devices;
systems with dissipative hysteretic fusible elements, structural components, joints and connections from special materials with great plastic deformation capabilities (low yield steel, pure aluminum), respectively;
systems with post-tensioned elements and self centering capabilities, that reduces or eliminates the remanent drift;
Replacing the force based design with the design based on capacity spectrums and displacement based control design, together with performance base design

objectives and criteria.

The hysteretic devices based on dissipative steel plate shear walls (low yield steel, pure aluminum) have been used since 1970's. The occurrence of Northridge 1994 (California) and Kobe 1995 (Japan) earthquakes has demonstrated these systems are very effective in supporting strong ground motions. The excellent performance of a high rise building during the Kobe earthquake has brought more attention of the engineers to this system.
In comparison with traditional structural systems, SPSWs offer the potential for comparable or better seismic performance at a reduced construction cost. SPSWs have high rigidity that allows for fewer bays of lateral load resisting framing. They utilize moment resisting beam to-column connections that must only qualify for ordinary moment resisting frames (medium ductility class) and thus have fewer restrictions and limitations than special moment resisting frames (high ductility class). Also, they employ infill connection details using fillet welds or bolts that can accommodate traditional erection tolerances.

Despite the benefits of SPSWs, they are not widely used yet. The limited implementation of SPSWs may be a direct result of:
traditional SPSW configurations result in large column dimensions and prohibit the use of narrow walls, thereby reducing the system's economy;
numerical models of SPSW systems are cumbersome and overly time consuming for engineers;
SPSW system behavior is not well understood, leading to conservative design requirements and further reduction in economy;
SPSWs have a lower flexural stiffness relative to concrete walls, making their use in taller buildings more challenging. Further, SPSW systems must be studied in the context of performance-based design as this will result in reliable and robust systems. Performance objectives must be identified and a procedure for reliably achieving those objectives for various levels of seismic hazard must be developed.

A major role on the recent development of SPSW systems can be attributed to the introduction of design rules in the code provisions, e.g. AISC (2005) or NBCC (2006). Unfortunatelly, there are no recomandations in Eurocodes, and as a consequence, there are no important applications to multi-storey buildings in Europe.
Concluding, there is a big interest for developing design procedures and detailing criteria for SPSW systems to be added to the relevant Eurocodes. The research work done by the author aimed at investigating the seismic performance of unstiffened SPSW systems, focusing on experimental and numerical evaluation of behavior factor q as well as acceptance criteria for performance based seismic evaluation.

1.2. Objectives

The aim of the thesis is the investigation, evaluation and characterization of performance parameters in terms of strength, stiffness and ductility of multi-storey steel moment resisting frames of dissipative steel plate shear walls (SPSW). The

associated targets can be resumed as follows:
- The first objective is a review on the present state of knowledge concerning the theoretical background and applications of this system to multi-storey buildings worldwide.
- The second objectiv is to conduct an experimental program in order to characterize and quantify the parameters used for controling structures with SPSW. The targeted parameters are the behavior factor q, the overstrength factor and the ductility criteria.
- The third objectiv is the extension of the findings from the experimental program to real multi-storey building frames by means of a numerical study. Different typologies of structures having as main parameters the height and the beam to column connection properties are investigated.
- The final objective is the developing of a methodology for performance based seismic design (PBSD) of SPSW structures that can be adopted in design codes.

2. State of art

2.1. Introduction

First studies on steel plate shear wall structures began in the 1970s. Since then, many experimental and analytical studies were conducted all over the world, to demonstrate the structural efficiency and cost competitiveness of this new lateral resisting system. Several buildings have utilized steel plate shear walls as a lateral load resisting system. In early applications, the designs were based on the concept of preventing buckling of the infill plate due to shear. In Japan, this was accomplished by using heavily stiffened thin plates, while in the United States, moderately thick plates were used. However, following numerous experimental results and numerical studies, unstiffened thin infill plates for the shear resisting system have been also considered.

The idea of using steel plates to resist lateral loads is based on the fact that buckling of a plate with a stiff boundary frame does not necessarily represent the limit of plate capacity in shear. Thus, Wagner (1931) [1] shown that a diagonal tension field would form after buckling in thin aluminum aircraft shear panels supported by stiff boundary members. He developed the "pure" tension field theory whereby the diagonal tension field that forms in a thin plate supported by stiff boundary members is the primary mechanism for shear resistance.

Kuhn et al. (1952) [2] proposed the "incomplete" diagonal tension theory, which assumes plate shear capacity is a combination of pure shear and the inclined tension field. Following the research of Wagner and Kuhn, Basler (1961) [3] developed an incomplete diagonal tension field model to predict the shear capacity of steel plate girders with intermittent transverse stiffeners to anchor the tension field. Basler's work has been widely accepted and can be found as the basis for the design of plate girders in several steel design standards and specifications (e.g., CAN/CSA S16-01 [4], AISC 2005 [5]).

Takahashi et al. (1973) [6], who is believed to have conducted the first extensive research program on the behavior of steel plate shear wall panels, found that under cyclic loads heavily stiffened steel panels perform better in shear than unstiffened steel panels, although it is unlikely that they would be economical in most markets.

The next two sections describe the main research developments related to steel plate shear walls and some important applications of steel plate shear walls as main lateral resisting systems of multi-storey frame buildings.

2.2. Literature review

2.2.1. Thorburn et al., 1983

The first comprehensive analytical investigations of conventional unstiffened steel plate shear walls were conducted at the University of Alberta. Thorburn et al. [7] recognized that buckling of the infill plate due to lateral loads does not represent the ultimate capacity of steel plate shear walls and that the inclined tension field dominated the post-buckling behavior of the infill plates. An analytical model termed the strip model—was developed to simulate the tension field behavior, wherein the

infill plate is modeled as a series of tension–only strips oriented at the same angle of inclination, α, as the tension field. A typical panel, representing a one storey "slice" of the shear wall, is shown in Figure 2-1. It was demonstrated that summing the responses of individual storeys gave a good approximation of the response of a strip model of the entire shear wall, resulting in savings in modeling effort where several identical panels are present. The strip model assumes that the boundary beams are infinitely stiff in order to reflect the presence of opposing tension fields above and below the modeled panel. The model studied in this research program used hinged connections at the beam ends, although the researchers indicated that frame behavior could also be included. The tensile yield strength of the plate material was considered to be the limiting stress and the shear resistance of the infill plate prior to buckling was neglected. The authors showed that ten strips per panel adequately represent the tension field action developed in the plate. All analyses conducted in this research were elastic. The Canadian steel design standard, CAN/CSA S16-01 [4], recommends the strip model as a design tool for steel plate shear walls.

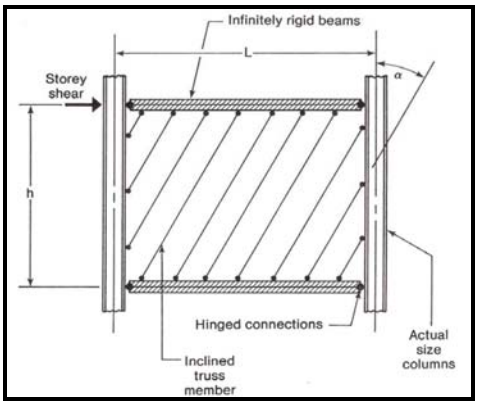

Figure 2-1 - Strip Model (Thorburn et al. 1983 [7])

Using the principle of least work, Thorburn et al. (1983) [7] derived an equation for α that takes the following form:

$$\tan\alpha = \sqrt{\frac{1+\frac{Lt}{2A_c}}{1+\frac{ht}{2A_b}}} \tag{2.1}$$

where t is the thickness of the infill plate, A_c and A_b are the cross-sectional areas of the column and beam, respectively. The derivation included the effect of the axial stiffnesses of the boundary members, but not the flexural stiffness.

In order to simplify the iterative process of designing a steel plate shear wall, Thorburn et al. (1983) [7] developed a Pratt truss model, known as the equivalent brace model, that is illustrated in Figure 2-2. The infill plate at a single storey is modelled as a single diagonal tension-only brace intersecting the working points of the frame. The diagonal brace represents the stiffness characteristics of the tension field in the infill plate, assuming rigid boundary elements. The equation

for the area of the brace is as follows:

$$A = \frac{tL\sin^2 2\alpha}{2\sin\phi\sin 2\phi} \tag{2.2}$$

where ϕ is the acute angle of the brace with respect to the column and all other parameters are as defined above. CAN/CSA S16-01 (Clause 20.2) [4] recommends the equivalent brace model as a preliminary design tool for steel plate shear walls.
Thorburn et al. (1983) [7] conducted a parametric study to assess the effect on the panel stiffness and strength of the plate thickness, the panel height, the panel width, and the column flexural stiffness. It was found that the parameters were closely interdependent with one another and their interaction complex.

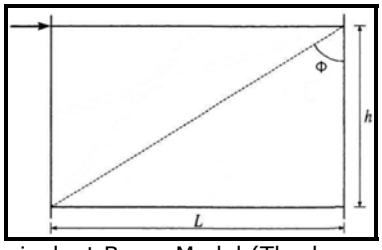

Figure 2-2 - Equivalent Brace Model (Thorburn et al. 1983 [7])

2.2.2. Timler and Kulak, 1983

To verify the analytical method developed by Thorburn et al. (1983) [7], Timler and Kulak (1983) [8] tested a full-scale specimen that represented two single–storey, one–bay steel plate shear wall elements. Due to the testing procedure implemented in this research, the columns were the horizontal elements while the beams were vertical. As seen in Figure 2-3, the interior beam of the test specimen incorporated moment–resisting beam to column connections, while the exterior beams utilized pin connections. The specimen was loaded in an incremental manner to both service and ultimate levels. A cyclic load test up to the allowable deflection limit was also performed. The researchers recognized that the flexural stiffness of the columns affects the value of α. Thus, the equation for α, originally developed by Thorburn et al. (1983) [7], was modified as follows:

$$\tan\alpha = \sqrt{\frac{1+\frac{t_w L}{2A_c}}{1+t_w h\left(\frac{1}{A_b}+\frac{h^3}{360I_c L}\right)}} \tag{2.3}$$

where I_c is the moment of inertia of the column about an axis perpendicular to the panel and all other parameters were defined earlier. It was found that for the case of beams that have an infill plate on one side only, and are therefore free to bend, such as the beam at the top of a shear wall (or the edge of the test specimen), the flexural stiffness of the beam affects α. Thus, the equation for α was re-derived for

the infill plate at the top of a steel plate shear wall and was presented as follows:

$$\tan\alpha = \sqrt{\frac{1+Lt\left(\frac{1}{2A_c}+\frac{L^3}{120I_b h}\right)}{1+th\left(\frac{1}{2A_b}+\frac{h^3}{320I_c L}\right)}} \tag{2.4}$$

where I_b is the moment of inertia of the beam about an axis perpendicular to the panel and all other parameters were defined previously. All equations were all derived assuming pinned beam-to-column connections.
Timler and Kulak (1983) [8] modeled their test specimen using the strip model. Since an elastic analysis program was utilized, inelastic behavior was simulated in the boundary members by successive reductions in the cross-sectional properties of the entire length of the members and in the strips by limiting the stress to the static yield stress measured from tension coupons. Good correlation was found between predicted and actual values of the infill plate stresses, axial strains, and the load vs. deflection response. The discrepancies found in using the Thorburn et al. (1983) [7] equation for α were minor. However, it was recommended that the revised equation (2.3) be used to describe more accurately the angle of the tension field.

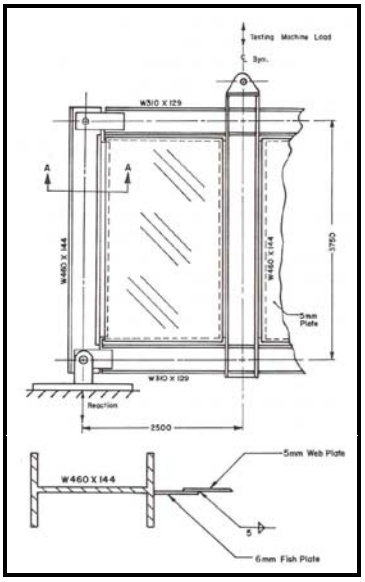

Figure 2-3 – One storey test specimen (Timler and Kulak 1983)

2.2.3. Xue and Lu, 1994

Xue and Lu (1994) [9] conducted analytical studies on four twelve-storey three–bay steel plate shear wall configurations. For each case, the exterior bays had moment–resisting beam-to-column connections and the interior bay had steel infill plates at each storey. The interior bay consisted of either rigid or simple beam-to-column

connections and the infill plate was either connected to all the boundary members or to the beams only. For comparison, upper and lower bound cases of the twelve-storey three–bay steel plate shear walls were included in the analyses. The interior bay of the upper bound case had infill plates, which were assumed not to buckle under load, that were connected to all boundary members and the beam-to-column connections at all frame joints were rigid. The lower bound case consisted of a frame with simple beam-to-column connections in the interior bay and no infill plates.

The six frame–wall structures were modeled using elastic line elements for the columns and beams and four-node shell elements with large-deformation capacity for the infill plate. A 6×6 mesh was used for all panels, with the exception of the bottom panel where a 6×8 mesh was used. The structures were loaded monotonically with lateral forces at each floor. Gravity loads were not applied. Based on the analysis results, Xue and Lu (1994) [9] concluded that the beam to column connection type had a very small effect on the lateral stiffness of the frame. It was found that the frames with the infill plates connected to all surrounding boundary members had a stiffness that was almost as high as the upper bound case. The frames with infill plates connected only to the beams were found to have a stiffness that was much higher than the lower bound case, but was lower than if the infill plates were connected to all surrounding boundary members. Despite this observation, Xue and Lu (1994) [9] recommended that the infill plate be connected to the beams only. The main factor that led to this conclusion is that the analysis predicted that the columns of the stiffer system would carry a proportionally larger share of the storey shears, which could lead to early failure of the columns. It should be noted that no tests were performed to verify the analytical results.

2.2.4. Driver et al., 1997; 1998a, b

Driver et al. (1997 [10]; 1998a [11]) performed tests on a large–scale, four–storey, single bay steel plate shear wall specimen, as shown in Figure 2-4. The specimen had moment–resisting beam-to-column connections and the infill plates were welded to fish plates that were also welded to the boundary members. Gravity loads were applied to the tops of the columns and cyclic lateral loads of equal magnitude were applied at each floor level, as per the requirements of ATC-24 (Applied Technology Council 1992) [12]. The specimen was able to resist increasingly higher loads at each successive cycle until a deflection of five times the yield deflection ($5\delta_y$) was reached. After the ultimate strength (3080 kN) was attained, the deterioration of the load-carrying capacity was gradual and stable. The maximum deflection attained by the lowest storey before failure occurred was nine times the yield deflection ($9\delta_y$). The hysteresis curves were also very stable throughout the test. It was found that the amount of energy dissipated during the loading cycles was significantly greater than that shown by similar specimens, but with shear-type beam-to column connections. Overall, the test behavior showed that a properly designed steel plate shear wall system is an excellent lateral load-resisting system for seismic loading.

Driver et al. (1997 [10]; 1998b [13]) also developed two analytical models to predict the structural behavior of the steel plate shear wall specimen. The first was a finite element model, which used quadratic beam elements to represent the beams and columns and quadratic plate/shell elements to model the infill plates. As-built dimensions and measured material properties of the test specimen were input into

the model. An estimated out-of-flatness of the panels and the experimentally obtained residual stresses were also incorporated. A monotonic analysis that included geometric and material nonlinearities was conducted up to a point where significant yielding occurred and where convergence became difficult to achieve. This nonlinear analysis was found to be in excellent agreement with the experimental data, but was unable to reach the full shear wall capacity. A full response analysis (with geometric nonlinearities excluded) was also performed and provided an excellent prediction of ultimate strength (almost exact, but model curve keeps increasing in capacity), but overestimated the initial stiffness by about 15%. A cyclic finite element analysis using a kinematic hardening rule was performed with the geometric nonlinearities excluded. The load vs. displacement results from this analysis showed good agreement with the test data, but they did not display pinching of the hysteresis curves. For the second model, Driver et al. (1997 [10]; 1998b [13]) used as its basis the strip model (Thorburn et al. 1983 [7]) to predict the envelope of the cyclic curves obtained in the test. The purpose of this model was to analyze the specimen using structural analysis software that is widely used in the design office. Inelastic behavior in this case was modeled using discrete plastic hinges, although since no common commercial structural analysis program was available at that time that could account for this behavior directly, hinging of both the inclined tension strips and the frame members were modeled iteratively using an elastic analysis program. When a column or a beam reached its plastic moment capacity, M_{pc} or M_p, respectively, a true hinge was placed at that point and a constant moment of the magnitude M_{pc} or M_p was applied at the hinged joint. The frame was modeled using member centerline dimensions and only the frame member endpoints were examined for flexural hinging behavior. When a tension strip reached yield, it was removed from the model and the tensile yield force of the strip was applied in the direction of the strip axis where the ends of the strip had been connected to the frame. After each hinging "event," the revised softened model was reloaded and the process was repeated until a plastic mechanism formed. The gravity loads used in the test and P-Δ effects were included in the analysis. It was found that this model slightly underestimated the elastic stiffness of the test specimen, while providing excellent agreement with the ultimate strength.
Driver et al. (1997 [10]; 1998b [13]) discussed various phenomena that could account for the underestimation of the initial stiffness of the test specimen by the strip model. One is the localized compression field that form in the diagonally opposite corners of the frame that form acute angles in the deformed structure where the compressed length of plate is short. Another factor is the increase in axial stiffness of the tension column arising from the presence of the infill plate connected to it; there will be some region that will be effective in tension in the vertical direction. Driver et al. (1997 [10]; 1998b [13]) also demonstrated that for their shear wall specimen, varying the angle of inclination of the tension field from 42º to 50º had little effect on the predicted storey shear vs. storey drift predictions and recommended a parametric study be conducted to examine this observation further. They also found that using twenty strips to model the infill plate did not provide a better prediction of the overall response than did the use of ten strips. Based on the strip model, the researchers also proposed a new hysteresis model that explicitly divides the steel plate shear wall behavior into two distinct components—that of the moment–resisting frame and that of the infill panel that was shown to provide good predictions of cyclic behavior.

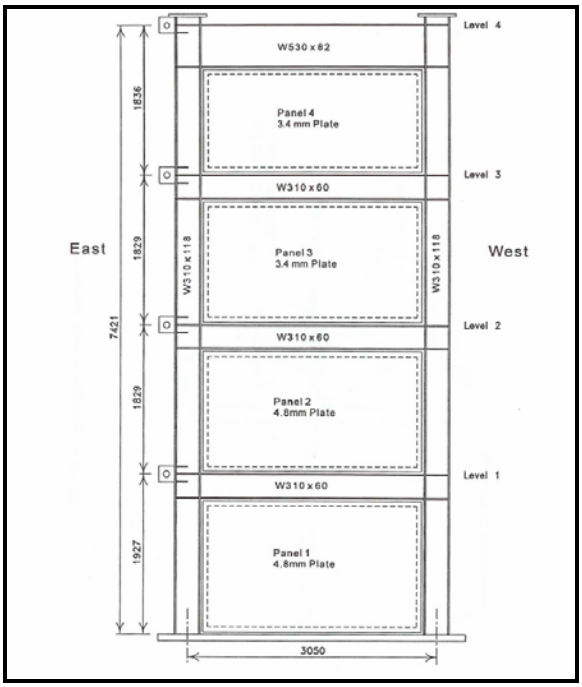

Figure 2-4 - Four–Storey Test Specimen (Driver et al. 1997 [10]; 1998a [11])

2.2.5. Rezai, 1999

Rezai (1999) [15] conducted shake-table testing on a quarter–scale, four–storey steel plate shear wall specimen to study the dynamic behavior. This was the first time a test of this kind was conducted on a steel plate shear wall specimen. All beam-to-column connections were moment–resisting. However, no stiffeners (continuity plates) were provided on the columns for these connections. Steel plates were placed on the beams at each storey to provide a mass of 1700 kg at each level. The specimen was subjected to various site-recorded and synthetically generated ground motions at varying intensities. Due to limitations of the shake table, the test results remained mainly in the elastic range. Thus, the nonlinear behavior of the steel plate shear wall specimen could not be explored in detail. Rezai (1999) [15] found that the first mode was the primary mode of vibration with very little contribution from higher modes. The top storeys exhibited behavior that suggested that flexural behavior dominated, while the bottom storey acted as a shear panel throughout the test sequence. Based on the load vs. deformation plots for all four storeys, it was shown that the first storey dissipated the majority of energy, while the top floors acted as a rigid body rotating about the first floor. Also, it was found that the flexural strains generated in the intermediate level beams could be considered negligible.
Rezai (1999) [15] also conducted sensitivity analyses using Equations 2.3 and 2.4 to assess the effects of various structural properties on the value of the angle of inclination of the infill plate tension field, α. One structural property was changed

while the remainder was kept constant. Five different test specimens were used: Timler and Kulak (1983) [8], Tromposch and Kulak (1983) [16], Caccese et al. (1993) [17], Driver et al. (1998a) [11], and Lubell (1997) [18]. It was found that α did not vary significantly for any change in beam and column cross-sectional area and for infill plate thicknesses, t, of 6 mm and greater, where Equation 2.3 was used. It was found that when Equation 2.4 was used, α varied significantly with changes in t.
Rezai (1999) [15] developed a "simplified" strip model for analyzing steel plate shear wall behavior, as illustrated in Figure 2-5. The tension–only strips for each panel are placed diagonally between opposite corners and from the corners to the mid-span of the boundary members, for a total of five strips per panel. The strips were set up in this manner to reflect the non-uniformity of α and to reflect the corner stiffness of each panel. Using this model, good agreement was obtained between the predicted and experimental elastic stiffness of the single–storey specimens of Lubell (1997) [18]. However, the model was found to be conservative in predicting the ultimate capacity. Rezai (1999) [15] also compared the results from the "simplified" strip model to the results from the original strip model using the specimen tested by Driver et al. (1998a [11]) as a basis. The "simplified" model had a higher estimated elastic stiffness and ultimate capacity than that provided by the conventional strip model.

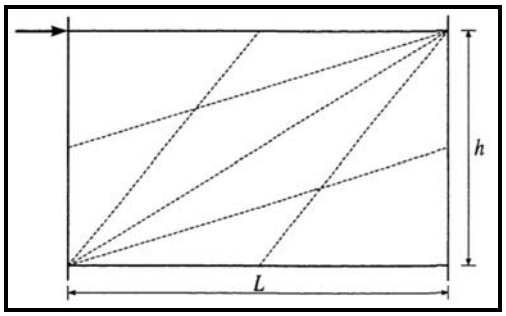

Figure 2-5 - Simplified Strip Model (Rezai 1999 [15])

2.2.6. Abolhassan Astaneh-Asl, 2001 [19]

Steel plate shear wall systems have been used in recent years in highly seismic areas to resist lateral loads. Figure 2-6 shows two basic types of steel shear walls; unstiffened and stiffened with or without openings. Unstiffened shear walls have been very popular in North American applications while in Japan almost all steel shear walls used in recent years have been stiffened. Some of the advantages of using steel plate shear wall to resist lateral loads are:
The system, designed and detailed properly is very ductile and has relatively large energy dissipation capability. As a result, steel shear walls can be very efficient and economical lateral load resisting systems.
The steel shear wall system has relatively high initial stiffness, thus very effective in limiting the drift.
Compared to reinforced concrete shear walls, the steel shear wall is much lighter which can result in less weight to be carried by the columns and foundations as well as less seismic load due to reduced mass of the structure.

By using shop-welded, field-bolted steel shear walls, one can speed-up the erection process and reduce the cost of construction, field inspection and quality control resulting in making these systems even more efficient.
Due to relatively small thickness of steel plate shear walls compared to reinforced concrete shear walls, from architectural point of view, steel plate shear walls occupy much less space than the equivalent reinforced concrete shear walls. In high-rises, if reinforced concrete shear walls are used, the walls in lower floors become very thick and occupy large area of the floor plan.
Compared to reinforced concrete shear walls, steel plate shear walls can be much easier and faster to construct when they are used in seismic retrofit of existing building.
Steel plate shear wall systems that can be constructed with shop welded-field bolted elements can make the steel plate shear walls more efficient than the traditional systems. These systems can also be very practical and efficient for cold regions where concrete construction may not be economical under very low temperatures.

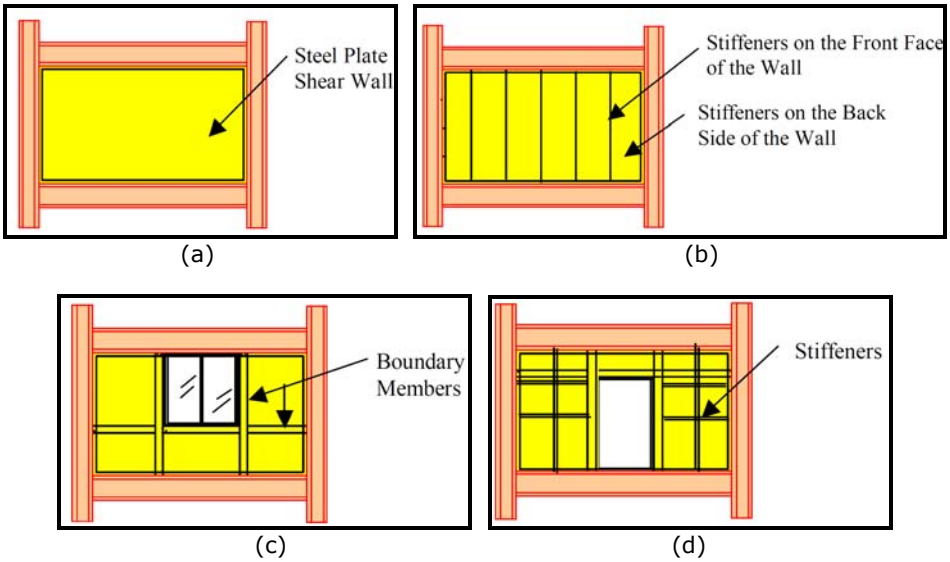

Figure 2-6 - Stiffened and Unstiffened Steel Shear Walls: a) Steel Plate Shear Wall (unstiffened); b) Steel Plate Shear Wall (stiffened); c) Stiffened Steel Shear Wall with Opening; d) Stiffened Steel Shear Wall with Opening

Typical systems include singular steel plate shear walls, where the shear wall is the only element resisting story shear and dual systems, where moment frames are parallel to it (Figure 2-7). Coupled Shear wall system is a particular dual system, where a coupling beam connects two shear wall bays. The frame or portion of it that contains the shear walls and coupling beams is special moment frame.

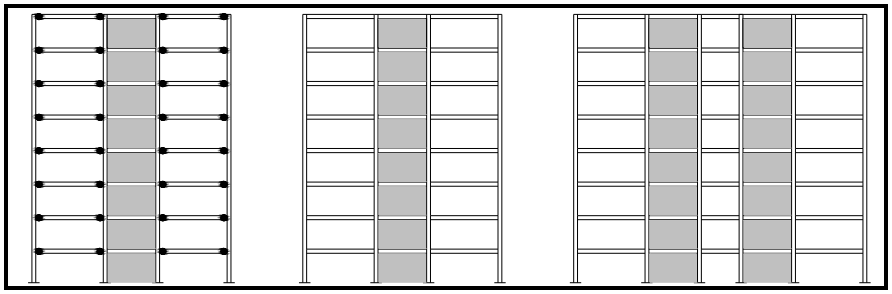

(a) (b) (c)

Figure 2-7 - Typical Steel shear wall systems: a) Singular shear wall inside gravity frame; b) Dual system with shear wall inside moment frame; c) Dual system with coupling beams

2.2.7. Behbahanifard, Grondin and Elwi, 2003

A very comprehensive experimental and numerical research program on the behavior of SPSW structures was developed at the University of Alberta, Canada, by Behbahanifard, Grondin and Elwi, 2003 [20] (Figure 2-8). The primary objective of the experimental program was to increase the database of test results on large-scale multi-storey unstiffened steel plate shear walls under extreme cyclic loading, such as would be expected in a severe earthquake. Stiffness, ductility, energy absorption capacity, and strength degradation were all assessed. In the second phase of the study, a nonlinear finite element model was developed in order to accurately simulate the monotonic and cyclic behaviors of thin unstiffened steel plate shear walls.

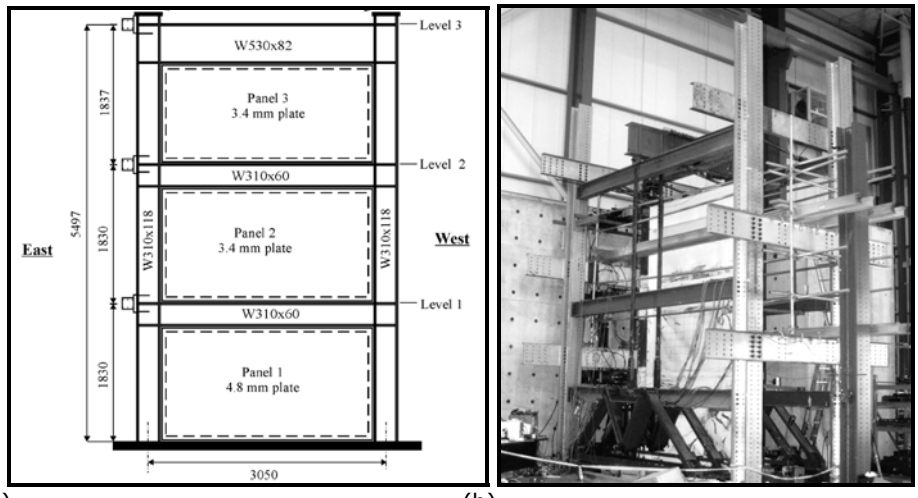

(a) (b)

Figure 2-8 - Schematic of three-storey steel plate shear wall a) and overview of test set up b)

Steel plate shear wall specimen demonstrated the excellent behavior of this system.

The specimen showed high initial stiffness, very ductile behavior, and stable hysteresis loops. Despite the fact that a beam to column connection fractured during the test, the ability of the system to resist the applied shear force was not noticeably affected, this shows the high redundancy of steel plate shear walls. Gradual decrease in the capacity, caused by plate tearing and local buckling, started when the test specimen reached a drift of about 3% of the storey height in the first and the second panels. This deflection is greater than the limiting storey drift specified by design standards for typical frame buildings. Therefore, if the system is properly designed, degradation of capacity is unlikely to occur.

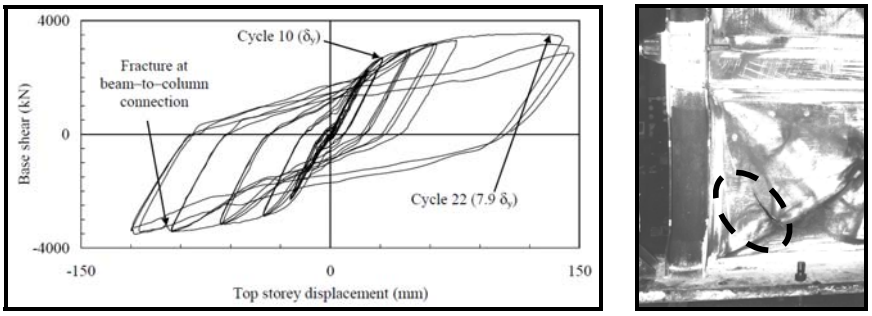

(a) (b)

Figure 2-9 - Base shear versus top storey displacement a); and tear at the bottom east corner of first panel (end of test) b)

2.2.8. Berman and Bruneau, 2003

Using plastic analysis theory and the assumption of discrete strips to represent the infill plate, Berman and Bruneau (2003) [21] derived equations to calculate the ultimate strength of single- and multi-storey steel plate shear walls with either simple or rigid beam-to column connections. For multi-storey shear walls, equations were developed based on two types of failure mechanisms that provide a rough range of ultimate strengths: soft storey failure and uniform yielding of the infill plates in all storeys simultaneously. To provide a lower bound estimate of capacity, the equation derived for single–storey steel plate shear walls with simple beam-to-column connections was used to predict the capacity of a variety of single- and multi-storey steel plate shear wall specimens from the literature having either pinned or semi-rigid connections. This equation was found to underestimate the experimental capacities by an average of about 6%, although it overestimated the capacity of one case by about 9%. The equation derived for the soft storey mechanism was found to overestimate the capacity of multi-storey test specimens with rigid connections by about 17%. This model provides only the ultimate capacity. The proposed equations do not describe the initial stiffness, the ductility, or the actual failure mechanism, nor do they provide a means of determining the frame forces for use in design.

Berman and Bruneau [21] also looked at the design of steel plate shear walls using CAN/CSA S16-01 [4]. The equivalent storey brace method (Thorburn et al. 1983 [7]) was used as an actual design case along with the traditional strip model. It was found that if the aspect ratio was not equal to one, the equivalent brace method would result in a higher ultimate capacity than the strip model. (It should be noted,

however, that the intended use of the equivalent brace method is for preliminary sizing only and not for detailed design.) The researchers observed that for design of the infill plate, the storey shear, V_s, found using the equivalent lateral force method, should be multiplied by a system overstrength factor, Ω_s, between 1.1 to 1.5. As such, the minimum thickness of the infill plate for each storey is:

$$t = \frac{2V_s\Omega_s}{F_y L \sin 2\alpha} \tag{2.5}$$

where V_s is the shear strength of the plate, Ω_s is the system overstrength and F_y is the nominal yield strength of the infill plate.

2.2.9. D. Vian and M. Bruneau, 2004 [22]

The authors tested specimens utilizing low yield strength (LYS) steel infill panels and reduced beam sections (RBS) at the beam-ends Figure 2-10. A total of three single bay, single story LYS SPSW specimens were designed and subjected to quasi-static cyclic testing using quasi-static loading protocol similar to ATC-24 [12]. Two specimens make allowances for penetration of the panel.
The frames measured 4000mm wide and 2000mm high between member centerlines, and consisted of 345MPa steel members. The infill panels were 2.6 mm thick, LYS steel plates with an initial yield stress of 165MPa, and ultimate strength of 300MPa, important properties that may aid in alleviating over-strength effects. The reduced beam sections (RBS) at each end was designed to ensure all inelastic beam action would occur at these locations.

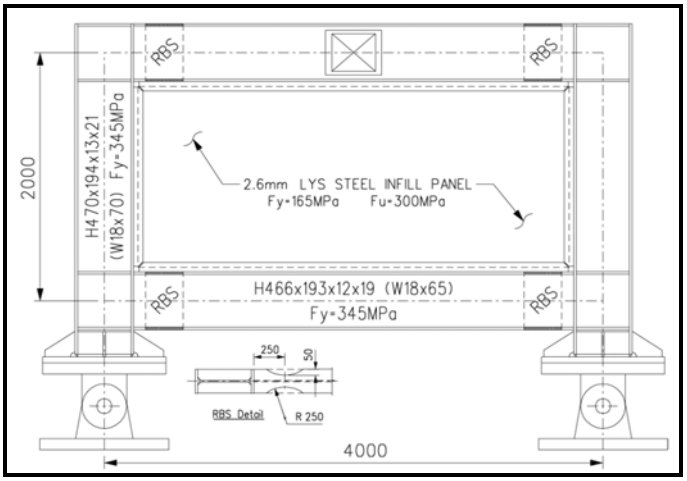

Figure 2-10 - Typical specimen dimensions

All specimens tested in this experimental program exhibited stable force-displacement behavior Figure 2-11, with very little pinching of hysteresis loops until the significant accumulation of damage at large drifts. The perforated panel specimen shows promise towards alleviating stiffness and over-strength concerns

and can also provide access for utilities to penetrate the system.

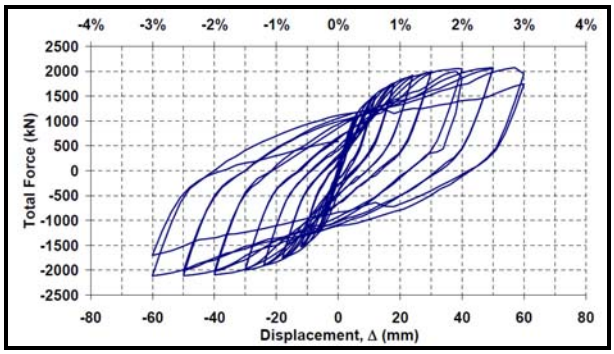

Figure 2-11 - Hysteretic behavior of the solid panel

2.2.10. Shishkin, Driver and Grondin, 2005

The study was then continued by Shishkin, Driver and Grondin, 2005, [23] who developed a new strip model for numerical analysis of SPSW. A detailed and a simplified model were developed and than validated based on several test results from the literature.
The detailed model proposed refinements to the strip model, as described by Thorburn et al. (1983) [7], to obtain a more accurate prediction of the inelastic behavior of steel plate shear walls using a conventional structural engineering software package. Multilinear rigid-inelastic flexural and axial hinges, generated from the stress vs. strain curves for the material of each member and neglecting local buckling, were used to model the pushover behavior of steel plate shear walls.

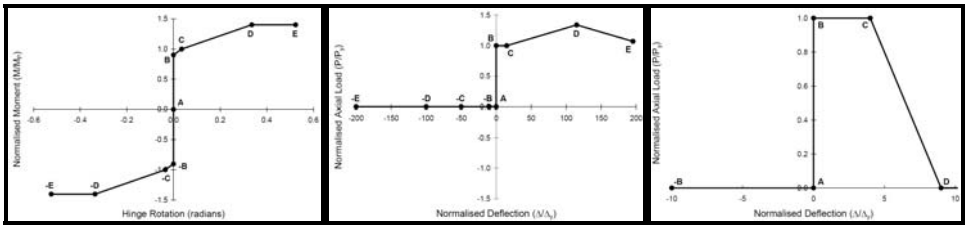

(a) (b) (c)

Figure 2-12 - Typical behavior for a) Flexural Hinges; b) Axial Tension Strip Hinges and c) Deterioration Hinge

The flexural hinges Figure 2-12a (columns and beam) were located a distance of one-half the member depth from the boundary of the panel zone and the axial hinges were located at a discrete point along the length of the tension–only strip. A compression–only diagonal strut was modeled to represent the small contribution of compressive resistance in each infill plate as well as other phenomena not captured by the representation of a continuous plate by a series of discrete tension strips. A bilinear axial hinge Figure 2-12b which defines the limiting stress of the strut was located at a discrete point along the length of the strut. The tearing of the infill plate

corners was modeled using deterioration axial hinges Figure 2-12c that were located on the strips that came closest to the corners of each panel.
Figure 2-13 shows the comparison between the specimen envelope curve and the detailed model pushover curve. The model provides an excellent representation of the elastic portion of the envelope curve. There is a very small kink in the elastic portion of the detailed model curve at a deflection of 0.7 mm, which is due to the early buckling of the compression strut in the bottom storey. The detailed model pushover curve overestimates the specimen strength slightly at a point just beyond the occurrence of initial yielding and underestimates the ultimate strength of the specimen by 2.9%. The peak of the first-storey pushover curve generated by the detailed model occurred at almost the same deflection as the specimen (44.3 mm for the detailed model vs. 42.5 mm for the specimen). The declining curve of the model descends at approximately the same rate as the specimen. At a very large first-storey deflection, the deterioration of the model ceased and was followed by a very slight gain in strength. This is attributed to the fact that only two tension strips deteriorate. As a conclusion, the pushover behavior of the detailed model is in very good agreement with the test specimen behavior.

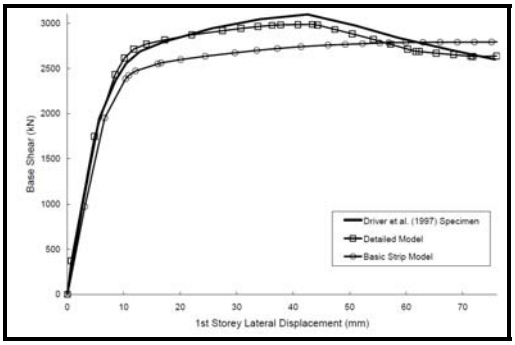

Figure 2-13 - First Storey Response Curves for Detailed Model, Basic Strip Model and Driver et al. (1998a) [11] Specimen

Based on the detailed model, the authors tried to make the model simpler and desirable for use as a design tool, while still retaining a good degree of accuracy. This simplified model was referred to as the modified strip model. The main differences from the detailed model consisted of:
- crosshatching technique was used to locate the tension strips. The crosshatching method uses the average angle of inclination and spaces the tension strips at equal intervals so that strips in panels above and below share common nodes at the beam;
- bilinear hinges instead of multilinear hinges in the beams, columns, and tension strips;
Figure 2-14 shows the pushover curves of the simplified (modified strip) models compared to that of the detailed model and the envelope curve of the specimen. The simplified model is a good model, and in some ways a better model than even the detailed model, for describing the specimen pushover behavior.

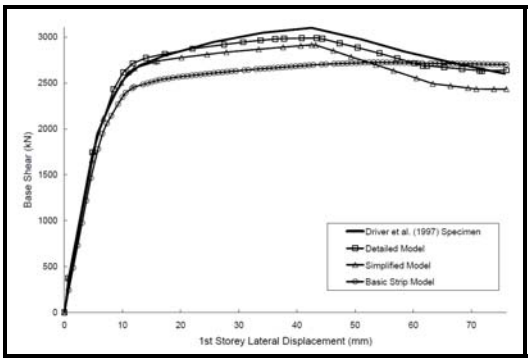

Figure 2-14 - First–Storey Response Curves for Detailed Model, Simplified Model, Basic Strip Model, and Driver et al. (1998a) [11] Specimen

2.2.11. M.M. Alinia, M. Dastfan, 2006 [24]

The study investigated the effects of surrounding members (i.e. beams and columns) on the overall behavior of TSPSWs. A variety of rectangular plates surrounded by a range of elastic structural members was considered. The panels were subjected to pure shear forces. The results shown the flexural stiffness of surrounding members has no significant effects, either on elastic shear buckling or on the post-buckling behavior of shear walls. It was also shown that the flexural rigidity does not influence the elastic shear buckling or the ultimate strength of shear panels and the extensional stiffness has only a slight effect on the ultimate strength. In addition, the beam-to-column connection type has no significant effect on the panel's behavior.

2.2.12. Chih-Han Lin et al., 2006 [25], Chih-Han Lin et al., 2007 [26]

To asses the behavior of SPSW systems Figure 2-15, Chih-Han Lin et all. performed a large experimental program:
- In the Phase I tests, experimental testing of specimens with out-of-plane displacements and the buckling sounds restrainers
- In the Phase 2 tests, damaged steel plates were removed and replaced with new plates without the use of any restrainer. In both phases, the specimens was pseudo-dynamically tested using three ground accelerations, which were recorded in the 1999 Chi-Chi earthquake and scaled up to represent seismic hazards of 2%, 10%, and 50% probabilities of exceedance in 50 years. Before the actual testing, analytical predictions were performed on the complete 2-story PISA3D structure model including the parameter MRF and the SPSW. For each SPSW frame, two series of strips with inclined angles of ±41 degrees were constructed. For the parameter MRF, all the beam and column members in MRF and boundary frame of SPSW adopt the bi-linear beam-column element.
- The results shown the responses of the SPSWF can be accurately predicted using the strip model and the tension only material property implemented in PISA3D computer program. The SPSWF specimen sustained three earthquake excitations without significant steel plate fracture or overall strength degradation.

- After Phase1 tests, the horizontal restrainers did not show any sign of damage. It appears that the 3% of the in-plane force assumption is appropriate for sizing the restrainers.
- The strip model can be conveniently used to study the deformation demands imposed in the center and corner of the steel shear wall. It is found from the analysis and the test results that the tension field action is much more severe in the center than that in the corner of a SPSW.

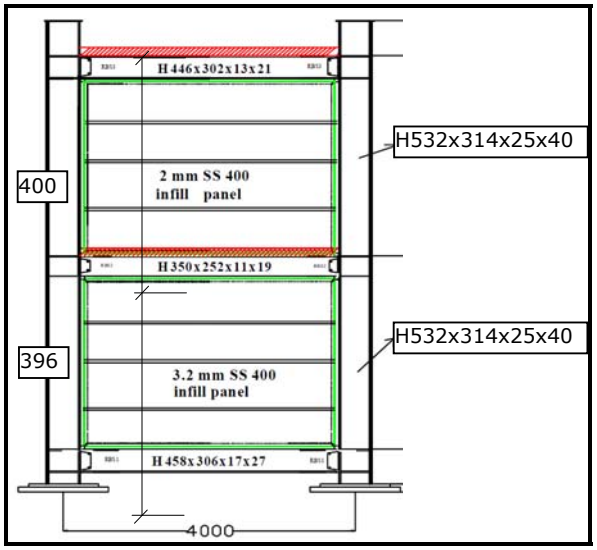

a)

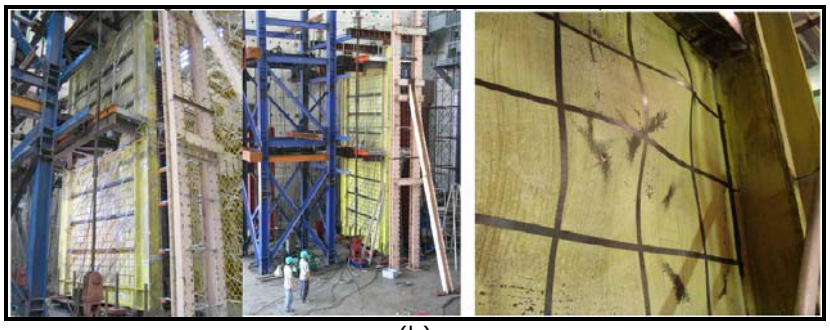

(b)

Figure 2-15 - Two-story SPSW specimen a); and Steel plate buckling b)

2.2.13.J. W. Berman, L. N. Lowes, T. Okazaki, M. Bruneau, K-C. Tsai, R. G. Driver, R. Sabelli, 2008 [27]

With many researchers that had important contributions to the development of SPSW systems, the paper addresses the recent developments and also future

needs. The authors propose also solutions for developing the next-generation of steel plate shear walls. Numerous advantages of steel plate shear walls (SPSWs) in comparison with traditional lateral load systems, such as steel braced frames, reinforced concrete walls and moment resisting frames, can be identified:
- SPSWs have fewer costly detailing requirements,
- require less stringent construction tolerances,
- allow for rapid construction, and
- result in fewer bays of lateral load resisting framing.

Despite these advantages, SPSWs are not widely used because:
- traditional SPSW configurations result in large column dimensions and prohibit the use of narrow walls, thereby reducing the system's economy,
- numerical models used to analyze SPSW systems are cumbersome and overly time consuming for engineers,
- SPSW system behavior is not well understood, leading to conservative design requirements and further reduction in economy, and
- SPSWs have a lower flexural stiffness relative to concrete walls, making their use in taller buildings more challenging.

The authors also identified important research needs:
- to develop SPSW systems that reduce column demands
- new modeling techniques are necessary to enable more efficient design of SPSWs
- improving the overturning stiffness of SPSWs (Splitting a SPSW into two coupled SPSWs, as shown in Figure 2-16 may also improve the overturning stiffness but there is little information available regarding how coupling beams should be designed within such a system)

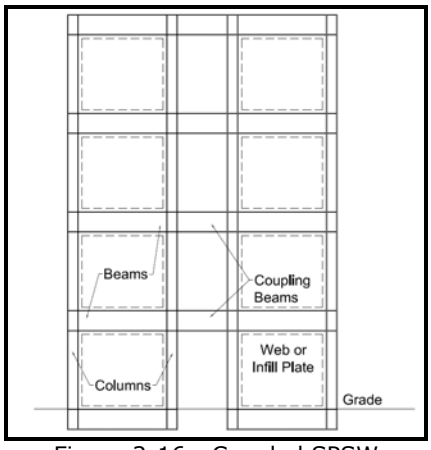

Figure 2-16 - Coupled SPSW

2.2.14. Mehdi H.K. Kharrazi, Helmut G.L. Prion, Carlos E. Ventura, 2008 [28]

The study investigated the implementation of modified-plate frame interaction (M-PFI) method in the design of a steel plate wall (SPW). To evaluate the application of

the M-PFI method as a design methodology, the finite element (FE) method was used to analyze different SPWs (Figure 2-17). Story height for all storeys was 3.5 m except for the first story, which was 5 m. The lateral resistance system consisted of four SPWs situated along the middle length of each side of the plan, see (Figure 2-17). Implementation of the M-PFI method to design an SPW contains the following steps:
Calculate and draw shear-load displacement diagrams (Figure 2-18)
Calculate the bending load displacement diagrams (Figure 2-19)
Modify the shear-load displacement diagram for the overhead overturning moments (Figure 2-20)
Check the combined axial compression and bending capacity of the columns
Check combined axial compression and bending capacity of the beams
Check that the steel plate dissipates more energy than the frame, and that the plate complies with of the infill plate (which is the fuse).
The results of the study shown that the M-PFI method is suitable for use in the design of an SPW system and enables engineers to meet specific performance requirements safely and efficiently.

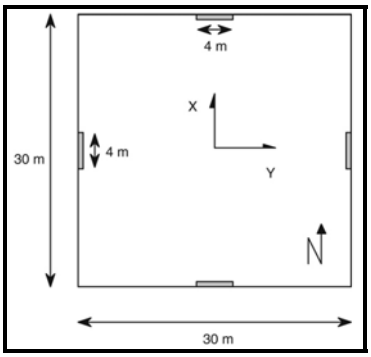

Figure 2-17 - Footprints of the 3, 9, and 27-story buildings

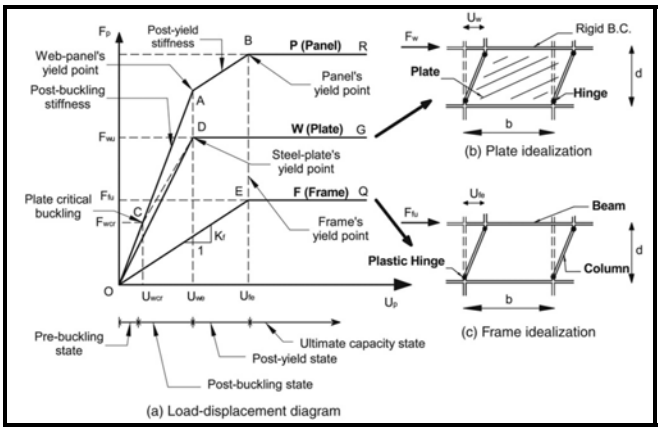

Figure 2-18 - Components of M-PFI model (a) shear-load displacement: frame only, plate only, and combined effects in panel; (b) idealized plate component; and (c) idealized frame component

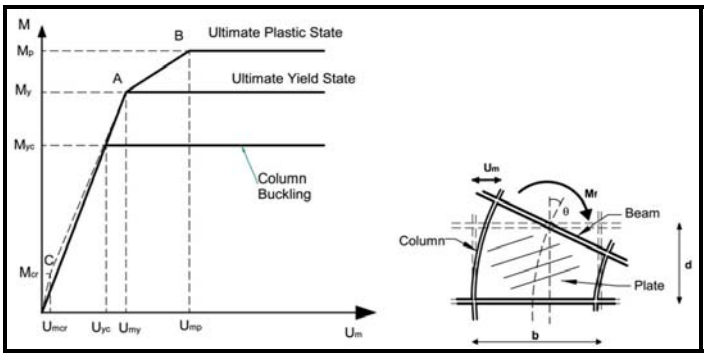

Figure 2-19 - M-PFI bending model load displacement of the panel (combined web plate and frame) (left), and M-PFI model plate idealization for bending deformation (right)

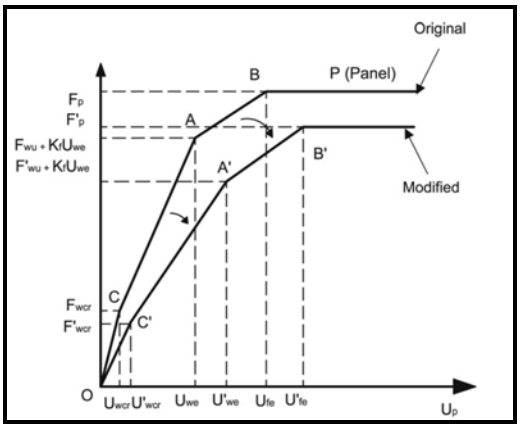

Figure 2-20 - Modified load displacement diagram for shear resistance of the SPW

2.2.15.S. Sabouri and M. Gholhaki, 2008 [29]

Sabouri and Gholhaki conducted an experimental program to evaluate the ductility factor of thin steel plate shear walls. Two types of ductile steel plate shear walls with one of third scale were designed and tested under cyclic loads . In these specimens Figure 2-21a and b, two types of beam-to-column connection, rigid Figure 2-21c and simple Figure 2-21d, were considered. For the plates of panels low strength steel and for the boundary frames high strength steel were used. The three-story ductile steel plate shear wall having the rigid beam-to-column connection has a ductility factor according to ATC-24 [12] equals to 6.63. The shear wall having simple beam-to-column connection (SPSW-S) has a ductility factor according to ATC-24 [12] protocol equals to 8.24. If the trilinear curve is used for obtaining the ductility factor instead of bilinear one, the yielding displacement (δ_{y1}) related to the trilinear curve Figure 2-22 is much smaller than the yielding displacement in the bilinear one (δ_{y2}). Therefore, the ductility factor can be considered much greater.

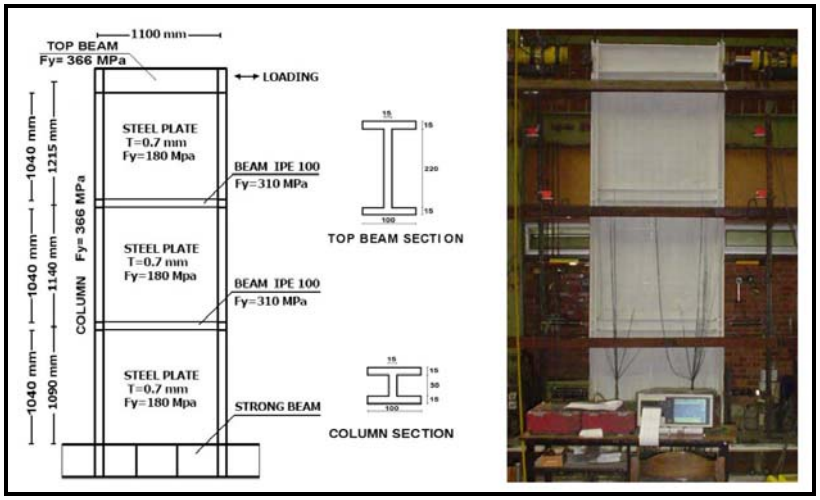

(a) (b)

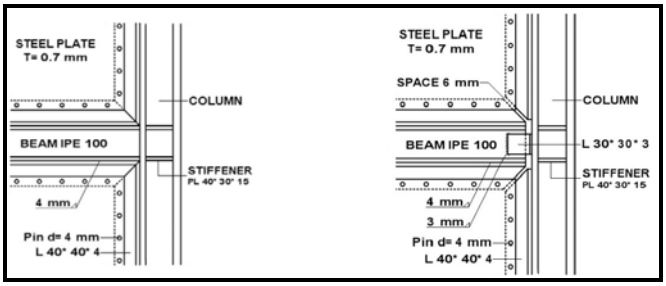

(c) (d)

Figure 2-21 - Schematic and photograph of specimens SPSW-R and SPSW-S and details of two types of beam-to-column connection

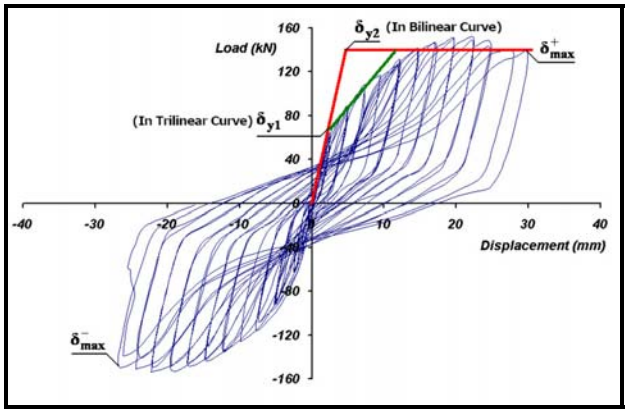

Figure 2-22 - Hysteresis loops, bilinear and trilinear curves of the first floor of the specimen SPSWR

2.2.16.A. K. Bhowmick, R. G. Driver, G. Y. Grondin, 2009

In their study, Anjan K. Bhowmick, Robert G. Driver, Gilbert Y. Grondin [30] investigated the capacity of current codes (NBCC 2005 [31]) to properly design SPSW structures using capacity design principals. Their work focused mainly the effects of strain rate on the dynamic flexural demand and the impact of P-delta effects on seismic performances. For study, a typical 4-storey and 15-storey steel plate shear wall for a building designed according to the NBCC 2005 [31] seismic provisions were analyzed under four spectrum compatible ground motions. The results obtained shown that the strain rate has an effect in the dynamic response of steel plate shear walls. With higher strain rates the ductility of the steel plate shear wall reduces and the average flexural demand at the base of the wall is increased. Thus, the strain rate effect increased the overturning moment by about 11% for the 4-storey and about 4% for the 15-storey steel plate shear wall. Regarding the P-delta effect, it does have a major influence if the shear wall structure meets the code specified inter storey drift limit (Figure 2-23).

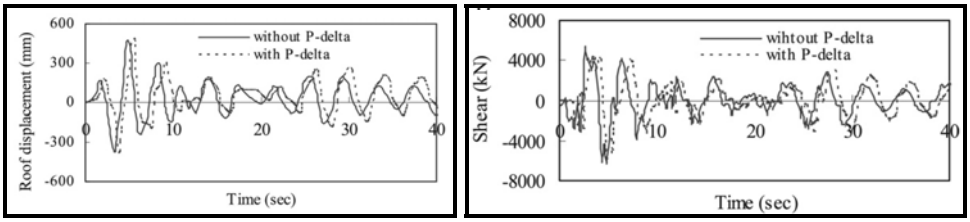

(a) (b)

Figure 2-23 - Inelastic seismic response: a) top storey displacement; b) base shear for El Centro 1940 earthquake record with and without P-delta effect

2.2.17.H.R. Habashi, M.M. Alinia, 2010 [32]

In their study, a number of SPSW models were analyzed in order to evaluate the degree of effectiveness of infill walls in resisting lateral loads and also their influence on the frame's behavior (Figure 2-24).

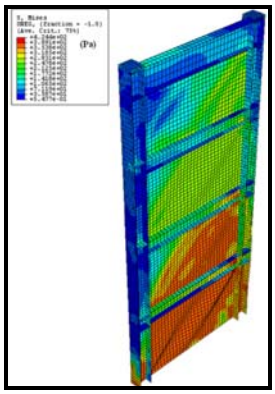

Figure 2-24 - FE model

Results shown that SPSWs designed according to design codes should have desirable sequences of yielding and that plastic deformations should primarily be provided by the infill plates. The infill plates are very effective in the initial stages of loading (up to the drift angle of 1%) and absorb substantial part of storey shear. However, once diagonal yield zones develop in the infill plates, they begin to lose their effectiveness and when yield zones spread throughout the wall, additional applied loads are essentially carried by the frame members (Figure 2-25).

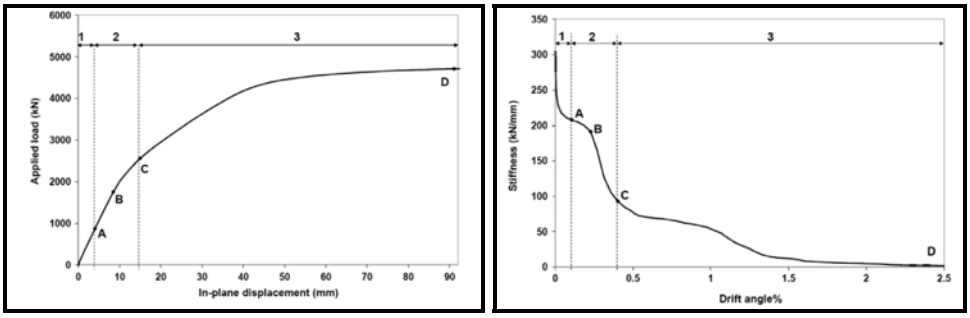

(a) (b)

Figure 2-25 - A typical lateral load-displacement curve a); and a typical lateral stiffness-drift angle curve b)

2.3. Applications of steel plate shear wall systems

2.3.1. SUA

2.3.1.1. Six-Storey Hospital in Los Angeles, California

The Olive View Hospital in Sylmar, California, is a good example of SPSWs used in an important structure such as a hospital, and is in an area of considerably high seismic activity (Figure 2-26). The existing hospital building replaced the initial reinforced-concrete Olive View Hospital that partially collapsed during the 1971 San Fernando earthquake and had to be demolished.

The new Sylmar Hospital building shown in Figure 2-26 is designed to resist the gravity load entirely through a steel space-frame, and to resist the lateral load through R.C. shear walls in the first two storieys and SPSWs in the upper four storeys. The steel plate panels in this structure are 7.6 m (25 ft) wide and 4.72 m (15.5 ft) high with steel plate panel thicknesses between 15.9 mm (5/8 in) and 19.1 mm (3/4 in) (Troy and Richard, 1988) [33] . The steel walls were designed for loads below the force necessary to trigger the global critical-buckling capacity of the stiffened walls, as well as local critical-buckling capacity of the sub-panels bounded by the stiffeners. The tension field action capacity was not used though the designers acknowledged its presence and considered the strength of tension field action as a 'second line of defense' mechanism in the event of high insensitive earthquakes. As a part of the California Strong Motion Instrumentation Program (CSMIP), seismic instruments were installed at the Sylmar hospital. These instruments recorded valuable data during the 1987 Whittier and the 1994 Northridge earthquakes including a valuable record of the response characteristics

of the structure. From the data recorded by the CSMIP instruments in this building during the 1994 Northridge earthquake, the accelerations at roof level were found to exceed 2.3g while the ground acceleration was approximately 0.66g. The damage investigation conducted for this building in the aftermath of the 1994 Northridge earthquake indicated severe damage found in some non-structural elements such as the suspended ceilings and sprinkler system resulting in breakage of a number of sprinklers and flooding of some floors. Additionally, the bolted connections of most TV sets hanging from the walls of patient rooms had been broken and the sets thrown to the floor. The non-structural damage was obviously an indicator of extreme stiffness of this structure. The intensive stiffness was also found to be the reason of relatively large amplification of accelerations from ground level to roof level (Celebi, 1997) [34].

Figure 2-26 - Olive View Hospital in Sylmar, California

2.3.1.2. 30-Storey Hotel in Dallas, Texas

The Hyatt Regency Hotel in Dallas (Figure 2-27), Texas described by Troy and Richard in 1988 [33] is a very good example of the efficient application of an SPW in areas with low seismic activity but with relatively high wind loads. The lateral-resisting system of the 30-storey structure is made of a steel braced frame in the longitudinal direction and SPSWs in the transverse direction. The SPSWs in this structure are designed to carry about 60 % of the tributary gravity load while the wide flange columns at the SPW boundary of is designed to resist the remaining 40 %.

By implementing the SPW system as gravity load-carrying elements, the designers claim they have saved a significant quantity of steel from use in beams and columns, and that the SPW system used one-third less steel compared to an equivalent steel moment-resisting frame (Troy and Richard, 1988 [33]). Since the building was located in Dallas, the wind loads were the governing lateral loads. Maximum drift was found to be only 0.0025 under the design wind load. The relatively low drift is due to relatively high in-plane stiffness of the SPWs.

Figure 2-27 - Hyatt Regency Hotel in Dallas

2.3.1.3. A 52-story residential building in San Francisco, California

The 52-story building in San Francisco was designed by Skilling, Ward, Magnusson, Barkshire of Seattle. The building is a residential tower and has 48 storeys above ground and four basement parking levels. A rendering of the building is shown in Figure 2-28.

The gravity load carrying system in this building consists of four large concrete-filled steel tubes at the core and sixteen concrete-filled smaller steel tube columns in the perimeter. The floors outside the core consist of post-tensioned flat slabs and inside the core and lower floors are typical composite steel deck-concrete slab. The foundation consists of a single reinforced concrete mat foundation.

Figure 2-28 - 52-story building in San Francisco

The main lateral load resisting system of the structure consists of a core made of four large concrete field steel tubes, one at each corner of the core, and steel shear walls and coupling beams. There are built-up H columns between the two corner pipe columns. The steel shear walls are connected to concrete filled steel tubes by coupling beams. The shear wall units are primarily shop-welded and bolt spliced at the site at each floor mid-height. The only field welding is the connection of the girders and steel plate shear wall to the large concrete-filled steel tube columns.

2.3.1.4. 24-Storey Office Building in Seattle, Washington

The U.S. Federal Courthouse in Seattle is shown in Figure 2-29. The typical floor framing of this building consists of steel deck - concrete floors supported on wide flange beams and columns. As shown in Figure 2-29, the lateral load-resisting system consists of a core with four large concrete-filled tubes at its corners and an SPW and coupling beams connecting the tubes to each other in one direction and a steel-braced frame in the other. The SPW system in this building is primarily shop-welded and field-bolted. The steel plates and girders are connected to the round columns in the field by welding. The four round concrete-filled tubes carry the gravity load in the interior of the building. The H-shaped columns within the steel box core are not designed to carry gravity load but are designed to be the main part of the lateral-load resisting system. This can be considered as a dual system consisting of SPWs and special moment-resisting frames.

Figure 2-29 - U.S. Federal Courthouse in Seattle

Two SPWs systems were used with thicknesses between 1.3 mm and 35.0 mm, and a height-to-width varying in size from 3 m by 3 m, and 3.7 m by 5.5 m, depending on floor height. These walls rise from the building base up to the structure's mechanical penthouse. Spaced approximately 3.7 m apart, the north and south facing walls are joined at the east and west sides by steel-braced frames, forming a rectangular shaped core as shown in Figure 2-29. These thin SPSWs are designed to absorb seismic energy by buckling when an earthquake hits. As the plates buckle,

diagonal tension field action provides lateral force resistance. At the four corners of the core, the concrete-filled steel pipe columns anchor the SPSWs and resist the intense forces being applied to the shear walls. Pipe columns range in diameter from 1.7 to 1.1 m.

2.3.1.5. 55-storey hotel (Convention Center) in Los Angeles

The Los Angeles Convention Center Hotel is a 55-storey (Figure 2-30) steel-framed steel plate shear wall high-rise building that takes full advantage of many of the performance-based design approaches and philosophies. The primary lateral resistance system consists of thin steel plates (6– 9 mm thick) within fully welded WUF-W moment frames. Additional system stiffness is provided by several storey-high outrigger trusses at the mid-height and top of the tower while using buckling-restrained braces (BRBs) as fuse elements to control the maximum force that the outrigger trusses can develop.

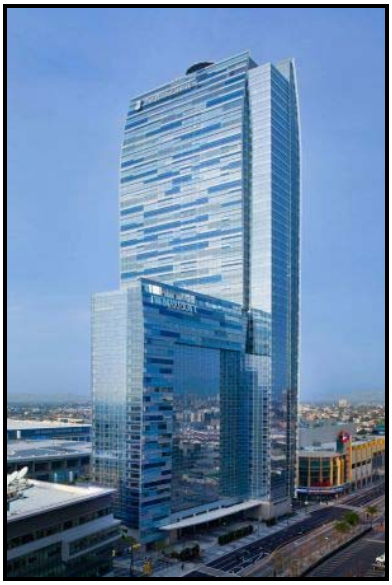

Figure 2-30 - Los Angeles Convention Center Hotel tower rendering

The tower is a 55-storey steel-framed structure over three storeys of a reinforced cast-in-place concrete basement. As much as possible, the steel columns on the exteriors of the tower slope from one floor to the next to maintain a constant slab edge distance and minimize disruption to useable floor space as the floor footprints expand and contract. Beams were located at demising walls of hotel units with the metal deck clear spanning across the rooms to maximize the ceiling heights while minimizing the floor heights. Large horizontal thrust forces develop where the column slopes shift from one floor to the next, which need to be resisted by cross-ties into the building (see Figure 2-30), creating loading upon much of the lateral seismic-resisting systems with gravity forces that need to be accounted for in their design, making the rigorous system capacity verification associated with the performance-based design all the more critical.

The lateral force-resisting system of the tower is provided by thin steel plate shear walls (SPSWs) at critical locations and typically adjacent to vertical circulation elements. The thin shear wall infill plates are 3/8–1/4 in. thick, A36 grade and are bounded by wide flange horizontal boundary elements (HBEs) and steel built-up composite box columns (see Figure 2-31). Full moment connections between the horizontal and vertical boundary elements (VBEs) of the wall provided a back-up moment frame which provided additional frame stiffness to the walls, as well as resisting cyclic force reversals before the steel plate engaged during post-bucking behavior. To further control the building drifts, a system of outriggers is used at the mid-height and top of the tower (see Figure 4). With depths of a full floor or more, the outrigger system effectively engaged the entire building width and reduced the aspect ratio of the tower from 20:1 to 10:1. Buckling restrained braces (BRBs) and portal frame sections were utilized in strategic locations within each outrigger truss to control the maximum amount of force that could be delivered to the exterior building columns, thereby providing for capacity protection of the gravity column elements. The system of thin steel plates, moment connections between the HBEs and VBEs and the BRBs within the outriggers provide a redundant and enhanced level of energy dissipation and ductility for resisting large-magnitude seismic events.

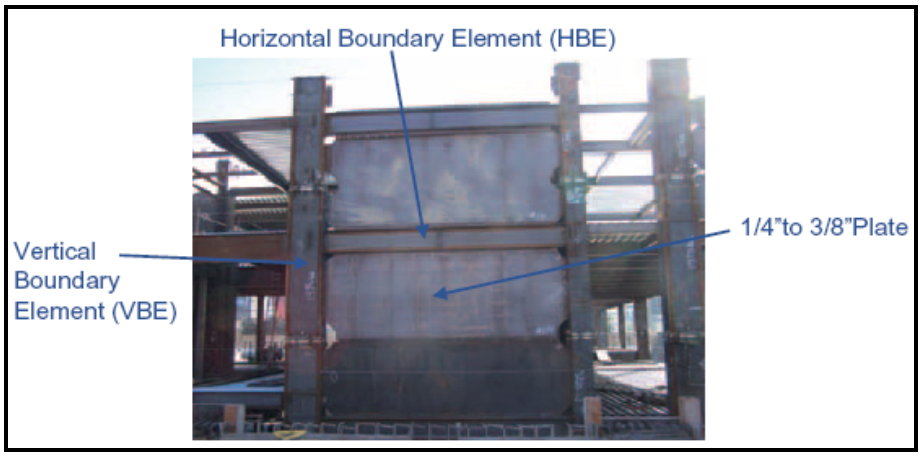

Figure 2-31 - Lateral force-resisting system overview

2.3.2. CANADA

2.3.2.1. Six-Storey Building in Saint Georges, Quebec, Canada

For the application of SPW within a new built structure in Canada, a thin steel infill panel concept was first deployed within a six-storey office structure for a major steel fabricator in St. Georges, Quebec, (in early nineties). The shear core panels were fabricated in two lifts, which were three-storey and were bolted at the base of the fourth storey infill panel. By using this least obtrusive system the usable floor space of the facility was maximized (Figure 2-32).

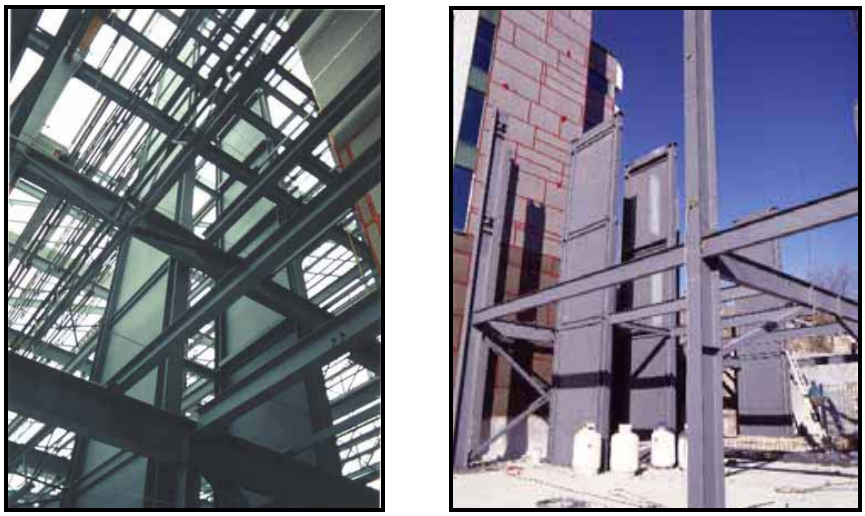

Figure 2-32 – 6 storey building in Saint Georges

2.3.2.2. Five-Storey Building in Saint Hyacinthe, Quebec

The six-storey 'ING' building is located in Saint Hyacinthe, Quebec. This building has SPW in each direction to provide sufficient lateral capacity as well as torsional resistance. This building was designed with a two-sided plate wall cage that is located in the centre of the rectangular building, stretching up 25 m (Figure 2-33). The designers reported that the plate wall was desired since it used not only much less steel but also much less construction time than other conventional construction types. Also these characteristics made this type of structure very cost effective.

Figure 2-33 – 6 storey "ING" building

2.3.3. JAPONIA

2.3.3.1. 35-Storey Office Building in Kobe, Japan

The 35-storey high-rise in Kobe, Japan is one of the most significant buildings with an SPW system and is located in an area burdened with high seismic activity. The construction of this structure was completed in 1988 and withstood the 1995 Kobe earthquake with no important damages. By contrast, the adjacent lower building suffered a complete intermediate soft storey mechanism and stories above were complete removed. Figure 2-34a shows the lower building after rehabilitation.

The structural system of the 35 storey building is a dual system consisting of steel moment frames and shear walls. The shear walls in the three basement levels are reinforced concrete shear walls. In the first and second floors of the building, the walls are composite walls of SPW and R.C. shear walls. Above the second floor, the walls are stiffened SPWs. Figure 2-34 shows the building and a typical plan and frames.

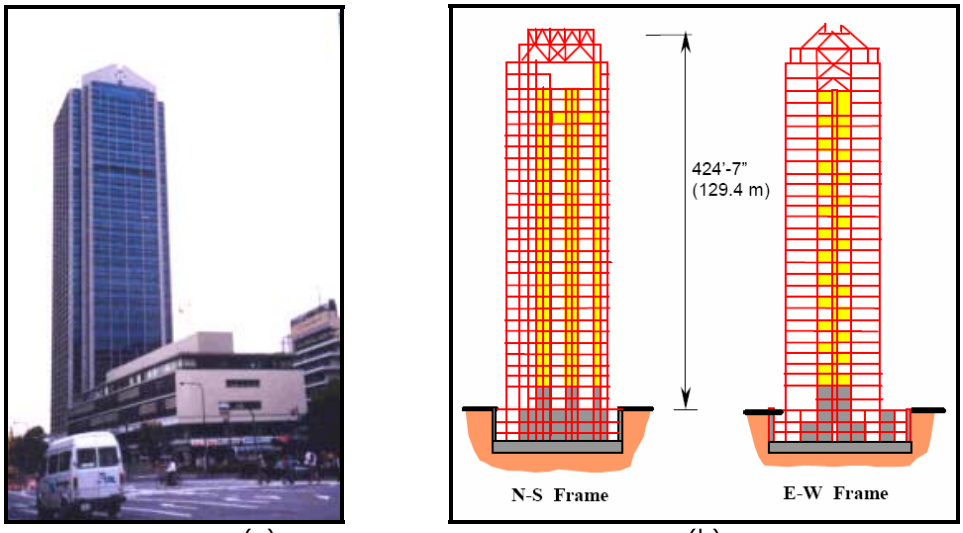

(a) (b)

Figure 2-34 - 35-storey high-rise in Kobe a); transversal and longitudinal view b)

This building survived the 1995 Kobe earthquake with only minor damage reported after the quake. Based on studies of this structure conducted by Fujitani et al., (1996) and AIJ, (1995), [35] indications were that the damage induced was minor and consisted of local buckling in the sub-panels of the stiffened SPW at the 26th storey (Figure 2-35). As well, a permanent roof drift of 225 mm was evident in the northern plane, and a 35 mm drift in the western plane, which is in the same direction of the SPW wall.

The results of the post-earthquake inelastic analyses of this structure, also reported in the mentioned-above references, indicate that soft storeys may have formed at the floors between the 24th and 28th level of the building. From post-earthquake inelastic analyses, the maximum storey drift was determined about 1.7 % at the 29th floor of the N-S frame.

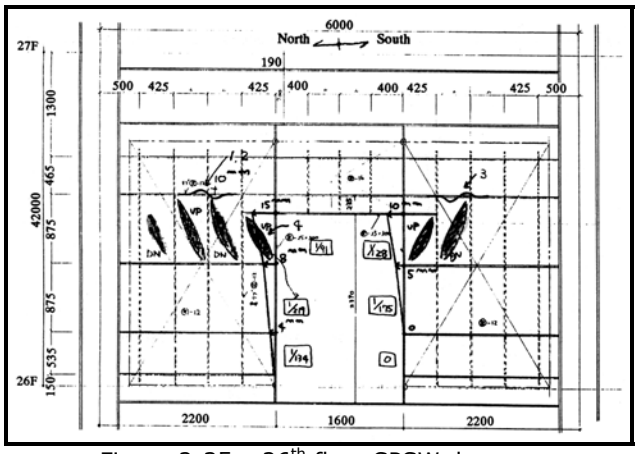

Figure 2-35 – 26th floor SPSW damage

2.3.3.2. 20-Storey Office Building in Tokyo, Japan

According to Thorburn et al. (1983), it is believed that the building referred to as the Nippon Steel Building (Figure 2-36), was the first major building construction using an SPW system. This building is located in Tokyo and was completed in 1970. The building's lateral-load resisting system is in a longitudinal direction and consists of a combination of moment frame and SPW units in an H-shape configuration (Figure 2-37). The building's lateral-load resisting system in the transverse direction is comprised of only an SPW system (Figure 2-38). The steel plate panels consist of 2.74 m by 3.71 m steel plates with horizontal and vertical steel channels as stiffeners. The thickness of the steel plates ranged from 7.8 mm to 12.7 mm. During structural design, it was decided that the gravity loads were not to be carried by the SPW system, and thus were designed to resist only lateral loads without formation of any buckling in the steel plates.

Figure 2-36 – Nippon Steel Building in Toyo

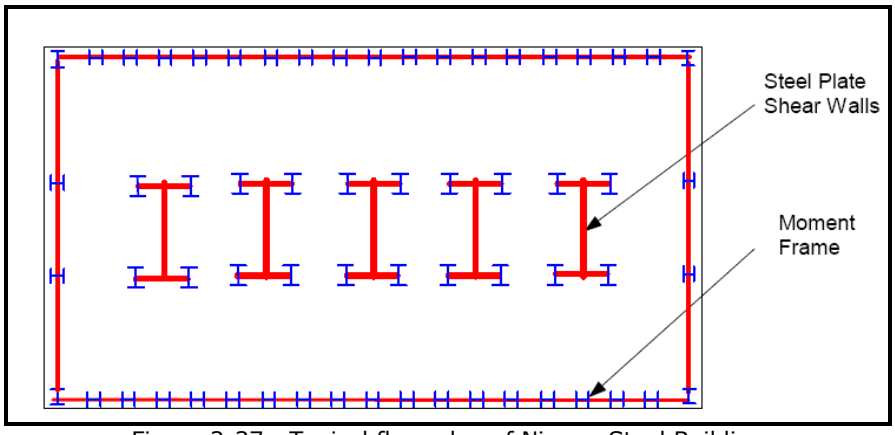

Figure 2-37 - Typical floor plan of Nippon Steel Building

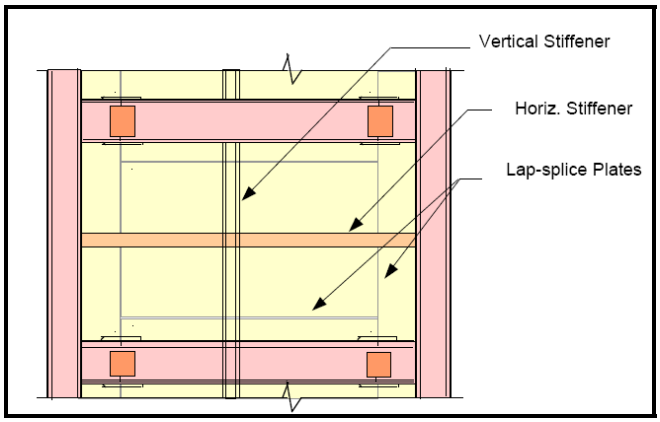

Figure 2-38 – Details of steel shear walls used in Nippon Steel Building

2.3.3.3. 53-Storey High-Rise in Tokyo

This 53-storey high-rise in Tokyo called the Shinjuku Nomura Building (Figure 2-39), was initially designed with reinforced concrete shear walls as the lateral-load resisting system. According to Engineering News Record (ENR 1978a), patent problems required conversion of the R.C. walls to SPWs later in the design phase. According to the same ENR article, "the contractor rejected a steel braced building core as too expensive" compared to an SPW. Figure 2-40 shows a typical plan view and elevation of the building. The structure consisted of moment perimeter frames and 'T'-shape stiffened SPW. The steel plate panels were approximately 3 m in height and 5 m in length. The panels had horizontal stiffeners at one side and vertical stiffeners at the other side. The panels were connected to H-steel columns and boundary boxes by bolted connections. The same ENR article stated that the construction contractor encountered problems with the steel panel connections and commented that their next high-rise building with an SPW system would not likely be designed with bolted connections.

Figure 2-39 - Shinjuku Nomura Building

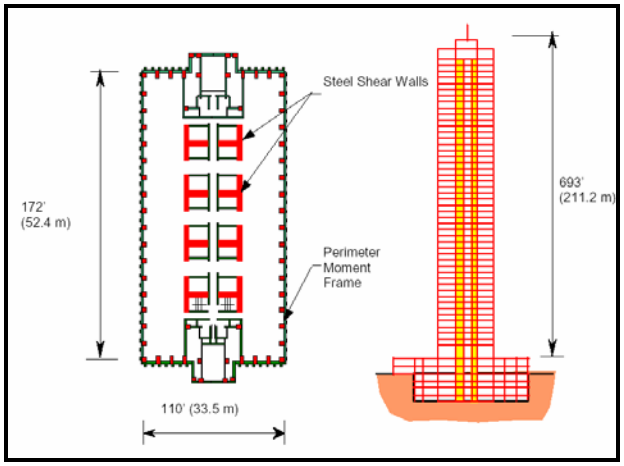

Figure 2-40 - Typical plan view and elevation

2.3.3.4. 26 and 31 storey buildings in Japan (LYS)

Figure 2-41 shows 26 and 31 storey buildings as examples of recent applications of LYP steel plate panels used as SPWs in Japan. According to Yamaguchi et al. (1998) [36], the LYP steel used in this structure had a 2 % offset proof stress (yield point) of approximate range of 80 to 120 MPa, a tensile strength of 200 to 300 Mpa, and the percent of elongation at fracture exceeding 50 %. The steel plate panels were designed to be approximately 6 mm to 25 mm thick with dimensions of 3 m height and 4.5 m width and stiffened by horizontal and vertical stiffeners. The prefabricated LYP wall units were connected to the boundary beams and columns using friction bolts. The walls were designed to remain elastic under wind load but to

yield under a "Level 1" earthquake.
The designers reported that the drift values decreased about 30 % as a result of using LYP steel. Based on the research of Yamaguchi et al. (1998) [36], the reason for using LYP steel in the SPW as an alternate solution was to decrease the overall bending effects and generate more shear behavior in the system. As well, it appears that such an alternative approach prevents gravity load from accumulating in the steel plate panels. Consequently, these walls were claimed to behave in relation to their shear characteristics and to reflect relatively small bending effects; therefore, the moment frames were designed to carry the overturning moments created by lateral loads.

(a) (b)
Figure 2-41 – 26 storey left building a); 31 storey right building b)

2.3.4. CHINA

2.3.4.1. 75-story office building in Tianjin, China

The Jinta Tower (Tower) is a 330 meter tall 75-story office building in Tianjin, China, with steel plate shear walls (SPSW) used as the primary lateral load resisting system (Wang 2008 [37] and Mathias 2008 [38]). It has an elliptical footprint approximately 42m by 81m at the base which changes with height to create an "entasis" effect, as shown in Figure 2-42. Given the tower's slender form, the SPSW structural system was selected because:
(1) a SPSW system's elastic stiffness is much higher than a brace structure's for the same steel tonnage, equivalent to that of a concrete shear wall;
(2) research and testing data for SPSW's demonstrate very significant ductility under moderate and rare earthquakes resulting from tension field action.
The lateral force resisting system for the tower can be classified as a frame-shear wall system, with perimeter and core ductile moment-resisting frames, and core SPSWs linked together with outrigger and belt trusses (Figure 2-43a). The ductile moment-resisting frames consist of concrete filled steel pipe composite
(CFT) columns and structural steel wide flange beams. The SPSWs consist of the

CFT columns—Vertical Boundary Elements (VBE)—and structural steel wide flange beams—Horizontal Boundary Elements (HBE)—in-filled with stiffened structural steel plates. Outrigger trusses, which are placed in the short direction of the tower plan, are used to engage the perimeter columns in resisting overturning (Figure 2-43b). Four sets of outrigger and belt trusses are provided and located at the mechanical levels of the tower. Strengthened diaphragm slabs are used at the outrigger levels. Buckling restrained SPSWs are used in the middle and lower portions of the building and are located in service core areas around the elevators, staircases and mechanical rooms. At the upper levels, where demands drop off sufficiently, concentric braces are used in lieu of SPSW panels in the core along with the CFT columns and wide flange girders.

Figure 2-42 - The architectural impression of Jinta

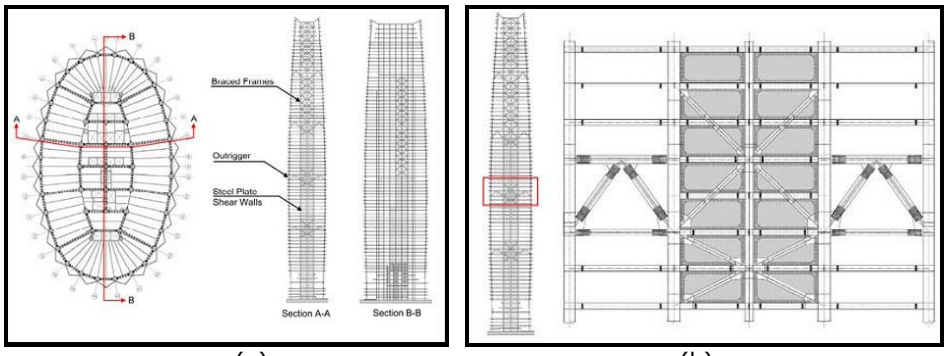

(a) (b)

Figure 2-43 - Typical plan and section a); Outrigger truss b)

Figure 2-44 shows a buckling restrained SPSW under construction. Gaps were introduced between the HBEs and the ends of the vertical stiffeners for the following reasons: (1) For ease of fabrication; (2) To minimize vertical gravity loads and thus prevent local buckling of the vertical stiffeners; (3) To enable the formation of

tension field effects when the structure experiences moderate and severe earthquakes.
The structural system is initially designed using elastic design (frequent seismic events) methods. The maximum story damage drift performance limit is set to 1/600 which is within the limit prescribed by the codes. The elastic analysis methods do not, however, reliably predict whether the stiffened SPSWs remain un-buckled as required by the Chinese code under this service level of drift. Sophisticated nonlinear dynamic earthquake analysis is necessary to demonstrate satisfaction of this performance goal.

Figure 2-44 - Buckling Restrained SPSWs

2.3.5. MEXIC

2.3.5.1. 22-story condominium building in Mexico

In Mexico, a 22-story condominium building located on a hillside was firstly planned to be built as a reinforced concrete building with 3 m. story heights and a total height of 68.5 m (Figure 2-45). Nonetheless, a steel framing was also designed for cost comparison due to owners' request.

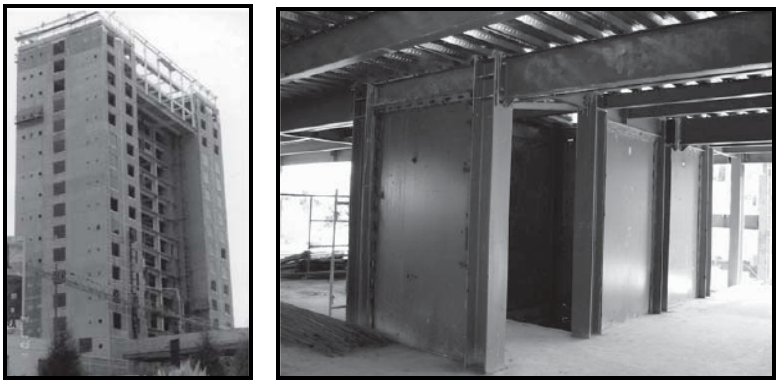

Figure 2-45 - 22 Story Building in Mexico

The preliminary calculations revealed that the steel frames combined with the concrete shear walls around the elevator cores were more economical. Consequently, this structural system was selected for construction.

2.4. Research needs

SPSW systems have numerous advantages such as high initial stiffness, substantial ductility, fast construction and reduction of seismic mass. Additional post-buckling resistance due to the diagonal tension field action improves the post-elastic behavior and increase the robustness in case of strong ground motions. Only a few design guidelines exist, e.g. NBCC 2005 (National Building Code of Canada) (2005) [31], FEMA 450 (Recommended provisions for seismic regulations for new buildings and other structures) (2004) [38], ANSI/AISC (2005) [5], AISC Design Guide 20, Steel Plate Shear Walls (2007). The lack of design guidelines is likely one of the barriers for application of this system in Europe, as the EN 1998 [40] code gives no indications regarding the conception and design of SPSW systems.
Significant research is needed for the developing of seismic design guidelines for SPSW:
- to develop SPSW systems that reduce column demands: the use of low yield point steel, composite columns, SPSW with adjacent outrigger beams can merit to be further investigated;
- approaches for improving the overturning stiffness of SPSWs: splitting a SPSW into two coupled SPSWs may improve the overturning stiffness. This idea has been considered by the author when designing the specimens for the experimental program and further for numerical study;
- a simple modeling technique is necessary to enable more efficient design of SPSWs. The element formulations should be aimed at satisfying the primary objectives of 1) accurate simulation of the global response of SPSW infill panels under the range of cyclic load histories that develop in typical SPSWs, 2) efficient model-building, including objective procedures for calibration that are based on panel geometric, material and design properties, 3) a simple model formulation, and 4) portability to commercial software for nonlinear analysis of structural systems [27];
- providing reliable values of behavior factor q: along the succesive editions of North American codes, different values of q factors were proposed. As an example, the response factor R (similar to European q factor) varied from 4 in 1996 edition to 8 in 2006 edition of NBCC. The author aimed at evaluating the q factor via experimental test and then extending the study to real multi-storey structures.
- overstrength factor to be used in capacity design approach: according to EN1998-1, in order to obtain a favorable plastic mechanism, the non-dissipative members should be designed with sufficient overstrength to avoid plastic deformations. The amount of overstrength depends, apart from the material overstrength factor γ_{ov} and reserve of strength in the seismic design situation Ω, on the the type of dissipative structural system. For example, it amounts $1.1\gamma_{ov}\Omega$ for MRF and CBF systems and $1.5\gamma_{ov}\Omega$ for EBF systems, respectively.
- acceptance criteria for Performance Based Seismic Evaluation: at present, there are no specifications regarding the selection of acceptance criteria for SPSW.
- The interaction between stiff SPSW system and more flexible un-braced frame system. For dual systems of SPSW and MRF, the MR frames can be sized to remain elastic until a certain drift to provide sufficient recentring capacity that allow for

repairing or easy replacement of damaged steel plates.
This is not an exhaustive list of research needs. The author tried to identify those ones that can allow the designers to deal with SPSW in real applications. In the following sections of the thesis, some of the research needs identified and presented above are investigated and finally a design methodology is proposed.

3. Experimental Program

3.1. Introduction

All the experimental programs developed worldwide in the past years (see Chapter 2), focused mainly on the behavior of steel plate shear walls, considering or not the influence of openings, perforations, type of connections, etc. Some tests also considered systems with several storeys or systems with composite shear walls. There are no important results regarding the influence of the boundary members and their connections on the behavior of SPSW systems coupled with moment resisting frames. The aim of this chapter is to evaluate the influence of boundary members and their connections on the performances of dual SPSW systems.
The main objective of the experimental program is the evaluation of the seismic parameters related to the local and global behavior, i.e. reduction factor q, modeling parameters and acceptance criteria in terms of resistance, stiffness and ductility. In order to asses the influence of the beam to column connections, two types of connections with different levels of strength and stiffness are considered. Results of the experimental tests are further used to calibrate a numerical model for nonlinear analysis.
Steel plate shear walls SPSW have been used as lateral force resisting systems since 80's, but till very recently the design specifications were rather absent or incomplete. During this period, numerous research programs and also seismic experiences have confirmed their effectiveness. Most research programs have focused on single span SPSW with one or several storeys (Chapter 2). A major role on their development can be attributed to the introduction of design rules in the code provisions, e.g. North American codes AISC (2005) [5] and NBCC (2005) [31].
The application of SPSW system in Europe is limited, partly due to the lack of design provisions in seismic code EN 1998-1 [40]. Particularly, there are no recommendations for behavior and system overstrength factors q and Ω, respectively. An additional problem refers to the prediction of the strength and stiffness capacity of the SPSW structures. Design practice requires simple models and conventional analysis software that are available and relatively simple to use.
In order to address the issues presented above with regards to the performances of SPSW systems, an experimental program was developed at the Politehnica University of Timisoara, Laboratory of Steel Structures. Monotonic and cyclic tests on different SPSW specimens were performed. Due to the limitations in testing capacity, models were half scaled.

3.2. Code provisions and Recommendations for cyclic testing of steel structures and hysteretic devices

Structural elements have different strength and deformation capacities therefore safety against collapse as well as damage control depends on designer's ability to assess these capacities with some confidence. Implicitly, we lump our knowledge of these capacities into parameters used in design, for example response modification coefficients (*q* factor or *R*-factor) for new structures (EC8 [40], ASCE 7-05 [41]), or *m*-factors (or estimates of plastic deformation capacities) for seismic retrofits (FEMA

273/356 [42]/[43] and ASCE 41-06 [44]). For some cases, our knowledge is adequate to assign reasonable values, but for many cases it is not. So, we have to resort to testing (in addition to analytical modeling) to evaluate performance of many conventional components, and particularly of new and innovative components (or systems) that show much promise for enhanced performance. Unfortunately, in case of earthquake engineering strength and deformation capacities depend (sometimes weakly and sometimes strongly) on cumulative damage, which implies that every component has a permanent memory of past damaging events and at any instance in time it will remember all the past excursions (or cycles) that have contributed to the deterioration in its state of health. Thus, performance depends on the history of previously applied damaging cycles, and the only reasonable way to assess the consequences of history (short of developing complex analytical models that can be used for damage state predictions) is to replicate, to the best we can, the load and deformation history a component will undergo in an earthquake (or several earthquakes if this is appropriate). The objective of a loading protocol is to achieve this in a conservative, yet not too conservative, manner. In the following are described some loading protocols applied for cyclic testing and hysteretic devices imposed by different codes around the world.

ECCS, 1985

According to this type of procedure, a monotonic test is done first in order to obtain the force vs. displacement relationship. Using this, a 10% slope at the maximum force is intersected with the tangent to the initial stiffness, thus obtaining the yielding displacement e_y and the corresponding yielding force F_y (Figure 3-1). The yielding displacement is then used to establish the cyclic loading. This consists of generating 4 cycles successively for the ranges of slip displacement $\pm 0.25e_y$, $\pm 0.5e_y$, $\pm 0.75e_y$, $\pm 1.0e_y$ followed up to failure by series of 3 cycles each with a range $\pm 2n\ e_y$ where n is =1,2,3……. As this procedure was initially developed for testing of beam-to-column joints, some modifications were necessary to take into account the particularities of SPSW systems.

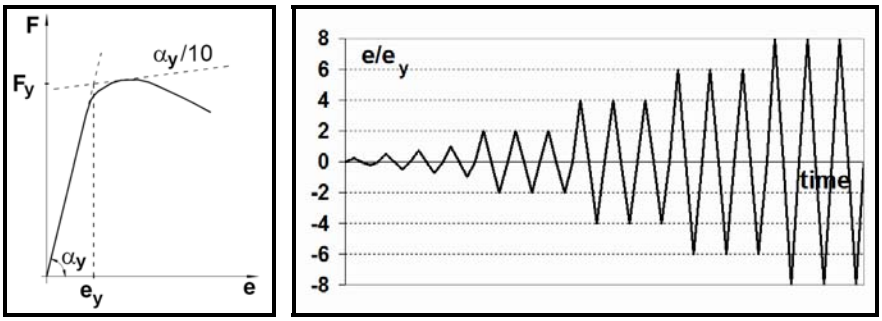

Figure 3-1 - Determination of yielding displacement a); and loading protocol b) (according to ECCS [45])

Steel - ATC 24 Protocols

This protocol, which was specifically developed for components of steel structures, was one of the first formal protocols developed in the U.S. for seismic performance evaluation of components using a cyclic loading history. It uses the yielding

deformation, Δ_{yield}, as the reference for increasing the amplitude of cycles. The history contains at least 6 elastic cycles (amplitude < Δ_{yield}), followed by three cycles each of amplitude Δ_{yield}, $2\Delta_{yield}$ and $3\Delta_{yield}$, followed by pairs of cycles whose amplitude increases in increments of Δ_{yield} until severe cyclic deterioration occurs (Figure 3-2). The relative and absolute amplitudes of the cycles were derived from statistical studies of time history responses of SDOF systems, and therefore represent global (roof or storey) drift history and not local deformation history such as those experienced, for instance, by links in eccentrically braced frames. The ATC-24 [12] document contains also a multi-specimen cumulative damage testing protocol that is based on constant amplitude testing and a cumulative damage hypothesis. Compared to ECCS protocol [45], ATC 24 [12] testing protocol is less severe for the fatigue resistance.

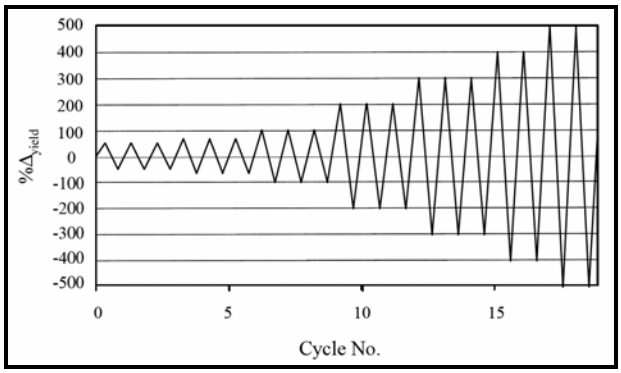

Figure 3-2 - Steel - ATC 24 loading protocol (ATC-24,1992 [12])

FEMA 461

This is a more recent testing protocol and was developed by a consortium led by ATC [12]. It was developed originally for testing of drift sensitive non-structural components, but it is applicable in general also to drift sensitive structural components.

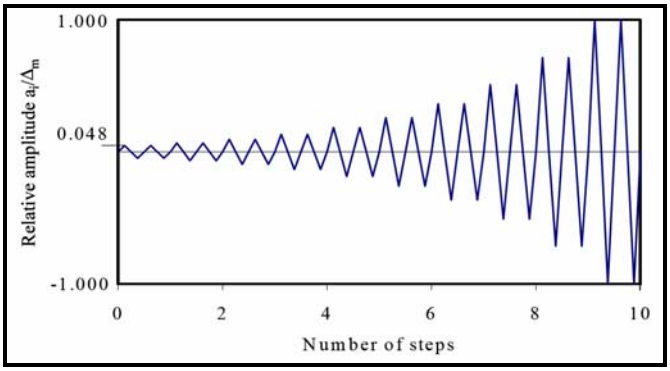

Figure 3-3 – FEMA 461 loading history (FEMA 2007 [46])

It uses a targeted maximum deformation amplitude, Δ_m, and a targeted smallest deformation amplitude, Δ_0, as reference values, and a predetermined number of increments, *n*, to determine the loading history (a value of $n \geq 10$ is recommended). The amplitude a_i of the step-wise increasing deformation cycles is given by the equation $a_{i+1}/a_n = 1.4\ (a_i/a_n)$, where a_1 is equal to Δ_0 (or a value close to it) and a_n is equal to Δ_m (or a value close to it). Two cycles are to be executed for each amplitude. If the last damage state has not yet occurred at the target value Δ_m, the loading history shall be continued by using further increments of amplitude of $0.3\Delta_m$ (Figure 3-3).

AISC 2005

According to this protocol, the test shall be conducted by controlling the level of axial or rotational deformation, Δ_b, imposed on the test specimen (Figure 3-4). As an alternative, the maximum rotational deformation may be applied and maintained as the protocol is followed for axial deformation.
Loads shall be applied to the test specimen to produce the following deformations:
(1) 2 cycles of loading at the deformation corresponding to $\Delta_b = \Delta_{by}$
(2) 2 cycles of loading at the deformation corresponding to $\Delta_b = 0.50\Delta_{bm}$
(3) 2 cycles of loading at the deformation corresponding to $\Delta_b = 1\Delta_{bm}$
(4) 2 cycles of loading at the deformation corresponding to $\Delta_b = 1.5\Delta_{bm}$
(5) 2 cycles of loading at the deformation corresponding to $\Delta_b = 2.0\Delta b_m$
(6) Additional complete cycles of loading at the deformation corresponding to $\Delta_b = 1.5\Delta$bm as required for the brace test specimen to achieve a cumulative inelastic axial deformation of at least 200 times the yielding deformation (not required for the sub assemblage test specimen) where the deformation is the steel core axial deformation for the test specimen and the rotational deformation demand for the sub assemblage test specimen brace.

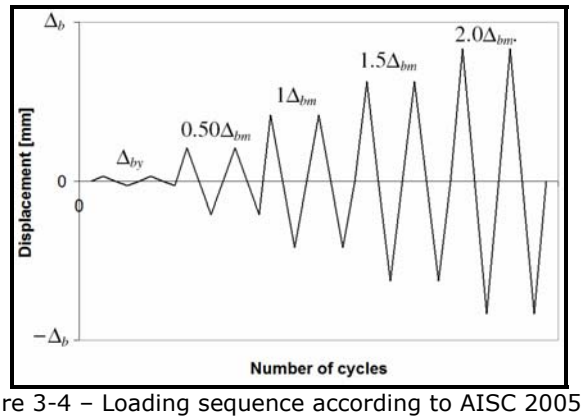

Figure 3-4 – Loading sequence according to AISC 2005 [5]

The design storey drift shall not be taken as less than 0.01 times the storey height for the purposes of calculating Δ_{bm}. Other loading sequences are permitted to be used to qualify the test specimen when they are demonstrated to be of equal or greater severity in terms of maximum and cumulative inelastic deformation. Additional increments of loading beyond those described above are also permitted.

3.3. Design of specimens

3.3.1. Design and Evaluation of Base Frame

The first step of an experimental program is the selection of a base frame to extract the experimental one. For this purpose, a dual base frame with the following characteristics was selected: two exterior moment resisting spans of 4.8 m, an interior 8.4 m span with 2 steel plates each with a span of 2.8 m and 2 additional columns. The storey height was taken 3.5 m (Figure 3-5).

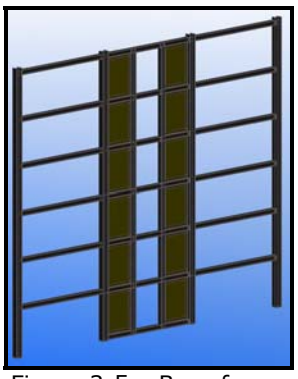

Figure 3-5 – Base frame

In order to pre-design the base frame, the steel plate shear walls were replaced by equivalent centrically X braces (Figure 3-6). This replacement is the simplest solution as the braces can predict quite well the behavior of the steel plates under applied loadings.

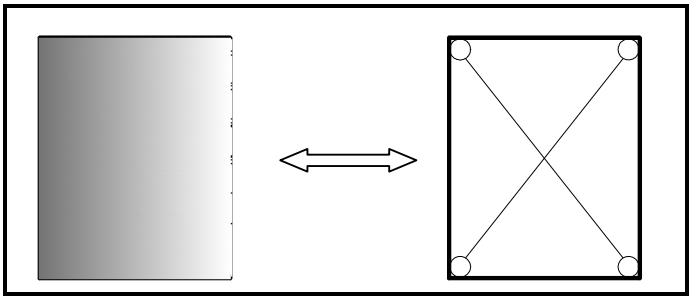

(a) (b)

Figure 3-6 – SPSW a); equivalent centrically X braces b)

The design of the base frame was carried out according to EN 1993 [47], EN 1998 [40] and P100/2006 [47]. The elements are made from hot rolled European steel sections with steel grades of S355 (f_y=355 kN/mm^2) for beams and columns and S235 (f_y=235 kN/mm^2) for the bracings. A 4 kN/m^2 dead load on the typical floor and 3.5 kN/m^2 for the roof were considered, while the live load amounts 2.0 kN/m^2. The building is located in a high seismic area (i.e. the Romanian capital, Bucharest), which is characterized by a design peak ground acceleration 0.24g for a returning

period of 100 years, and soft soil conditions, with T_C=1.6 sec. It is noteworthy the long corner period of the soil, which in this case may affect flexible structures. For serviceability check, the returning period is 30 years, while for collapse prevention it is 475 years.
The following figure (Figure 3-7) presents the normalized elastic spectrum for accelerations of the horizontal component of the ground motion specific for the zones having a corner period of T_c=1.6s

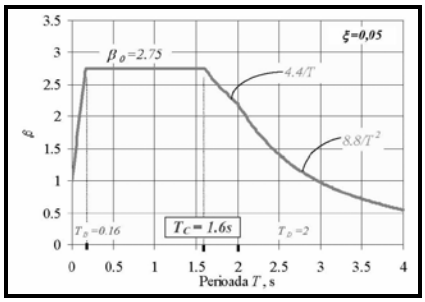

Figure 3-7 – Normalized elastic spectrum according to P100-2006

The load combinations were done according to EN 1991 [49] and P100 -2006 [47]. For the design of the non-dissipative members, the forces due to the design seismic action were amplified with the factor 1.1 γ_{ov} Ω = 2 (see annex F, P100/1-2006 [47]). After pre-design of the base frame, the experimental specimens were extracted from the interior stiffened frame of the 6 storey structure (highlighted with red in Figure 3-8) and selected at 1/2.

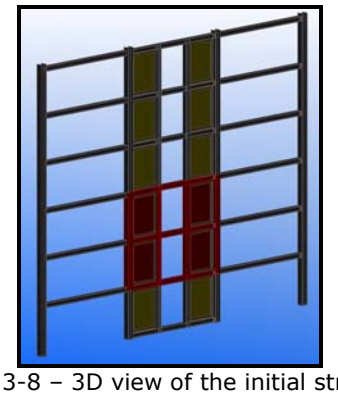

Figure 3-8 – 3D view of the initial structure

3.3.2. Design and preliminary numerical evaluation of specimens

3.3.2.1. Design of the experimental frames

A typical SPSW system consists of horizontal and vertical boundary elements (that may carry also gravity loads), and thin steel plates that buckle in shear and form a diagonal tension field to resist lateral loads. Due to testing capacity limitations, the

extracted frames where half scaled geometrically. The design was done according to EN 1993 [47] and for the design of the steel plates the American codes AISC (1999 [49], 2005 [5]) and FEMA 450 [38] were taken as guidance, as the European code does not provide any recommendation for this type of structures.
The frames measured 3500 mm high (2 storeys) and 4200 mm wide between main column centerlines. The beams and columns were design using European hot rolled H sections: HEB240 for the main columns, HEB180 for the internal columns and HEA180 for the beams (Figure 3-9).

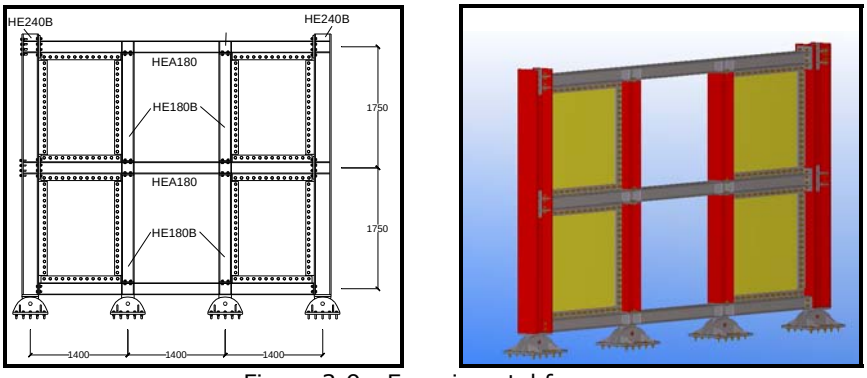

Figure 3-9 - Experimental frames

All elements are made from conventional mild carbon steel. The nominal materials used in design are S355 (f_y=355 kN/mm^2, f_u=510 kN/mm^2) for beams, columns and fishplates and S235 (f_y=235 kN/mm^2, f_u=360 kN/mm^2) for the infill plates.

Steel plates

Two thicknesses for the steel plates have been taken into consideration 2 mm, respectively 3 mm. The steel plates measure 1160x1559 mm for the specimen with flush-end plate beam to column connection and 1148x1559 mm for the specimen with extended end plate connection. The difference in the steel plate length is due to the presence of the extended end plate in the rigid connection. According to the Figure 3-10 (AISC 1999 [49]), depending on the slenderness of the shear wall L_{cf}/t_w, steel plates can range from compact to slender.

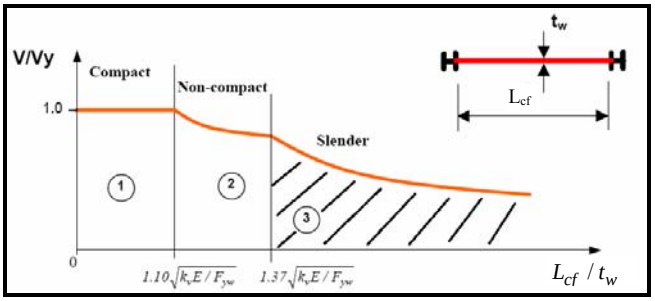

Figure 3-10 - The region of behavior of the steel shear walls

For the tested specimens, the plate's slenderness L_{cf}/t_w is 580 for the 2 mm plate and 387 for the 3 mm plate, categorizing them as slender. The plates that fall into this category are expected to buckle while some shear yielding has already taken place. In this case, the storey shear is resisted by the horizontal components of the tension and compression diagonal forces.
The nominal strength of the steel plate was evaluated to 300 kN by means of the equation (3.1) (AISC 2005 [5]), considering the design shear strength equal to ϕV_n, where $\phi=0.90$. The initial multiplier of 0.5 in the V_n formula was divided by an overstrength factor of 1.2 (Berman and Bruneau, 2003 [21]).

$$V_n = 0.42 F_y t_w L_{cf} \sin 2\alpha \tag{3.1}$$

Based on an elastic strain energy formulation, Timler and Kulak (1983) [8] derived an equation for the inclination angle of the tension field (3.2), α, in a SPSW infill plate. According to this equation the inclination of the tension field amounts 40°.

$$\tan^4 \alpha = \frac{1 + \frac{t_w L}{2A_c}}{1 + t_w h\left(\frac{1}{A_b} + \frac{h^3}{360 I_c L}\right)} \tag{3.2}$$

where:
h is the distance between horizontal boundary elements centerlines
A_b is the beam cross-section area
A_c is the column cross-section area
I_c is the column moment of inertia taken perpendicular of the steel plate line
L is the distance between vertical boundary elements centerlines

The flexural stiffness of the horizontal boundary elements was excluded in the derivation because the opposing tension fields that develop above and below these intermediate horizontal members almost cancel out and induce little significant flexure there.

Connection of steel plates to the boundary elements

The connection between the infill steel panels and the boundary elements were done with 8.8 grade bolts, preloaded at 50% of their capacity, and 6 mm fish-plates welded to the boundary elements on the entire length (Figure 3-11).

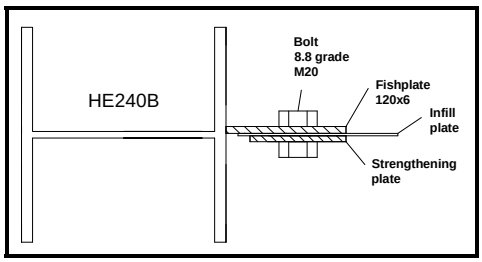

Figure 3-11 – Infill panel to boundary elements connection

In order to reduce the number of bolts and also to strengthen the panel, additional fishplates were welded to the sides of the infill panel. The 2 mm infill panel has a strengthening plate of 4 mm and the 3 mm infill plate has a strengthening plate of 3 mm. In this way, the required strength of the connection as recommended in AISC 2005 [5] is fulfilled.

Beams and columns

According to the capacity design principles, all edge boundary elements (HBE as beams and VBE as columns) were designed to resist the maximum forces developed by the tension field action of the webs fully yielded. Axial forces, shears, and moments develop in the boundary elements of the SPSW as a result of the response of the system to the overall overturning and shear, and this tension field action in the webs.
According to regulations from the two codes (AISC [5] and FEMA [43]), VBE and HBE are to remain essentially elastic under forces generated by fully yielded plates, but flexural hinges are allowed at the ends of HBE elements.
In order to prevent excessive deformations leading to premature buckling under the pulling action of the plates, the minimum moment of inertia of the columns was verified using Equation (3.3) (Montgomery and Madhekar, 2001 [51]). It has to be noted the fact that the average moment of inertia of the two columns bounding the steel plates was used in the calculation.

$$I_c \geq \frac{0.00307 t_w h^4}{L} \tag{3.3}$$

Beam to column connection

In order to evaluate the contribution of the boundary frames to the strength and stiffness of the structure, two types of beam-to-column connections were used. The first connection (joint 1) is a flush end plate bolted connection and the second one (joint 2) is an extended end plate bolted connection (Figure 3-12). According to EN1993-1-8 [47] classification, flush end plate connection can be classified as semi-rigid and *weak* partial strength ($M_{j,Rd}=0.53M_{b,Rd}$) (further denoted as *semi-rigid*) and extended end plate connection can be classified as rigid and *strong* partial strength, with a capacity almost equal to that of the connected beam ($M_{j,Rd}= 0.96M_{b,Rd}$), (further denoted as *rigid*) Figure 3-13.

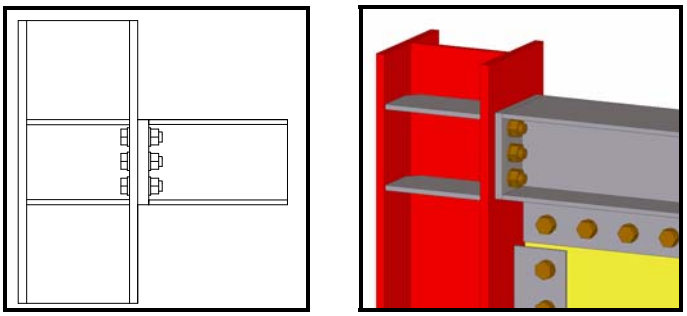

(a)

Figure 3-12 - Beam-column connection: a) Semi-rigid; b) Rigid

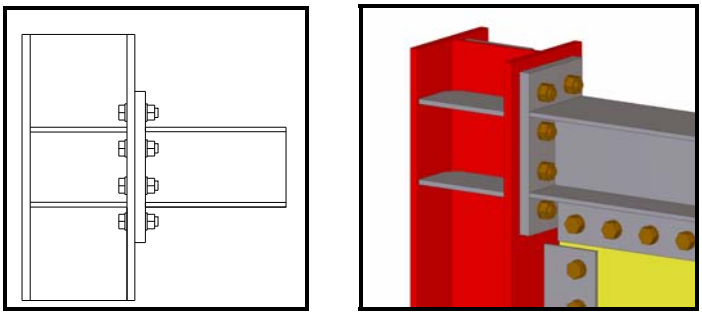

(b)

Figure 3-12 - (Continued)

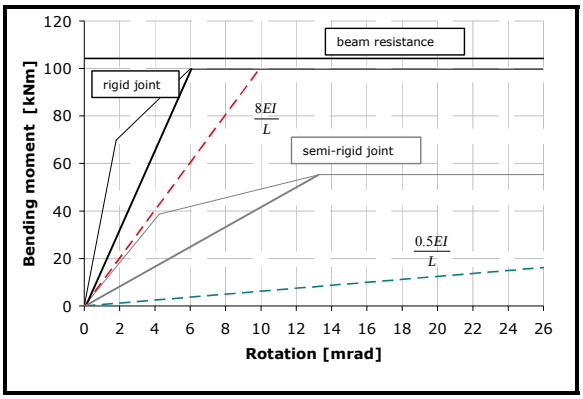

Figure 3-13 – Classification of joints by stiffness (EN1993-1-8 [47])

Table 3-1 and Table 3-2 show the characteristics of the joints and their classification for strength and stiffness according to EN1993-1-8 [47].

Table 3-1 – Joint classification for stiffness

Joint	K_w (S_j) [kNm/rad]	EN1998-1-8 boundaries [kNm/rad]		% of full rigid	Classification
		lower	upper		
Joint 1	4152	628	10042	41	Semi-rigid
Joint 2	16665	628	10042	100	Rigid

Table 3-2 – Joint classification for strength

Joint	$M_{j,Rd}$ [kNm]	Beam resistance [KNm]	% of beam resistance
Joint 1	55.1	104.2	53
Joint 2	99.8	104.2	96

The interior columns are connected to the beams using flush end plate bolted connections (Figure 3-14). This connection has a very low stiffness (pinned according to EN1993-1-8 [47] classification) and a capacity $M_{j,Rd}=0.2M_{b,Rd}$.

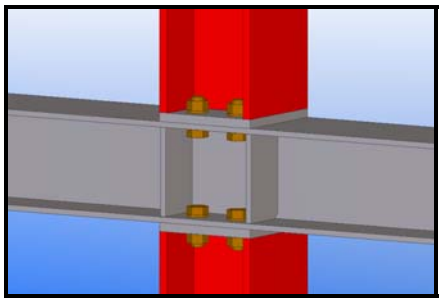

Figure 3-14 – Interior column to beam connection

The following table (Table 3-3) show all the specimens which were tested. Details regarding type of beam to column connection, type of loading and thickness of the infill plates are given. The first specimen which is tested monotonically has a rigid beam to column connection and a 2 mm infill plate (R-M-T2). The second specimen has the same configuration but is loaded cyclically (R-C-T2). The next two specimens are loaded cyclically and have semi-rigid beam to column connection but one has a plate thickness of 2 mm and the other 3mm.

Table 3-3 -Design of specimens

Specimen	Thickness SPSW [mm]	Beam-Column joint	Loading
R-M-T2	2	Rigid	Monotonic
R-C-T2	2	Rigid	Cyclic
SR-C-T2	2	Semi-rigid	Cyclic
SR-C-T3	3	Semi-rigid	Cyclic

3.3.2.2. Preliminary numerical analysis

In order to anticipate the overall behavior of the SPSW specimens prior testing but also to adjust the behavior of the experimental frames within the capabilities of the existing equipment, preliminary numerical analysis were carried out using the commercial software SAP2000 [52] for the specimen with rigid beam to column connection and 2 mm infill plate thickness.
Using the inclination angle of the tension filed given by Equation (3.2), an analytical model known as the strip model, in which the infill plates are represented by a series of pin ended tension only strips was used. The model was developed by Thorburn et al. (1983) [6] and subsequently refined by Timler and Kulak (1983) [8]. A typical strip model representation of a SPSW is shown in Figure 3-15.
The area of the strut is given as follows (3.4):

$$A_s = \frac{t_w}{2} \cdot \left(L\cos\alpha + H\sin\alpha \right) / n \tag{3.4}$$

where:

A_s is the area of a strip
L is the width of the panel
H is the height of the panel
n is the number of strips, which is taken as 10

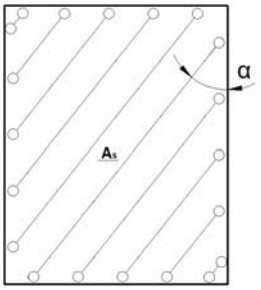

Figure 3-15 - Strip model

To simulate the yielding of the infill plate, an axial bilinear hinge is placed at the midpoint of each strip (Table 3-4 and Figure 3-16).

Table 3-4 – Bilinear axial hinge values (Driver et al, 1998 [10])

Hinge	A		B		C		D		E	
	P/P_y	Δ/Δ_Y	P/P_y	Δ/Δ_Y	P/P_y	Δ/Δ_Y	P/P_y	Δ/Δ_Y	P/P_y	Δ/Δ_Y
Tension	0	0	1.0	0	1.0	16.4	1.0	50	1.0	100

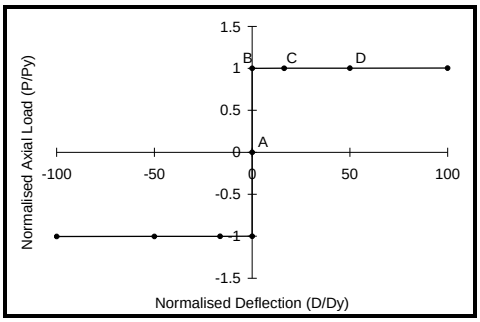

Figure 3-16 – Tension hinge definition

The frame elements (beams and columns) were modeled using the conventional plastic hinges placed at both ends of the elements, defined in the SAP2000 software [52] (according to FEMA 356 [43]) (Figure 3-17).

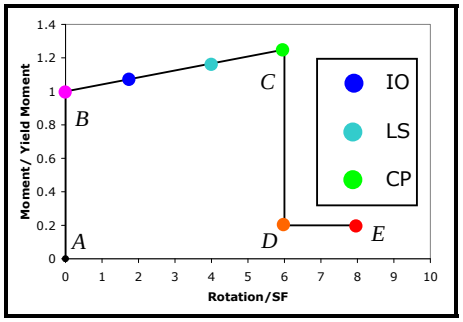

Figure 3-17 – Beam hinge definition

Figure 3-18 shows the results in terms of base shear force vs. top displacement. The yielding point occurs at a force of 410 kN corresponding to a displacement of 15.4 mm while the peak capacity is 636 kN for a displacement of 100 mm.

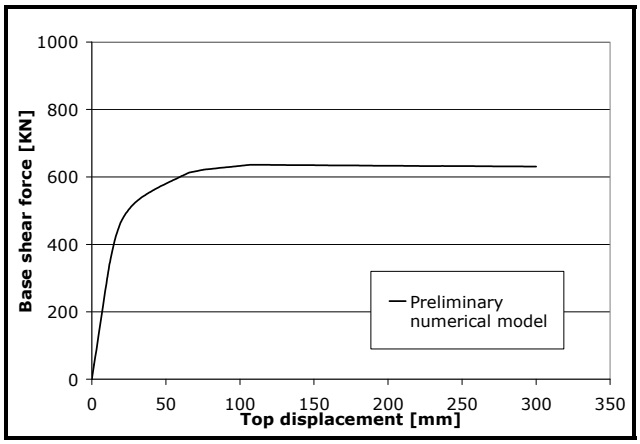

Figure 3-18 - Base shear vs. top displacement relationship

3.4. Test set-up and instrumentation

3.4.1. Test set-up

The tests were done within the Laboratory of Steel Structures from the "Politehnica" University of Timisoara. The load application system was the same for all specimens. A MTS digital servo-controller was used to operate two hydraulic actuators having the capacity of 1000 kN and 500 kN, respectively. The strokes of the actuators are ± 160 mm.

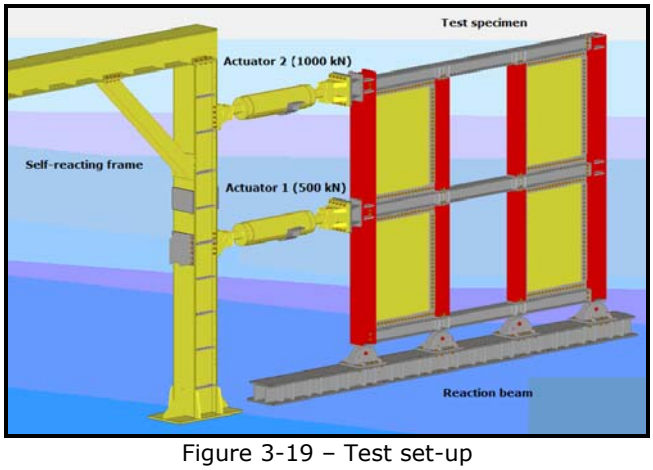

Figure 3-19 – Test set-up

The two actuators are placed at the level of the two storeys of the specimens and are fixed using connecting elements (Figure 3-19). They could rotate freely in vertical direction at the base of the actuators as well as at the loading joint at the specimen.
For testing purposes, the bases of the columns are connected to the reaction beam using pin connections (Figure 3-20). The supports were design to be reused after each test. The two lower 25 mm pins are connected to the upper 50 mm pin through a 50 mm diameter bolt. The upper pin is welded to the column base plate of the main column and to the bottom flange of the beam under the intermediary column. The system is bolted to the reacting beam using ten 20 mm bolts.

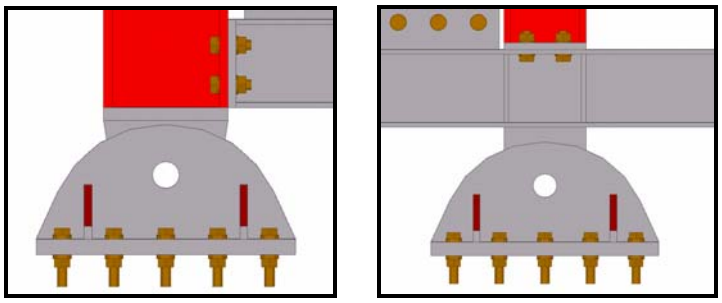

(a) (b)

Figure 3-20 – Base connection: a) Main column connection; b) Secondary column connection

As the steel plate shear wall is designed to resist a uni-directional motion, it was necessary to restrain it from out-of-plane movement. The important issues that were considered in implementing the lateral support system were the elimination of twist in the columns and bracing of the columns and beams in the out-of-plane direction at each storey. To fulfill the aforementioned tasks, the lateral bracing system consisted of two parallel frames mounted on each side of the specimens connected together, and laterally braced to a support (
Figure 3-21). The two beams of the lateral bracing system, at the 1st and 2nd level, act as guiding rails for the guiding elements connected to the testing specimens.

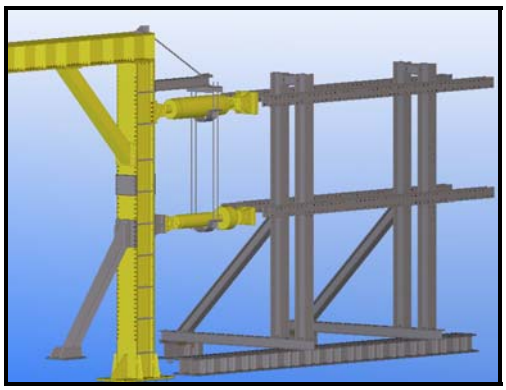

Figure 3-21 – Lateral support system

3.4.2. Instrumentation and monitoring scheme

Extensive instrumentation layout was used in order to asses the parameters used for controlling the test or for interpreting the results (Figure 3-22, a). The specimens were instrumented in the same manner in order to develop equal criteria for comparison of results. The actuator loads were recorded and monitored during the test. The top displacement was also monitored, together with the intermediary level displacement and base slippage, using LWG (http://www.dseurope.it) type displacement sensors. TRS type sensors (http://www.novotechnik.com) were used to measure specimen uplift at the two main columns, beam to column slippage and infill panel diagonals.

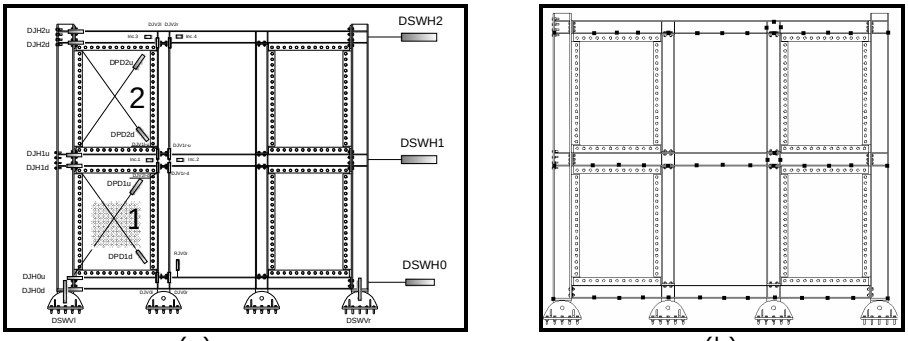

(a) (b)

Figure 3-22 – Instrumentation of the experimental frames: a) By cable potentiometers and VIC3D (described below); b) By laser based apparatus (LEICA TPS1200)

As the behavior of the 1st infill panel was expected to be the most critical, the initial imperfections and out of plane deformations were measured within a central 450x550 mm area using an optical measuring device called VIC 3D (Figure 3-23). A double measurement was done with a high performance apparatus based on laser measurement called Leica TPS1200 (http://www.leica-geosystem.com). Certain points were placed on the specimens in order to record the movement of the testing frames and out of plane displacements (Figure 3-22, b).

VIC3D and LEICA TPS1200

a) Based on digital image correlation techniques and stereoscopic principles of the setup of two cameras, a contact less measure is done on the highlighted area in Figure 3-23, in order to obtain the object contour and out of plane displacement of the infill panel.

The system has the following specifications (http://www.limess.com):

- Optical contact less measurement of 3D shape, displacement, deformation and strains;
- Point to point accuracy of displacement: 0.01 pixel;

- Point to point strain accuracy: 0.02%;
- Partial resolution 1392*1024 pixel / 10 Hz.

Figure 3-23 –VIC 3D system

b) The Leica TPS1200 possesses high accuracy angle measurements and precise long-range distance measurements backed by automatic fine pointing and fast, reliable reflector location (Figure 3-24). The readings are automatically corrected for any "out of level" by a centrally located twin-axis compensator (http://www.leica-geosystem.com).

Characteristics of the apparatus:

- Round prism (GPR1): 3000m
- 360° reflector (GRZ4): 1500m
- Mini prism (GMP101): 1200m
- Reflective tape (60 mm x 60mm) 250m
- Shortest measurable distance: 1.5m
- Standard mode: 1 mm + 1.5 ppm / typ. 2.4 s
- (Fast mode: 3 mm + 1.5 ppm / typ. 0.8 s
- Tracking mode: 3 mm + 1.5 ppm / typ. <0.15 s
- Display resolution: 0.1mm
- Special phase shift analyzer (coaxial, visible red laser)

Figure 3-24 – Laser measurement apparatus

The following describes the names for the measuring devices used in instrumentation scheme:

- DSWH0 -base slippage
- DSWH1 -1st level displacement
- DSWH2 -2nd level displacement
- DSWVl -left base uplift
- DSWVr -right base uplift
- DJH0d, DJH0u -base beam-column connection rotation
- DJH1d, DJH1u -1st level beam-column connection rotation
- DJH2d, DJH2u -2nd level beam-column connection rotation
- DJV0l, DJV0r -base beam connection uplift
- DJV1ld, DJV1r-d, -1st level interior connection rotation
- DJV1lu,DJV1r-u
- DJV2l, DJV2r -2nd level interior connection rotation
- RJV0l, RJV0r -base level interior connection rotation
- Inc 1 & 2 -1nd level interior connection rotation
- Inc 3 & 4 -2nd level interior connection rotation
- DPD1d, DPD1u -1st panel diagonal measurement
- DPD2d, DPD2u -2nd panel diagonal measurement

3.4.3. Loading protocol

In case of quasi-static cyclic testing, the seismic effects are replicated by slow cyclic application of loads (or deformations) whose history (in terms of the applied load or in terms of the deformation caused by an applied load) follows a predetermined pattern. Examples of structural components that may be tested in accordance with this protocol include shear walls, beam-column assemblies and frame assemblies. This loading protocol should not be used for components sensitive to dynamic effects or whose behavior is sensitive to strain rate effects. The most used type of loading is the incremental loading, because it allows a good comparison with the real seismic action. This model also allows more cycles with reduced speed in order to determine each problem occurred during the tests and it does not need the ultimate capacity of each specimen at the beginning stage.
Because the loading protocol requires the value of yielding drift Δ_y, a monotonic test needs to be performed first. In order to reduce the time and costs of the experimental program, only one monotonic test was performed. With this yielding drift, it can be determined the loading protocol for the cyclic test (see paragraph 3.2).
The testing procedure was done in displacement control. The displacement was fed from the computer to the controller, which then displaced the hydraulic actuator to match the demand. The rate of displacement of the monotonic test was 10 mm/min and for the cyclic tests 6 min/cycle.

Table 3-5 presents the loading protocol applied on the experimental frames (ECCS 1985 [45]) trough the top actuator (1000 kN).
The ratio between the two actuators was kept 0.5 for the entire time of the experiments (Figure 3-25), thus simulating an inverse triangular loading according to the 1st mode of vibration.

Table 3-5 – Loading protocol

Cycle number	Cycle demand	R-C-T2	SR-C-T2	SR-C-T3
1	$0.25x\Delta_y$	x1	x1	x1
2	$0.5x\Delta_y$	x1	x1	x1
3	$0.75x\Delta_y$	x1	x1	x1
4	Δ_y	x1	x1	x1
5,6,7	$2x\Delta_y$	x3	x3	x3
8,9,10	$4x\Delta_y$	x3	x3	x3
11,12,13	$6x\Delta_y$	x3	x3	x3
14,15,16	$8x\Delta_y$	x3	x3	x3

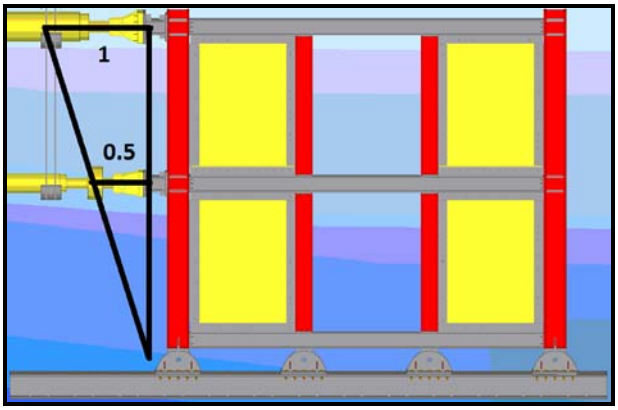

Figure 3-25 – Inverse triangular loading

3.5. Results

3.5.1. Material tests

Mechanical properties of materials used for experimental frame elements were determined prior the testing of the assemblies. Between 3 and 5 samples were taken from the flange and web of the columns and beams, as well as from the 2 mm and 3 mm steel plates. The scope is to determine the yield stress and the ultimate strength of these materials. This was conducted on test samples according to EN ISO 6892-1, 2009 [53]. The tensile tests on the steel samples were carried out using the universal testing machine TESTWELL/UTS (Figure 3-26) with the following specifications:

- hydraulic grips;
- tension and compression test;
- capacity:250 kN;
- computer aided control, acquisition and post processing of results.

Results of the tensile tests have shown values of yield stress higher then the nominal values. For the main columns, the increase was about 100 N/mm^2 (29%). This increase does not affect the behavior of the columns because they are design

to remain in elastic. For beams, the increase of the yield stress was much lower, amounting only 55 N/mm^2 (15%), which is in the safety margins provided by the code, i.e. γ_{ov}=1.25. For the infill panels, the increase was approximately 75 N/mm^2 (25%) which is in the safety margins of 25% provided by EN 1998-1 [40] also. Table 3-6 presents the results of tensile test for the hot rolled profiles while Table 3-7 presents the same results but for the infill plates.

Figure 3-26 –Universal testing machine TESTWELL/UTS

Table 3-6 - Material properties of hot rolled profiles

Section	Steel grade	Element	f_y [N/mm^2]	f_u [N/mm^2]	A_u [mm^2]	Actual steel grade
HEB240	S355	Flange	457	609	40	S460
		Web	458	609	31	
HEB180	S355	Flange	360	515	44	S355
		Web	408	540	40	
HEA180	S355	Flange	419	558	32	S420
		Web	415	542	22.5	

Table 3-7 - Material properties of flat steel (infill plates)

Section	Steel grade	Thickness [mm]	f_y [N/mm^2]	f_u [N/mm^2]	A_u [mm^2]	Actual steel grade
Plate	S235	2	305	429	24	S275
Plate	S235	3	313	413	25	S275

Figure 3-27 shows the stress-strain relationship for the infill panels of 2 and 3 mm thickness. In Figure 3-28 are shown photos taken during the material testing.

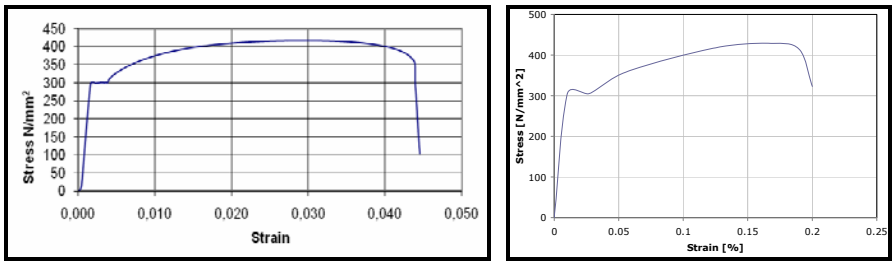

(a) (b)

Figure 3-27 – Infill plate stress vs. strain curve: a) 2 mm plate; b) 3 mm plate

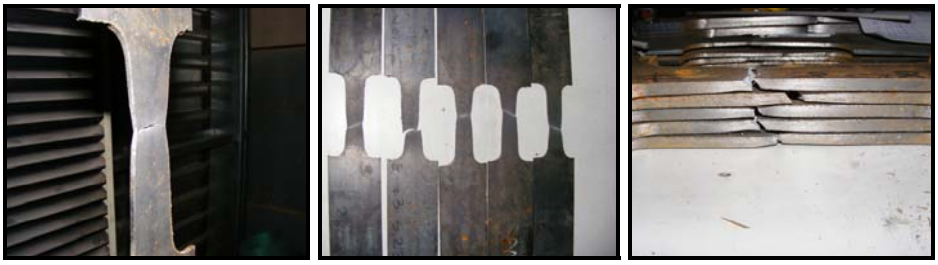

Figure 3-28 – Photos during test on materials

3.5.2. Initial imperfections

The effect of initial imperfections was also studied by Behbahanifard *et al.* (2003) [20]. The results of their research showed that initial out-of-plane imperfections in the infill plate could have a significant influence on the stiffness of the shear panel, but they have little effect on the ultimate shear capacity. As long as the imperfection magnitude is less than $0.01\sqrt{Lh}$, the effect is small and can be neglected. For imperfection sizes larger than $0.01\sqrt{Lh}$, the stiffness reduction is noticeable and should be accounted for in the design.

According to EN1993-1-5 [54], unless a more refined analysis of the geometric imperfections and the structural imperfections is carried out, equivalent geometric imperfections may be used. Figure 3-29 shows how to evaluate the geometric imperfection and Table 3-8 shows allowable equivalent geometric imperfections.

In order to evaluate the initial imperfections of the infill plates, an optical measurement system VIC 3D was used. The limit of allowable imperfection of $0.01\sqrt{Lh}$ proposed by Behbahanifard *et all.* [20] corresponds to an imperfection magnitude of 15.6 mm. The limit of imperfection given by EN1993-1-5 [54] corresponds to a value of 6 mm (Figure 3-29 and Table 3-8).

The values of initial imperfections measured for the 1st infill plate (first storey plate) of each specimen were between 8 and 9 mm, with exception of the SR-C-T2 specimen, for which it amounted 11.5 mm (Figure 3-30, Table 3-9). For all specimens, the values of imperfections are below the limit indicated by Behbahanifard *et al.* (2003) [20] but beyond the limit of EN1993-1-5 [54].

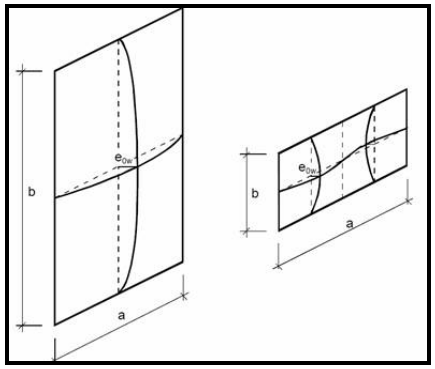

Figure 3-29 – Modeling of equivalent geometric imperfections, EN1993-1-5 [54]

It can be seen there is a big discrepancy between the two recommendations and

therefore they were carefully monitored for all test.

Table 3-8 – Allowable equivalent geometric imperfections (EN 1993-1-5 [54])

Type of imperfection	Component	Shape	Magnitude
Local	Panel or sub-panel with short span a or b	Buckling shape	min (a/200; b/200)

Table 3-9. Initial imperfections of the infill plates

Specimen	Measured e_{0w} [mm]
R-M-T2	8.2
R-C-T2	8.7
SR-C-T2	11.5
SR-C-T3	8.9

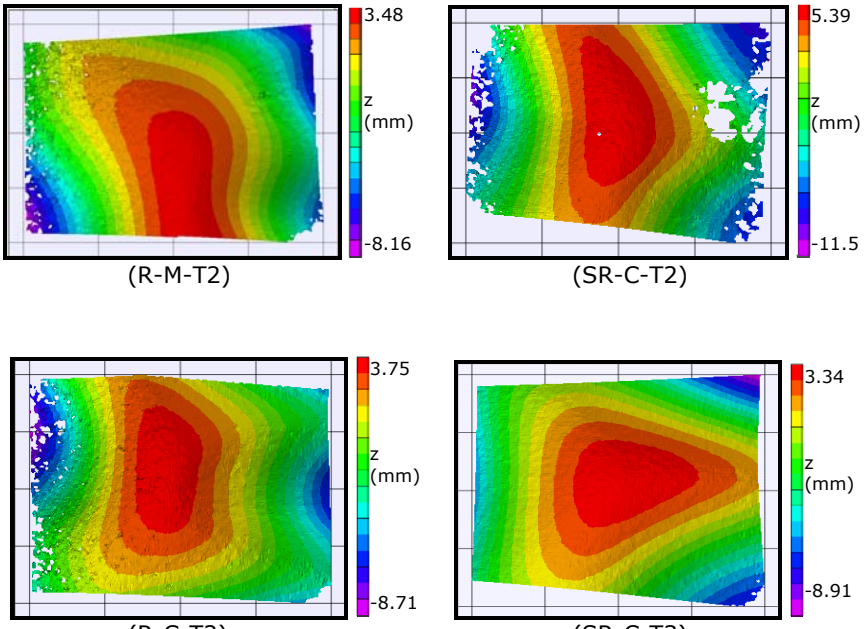

Figure 3-30 – Initial out-of-plane imperfections of specimen

3.5.3. Monotonic test

The specimen tested monotonically has rigid beam to column connections and 2 mm infill plates (R-M-T2). As presented above, the initial imperfection of the plate amounted 8.8 mm ($0.0065\sqrt{Lh}$). Up to 0.5% of the interstorey drift, the specimen exhibited a linear behavior. The yielding of the infill plates occurred at 0.5% of the interstorey drift and was indicated by a drop in stiffness as seen in Figure 3-31. In this point, the base shear force reached 482 kN and the corresponding top

displacement amounted 20.7 mm. The out of plane deformation of the infill panel corresponding to this drift was approximately $0.017\sqrt{Lh}$ (Figure 3-32). Following this point, some local fractures were initiated at the corners of the panels at 2% drift (Figure 3-33a, b). No plastic deformations occurred in beam-to-column connections up to 2% interstorey drift. The 2% drift was reached at a base shear force of 820 kN corresponding to a top displacement of approximately 70 mm. For drifts larger than 2%, local plastic deformations started to initiate at the beam flange in compression (Figure 3-33c) and the fractures at the panel corners started to open and propagate.

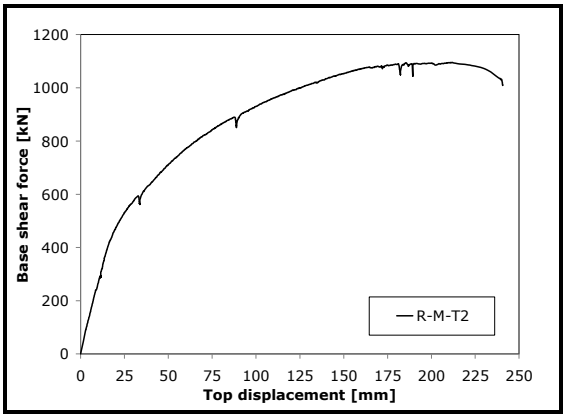

Figure 3-31 – Base shear vs. top displacement

The peak capacity was reached at 6% drift (Figure 3-34, a) at a top displacement of 210 mm and a corresponding base shear force of 1094 kN. Out-of plane deformations corresponding to this drift were about $0.02\sqrt{Lh}$ (Figure 3-34, b). The test was stopped at a displacement of 240 mm as the force started to drop but without reaching the infill panels full shear capacity. Figure 3-34c shows the fracture at the corner of the lower panel in the final stage.

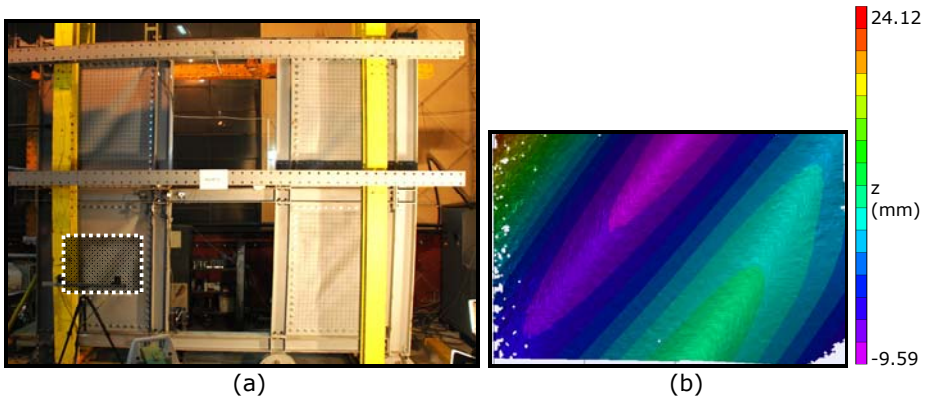

(a) (b)

Figure 3-32 – Yielding stage a) and out of plane deformations b) for 0.5% drift

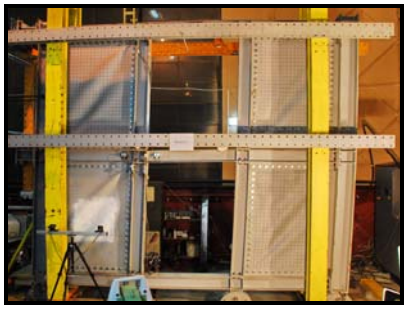

(a)

(b)

(c)

Figure 3-33 – 2% drift

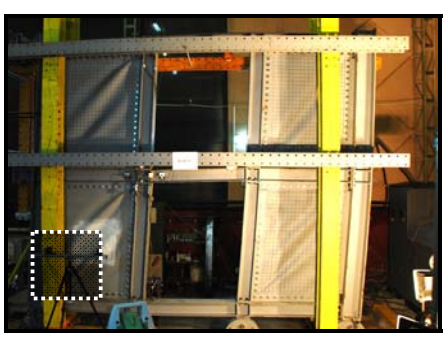

(a)

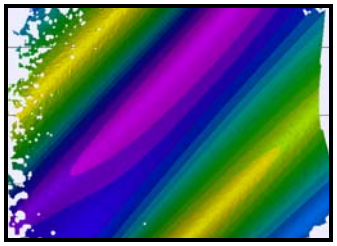

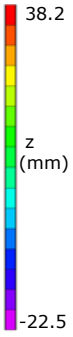

(b)

(c)

Figure 3-34 – Peak capacity (6% drift) a); Out of plane deformations b); Opening of fracture

The monotonic test is necessary mainly for the evaluation of the yielding displacement which is the main parameter in the cyclic loading history (see paragraph 3.2). According to ECCS [45] procedure, a 10% slope at the maximum force is intersected with the tangent to the initial stiffness, thus obtaining the yielding displacement Δ_y and the corresponding yielding force F_y. The original ECCS [45] procedure was developed for the testing of beam to column joints, mainly. As shear walls manifest a different behavior, especially in terms of strain hardening, the estimation of yield displacement considered other methods, also. Thus, based on the behavior of the specimen in the monotonic test, the calculation based on ECCS [45] method was modified. ECCS [45] uses a secant and a tangent line to two sections of the load-deformation curve to determine the yield point. The first line represents the initial stiffness (K_α), which is usually 10% but in SPSW case was increased to 20% of the peak load. This secant line forms an angle a with the displacement axis. The second line (K_β), is drawn at a slope equals to one sixth of the slope of the secant line of the load– displacement curve. The yield point is determined as the intersection of those two lines (K_α and K_β) as can be seen in Figure 3-35. Figure 3-36 plots the load– displacement curve and the location of yielding displacement Δ_y and corresponding yielding force.

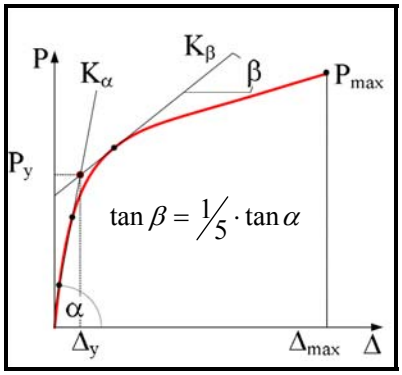

Figure 3-35 – ECCS analysis method for the determination of the yield point [45]

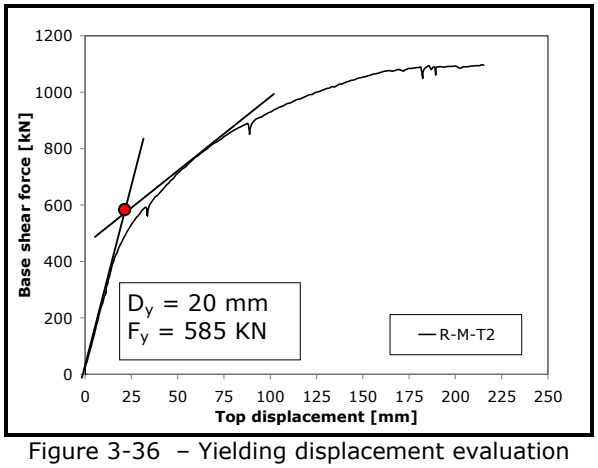

Figure 3-36 – Yielding displacement evaluation

It is worthwhile to mention the nominal shear strength of the infill plates is correctly estimated by using relation (3.1). Thus, the yielding force obtained in the monotonic test amounts 585kN, while the initial prediction amounts 591 KN (for two infill plates).

3.5.4. Quasi-static cyclic tests

Three specimens have been tested cyclically using ECCS [45] procedure, i.e. R-C-T2, SR-C-T2 and SR-C-T3. After evaluating the yielding displacement from the monotonic test (Δ_y=20 mm), the loading protocol for the quasi-static cyclic test can be calibrated. According to ECCS [45] recommendations, the loading history begins with 4 elastic cycles at 5 mm, 10 mm, 15 mm and elastic limit of 20 mm, and then 3 cycles for each of the following top displacements: 40 mm, 80 mm, 120 mm and 160 mm (stroke limit of the actuators). In order to consider the load as quasi-static, the strain rate has been 5 mm/min. The loading history is presented in Figure 3-37 in terms of normalized top displacement Δ/Δ_y and number of cycles.

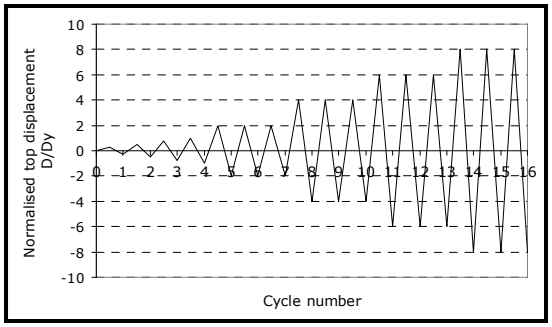

Figure 3-37 – Calibrated loading history

As presented in previews sub-chapter, the initial imperfection of the 2nd specimen having rigid beam to column connection and 2 mm infill plates (R-C-T2) plate, amounted 8.7 mm ($0.0064\sqrt{Lh}$). The elastic limit was reached at a top displacement of approximately 19.4 mm, equivalent to 0.55%. The corresponding base shear force amounted 420 kN. The out of plane deformation of the 1st plate, in this point, was 24 mm ($0.018\sqrt{Lh}$). The specimen exhibited a stable behavior up to cycles of $6\Delta_y$, see Figure 3-38. At this point, the top displacement reached 120 mm with a corresponding base shear force of 824 kN. Some local fractures were initiated at the corners of the panels at drifts of approximately 2.2% and the corresponding base shear force of 920 kN. For drifts larger then 2%, local plastic deformations were observed at the beam flange in compression, similar to the monotonic test. The peak capacity is reached at 4.6% drift for a top displacement of 160 mm and a corresponding base shear force of 1230 kN. The out of plane deformation in this point was 29 mm ($0.022\sqrt{Lh}$).

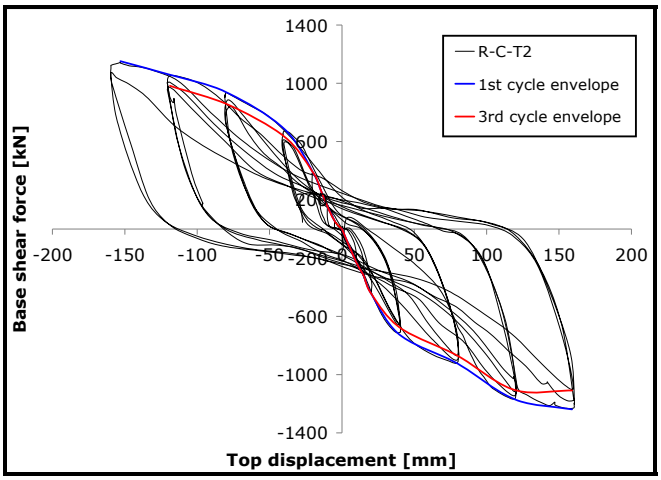

Figure 3-38 – Hysteretic curve for R-C-T2 specimen

The connections between infill panels and the fish plates showed small slippages but no plastic deformations either in plates or bolts. Figure 3-38 plots the test hysteresis of specimen with rigid beam to column connection (R-C-T2) and the envelope curves for the 1st and 3rd cycles.

The second specimen tested cyclically had semi-rigid beam to column connections and 2 mm infill plates (SR-C-T2). The out of plane initial imperfection of the panel was 11.5 mm ($0.008\sqrt{Lh}$). The specimen showed an elastic behavior up to 0.7% storey drift (or a top displacement of 25 mm), with a corresponding base shear force of 469 kN. Cracks were initiated at the corner of the infill panels at 2.1% storey drift and a corresponding base shear force of 813 kN. In this point the out of plane deformations for the panel amounted 32 mm ($0.023\sqrt{Lh}$).

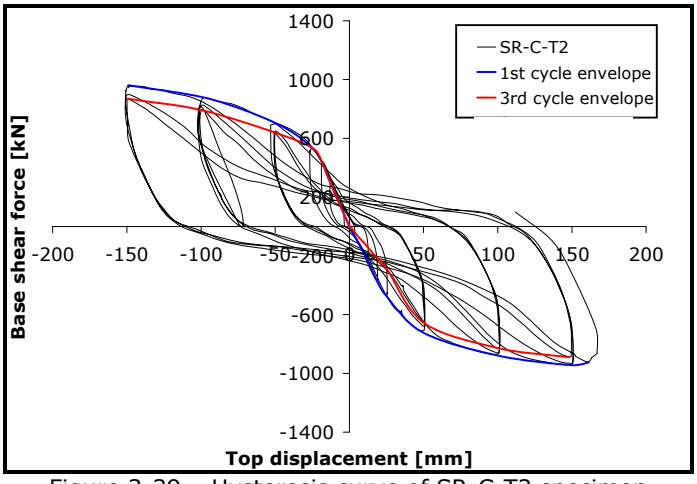

Figure 3-39 – Hysteresis curve of SR-C-T2 specimen

The histeresis loops indicated a stable behavior (Figure 3-39) up to a drift of 4% (equivalent to a top displacement of 143 mm) and a corresponding base shear force of 939 kN. However, pinching was visible for large drifts, caused by the semi-rigid connections between boundary beams and columns. This is particularly important at the evaluation of the q factor, as the pinching needs to be taken out at the evaluation of the ultimate displacement. The ultimate capacity was reached at 4.3% drift (a top displacement of 149 mm) and a corresponding base shear force of 960 kN. In the final stage the infill plate had a 52 mm ($0.038\sqrt{Lh}$) out of plane deformation.

For the 3rd specimen tested cyclically, which has rigid beam to column connections and 3 mm infill plates (SR-C-T3), the initial imperfections amounted 8.9 mm ($0.0066\sqrt{Lh}$). The specimen reached its elastic limit at approximately 0.57% drift (for a top displacement of 20 mm) and a corresponding base shear force of 486 kN. The plate's out of plane deformation was 21.3 mm ($0.016\sqrt{Lh}$).

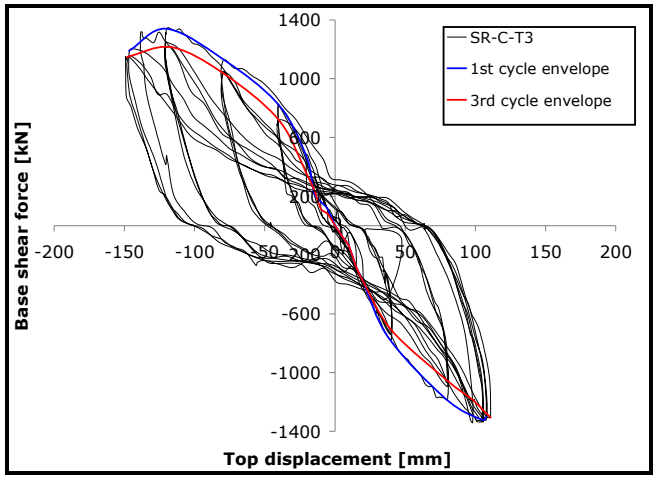

Figure 3-40 – Hysteretic curve of SR-C-T3 specimen

Some pinching was recorded also at this specimen but for large drifts only. The ultimate capacity was reached at a top displacement of approximately 118.3 mm and a corresponding base shear force of 1345 kN. In this point, the out of plane deformation amounted 30 mm ($0.022\sqrt{Lh}$) similar as for the specimen with 2 mm infill plate. Figure 3-40 plots the histeretic behavior with the specification that the load cycles were asymmetrical.

3.6. Interpretation of results

3.6.1. General behavior

In many experimental programs performed throughout the world, steel plate shear wall were done from lower yield strength steel compared to boundary members. In

case of specimens tested at PU Timisoara, in the initial design the steel grade was S235 for the infill plates and S355 for the boundary elements. The steel supplied was different than ordered, but the hierarchy among the system components did not change. As a result, the energy dissipation concentrated in the infill plates.
Experimental results have shown that slender SPSW systems have good initial stiffness, stable hysteresis characteristics and increased energy absorbing capacity in each of the cycles. The hysteretic response of the slender steel plate shear walls is characterized by a typical pinching effect when loaded cyclically. This pinching of the hysteresis curve is accompanied by a substantial drop of the initial stiffness due to the release of the tension field developed in the previous load excursion. Figure 3-41 shows a typical hysteresis loop taken from the response of the SR-C-T2 specimen at cycle 11 corresponding to $6\Delta_y$.

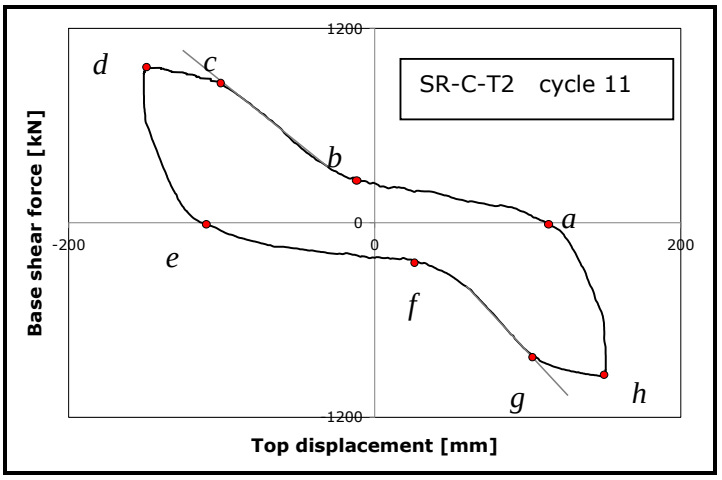

Figure 3-41 – SR-C-T2 specimen hysteresis curve, cycle 11

Point *d* shows the peak displacement in this cycle while the specimen is loaded in the left direction. When unloading the specimen from point *d*, the response follows path *d-e* and has a similar stiffness to the elastic stiffness of the specimen during loading. When loading starts in the opposite direction (point *e*), the specimen shows a substantial drop in stiffness, as indicated by the slope of segment *e-f*. This reduction in stiffness is due to the absence of tension field action. In this region of the base shear force versus top drift curve, the frame is the main lateral load resisting system. Obviously, if singular shear walls are considered instead of dual systems, this region of the curve is horizontal. After point *f*, the structure deforms sufficiently to allow the redevelopment of tension field and the stiffness increases. As the load goes beyond point *g*, the stiffness decreases due to the yielding of the walls. At point *h*, the maximum displacement is attained and starts the unloading phase. Segment h-a-b-c-d represents unloading and reloading in the opposite direction with similar behavior compared to segment d-e-f-g-h. As mention above, stiffness along the segment e-f (or a-b) is given mainly by the frame. When rigid connections between beams and columns are used, the pinching effect is considerably alleviated.
Beam to column connections do not have a major effect in the initial elastic phase, where the plates behavior is dominant. Their contribution can be observed for large

drifts, and increases with the increase of the connection stiffness. The design requirement for such dual frames can be to prevent yielding in frame components up to the attainment of certain deformation capacity in the infill plates.
Perfectly flat walls have very high stiffness but even slight out-of-plane initial imperfections reduce the shear stiffness. Due to the fabrication process, but also due welding and assemblage, the thin plates of all specimens shown initial out-of-flatness with the magnitude less than $0.01\sqrt{Lh}$ (or 15.65mm), where L is the length and h is the height of the panel. These initial imperfections affected the initial stiffness and the yield strength of the specimens' plates but had small effects on the ultimate capacity. Table 3-10 and Figure 3-43, Figure 3-44, Figure 3-45 show the out-of-plane deflections for initial state (initial imperfections), yielding and ultimate load for the left hand side panel of the first storey.

Table 3-10. Out of plane initial imperfections and deformations for yielding and ultimate load

Specimen	e_{0w} (initial)	e_w (yielding)	e_w (ultimate)
R-M-T2	8.8	23.6	27
R-C-T2	8.7	-	-
SR-C-T2	11.5	32.6	52.6
SR-C-T3	8.9	21.3	31.9

Figure 3-42 shows the corresponding stages during the experimental testing for the plots given by the optical measurement system VIC 3D.

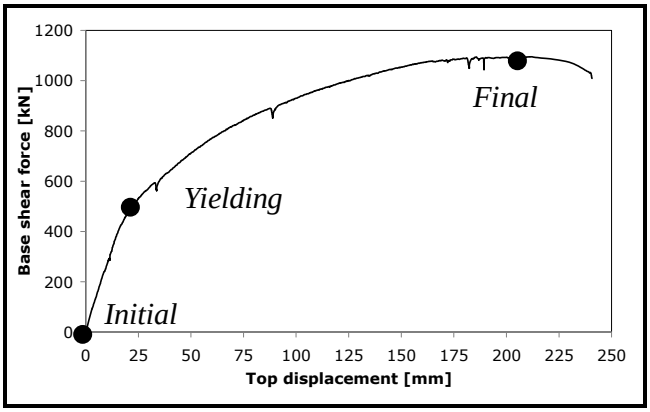

Figure 3-42 – The 3 points of VIC 3D plots

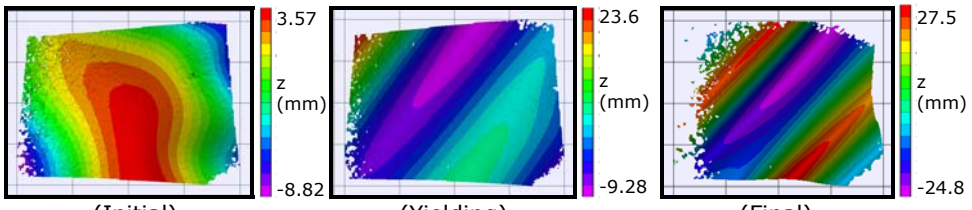

(Initial) (Yielding) (Final)

Figure 3-43 – Out-of-plane deformations for the R-M-T2 specimen

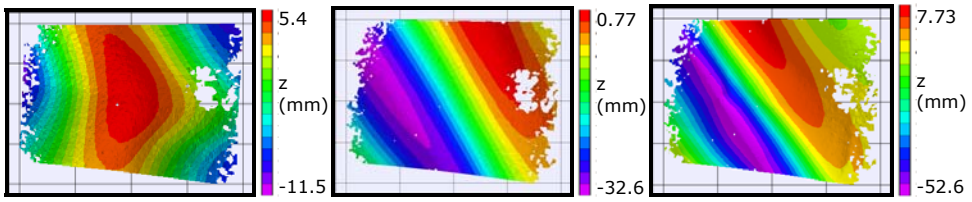

(Initial) (Yielding) (Final)

Figure 3-44 – Imperfections for the SR-C-T2 specimen

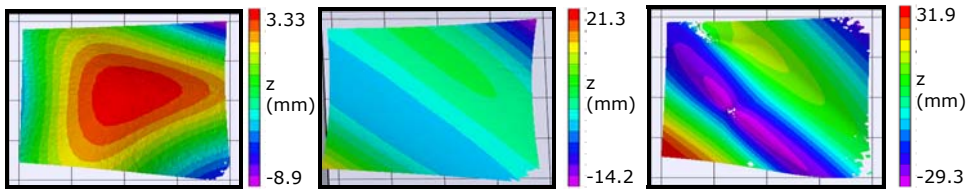

(Initial) (Yielding) (Final)

Figure 3-45 – Imperfections for the SR-C-T3 specimen

3.6.2. Stiffness and strength of dual frames with SPSW

If linear static analysis is performed, the initial configuration of the system can be done if initial stiffness and elastic strength are computed with appropriate accuracy. According to FEMA 356 (2000) [43], the stiffness of the wall, K_w, is calculated in accordance with equation:

$$K_W = \frac{G \cdot a \cdot t_w}{h} \tag{3.5}$$

where:

G = Shear modulus of steel
a = Clear width of wall between columns
h = Clear height of wall between beams
t_w = Thickness of plate wall

For a 2 mm thickness infill plate, the stiffness, K_w, amounts 120.46 kN/m and for 3 mm infill plates, K_w amounts 180.7 kN/m. For comparison, if steel plates are replaced by equivalent X braces, the stiffness of the wall is given by the equation:

$$K_{brace,tension} = \frac{E \cdot A_{eq}}{L_{brace}} \tag{3.6}$$

where:

E = Young modulus of steel
L_{brace} = length of the diagonal brace
A = area of the equivalent brace, calculated with the following relationship:

$$A = \frac{t_w L \sin^2 2\alpha}{2 \sin\phi \sin 2\phi} \tag{3.7}$$

where

- ϕ is the acute angle of the brace with respect to the column;
- L is the centre-to-centre distance of columns;
- α is the angle of inclination of the average principle tensile stresses in the infill plate with respect to the boundary column;
- t_w is the infill plate thickness.

In Table 3-11 are given the values of initial stiffness for the steel plates calculated with equation (3.5) and with the general equation (3.6) for a tensioned equivalent brace. The two methods for the evaluation of wall stiffness give similar values. For further evaluations, only K_w will be used for the evaluation of wall stiffness.

Table 3-11 – Wall stiffness

Wall thickness	K_w	$K_{brace,\,tension}$
2 mm	120.46	120
3 mm	180.69	180

The stiffness of the frame (K_{frame}) contributes also to the total stiffness of the SPSW system. The contribution is given by the frame surrounding the infill plates (K_1) and internal coupling beam (K_2) connecting the two plates. If rigid connections beam to column connections are used, the stiffness K_1 can be evaluated with the following relationship:

$$K_1 = \frac{2}{H^2\left(\frac{L}{6EI_b} + \frac{H}{12EI_c}\right)} \tag{3.8}$$

For coupling beam, the stiffness K_2 can be evaluated with the following relationship:

$$K_2 = \frac{6 \cdot E \cdot I_{c.beam}}{L_{c.beam} \cdot H^2} \tag{3.9}$$

The total stiffness K_{frame} is therefore obtained by combining the contribution of the stiffness K_1 and K_2 as follows:

$$K_{frame} = \frac{2}{H^2\left(\frac{L}{6EI_b} + \frac{H}{12EI_c}\right)} + \frac{6 \cdot E \cdot I_{c.beam}}{L_{c.beam} \cdot H^2} \tag{3.10}$$

Once the stiffness of the frame and the walls are calculated, the total stiffness of the SPSW system can be determined as:

$$K_{SPSW} = \frac{K_W \cdot K_{frame}}{K_W + K_{frame}} \tag{3.11}$$

Table 3-12 shows the stiffness of the specimens evaluated with the formulas above and then compared to experimental values.

Table 3-12 – SPSW stiffness for specimens

Specimen	Analytic [kN/m]	Experimental [kN/m]
R-M-T2	27.03	27.1
R-C-T2	27.03	22.3
SR-C-T2	16.93	18.5
SR-C-T3	27.5	29

In case of specimen with rigid connections tested under monotonic load (R-M-T2), there is a very good agreement between the analytical and the experimental stiffness. In case of specimen SR-C-T2, tested under cyclic loading, the stiffness calculated analytically is underestimated with approximately 8% while for specimen SR-C-T3, the stiffness calculated analytically is less with 5%. These differences can be attributed to the shear walls plates, which act as gusset plates above and below the connection and result in stiffness increase and much less rotation demand.
The rigid beam to column connection showed a greater influence on the strength in case of the cyclic test (1238 kN) (R-C-T2) then in the monotonic one (1090 kN) (R-M-T2) with approximately 12%. When the semirigid connection and 2 mm infill plates were used (SR-C-T2), the strength of the system (944 kN) was smaller with approximately 24%. The increase in infill plate thickness from 2 mm to 3 mm in case of the specimen with semirigid connection (SR-C-T3) brings an increasing of the strength (1345) with 30%. In Table 3-13 and Figure 3-46 is presented the degradation of strength of the specimens due to repeated loading cycle.

Table 3-13 – Degradation of the specimen due to repeated cycles

Specimens		R-C-T2	SR-C-T2	SR-C-T3
Strength [KN]	1st cycle	1238	944	1345
	3rd cycle	1136	890	1214
Degradation [%]		8.2%	5.7%	9.7%

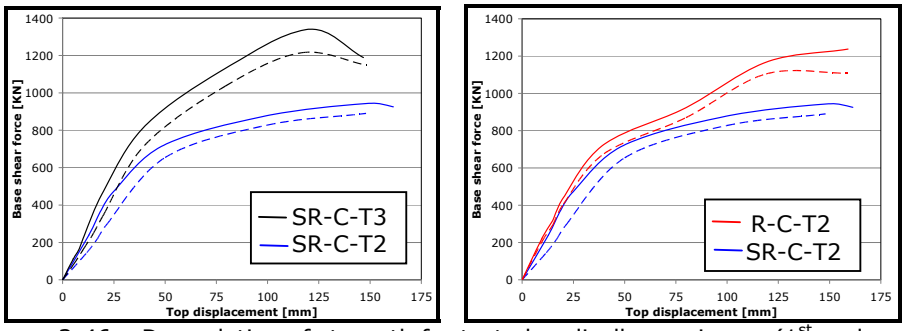

Figure 3-46 – Degradation of strength for tested cyclically specimens (1st cycle and 3rd cycle)

As it can be seen from the Figure 3-46 and Table 3-13, the degradation of the specimens with semirigid joints is greater then in case of rigid one. This degradation can be seen for initial stiffness as well as for the strength.

3.6.3. Energy dissipation and ductility

The main parameters associated to the global performance of the SPSW systems are the energy dissipation and global ductility (given by behavior factor q). The cyclic tests on three SPSW systems with coupling beams have shown significant ductility and energy dissipation capacity. The specimens were capable of follow large number of inelastic cycles, reaching relatively large drift values (beyond 4%).

3.6.3.1. Energy dissipation

The area enclosed by a hysteresis curve is a measure of the energy dissipated by the system during a load cycle. The hysteresis curves of all specimens are fairly wide, indicating good energy absorption of the system. In order to assess the performance of the test specimens quantitatively, the energy dissipated was calculated for each test specimens.
Figure 3-47 shows the energy absorbed by the specimen with rigid beam to column connection (R-C-T2) during the cyclic loading. For the elastic cycles up to Δ_y, the absorbed energy is very small. The increase of the amplitude of the cycles (plastic cycles) leads to an increase in energy absorption. Due to the cyclic degradation, the 2nd cycle shows a decrease in energy absorption of 26% for $2\Delta_y$ and $4\Delta_y$, while for $6\Delta_y$ and $8\Delta_y$ the decrease is about 20%, compared to 1st cycle. The 3rd cycle shows a 15% decrease for $2\Delta_y$, 13% decrease for $4\Delta_y$ and $6\Delta_y$, while for $8\Delta_y$ the energy absorption is less with about 19%, compared to 2nd cycle.

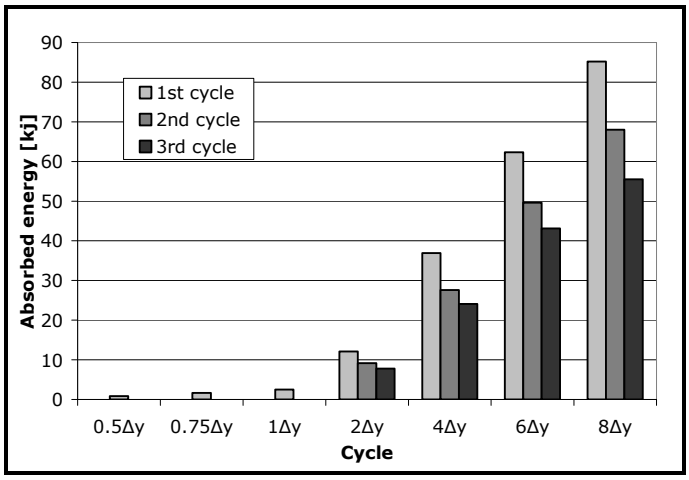

Figure 3-47 – Energy dissipation for R-C-T2 specimen per cycles

For the specimen with semi-rigid beam to column connection (SR-C-T2) (Figure 3-48), the 2nd cycle leads to a reduction of the absorbed energy by 27% for 2 Δ_y, while for 4 Δ_y and 6 Δ_y the reduction amounts 27% and 20%, respectively. For the 3rd cycle, the reduction is 16% for 2 Δ_y, 4 Δ_y and 6 Δ_y.

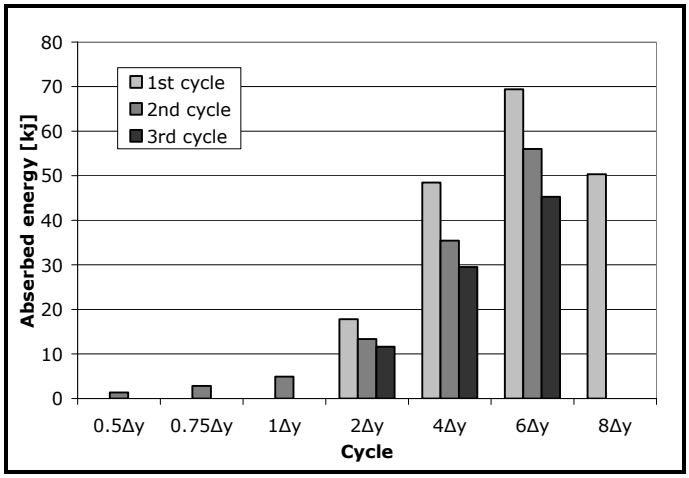

Figure 3-48 – Energy dissipation for SR-C-T2 specimen per cycles

For the specimen with semi-rigid beam to column connection and a thickness of the infill plates of 3 mm (SR-C-T3), the 2nd cycle leads to a reduction of the absorbed energy by 25% for 2 Δ_y, 36% for 4 Δ_y and 28% for 6 Δ_y and 3% for 8 Δ_y. For the 3rd cycle, the reduction is negligible for 2 Δ_y and 4 Δ_y, while for 6 Δ_y and 8 Δ_y the reduction amounts 9% and 14%, respectively.

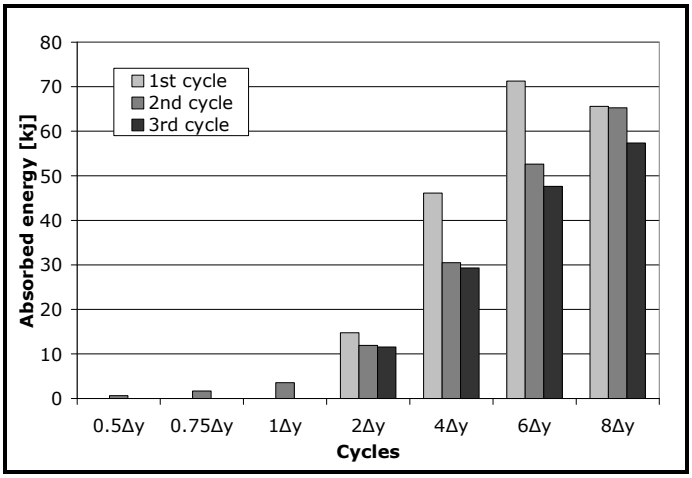

Figure 3-49 – Energy dissipation for SR-C-T3 specimen per cycles

The values of the cumulative energy dissipation were calculated and are presented comparatively in Figure 3-50. The results showed that in specimen SR-C-T3, the amount of energy dissipated (510 kJ) during the loading cycles was significantly greater than those in SR-C-T2 (330 kJ) by almost 50%. The specimen with rigid beam to column connection (R-C-T2) presented higher cumulative energy dissipation of about 46% (485 kJ) than the one with semirigid conennection.

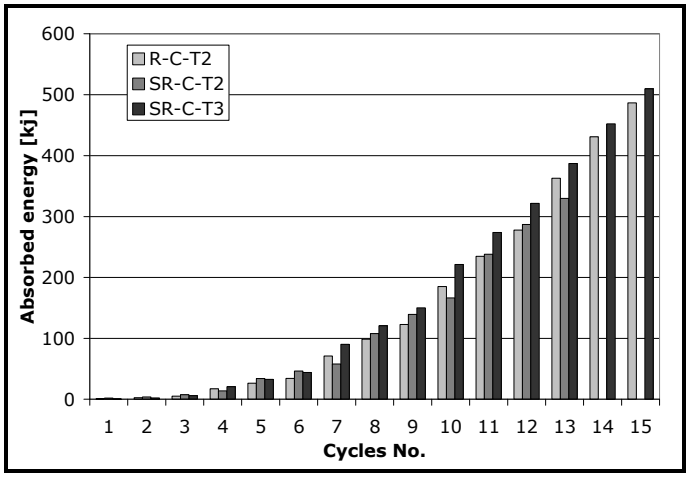

Figure 3-50 – Cumulative energy dissipation

3.6.3.2. Ductility

One of the objectives of the experimental program was the evaluation of the behavior factor or q factor. Seismic codes provide values of q factor (or reduction factor) for common structural systems, like moment resisting frames or centrically braced frames. Starting with 2005 edition, North American codes AISC 2005 [5] and NBCC 2005 [31] introduced provisions regarding the selection of reduction factor R (equivalent to q factor) for SPSW systems. Unfortunately, European codes (eg. EN1998-1 [40] or Romanian code P100-1/2006 [48]) do not provide any recommendations regarding q factor for singular SPSW or dual systems with SPSW and moment frames. Therefore, this task is very important for the development of such systems in Europe. The q factor can be subdivided in two components, as expressed in the equation below (Figure 3-51):

$$q = q_{\mu} \cdot q_{\Omega} \tag{3.12}$$

where:

q_{μ} is the ductility reduction factor and q_{Ω} is the overstrength factor.

The overstrength factor q_{Ω} may vary significantly and it is affected by the different contribution of gravity loads, material overstrength, structural redundancy, member oversize due to design, other non seismic load combinations and serviceability requirements. Therefore, its evaluation based on limited experimental tests cannot be relevant. The overstrength factor q_{Ω} for a structural system can be conservatively evaluated and prescribed in codes. For example, NBCC (2005) [31] indicates for ductile steel plate shear walls overstrength factor R_s (equivalent to q_{Ω}) equal to 1.6. Similar recommendations are given by Berman and Bruneau (2003) [21], but they recommend an overstrength factor R_s=1.2.

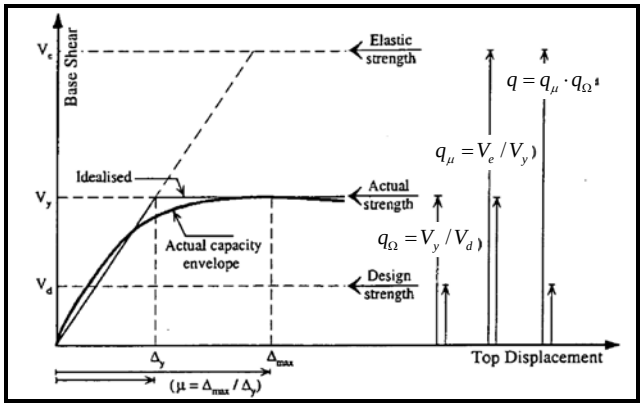

Figure 3-51 – Definition of the q factor and its components

For structures that exhibit a period > 0.5 s, the ductility reduction factor (q_μ) may be taken equal to the displacement ductility factor (μ). This approximation follows the equal displacement assumption proposed by Newmark and Hall (1982) [55]. The ductility is the structure's ability to sustain large plastic displacement before failure. Based on this definition, the displacement ductility factor for a system can be obtained from equation:

$$\mu = \frac{\Delta_u}{\Delta_y} \tag{3.13}$$

where
Δ_u is the maximum plastic displacement (or ultimate displacement) that the system sustains the loads up to the failure and Δ_y is the displacement at the point of significant yielding.

The ductility reduction factor q_μ is therefore defined as the ratio of the ultimate displacement Δ_u and the yielding displacement Δ_y:

$$q_\mu = \frac{\Delta_u}{\Delta_y} \tag{3.14}$$

According to AISC 2005 [5], the parameter Δ_u corresponds to a reduction of the load carrying capacity of 20% compared to the maximum one. Due to the stroke limitation of the actuators, a 10% reduction was used.
Yielding displacement Δ_y has no standardized or at least harmonized definition for steel plate shear wall systems. In the monotonic test, the evaluation of the yielding displacement, Δ_y, was based on the ECCS methodology [45] (see paragraph 3.5.4). In the cyclic tests, apart from ECCS methodology [45], the "stiffness method", where the yield point corresponds to the modification of the elastic stiffness, was considered. Based on the observation of the hysteretic curves, the ultimate displacements Δ_u for SR-C-T2 and SR-C-T3 were corrected to take into account the pinching during the load reversal. Figure 3-52, Figure 3-53 and Figure 3-54 show the evaluation of yielding displacements for the three specimens.

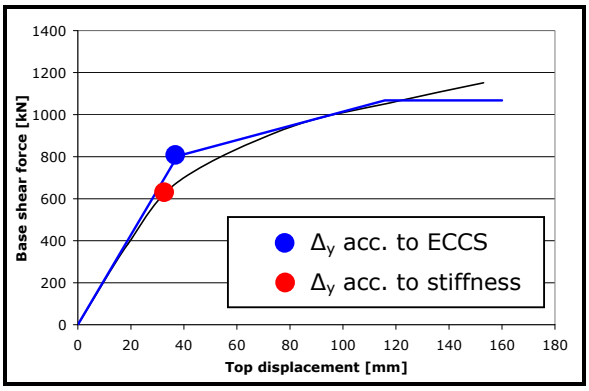

Figure 3-52 – Evaluation of Δ_y for R-C-T2

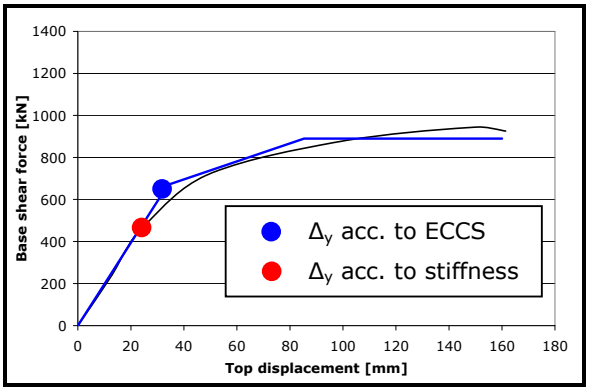

Figure 3-53 – Evaluation of Δ_y for SR-C-T2

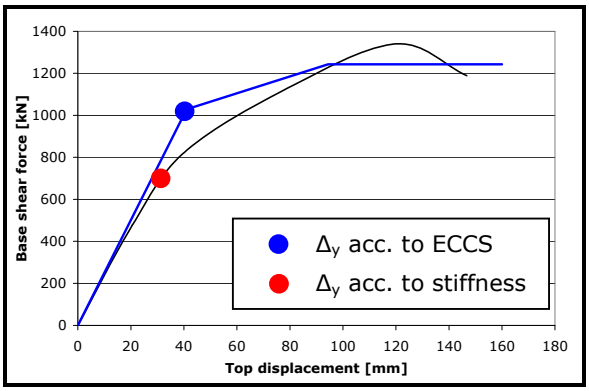

Figure 3-54 – Evaluation of Δ_y for SR-C-T3

Table 3-14 shows the q_μ factor values for the specimens. Comparing these values, it may be seen the specimens have similar ductility factors q_μ, with values between 4.9 and 5.2. The lower values of the elastic resistance of semi-rigid specimens compared to rigid ones caused the larger values of q_μ. These values show SPSW

structures can provide q factors similar to those corresponding to other dissipative structure, like for example moment resisting frames or eccentrically braced frames.

Table 3-14 - q factor values

Structure	Δ_y		Δ_u	q_u	
	ECCS	stiffness		ECCS	stiffness
R-C-T2	38	31	153	4.0	4.9
SR-C-T2	33	26	163	4.9	6.3
SR-C-T3	40	33	147	3.7	4.5
Average value				4.2	5.2

3.7. Conclusions

The main parameters of the specimens were the beam to column connection and the thickness of the infill plates. Rigid and seimirigid beam to column connection and 2 mm, respectively 3 mm thick infill plates were used.
All specimens showed appropriate behavior during the tests, and the use of thin plate made of lower strength steel made the plates manifest good energy absorption with the maximum displacement.
Rigid connections increased the "yield resistance", ultimate capacity and initial stiffness of the structures. It also reduces the degradation of the structure true repeated cycles and diminished considerably the effect of pinching at load reversal.
When the infill plate thickness was increased to 3 mm, there was no change in evolution of out of plane deformations of the plates, but improved the initial stiffness and the ultimate capacity, considerably.
Because no plastic deformation were recorded in the bolts or fishplates this enabled a very easy dismantling of the steel panels after the test. Associated with a small residual drift (for rigid structure), this can assure an easy intervention after a moderate earthquake to replace the damaged panels.
Behavior factor q_μ (considering the contribution of the ductility, only), was evaluated using two methods: ECCS [45] and stiffness, based on the results of the cyclic tests. The amount of ductility factor obtained, 4.2 from ECCS method [45] and 5.2 from stiffness method, demonstrates the significant ductility of steel plate shear walls even with existing residual stresses and strains. Since, the most damages occur during the main earthquake in structure; this system demonstrates the efficiently seismic performance even after earthquake.
Results were compared with other similar tests performed worldwide. Thus, two multi-story steel plate shear walls were tested in University of Alberta (Driver et all. 1998) [10]. The ductility factor of the first shear wall according to ATC-24 [12] protocol equals to 8.5 and for the second it equals 6.4. Values are very close to the ones reported by the author. Other tests were performed at the University of British Columbia (Kharrazi, 2005 [28]). For the specimen with the mild carbon steel plate, the ductility factor according to ATC-24 [12] protocol equals to 7.4.
It is noteworthy to be mentioned the fact that, the ductility factor is very sensible regarding the method of determination of yielding displacement. Although there are lots of methods for determination of yielding displacements, in case of SPSW systems is much more difficult then for other type of systems.

4. Numerical Program

4.1. Introduction

The numerical study conducted in this chapter investigates the seismic performances of dual systems of steel plate shear walls and moment resisting frames. Experimental study presented in the previous chapter demonstrated the effectiveness of the steel plate shear walls as a lateral load resisting system against earthquake forces. The main objective of the chapter is to asses the seismic performance of different typologies of SPSW structures using the modeling parameters obtained for the steel plates tested in chapter 3. The evaluation of the behavior factor *q* is the main target of the numerical study. The possibility of using different types of beam to column connection in SPSW systems is also explored. Test data presented in Chapter 3 were used in the calibration of the numerical models which were capable of accurately simulating the initial stiffness, post-yield stiffness and ultimate capacity of the system. The evaluation of frame-shear wall interaction was done in order to obtain the influence of macro-components (i.e. the open frame, overstrength factor Ω, joint's properties and steel plates) on the values of q factor. Having these objectives complete, acceptance criteria to be used in Performance Base Seismic Engineering can be identified.
The nonlinear static and dynamic analyses were conducted using the commercial software SAP2000 [52].

4.2. Modeling of shear walls for nonlinear static and dynamic analysis

The development of diagonal tension field within the infill plates is the primary mechanism to resist storey lateral forces. This behavior should be considered in the analysis by modeling shear plates using shell elements that can buckle. This complex plate buckling formulation (geometric nonlinearity) is not readily available in conventional structural analysis programs used for routine seismic design. To facilitate the analysis and design of structural elements for building applications, including the gravity beams and columns, a simplified methodology for modeling the steel plates has been employed. The model can be used in conventional structural analysis programs, eg. SAP2000 [52]. The idea behind the modeling approach is based on the results of Thorburn et al. (1983) [7], which developed an analytical method to study the shear resistance of thin un-stiffened steel plate shear walls. The so called "strip model" represented the shear panels as a series of inclined strip members, capable of transmitting tension forces only, and oriented in the same direction as the principal tensile stresses in the panel. Figure 4-1 shows the strip model representation of a typical steel plate shear panel. By replacing the plate panel with these tension strips, the resulting steel structure can then be analyzed using currently available computer analysis software.
The modeling of the plates using the strip model as presented above can be used for static nonlinear analysis. For the nonlinear dynamic analysis, where the structure is loaded in both directions, was used a different model, called dual strip model (Figure 4-2). This model uses the idea of the strip model, but with the struts arranged in

the same manner in both directions. This model was also used by B. Qu and M. Bruneau (2007) [56] in an analytical study on SPSW system in order to replicate the result of MCEER/NCREE Phase II cyclic tests done at University at Baffalo, New Tork. It has been found that the adequacy of the dual strip model using tension-only strips was accurate to predict the nonlinear behavior of SPSW under earthquake loads.

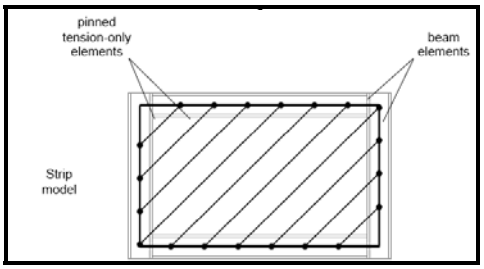

Figure 4-1 – Strip model representation of typical steel plate

The strip model was presented in detail in chapter 3, presenting the relationships for the angle of inclination of the tension field (α) and area of one pinned tension-only element (A_s) (equations (3.2) and (3.4)).

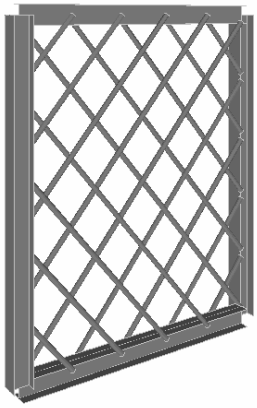

Figure 4-2 – Dual strip model

4.3. Calibration and validation of numerical models

The main parameters that define the strip model of a steel plate shear wall are the area of the pin ended tension strips, A_s, the angle of inclination of the tension field, α, and the tension plastic hinge which gives the post-elastic behavior.
In the initial numerical evaluation of the specimens that were tested experimentally (see chapter 0), the modeling was based on AISC [5] provisions, using the bilinear curve proposed by Driver (1998) [10]. Based on these parameters, the initial stiffness and the elastic limit have been predicted with good accuracy but the ultimate capacity was very poorly estimated compared to the experimental value

(42% less), see Figure 4-3. As the initial stiffness offered by this model is predicted with accuracy, the equivalent area calculated according to AISC 2005 [5] and the angle of inclination can be used with confidence. Thus, the error in the model is related to the bilinear plastic hinge which has to be calibrated in order to have a better prediction of the post-elastic behavior of the system. The calibration was done on the experimental monotonic curve using a multi-linear curve. Figure 4-4 shows the multilinear curve in terms of normalized force P/P_y vs. normalized displacement Δ/Δ_y and Table 4-1 shows the values of the component modeling and acceptability.

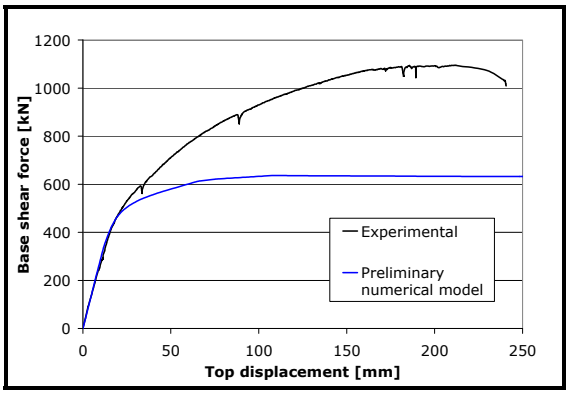

Figure 4-3 – Experimental vs. preliminary numerical analysis

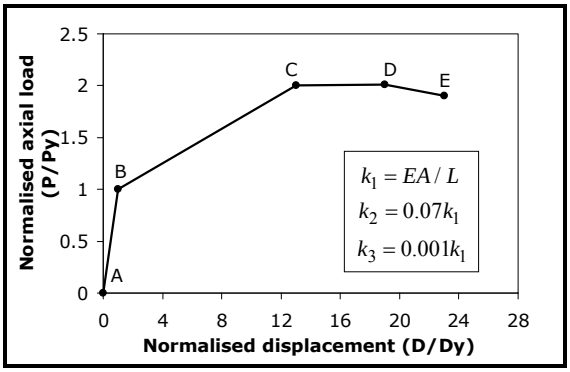

Figure 4-4 – Calibrated tension hinge according to experimental

Table 4-1 - Calibrated axial hinge

Hinge	A		B		C		D		E	
	P/P_y	Δ/Δ_y	P/P_y	Δ/Δ_y	P/P_y	Δ/Δ_y	P/P_y	Δ/Δ_y	P/P_y	Δ/Δ_y
Tension	0	0	1.0	0	2.0	13	2.0	19	1.8	23

Based on the improved model, the behavior of the SPSW system is very much improved and the two curves (i.e. numerical and experimental) are closed. The new

model predicts with good accuracy the entire behavior of the steel plate shear wall, including the softening branch. Some differences exist but they can be attributed to imperfections in testing set-up and larger than expected contribution of beam to column connections (frame - panel interaction in the vicinity of the beam ends).

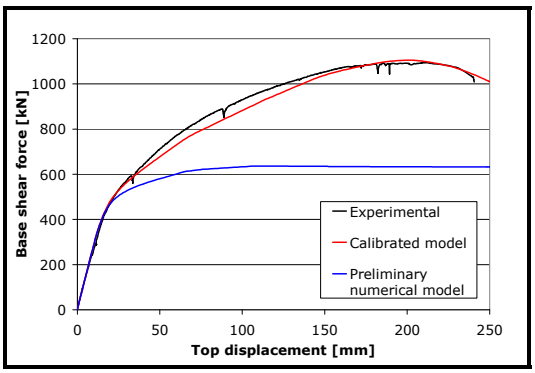

Figure 4-5 – Experimental vs. calibrated numerical model

4.4. Interaction between framing and shear walls: contribution of macro-components

In order to determine the interaction between framing (HBE and VBE) and shear walls, some supplementary analysis were done. Thus, the behavior of the frame without the infill plate's contribution and behavior of the infill plates only can be assessed from numerical analysis and compared then to experimental tests (with the infill plates in). First, the behavior of the moment frame alone (rigid beam to column connections) is plotted in Figure 4-6, curve 1. It was found that the frame has a weak contribution, characterized by a low initial stiffness (2071 KNm) and poor strength (150 kN). In order to asses the behavior of the infill plates only and to neglect the frame contribution, the connections between beams and columns are pinned (curve 2). The initial stiffness is approximately 12 times larger (26063 KNm) and the strength almost 6.4 times (961 kN). If the two system act together (dual system) (curve 3), the cumulated strength increases accordingly (1100 kN) but the gain in initial stiffness (up to yielding) is negligible. For comparison, the experimental curve is also plotted and shows a very good agreement. The model is therefore capable of representing with very good accuracy the behavior of the dual frame-panel system. In the same way, the behavior of the structure with semirigid connections can be evaluated. Curve 5 shows the behavior of the dual structure (frame + panel) with semirigid beam to column connections. The initial stiffness is relatively the same and there is a reduction in strength compared to the dual rigid structure.

As the behavior and the contribution of each component can be easily evaluated, their relative capacity in stiffness and strength can be adjusted to meet the specific requirements. Thus, the vertical line marked with I shows the limit of elastic behavior for the panel, while the frame (including connections) is still elastic. Between lines I and II, the plate is in post-elastic state and the frame (connection) is in elastic state. Line II shows the initiation of yielding in frame (connection), at

approximately 65 mm or 2%. This point is also visible on the cumulative behavior, when the slope of the curves changes (curve 3 - numerical and curve 4 - experimental). The frame can be therefore sized to remain elastic until a certain drift (eg. 2%) to allow for repairing or easy replacement of damaged steel plates. Zone between II and III is characterized by a degradation of both frame and plate, as the plastic deformations progress. The line III represents the maximum capacity attained in the structure, followed after by a decrease of capacity and then failure. At the point of maximum capacity, the storey drift reaches 6% and the plastic rotation in beams reaches 0.032 rad. The plastic rotation demand in frame (or connection) can be evaluated and then compared to the available one. The demand can be reduced by increasing the elastic limit of the frame, for example by increasing the steel grade. In the experimental test performed by the author, the nominal steel grade in the frame was S355, compared to S235 in plates. The material supplied was different from what was ordered but still the yield strength of plates was lower than the yield strength of frame components.

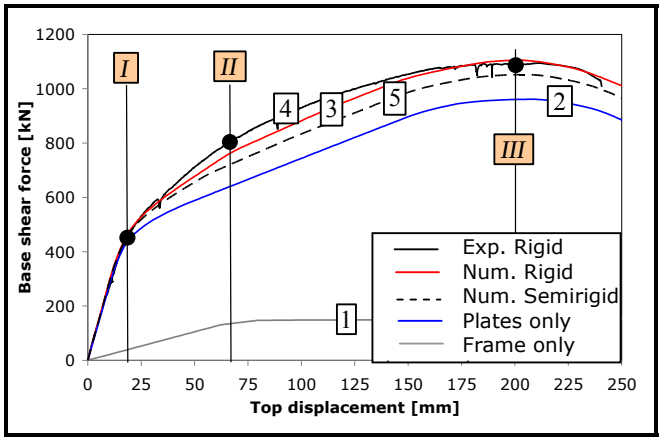

Figure 4-6 – Contribution of components

4.5. Parametrical study

4.5.1. Design of frames selected for analysis

4.5.1.1. Selection of frames

In order to hopefully reflect the findings obtained in the experimental program different typologies of structures were selected to be analyzed. The structures selected for the numerical investigation are similar to those tested experimentally. As the experimental frames were scaled geometrically to one half, the infill plates that had originally the dimensions of 1400 by 1750 mm were scaled to double (2800 by 3500 mm), thus maintaining the aspect ratio *L/H* of the plates of 0.8 (see paragraph 3.3.2). Engineering judgment in seismic regions indicates the dual frame-wall structures as an excellent lateral force resisting system, able to guarantee an

efficient control both on drift and displacement deformations. Moreover, the use of SPSW system and moment revisiting frame provides the retention of a satisfactory energy dissipation capacity during earthquake motions. In addition, if it is extended over the full height of the building, the system can also boast a great maintenance of lateral strength and stiffness properties. For this reason, the structures selected for the study have dual systems MRF+SPSW, where the MRF system has to contribute with more than 25% (1) to the lateral load resisting system, otherwise, it is referred to as a combined system. Figure 4-7 shows the seismic response of the MRF (left) and dual systems (right).

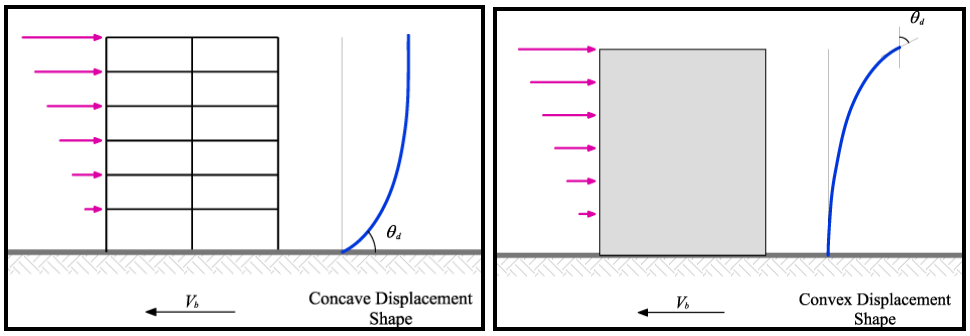

(a) (b)

Figure 4-7 – Seismic behavior for building structures: a) Moment resisting frame (MRF); b) Dual frame MRF+SPSW

Another important requirement for the structures was the beam to column connection surrounding the infill plates. Two types of connections were considered fully rigid (further referred to as rigid) connection and pinned connection (further referred to as pinned). The selection was made in order to reflect the two types of joints used for the experimental specimens (see paragraph 3.3.2).
In order to better understand the behavior of the SPSW structures in seismic areas, 3 different structure heights were chosen: low, mid and high. A total of 6 SPSW structures were selected to be designed and analyzed in order to asses their seismic performance. The systems are similar to those tested experimentally and presented in chapter 3. The geometry of the structure is presented in Figure 4-8. The storey height is 3.5 m, the span of the outer moment resisting frames is 6 m and the total interior span is 7.5 m. The interior frame is a braced frame with two vertical rows of steel plate shear walls of 2.8 m each. Due to the internal coupling beam, the system is also called "dual system with coupling beams". The total height of the structures amounts 21 m for the 6 storey structures, 42 m for the 12 storey structures, respectively 63 m for the 18 storey structure.

The preliminary selection of steel materials is as follows: S235 (f_y=235 N/mm^2) for the infill panels; S355 (f_y=355 N/mm^2) for beams and columns respectively S460 (f_y=460 N/mm^2) if needed for the main column. The hierarchy of the steel grades from the experimental frames (see paragraph 3.5.1) is maintained also in the numerical investigations.

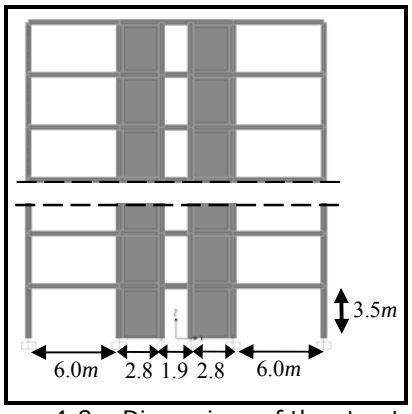

Figure 4-8 – Dimensions of the structure

4.5.1.2. Code based design

The design was carried out according to EN1993-1-1 [57], EN1998-1 [40], AISC 2005 [5] and P100-1 [47]. Regarding the design of the steel plates shear walls for seismic conditions, the provisions from AISC 2005 [5] were compared with experimental results. Thus, based on the results of the experimental program, a behavior factor q of 6 was considered (paragraph 3.6.3). The dead load amounts 4 kN/m^2 and live loads (office building category) amounts 2.0 kN/m^2, respectively.

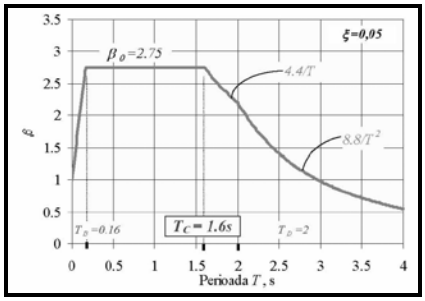

Figure 4-9 – Normalized elastic spectra [47]

The structure is located in a high seismic area (i.e. the Romanian capital, Bucharest), which is characterized by a design peak ground acceleration of 0.24g for a returning period of 100 years, soft soil conditions and a corner period of T_C=1.6 sec. This last characteristic has a detrimental effect against flexible buildings (eg. mid-rise buildings), with periods of vibrations around 1.5 sec.
After the selection of the dimensions and steel grades, the next step is the preliminary design of the structures. The SPSW walls were approximated by means of a vertical truss with tension diagonals for preliminary proportioning of HBE, VBE and webs (infill plates). Each web is represented by a diagonal tension brace within each storey. The area of the equivalent brace is then adjusted to fulfill the requirements for SLS (0.005H_e) and ULS (appropriate strength) using a response spectrum analysis. After performing a spectral analysis of the structures, using

Sap2000 software, the configuration of the 3 structures could be obtained. The main dissipative elements (braces) are designed taking into account the design seismic action. Thus, the areas obtained for braces are 7700 mm^2 for 6 storey structures, 9000 mm^2 for 12 storey structures and 13000 mm^2 for 18 storey structures, respectively. Beams are also considered as dissipative elements and designed accordingly. For non-dissipative elements (i.e. columns), EN1998-1 and P100-1/2006 amplifies the design seismic action by a multiplicative factor $1.1\gamma_{ov}\Omega$. Factor 1.1 accounts for the strain hardening of the material and can be taken equal to 1.2 (see Table 3-6). As a comparison, the same factor amounts 1.1 for MRF and 1.5 for EBF systems. γ_{ov} is a factor that accounts for the increase of the steel grade supplied for main dissipative elements and amounts 1.25. For the infill panels, results of the tensile tests (see
Table 3-7) have shown values of yield stress higher by maximum 75 N/mm^2 (25%) than the nominal value, which are in the safety margins of 25%. Ω factor accounts for the strength reserve in main dissipative elements and can be evaluated after a first structural analysis. In a simplified analysis, the factor $1.1\gamma_{ov}\Omega$ can be considered as 2 for dual frames of MRF and CBF.
Figure 4-10, Figure 4-11 and Figure 4-12 show in very short steps the design of the structures and the resulted configuration of the structure (Table 4-2).

Table 4-2 – Structures section members

Frames	MRF column	SPSW column	Inner column	Beam
6	HEB400	HEB400	HEB400	IPE360
12	HEB600/HEB550	HEB600/HEB550	HEB400	IPE450/IPE400
18	HEB600/HEB550	HEB700/HEB650	HEB500/HEB400	IPE450/IPE400

At this point, the thickness of the steel plate t_w can be calculated using the equivalence between diagonal brace and steel plate:

$$t_w = \frac{2A\Omega_s \sin\theta}{L \sin 2\alpha} \tag{4.1}$$

where
A is the area of the equivalent tension brace
θ is the angle between the vertical and the longitudinal axis of the equivalent diagonal brace;
L is the distance between VBE centerlines;
α is the angle of inclination of the tension field measured from the vertical using equation.
Ω_s is the system overstrength factor, as defined by FEMA 356 [43], and taken as 1.2 for SPSW (Berman and Bruneau, 2003 [21], NBCC 2005 [31] (different from Ω described in the previous section).
Table 4-3 present the thickness of the plates obtained from the equivalence with the brace.

Table 4-3 – Area of equivalent brace

Equivalent brace [mm^2]	7700	9000	1300
Plate thickness [mm]	4	5	7

The plate thicknesses of 4, 5, and 7 mm turned out to be larger that the minimum thickness required by the FEMA [43]/AISC [5] guidelines, which resulted in SPSW models having the same plate thickness at all storeys (constant plate thickness).

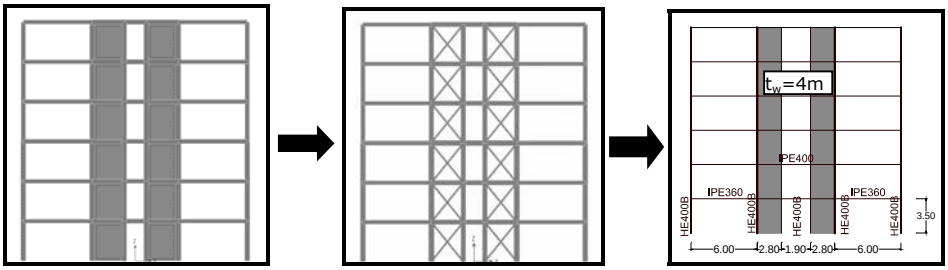

(initial) (pre-design) (final)

Figure 4-10 – Design of 6 storey structure

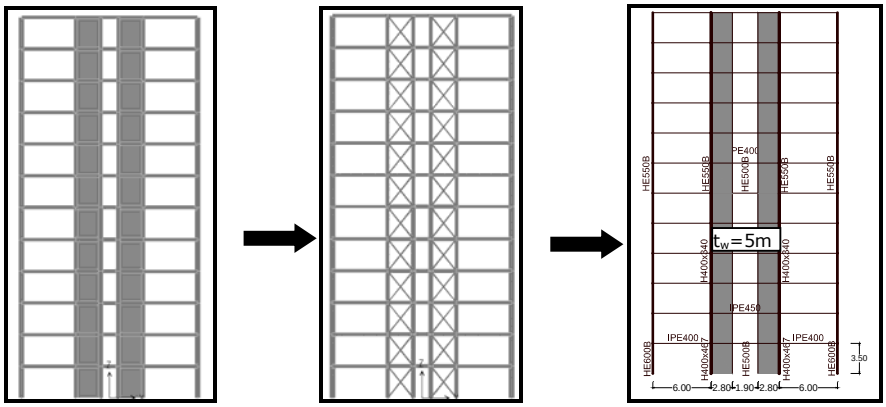

(initial) (pre-design) (final)

Figure 4-11 – Design of 12 storey structure

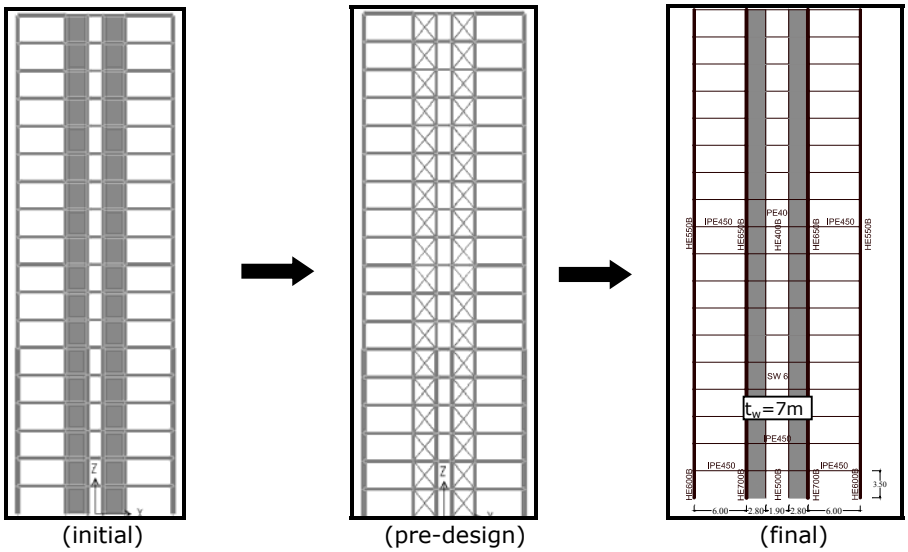

(initial) (pre-design) (final)

Figure 4-12 – Design of 18 storey structure

Horizontal and Vertical Boundary Elements

The boundary beams were checked to resist fully yielding plates, without developing mid-span hinges:

$$W_{pl(beam)} \geq \frac{f_{yp} t_w \cos^2 \alpha L^2}{4 f_{y(beam)}} \tag{4.2}$$

where:

f_{yp} is the steel plate yielding resistance;

f_{ym} is the beam yielding resistance.

The moment of inertia of the column was verified to fulfill the minimum value offered by AISC 2005 [5] (equation (3.2)), in order to prevent excessive deformations leading to premature buckling under the pulling action of the plates.

Classification of beam to column connections

In the numerical study, two types of beam to column connection are used. Rigid connection which may be assumed to have sufficient rotational stiffness to justify analysis based on full continuity and nominal pinned connection which is capable of transmitting the internal forces, without developing significant moments which might adversely affect the members or the structure as a whole.

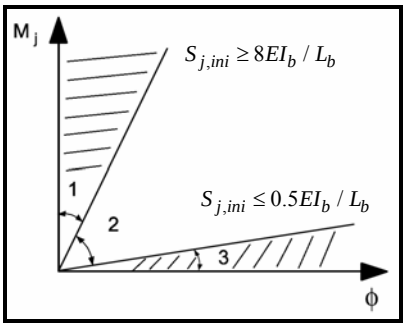

Figure 4-13 – Classification of joints by stiffness for braced structures, according to EN1993-1-8 [47]

The joints can be classified according to strength by comparing its design moment resistance $M_{j,Rd}$ with the design moment resistance of the connected members. Thus, the full strength joint does not have its design resistance less that of the beam element and meets the criteria given in Figure 4-14.

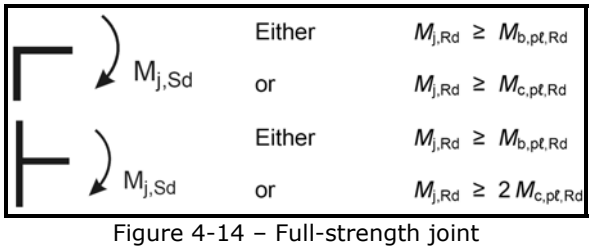

Figure 4-14 – Full-strength joint

A dual frame, according to EN 1993 [47], represents a structure combined from a moment resisting frames (MRF) and braced frames. The MRF must take at lest 25% from the lateral loads acting on the structure. The dual frame was a selection criterion for the structures to be analyzed as described in paragraph 4.5.1.1.

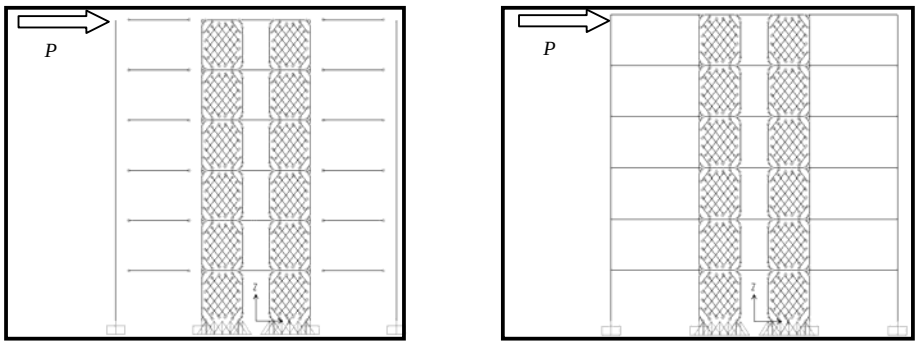

(a) (b)

Figure 4-15 – Dual frame a); simple braced frame b)

Using a 1000 kN force applied at the top of the structures and alternating between pinned (Figure 4-15a) and rigid (Figure 4-15b) connection in the moment resisting frame, it was determined that the contribution of MRF in case of 6 storey structure was about 25%, 27% for the 12 storey structure and 53% for 18 storey structure (acc. Figure 4-16).

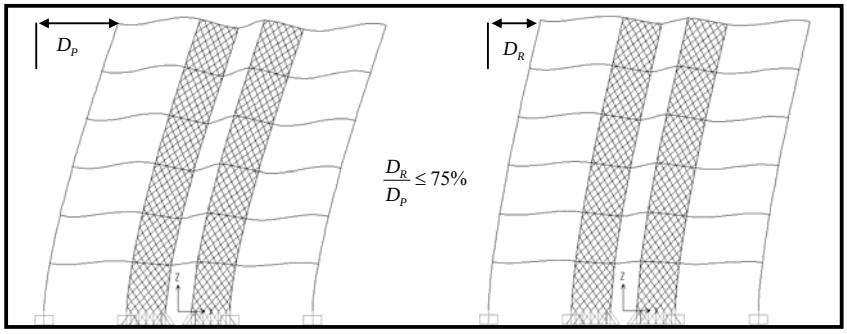

Figure 4-16 – Contribution of MRF, in %

4.5.2. Performance Based Seismic Evaluation (PBSE)

4.5.2.1. Scope and definition

Performance-based seismic evaluation is a new approach that couples the structural damage or performance with the ground shaking hazard. It aims to avoid the prescriptive approach currently prevailing in the seismic codes worldwide and promotes the use of nonlinear analysis techniques in order that seismic demands at different levels of intensity of seismic ground motion can be reliably estimated. The corresponding multi-level structural and non-structural performance objectives are

explicitly specified in compliance with the needs and interests of the society and individual stakeholders. A performance level is an expression of the maximum desired extent of damage to a building. There is a minimum level of protection demanded by society to safeguard adequately against various types of collapse or falling hazards that endanger human lives. It is widely acknowledged that seismic design explicitly should consider multiple performance objectives but the number and the definition of the objectives may vary from author to author. They range from a minimum two levels but there are also methodologies that propose four levels. The most widely known documents are Vision 2000 (SEAOC, 1995 [58]), FEMA 273 [42] and ATC-40 (1996) [59].
In Vision 2000 [58] document, efforts have been made in relating performance levels to structural and nonstructural damage. For example, damage descriptions are available to aid the designer in validating that performance levels are being met. They contain descriptions of behavior meeting an established performance level. For example, in the case of primary steel moment frames, the life safety seismic performance level includes "formation of plastic hinges; local buckling of some elements; severe joint distortion; isolated connection failures; and a few elements with a chance of experiencing fracture". While these tabular descriptions are very useful for qualitative assessment, the structural engineer needs much more quantitative performance measures. The Vision 2000 [58] document defines four performance levels:
1. Fully Operational, where the facility continues in operation with negligible damage after frequent events.
2. Operational, in which the facility sustains minor damage and minor disruption in non-essential services after occasional seismic events.
3. Life Safe, where life-safety is substantially protected and damage to the structure is moderate to extensive after the rare event.
4. Near Collapse, in which life-safety is at risk, damage to the structure is severe, but structural collapse is prevented after the very rare earthquake.

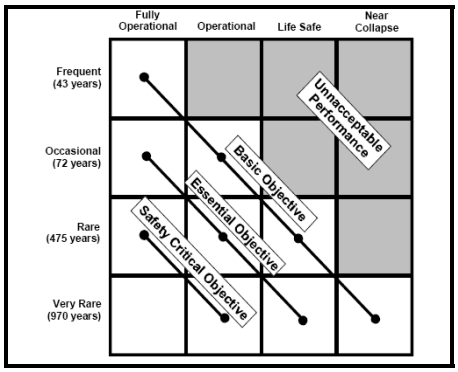

Figure 4-17 – Performance Objective and Hazard Level Matrix for Seismic Events [58]

In parallel with the Vision 2000 [58] effort, the U.S. Federal Emergency Management Agency funded a large project to develop national guidelines for the seismic rehabilitation of buildings. This project resulted in the FEMA 273 (1996) [42] reports, which later were reevaluated and modified, and then published as an ASCE Standard. FEMA 273 [42] defines performance levels somewhat differently, but in

concept use a very similar framework. The importance of the building is tied in with the notions of "basic," "essential" (such as hospitals and police stations), "hazardous" (containing hazardous materials, but of confined impact), and "safety critical" (such as buildings containing explosives and radioactive materials).

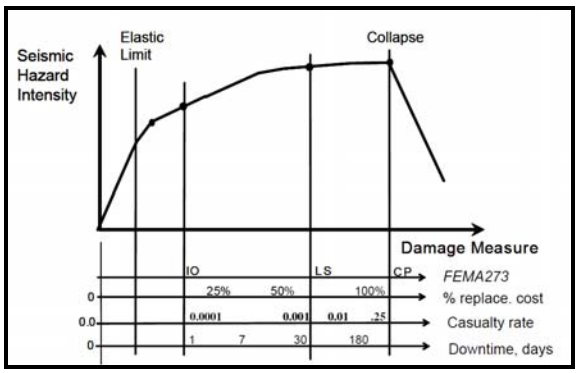

Figure 4-18 - Conceptual relationship between seismic hazard intensity and structural performance

The performance-based framework is similar to that of Vision 2000 [58], i.e., it associates discrete performance levels with discrete hazard levels, but it uses somewhat different hazard levels (50/50, 20/50, 10/50 and 2/50) and defines the performance levels as operational, immediate occupancy (IO), life safety (LS) and collapse prevention (CP).

In parallel with the FEMA [42], the State of California commissioned the development of seismic evaluation and retrofit guidelines for existing reinforced concrete structures. This project resulted in the ATC-40 [59] document. The PBEE framework is again similar to that of Vision 2000 [58]. Like any other PBSE approach, implementation strongly depends on the ability to predict seismic demands, such as storey drifts and plastic hinge rotation demands. As mentioned in the preceding paragraph, the pushover analysis has become the method of choice for many structural engineers. In the ATC-40 [59] document the prediction of the target displacement is based on the capacity spectrum method.

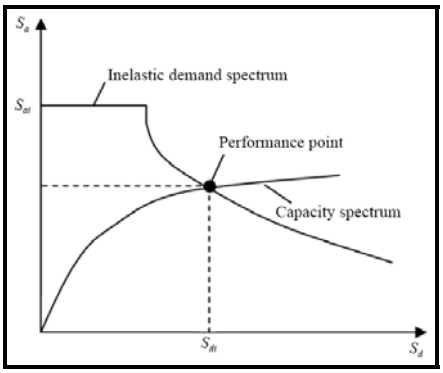

Figure 4-19 - Illustration of capacity spectrum method

The Eurocode 8 [40] has similarities with the U.S. documents referred above but also distinct differences. It states two explicit performance objectives: (a) to protect life under a rare seismic action, by preventing collapse of the structure or parts thereof and maintaining structural integrity and residual load capacity, and (b) to reduce property loss due to a frequent event, by limiting structural and nonstructural damage. The no-local-collapse performance objective is achieved by dimensioning and detailing structural elements for a combination of strength and ductility, with a defined safety factor, against a substantial loss of gravity load capacity and lateral load resistance. The damage limitation performance objective is achieved by limiting overall deformations (lateral displacements) of the system to levels acceptable for the integrity of all its parts (including nonstructural ones). The Eurocode [40] specifies spectral shapes, but does not specify hazard levels for the two performance objectives, because the choice of the level of safety and serviceability is left to the discretion of the national members. The recommendation is to use a 10/50 hazard (475 years return period) for collapse prevention and a 10/10 hazard (95 years return period) for damage limitation. In the Romanian Seismic Code P100-1/2006 [47], the hazard is 30 years for the damage limitation and 100 years for collapse prevention. Apart from the two basic performance levels - limit state defined in EN1998 [40], the collapse prevention is also introduced, with the hazard defined by a 475 years return period. In the design process for strength and ductility, the EN1998 [40] employs a behavior factor q, however, it explicitly incorporates the overstrength by incorporating the ratio of structure strength at mechanism to structure strength at first plastic hinge formation.
In this study, three performance levels or limit states were defined (similar to P100/2006) [47] :
- Serviceability limit state (SLS)
- Ultimate limit state (ULS)
- Collapse prevention limit state (CPLS).

The performance objective (Figure 4-20) is described as the combination of an expected performance level with expected levels of hazard (e.g. ground motion).

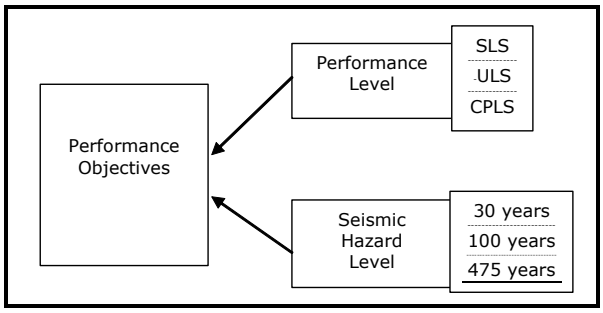

Figure 4-20 – Performance objectives

The seismic hazard and acceptance criteria are discussed and defined below.

4.5.2.2. Seismic hazard

The first aspect to PBSE is the definition of the expected hazard level that may occur at the given site. The seismic hazard is described thru the peak ground acceleration

corresponding to a recurrence interval (or to the probability of exceeding the peak ground acceleration in 50 years). The recommended recurrence intervals considered for the performance base seismic evaluation of the buildings is given in Table 4-4 (P100 part 3-2006 [60]).

Table 4-4 – Average recurrence interval of recommended peak ground acceleration used in performance base seismic evaluation of the buildings and the corresponding probability of exceeding it in 50 years

Frequency	Recurrence Interval [years]	Probability of excedance in 50 years [%]
Frequent	30	80
Occasional	100	40
Rare	475	10

The design seismic hazard is that corresponding to life safety performance level (ULS). Table 4-5 shows the simplified coefficients for conversion of the peak ground acceleration (PGA) corresponding to a recurrence interval (IR) of 100 years to values of PGA corresponding to IR of 30 and 475 years.

Table 4-5 – Simplified coefficients for conversion of PGA for seismic hazards

Seismic source	a_g(30 years)/ a_g(100 years)	a_g (475 years)/ a_g(100 years)
Vrancea	0.5	1.50

Figure 4-21 shows the elastic design spectrum for the 100 years recurrence interval. For the recurrence intervals of 30 years and 475 years, the design spectra are obtained by using the conversion coefficients shown in Table 4-5.

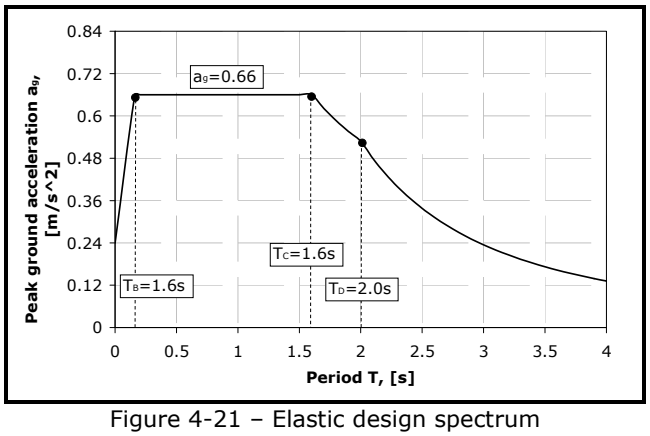

Figure 4-21 – Elastic design spectrum

In order to include the variations in ground motion characteristics, 6 earthquake records were selected to be used in the numerical investigation. Earthquake records with differing intensities are expected to produce different levels of ductility demands (such as interstorey drift) on a particular wall system. The 6 ground motions were selected from the main 3 Vrancea earthquakes of 04.03.1977,

30.08.1986 and 30.05.1990 and were recorded by different stations located in Romanian capital Bucharest. Table 4-6 presents the earthquakes magnitude and corresponding recording stations and components.

Table 4-6 – Vrancea earthquake records for T_C=1.6s accelerograms

Earthquake	Magnitude,M_w*	Station	Comp.	Abbreviation
Vrancea, 4.03.1977	7.5	B- INCERC	NS	VR77-INC-NS
Vrancea, 0.08.1986	7.2	B- EREN	N10W	VR86-ERE-N10W
		B-Magurele	NS	VR86-MAG-NS
Vrancea30.05.1990	6.9	B-Armeneasca	S3E	VR90-ARM-S3E
		B- INCERC	NS	VR90-INC-NS
		B-Magurele	NS	VR90-MAG-NS

Table 4-7 – Characteristics of the original records, T_C=1.6 accelerogram set

Record	PGA, m/s^2	PGV, m/s^2	EPA, m/s^2	EPV, m/s^2	T_c, s	T_d, s
VR77-INC-NS	-1.949	-0.712	2.373	0.535	1.42	2.02
VR86-ERE-N10W	1.56	0.144	1.364	0.157	0.72	1.85
VR86-MAG-NS	-1.355	0.223	1.284	0.21	1.03	1.52
VR90-ARM-S3E	0.557	-0.047	0.562	0.045	0.5	1.58
VR90-INC-NS	0.373	-0.064	0.307	0.04	0.81	1.87
VR90-MAG-NS	-0.896	0.047	0.868	0.043	0.31	4.29

The set denoted with T_C=1.6 (see Table 4-6) was based on EPA≥0.9 m/s^2, and T_C approximate 0.6 sec criteria, but there were not enough records with these parameters. Initially, this set of records denoted as T_C=1.6 (see Table 4-6), were selected to manifest 6 accelerograms with corner period of 1.6s and a minimum EPA of 0.9m/s^2 from the seismic source Vrancea, but there were not enough. Therefore, semi-artificial accelerograms were derived from six original accelerograms recorded in Bucharest, and oriented approximately in the N-S direction (see Table 4-7) (Figure 4-22,a).

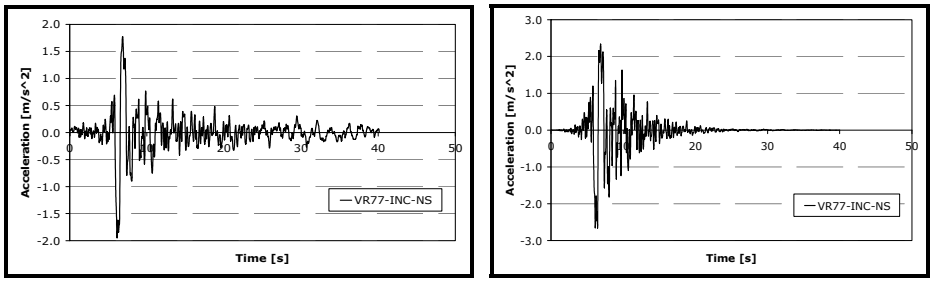

(a) (b)

Figure 4-22 – Vrancea 1977, INCERC station, N-S component: a) Original ground motion; b) Scaled ground motion

Figure 4-23 and Figure 4-24 show the maps with levels of peak ground acceleration for 100 years and 475 years, while Figure 4-25 shows the distribution of corner periods during last strong earthquakes. Table 4-7 shows in detail the characteristics of the original ground motion records for T_c=1.6 accelerogram sets.

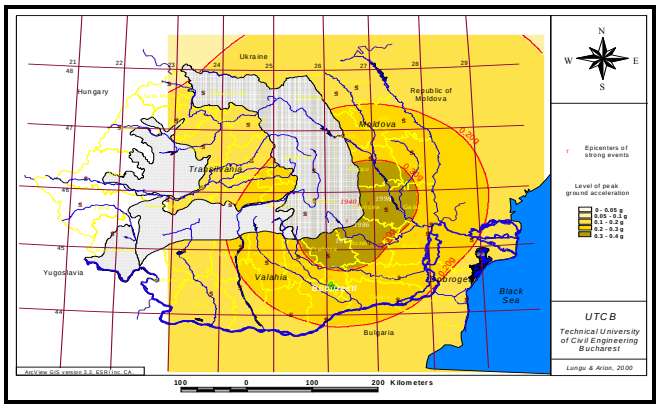

Figure 4-23 - Level of peak ground acceleration for 100 years and epicenters of strong events, Lungu&Arion, 2000 [61]

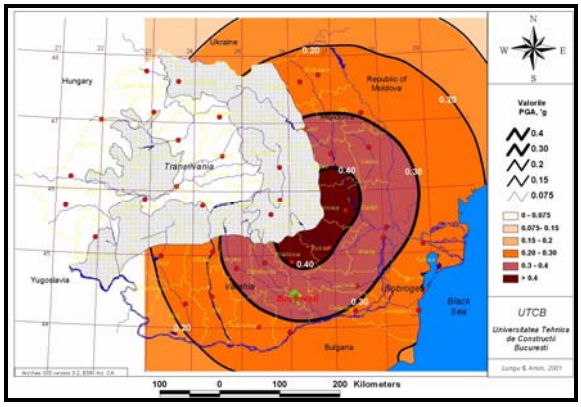

Figure 4-24 - Level of peak ground acceleration for 475 years, Lungu&Arion, 1999 [62]

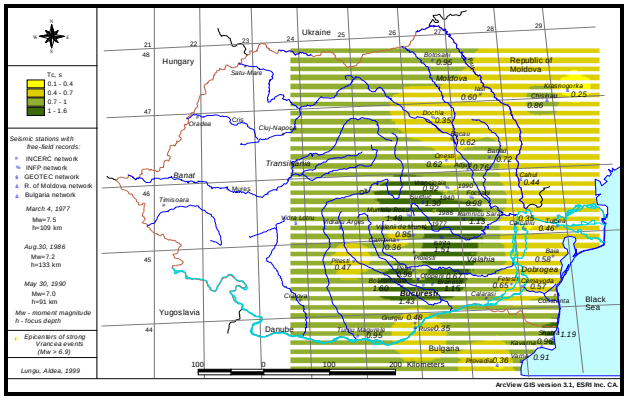

Figure 4-25 –Corner periods distribution for the strong seismic motion recorded in 1977, 1986 and 1990

The starting point was SIMQKE-1 software [63], used for generation of compatible artificial accelerograms with an elastic target spectrum. The calculus procedure is based on a relationship between the response spectrum ordinate and Fourier amplitudes of the ground motions which must be generated, proposed by Vanmarcke [63]. This procedure was modified in order to generate semi-artificial accelerograms, obtained by modification of an existing record such as its spectra to be compatible with targeted one. The results are presented in Figure 4-25b and Figure 4-26.
A smooth elastic spectrum in EC8 [40] format was associated to each of the accelerogram set: T_B=0.16, TC=1.6, T_D=2.0 sec for Bucharest soil conditions.

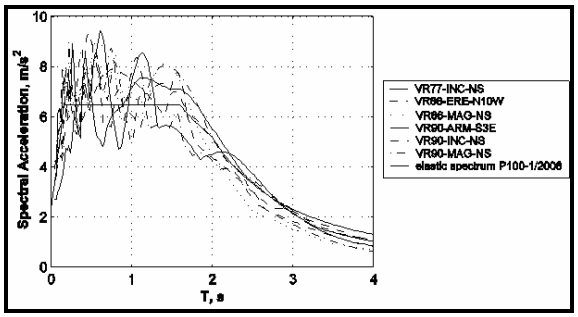

Figure 4-26 - Elastic response spectra of semi artificial records and EN1998 [40] elastic spectrum

4.5.2.3. Performance Levels

The performance levels of the buildings describe the expected seismic performance through level of degradations, economic losses and functionality problems. A performance level is an expression of the maximum desired extent of damage to a building. Thus, the Romanian seismic code P100-2006 [47] recommends taking into account tree performance levels (or limit states):
Serviceability limit state (SLS) - the facility sustains minor damage and minor disruption in non-essential services after occasional seismic events (damage control).
This performance level is defined as the post earthquake damage state in which only limited structural damage has occurred. Damage is anticipated to be so slight that it would not be necessary to inspect the building for damage following the earthquake, and such little damage as may be present would not require repair. The basic vertical-and lateral-force-resisting systems of the building retain nearly all of their pre-earthquake strength and stiffness. The risk of life-threatening injury as a result of structural damage is very low. Buildings meeting this performance level should be safe for immediate post earthquake occupancy, presuming that damage to nonstructural components is suitably light and that needed utility services are available.
In order to be used in analysis, quantitative acceptance criteria need to be provided. Based on the results of the experimental tests, the acceptance criteria can be considered the limit of elastic behavior of the infill plates, which is associated to a transient storey drift of 0.5%. Main structural elements suffer no damages (or very slightly), therefore no limiting local acceptance criteria need to be provided.

Ultimate limit state (ULS) - life-safety is substantially protected and damage to the structure is moderate to extensive after the rare event.
This level is a damage state in which significant damage has been sustained, although some margin remains against either partial or total collapse. In FEMA 273 [42] this margin is taken as 1/3. That is, it is anticipated that a ground motion level that is 1/3 larger than that which results in the Life Safety performance level for a building would be required to bring the building to the Collapse Prevention level. In FEMA 302 [64], this margin is taken as ½, i.e., it is believed that buildings designed for Life Safety performance can experience approximately 50% greater motion before they reach the Collapse Prevention level. For the evaluation of buildings for the Life Safety performance level is done by interpolating between the acceptance criteria provided for the Collapse Prevention and Immediate Occupancy levels.
Based on the results of the experimental tests and also on the provisions of P100/2006 [47], a transient storey drift of 2.5% can be associated to this level as a global parameter. Damage control needs to be included also in the verification of the acceptance of the performance level. As presented in paragraph 4.4 and 3.5, for 2.5% storey drift, the damage state of the infill plates is minor, and cracks are just initiated at the corners. At the same storey drift, plastic hinges take place in beams but the plastic rotation demand is reduced (2% storey drift represents the onset of yielding). If plastic hinges take place in beams, the permissible plastic rotation shall be limited to $3\theta_y$, where θ_y is the beam yield rotation. If partial strength connections are used, the plastic hinges takes place in connection and the permissible plastic rotation shall be limited to 0.025rad. Observations after the experimental tests shown in chapter 3, limited plastic rotations develop in connections between boundary beams (HBE) and columns (VBE) up to 2.5% storey drift. The same limits of plastic rotations can also be used for moment frames outside the braced bays.

Collapse prevention limit state (CPLS) - life-safety is at risk, damage to the structure is severe, but structural collapse is prevented after the very rare earthquake
The Collapse Prevention structural performance level is defined as the post earthquake damage state in which the structure is on the verge of experiencing partial or total collapse. Substantial damage to the structure has occurred, potentially including significant degradation in the stiffness and strength of the lateral-force-resisting system, large permanent lateral deformation of the structure, and, to a more limited extent, degradation in the vertical-load-carrying capacity. However, all significant components of the gravity-load-resisting system must continue to carry their gravity-load demands. The structure may not be technically or economically practical to repair and is not safe for re-occupancy; aftershock activity could credibly induce collapse.
Based on the results of the experimental tests (see paragraphs 4.4 and 3.5), a transient storey drift of 4.0% corresponds to a major state of damage but the maximum capacity is not attained, and shall be used as a global parameter associated to this level. If plastic hinges take place in beams, the permissible plastic rotation shall be limited to $4\theta_y$, where θ_y is the beam yield rotation. If partial strength connections are used, the permissible plastic rotation shall be limited to 0.035rad. Observations after the experimental tests shown in chapter 3 limited plastic rotations develop in connections between boundary beams (HBE) and columns (VBE) up to 2.5% storey drift. The same limits of plastic rotations can also be used for moment frames outside the braced bays.

Table 4-8 – Structure 1st to 3rd mode periods

Performance level		SLS	ULS	CPLS
Damage state				
Drift		0.5%	2.5%	4%
Plastic deformations	Beams	-	$3\theta_y$	$4\theta_y$
	Connections	-	0.025rad	0.035rad

4.5.2.4. Analysis procedures

The final ingredient necessary for PBSE is a mean to verify that the design is meeting the performance objectives. Some of the difficulty in implementing PBSD in the past was the result of limited computational power and analytical tools. One can surmise that the analysis employed to validate achievement of the life-safe performance level during the very rare earthquake might involve a nonlinear static pushover analysis or nonlinear time-history analysis. To the contrary, assessment that the degradation limit level is being met during the frequent earthquake may involve elastic time-history analysis or even a linear static lateral load analysis. Therefore, the verification of performance may require significantly different analysis methods and/or analytical assumptions (e.g. damping levels). Once these analyses have been carried out, the engineer is left with the need to assess satisfaction of performance objectives using information obtained through the analysis.
Several methodologies have been developed in order to analyze structural models so as to estimate the demand from a seismic action and to determine the level of seismic intensity that may cause a structure to exceed a certain limit state or performance level.
As linear procedures can't estimate the post-elastic behavior associated to life safety (LS) and collapse prevention performance levels, the static and dynamic nonlinear procedures are more appropriate. These procedures are used also in case of torsional irregularities and non-orthogonal systems of buildings.
The term "nonlinear" in nonlinear analysis procedures implies explicit material nonlinearity or inelastic material response, but geometric nonlinearity may also be included. Geometric nonlinearities play a fundamental role in the global response of the structure when the occurrences of large deformation in the structural elements induce displacements not more proportional to the loads effectively applied. Involving both local and global aspects, three are the most important sources of geometric nonlinearities: the beam-column effects, the large displacement/rotation effects and the P-delta effects.

4.5.2.5. Nonlinear Static Procedure

Nonlinear static procedures have seen a growing interest in the seismic design of buildings. One of the several procedures developed, mainly as an alternative to more advanced nonlinear time history analysis is the static nonlinear procedures used by the Performance Based Evaluation or Design (PBSE, PBSD). One of the most known methods of the static nonlinear analysis is the N2 method [65].
In this procedure, the comparison between the seismic demand and the capacity is made in terms of displacements by applying the equivalent single degree of freedom (SDOF) substitution approach and by plotting a force-displacement curve, namely

the "capacity curve", or a spectral acceleration-displacement curve, namely the "capacity spectrum".
This method may be used for any structure and any performance level with some limitations. The procedure should not be used for structures in which higher-mode effects are significant. Higher-mode effects shall be considered significant if the shear in any storey calculated from the analysis with 90 percent mass participation exceeds 130 percent of the corresponding storey shear from the analysis considering only the first mode response.
According to NSP, the model that incorporates the inelastic response is pushed to a certain displacement, called "target displacement", and the forces and deformations are evaluated. The target displacement represents the maximum displacement to be experienced during the design earthquake.
In the following is given a brief description of how to determine the target displacement for nonlinear static analysis (N2 procedure) (P100-2006-Annex [47]).

Step 1 - *General*

The target displacement is determined from the elastic response spectrum. The capacity curve, which represents the relation between base shear force and control node displacement, is determined in accordance with EN 1998 [40]**.** The following relation between normalized lateral forces F_i and normalized displacements Φ_i is assumed:

$$\overline{F}_i = m_i \Phi_i \tag{4.3}$$

where m_i is the mass in the *i*-th storey.

Displacements are normalized in such a way that $\Phi_n = 1$, where *n* is the control node (usually, *n* denotes the roof level). Consequently, $F_n = m_n$.

Step 2 - *Transformation to an equivalent Single Degree of Freedom (SDOF) system*

The mass of an equivalent SDOF system m^* is determined as:

$$m^* = \sum m_i \Phi_i = \sum \overline{F}_i \tag{4.4}$$

and the transformation factor is given by:

$$\Gamma = \frac{m^*}{\sum m_i \Phi_i^2} = \frac{\sum \overline{F}_i}{\sum \left(\frac{\overline{F}_i^2}{m_i} \right)} \tag{4.5}$$

The force F^* and displacement d^* of the equivalent SDOF system are computed as :

$$F^* = \frac{F_b}{\Gamma}, \quad d_t = \frac{d_n}{\Gamma} \tag{4.6}$$

where F_b and d_n are, respectively, the base shear force and the control node displacement of the Multi Degree of Freedom (MDOF) system.

Step 3 - Determination of the idealized elastic-perfectly plastic force – displacement relationship

The yield force F_y^*, which represents also the ultimate strength of the idealized system, is equal to the base shear force at the formation of the plastic mechanism. The initial stiffness of the idealized system is determined in such a way that the areas under the actual and the idealized force – deformation curves are equal (Figure 4-27). Based on this assumption, the yield displacement of the idealized SDOF system d_y^* is given by:

$$d_y^* = 2\left(d_m^* - \frac{E_m^*}{F_y^*}\right) \tag{4.7}$$

where E_m^* is the actual deformation energy up to the formation of the plastic mechanism.

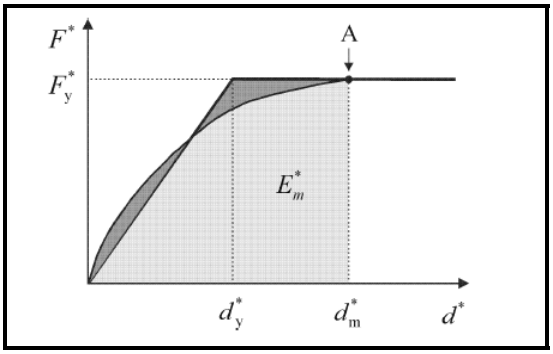

Figure 4-27: Determination of the idealized elastic - perfectly plastic force – displacement relationship.

Step 4 - *Determination of the period of the idealized equivalent SDOF system*

The period T^* of the idealized equivalent SDOF system is determined by:

$$T^* = 2\pi\sqrt{\frac{m^* d_y^*}{F_y^*}} \tag{4.8}$$

Step 5 - *Determination of the target displacement for the equivalent SDOF system*

The target displacement of the structure with period T^* and unlimited elastic behavior is given by:

$$d_{et}^* = S_e\left(T^*\right)\left[\frac{T^*}{2\pi}\right]^2 \tag{4.9}$$

where $S_e(T^*)$ is the elastic acceleration response spectrum at the period T^*.

For the determination of the target displacement d_t^* for structures in the short-period range and for structures in the medium and long-period ranges different expressions should be used as indicated below. The corner period between the short and medium period range is T_C (see Figure 3.1 and Tables 3.2 and 3.3 from [40]).

a) $T^* < T_C$ (short period range)

If $F_y^* / m^* \geq S_e\left(T^*\right)$, then response is elastic and thus

$$d_t^* = d_{et}^* \tag{4.10}$$

If $F_y^* / m^* < S_e\left(T^*\right)$, then response is nonlinear and

$$d_t^* = \frac{d_{et}^*}{q_u}\left(1 + \left(q_u - 1\right)\frac{T_C}{T^*}\right) \geq d_{et}^* \tag{4.11}$$

where q_u is the ratio between the acceleration in the structure with unlimited elastic behavior $S_e(T^*)$ and in the structure with limited strength F_y^*/m^*.

$$q_u = \frac{S_e\left(T^*\right) m^*}{F_y^*} \tag{4.12}$$

b) $T^* > T_C$ (medium and long period range)

$$d_t^* = d_{et}^* \tag{4.13}$$

d_t^* need not exceed 3 d_{et}^*

The relation between different quantities can be visualized in Figures B.2 a) and b). The figures are plotted in acceleration - displacement format. Period T^* is represented by the radial line from the origin of the coordinate system to the point at the elastic response spectrum defined by coordinates $d^* = S_e(T^*)(T^*/2\pi)2$ and $Se(T^*)$.

Iterative procedure (optional)

If the target displacement d_t^* determined in the 4th step is much different from the displacement d_m^* (Figure 4-28) used for the determination of the idealized elastic-perfectly plastic force – displacement relationship in the 2nd step, an iterative procedure may be applied, in which steps 2 to 4 are repeated by using in the 2nd step d_t^* (and the corresponding F_y^*) instead of d_m^*.

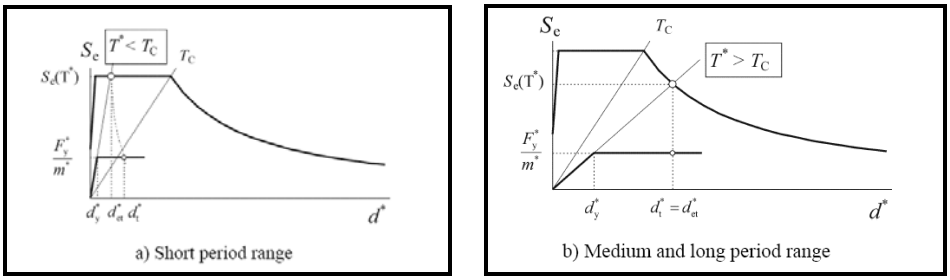

Figure 4-28 - Determination of the target displacement for the equivalent SDOF system

Step 6 - Determination of the target displacement for the MDOF system. The target displacement of the MDOF system is given by:

$$d_t^* = \Gamma d_t \tag{4.14}$$

4.5.2.6. Nonlinear Dynamic Procedure

In order to estimate structural performance under seismic loads, an incremental dynamic analysis IDA was employed [66]. The IDA approach is new methodology which can give a clear indication of the relationship between the seismic capacity and the demand. With respect to seismological intensity measures (IM), such as peak ground acceleration, engineers can estimate principal response quantities in terms of governing engineering demand parameters (EDP), such as the maximum deflection or drift of the structure. The IDA approach involves performing nonlinear dynamic analyses of a structural system under a suite of ground motion records, each scaled to several IM levels designed to force the structure all the way from elastic response to final global dynamic instability (collapse).

While it is a simple concept, performing an IDA requires several important steps:

Step 1 – Select the models for the structure under investigation.

Step 2 - Select a suite of ground motion records.

Step 3 - For each record, incrementally scale it to multiple levels and run a nonlinear dynamic analysis each time. Stop incrementing when numerical non-convergence is first encountered.

Step 4 - Select a ground motion Intensity Measure IM (e.g., Sa(T1,5%), the 5%-damped first-mode spectral acceleration) and a Damage Measure DM (e.g., q_{max}, the maximum over all storeys peak interstorey drift ratio) and post-process the results of the dynamic analyses.

As described above, the dynamic analysis involves scaling of the seismic records. In the Table 4-9 is presented the scaling coefficient necessary to obtain the level of records for the 3 performance levels.

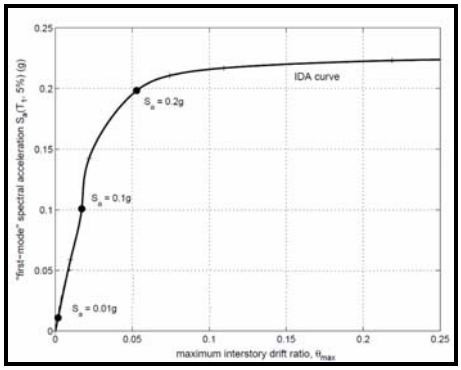

Figure 4-29 - IDA curve

Table 4-9 – Response spectrum multiplier

Performance Level	P100-2006		Conversion Coefficient, λ
	MRI	PE	
IO (SLS)	30	80	0.5
LS (ULS)	100	40	1.0
CP (CPLS)	475	10	0.5

4.6. Results

4.6.1. Nonlinear static analysis

The nonlinear response of the structures was analyzed using N2 method (paragraph 4.5.2.5). In Figure 4-30 is presented the structures modeled with equivalent strips members.

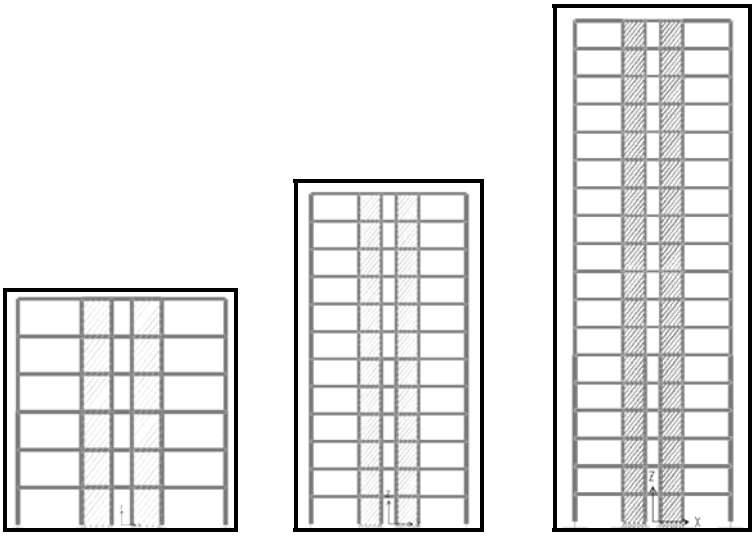

Figure 4-30 – Structures with strip model for static nonlinear analysis

In order to reduce the amount of analysis, the modeling of the structures for static nonlinear analysis was made using the dual strip model with the specifications that the strip elements used in SAP2000 [52] had the axial compression behavior restricted.
The results of the push-over analysis (Figure 4-31) have shown the main columns adjacent to the steel plates are too weak to resist against the axial load developed in the structure. This is a problem reported by other investigations on this type of systems. One solution can be the increase of the column sections in order to be able to resist against axial load. But, the increase in column section can be done till a point because this increase draws more axial force. Thus, a solution of this problem is to raise the material resistance of the column steel from S355 to S460 (our papers, [67], see 6.3). This solution alleviates the amplification of the column stiffness and offers the possibility to raise the resistance against axial loads.

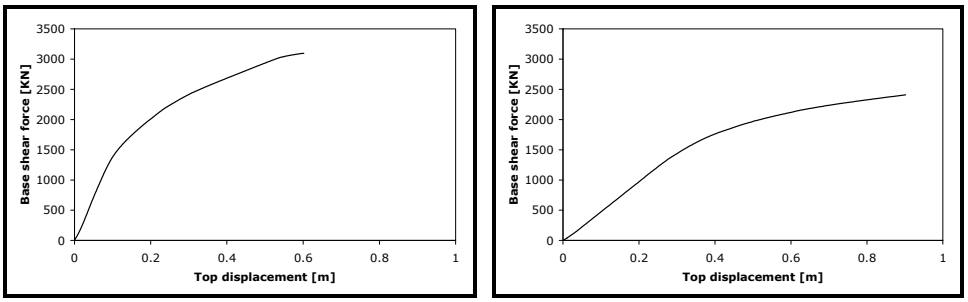

(a) (b)

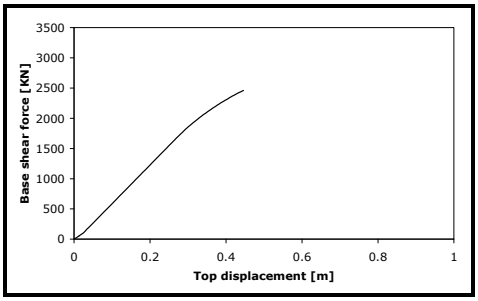

(a)

Figure 4-31 – 6 storey a); 12 storey b); 18 storey structures c)

The results with the new cross-section of the structural members are given in Figure 4-32. It can be seen that the columns adjacent to the SPSW were very much increased which led to increase in MRF elements after case.

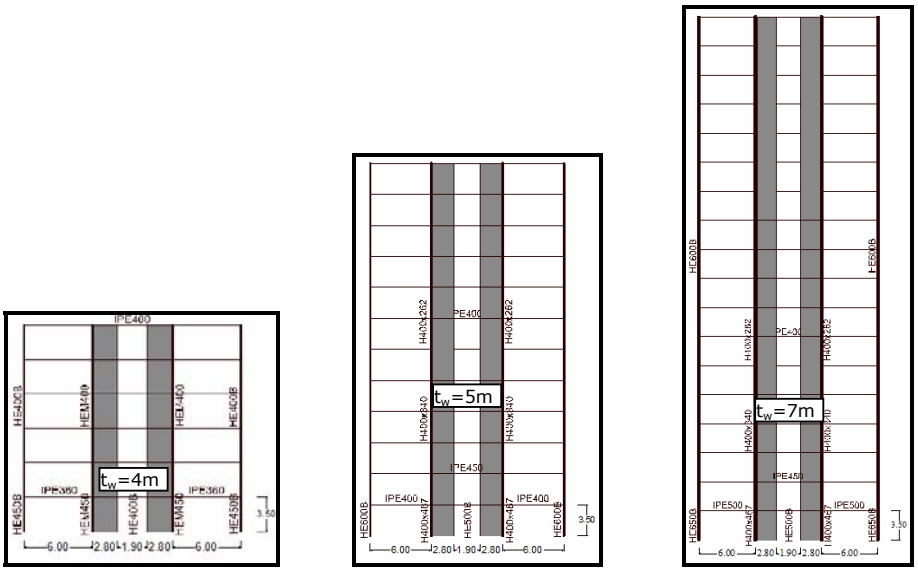

(6 storey) (12 storey) (18 storey)

Figure 4-32 – New structural systems

Figure 4-33, Figure 4-34 and Figure 4-35 plot the result of push-over analysis in terms of base shear force versus top displacement. Both structures with rigid connections and pinned connections between HBE and VBE show similar values of initial stiffness. The strength of the structures with rigid beam to column connections is higher with approximately 12% in each case. Using the N2 methodology, the target displacement for each performance level has been determined and shown in the figures. The yielding of the structures, taken as the point where the initial stiffness drops for the first time, takes place almost in the same time with the attainment of serviceability limit state (also observed in experimental tests).

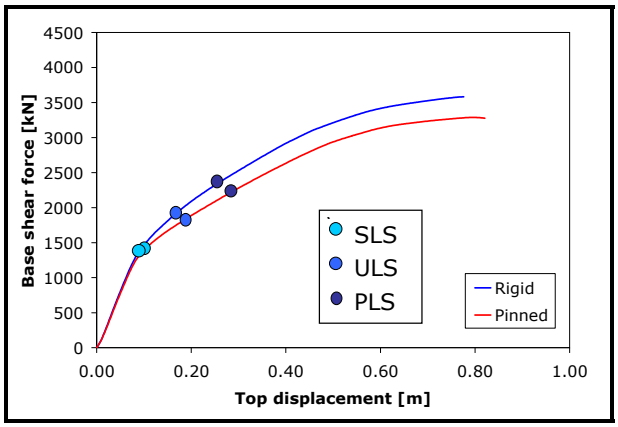

Figure 4-33 – Target displacement for 6 storey frame (N2 method)

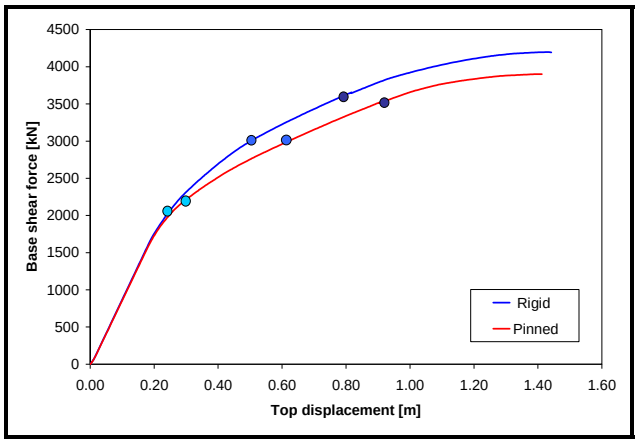

Figure 4-34 – Target displacement for 12 storey frame (N2)

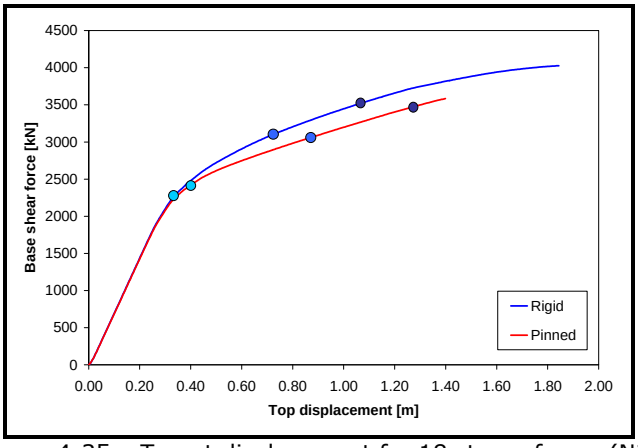

Figure 4-35 – Target displacement for 18 storey frame (N2)

Table 4-10 shows the values of target displacement, D_t, for the studied frames, calculated using N2 procedure. The target displacements of the pinned structures are slightly higher with approximately 10% than of the structures with rigid beam to column connections.

Table 4-10 – Target displacements for the 6 structures

	6		12		18	
Levels	Rigid	Pinned	Rigid	Pinned	Rigid	Pinned
SLS	0.095	0.106	0.252	0.302	0.383	0.423
ULS	0.190	0.212	0.505	0.605	0.766	0.890
CPLS	0.286	0.318	0.791	0.921	1.150	1.320

Figure 4-36 show the calculation of target displacement for SLS, ULS and CPLS of 6 storey structure with rigid and pinned joint.

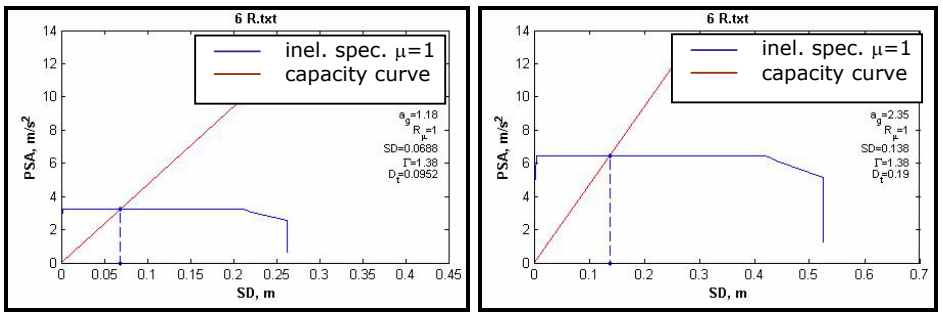

(a) (b)

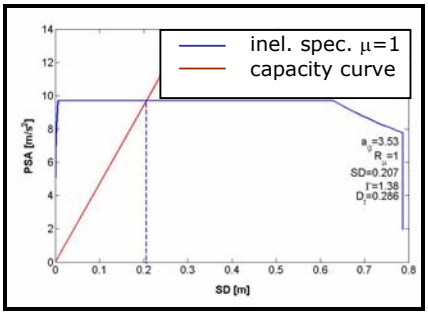

(c)

Figure 4-36 - D_t for 6 storey structure, rigid joint: a) SLS; b) ULS; c) CPLS

Figure 4-3, Figure 4-38 and Figure 4-39 present the plastic hinges mechanism up to the target points.

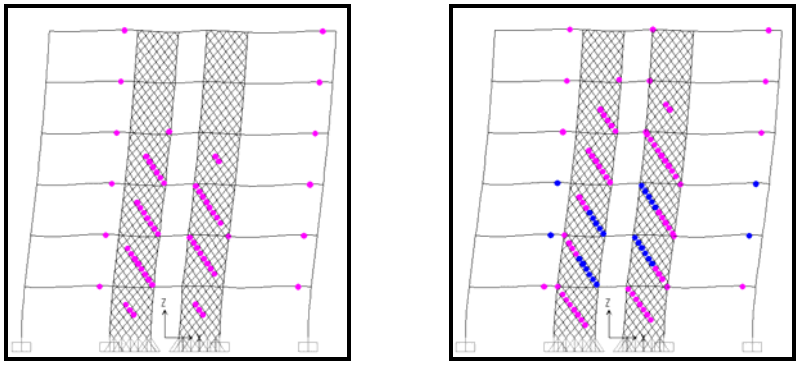

(ULS) (Rigid) (CPLS)

Figure 4-37 – Plastic hinges at ULS and CPLS for 6 storey structures

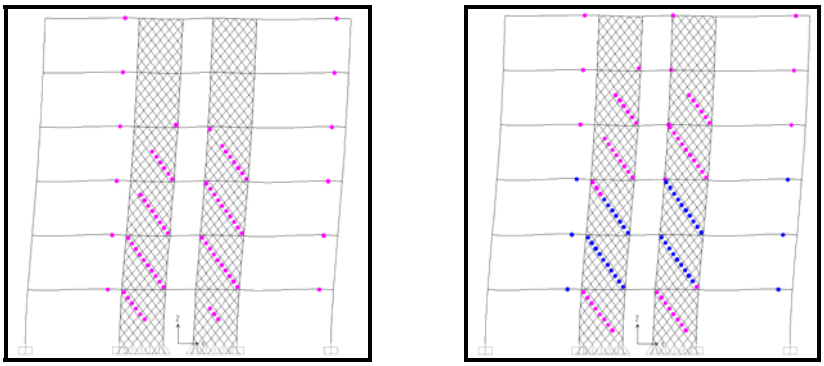

(ULS) (Pinned) (CPLS)

Figure 4-37– (Continued)

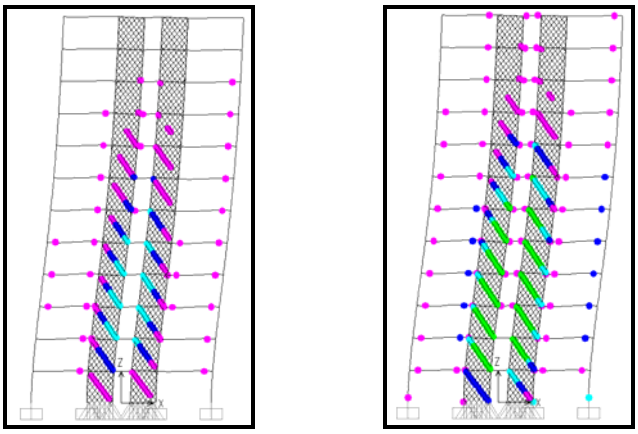

(ULS) (Rigid) (CPLS)

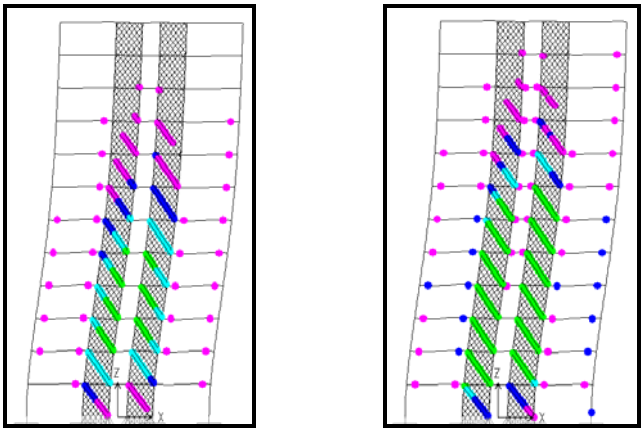

(ULS) (Pinned) (CPLS)

Figure 4-38 - Plastic hinges at ULS and CPLS for 12 storey structures

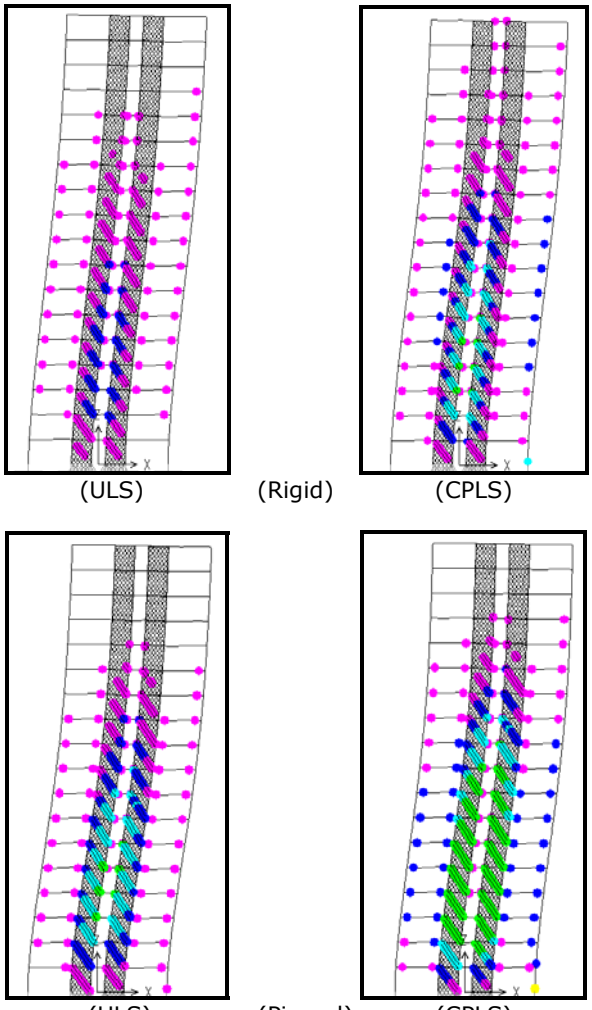

Figure 4-39 - Plastic hinges at ULS and CPLS for 18 storey structure: rigid and pinned

All structures satisfy the criteria for life safety performance level which states that no plastic hinges should be recorded before SLS with the exception of the 6 storey structure with rigid and pinned connection and pinned joints 12 storey structure. Plastic deformation demands in beams are more severe for the structures with pinned beam to column connection compared to the rigid one. The plastic mechanisms develop almost on entire height of the structures. Shear wall frames show a very good ductility and provide a high stiffness for the structures. For the six storey structures, no plastic hinges are recorded in columns, while for 12 and 18 storey buildings plastic hinges are recorded at the bottom part of the first storey columns only at collapse prevention limit state. Also, plastic hinge was recorded in the second storey outer column just for 18 storey structure with pinned connection.

This shows that in case of higher buildings, when the contribution of the gravity loads (i.e. dead loads, live loads) is lower, the Ω factor is more effective in design of non-dissipative members.

Table 4-11 – Plastic hinge values of the elements

	Storey	6		12		18	
	Elements	Beam	Column	Beam	Column	Beam	Column
Rigid	SLS	0.006	-	-	-	-	-
	ULS	0.015	-	0.013	-	0.0105	-
	CPLS	0.025	-	0.024	0.001	0.022	0.002
	Levels						
Pinned	SLS	0.007	-	0.003	-	-	-
	ULS	0.018	-	0.018	-	0.015	0.0007
	CPLS	0.029	-	0.030	0.002	0.025	0.004

Asdasd Table 4-11 presents the plastic hinge values developed in beams and columns during till the attainment of each performance level. Structures designed using the dissipative approach, may experience structural damage even under moderate (SLS) earthquakes. This can be clearly seen in the table, for both cases of connections, of the 6 storey structure. Plastic deformations in the dissipative members indicate a moderate damage to the structures at serviceability limit state (SLS).

4.6.2. Incremental dynamic analysis

Having the semi-artificial accelerograms, it can be shown the amount of influence that the ground motions will have on the structures Figure 4-40. It can be seen that the structures having 6 and 12 storeys have the first 3 periods of vibration in the acceleration sensitive zone (between T_B and T_C). The 18 storey structure has the 1st period of vibration in the displacement sensitive zone (beyond T_D) while the 2nd and the 3rd periods in the acceleration sensitive zone. Thus, the 18 storey structure will be much more sensitive to higher modes of vibration as they tend to be amplified significantly.

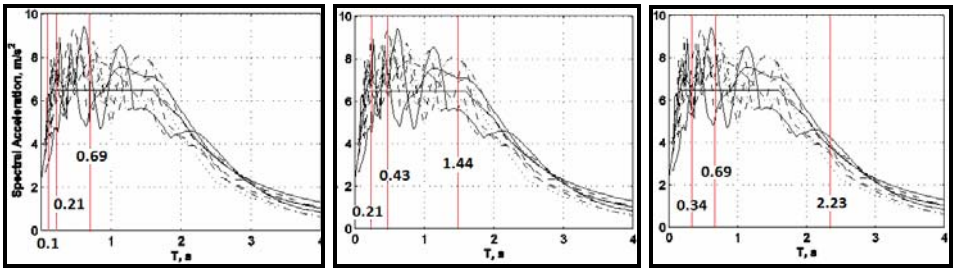

(a) (b) (c)

Figure 4-40 – Structures periods versus spectral acceleration – T curves

Table 3-12 presents the 1st, 2nd and 3rd fundamental mode period of the structures.

Table 4-12 – Structure 1st to 3rd mode periods

Storey	T1 [s]	T2 [s]	T3 [s]
6	0.69	0.21	0.10
12	1.44	0.43	0.21
18	2.23	0.69	0.34

Dynamic time historey inelastic analyses were carried out for the 6 selected earthquake records using the nonlinear structural analysis program SAP2000 [52]. One part is done by assessing the behavior of the structure for the three important levels of performance characterized by the ground motion intensity a_g with the corresponding intensity factor λ. Figure 4-41 plots Vrancea 1977 ground motion, scaled down to SLS by a factor λ=0.5 and up to CPLS by a factor λ=1.5.

The second part is to obtain the behavior factor q for which acceleration time history motion records have been scaled to multiple levels, up to the collapse or the attainment of certain limiting criteria (eg. exhaustion of rotation capacity in elements).

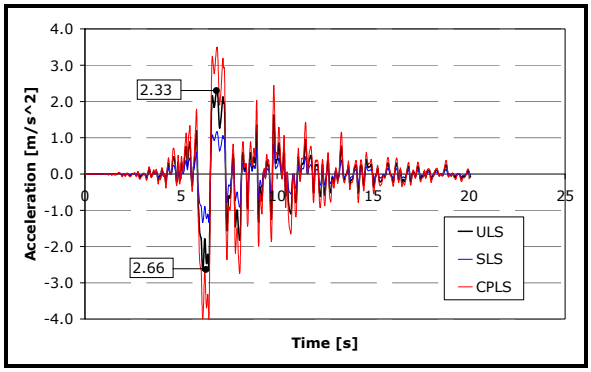

Figure 4-41 – Vrancea 1977, Incerc station, N-S component (SLS, ULS and CPLS)

As described in paragraph 4.2, the structures are modeled using the dual strip model for the dynamic nonlinear analysis. Figure 4-42 shows the numerical model of the 6 storey structure.

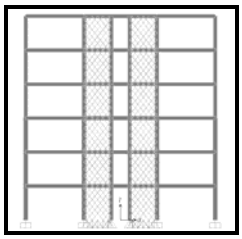

Figure 4-42 –Dual strip model for dynamic nonlinear analysis

Figure 4-43 and Figure 4-44 show the maximum interstorey drift ratio vs. spectral acceleration S_a for all records. Based on the results of the experimental test, first yielding develops in infill plates at a corresponding interstorey drift of 0.5%. The

collapse criterion is given by the attainment of dynamic instability or plastic deformation capacity of dissipative members (infill panels and beams). The experimental tests demonstrated that steel panels can sustain an interstorey drift of 4%, which is equivalent to 0.035 radian plastic rotation in beams.

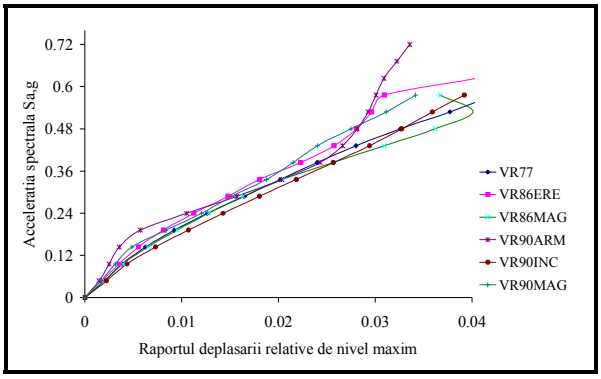

(a)

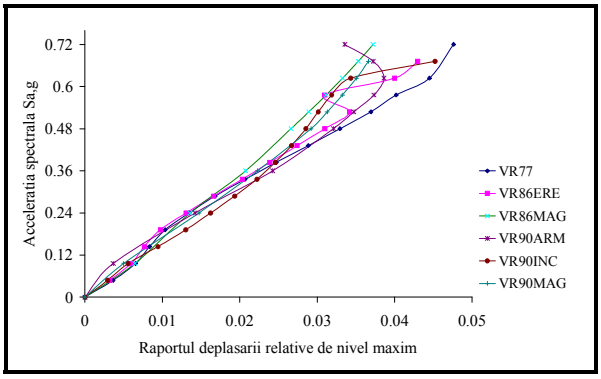

(b)

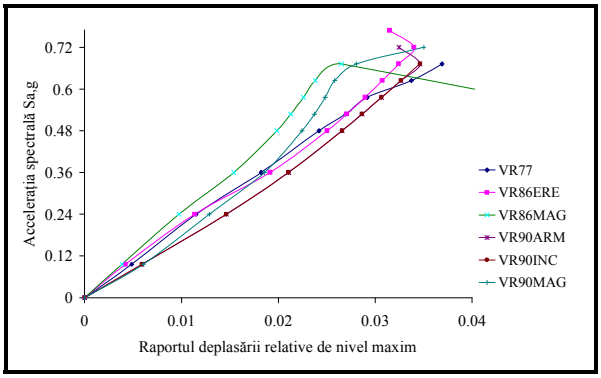

(c)

Figure 4-43 – Rigid structures: a) 6 storey; b) 12 storey; c) 18 storey

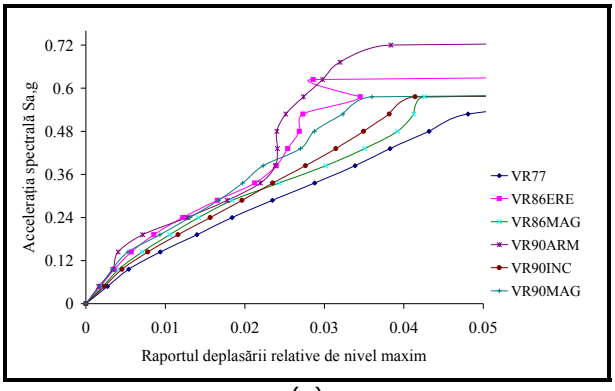

(a)

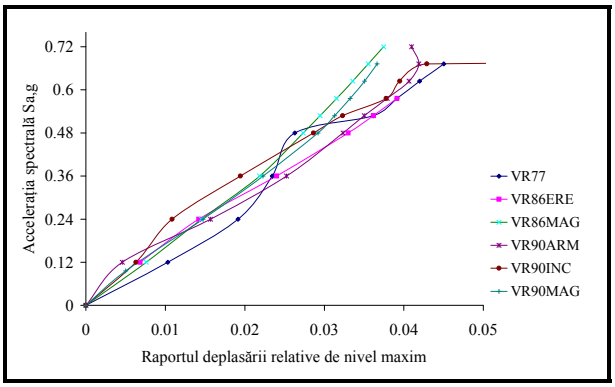

(b)

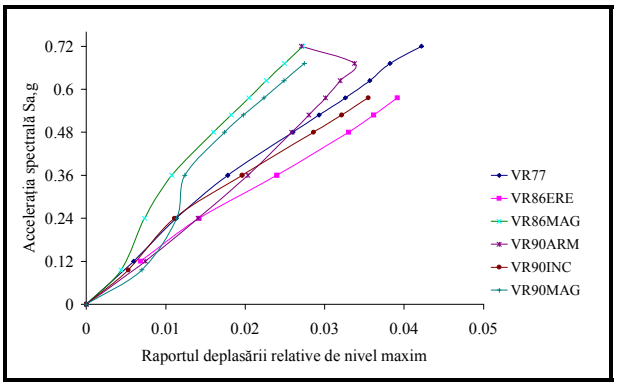

(c)

Figure 4-44 – Pinned structures: a) 6 storey; b) 12 storey; c) 18 storey

Figure 4-45, Figure 4-4 and Figure 4-4 show the development of plastic hinges for the most undesirable earthquake VR77INC.

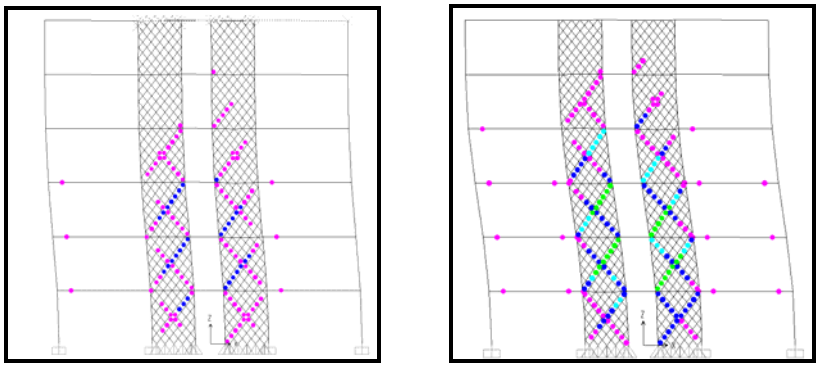

(ULS) (Rigid) (CPLS)

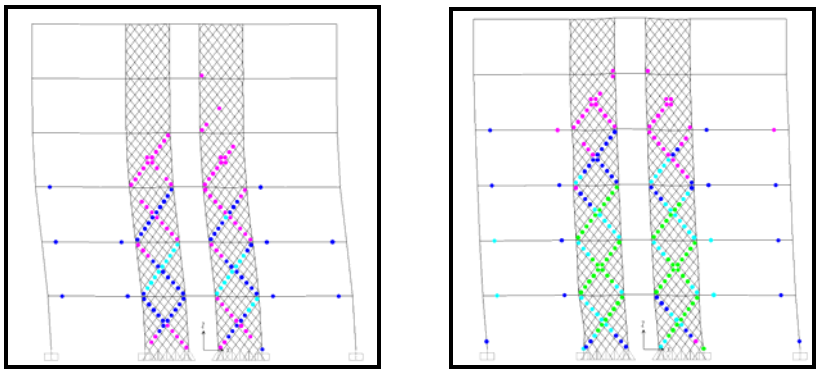

(ULS) (Pinned) (CPLS)

Figure 4-45 – Distribution of plastic hinges for 6 storey structure: rigid and pinned

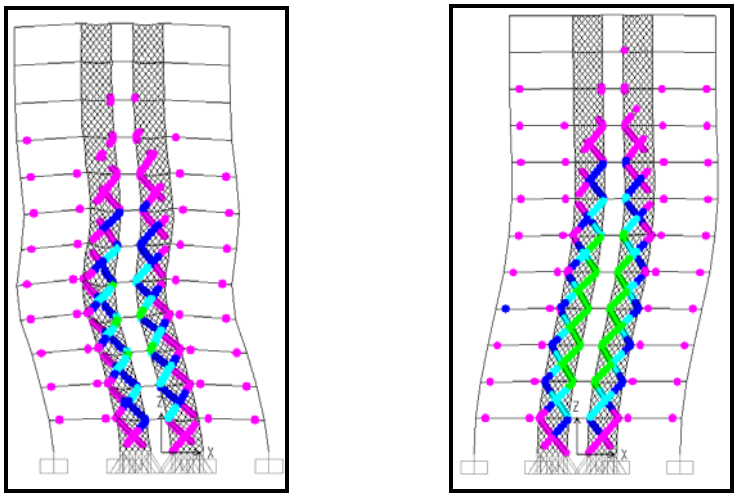

(ULS) (Rigid) (CPLS)

Figure 4-46 - Distribution of plastic hinges for 12 storey structure: rigid and pinned

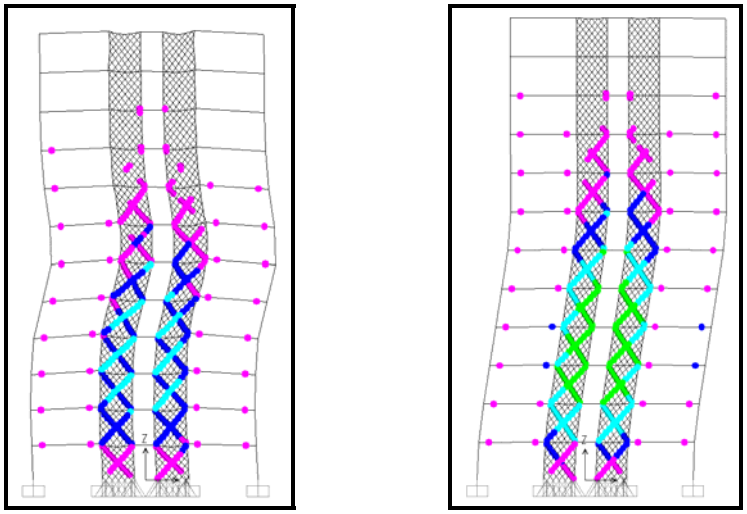

(ULS) (Pinned) (CPLS)

Figure 4-46- (Continued)

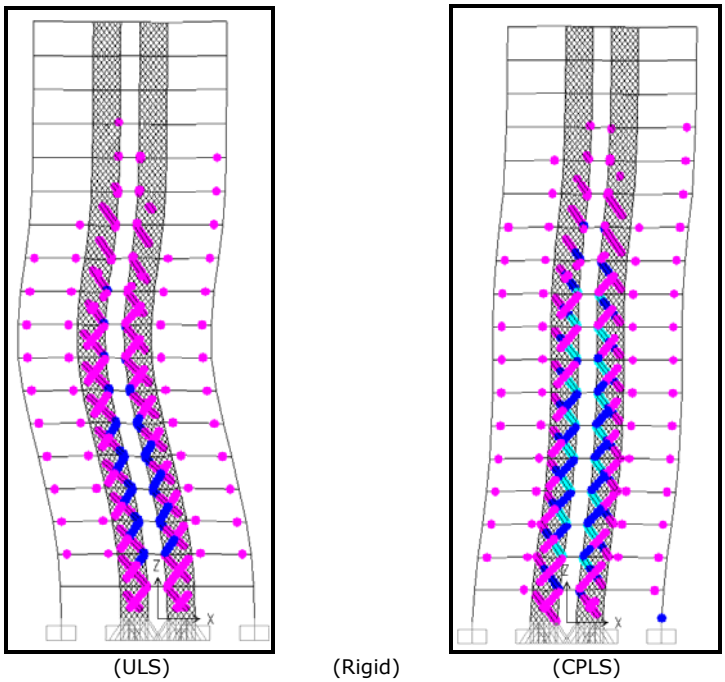

(ULS) (Rigid) (CPLS)

Figure 4-47 - Distribution of plastic hinges for 18 storey structure: rigid and pinned

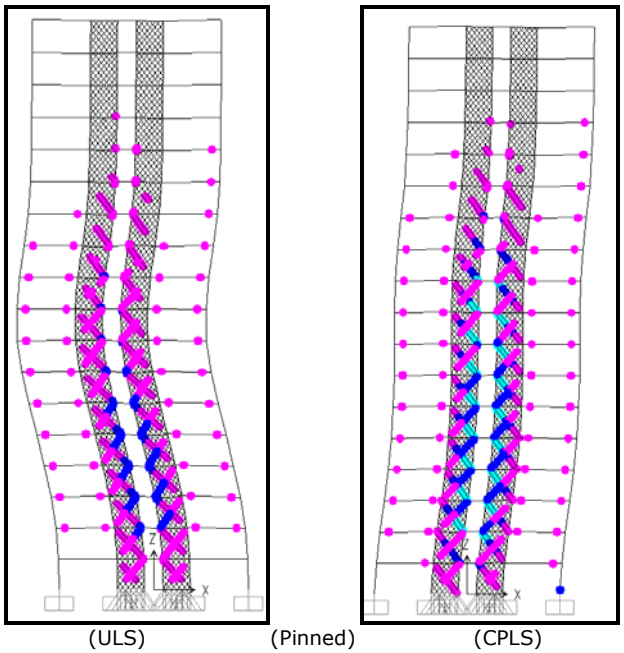

(ULS) (Pinned) (CPLS)

Figure 4-47- (Continued)

Table 4-13 and Table 4-15 to Table 4-20 show the interstorey drift values at the 3 performance levels for the 6 structures subjected to the considered ground motions. Table 4-14 show the plastic rotation in hinges developed at the attainment of the life safety and collapse prevention performance levels. No plastic deformations were recorded in the columns for 6 and 18 storey structures while for 12 storey structures the plastic deformations in columns develop for first two ground motion records, only. As it can be seen from these tables, the type of ground motion affects the amount of plastic deformations occurred in the elements. The structure with pinned beam to column connection takes more damage then the structure with rigid connection.

Table 4-13 – Plastic hinge values for rigid structures

6 storey	Beams [R3] [rad]					
	VR77INC	VR86ERE	VR86MAG	VR90ARM	VR09INC	VR90MAG
SLS	-	-	-	-	-	-
ULS	0.006	0.004	0.005	0.003	0.008	0.005
CPLS	0.019	0.022	0.023	0.019	0.02	0.017
12						
SLS	0.002	0.002	-	-	-	-
ULS	0.014	0.013	0.012	0.009	0.011	0.009
CPLS	0.023	0.022	0.016	0.02	0.018	0.017
18						
SLS	-	-	-	-	-	-
ULS	0.006	0.003	0.0013	0.008	0.007	0.006
CPLS	0.013	0.011	0.0083	0.014	0.013	0.012

Table 4-15 to Table 4-20 show the interstorey drift values at the 3 performance levels for the structures subjected to the 6 ground motion earthquakes.

Table 4-14 – Plastic hinge values for pinned structure

6 storey	Beams [R3] [rad]					
	VR77INC	VR86ERE	VR86MAG	VR90ARM	VR09INC	VR90MAG
SLS	-	-	-	-	-	-
ULS	0.013	0.006	0.009	0.006	0.01	0.009
CPLS	0.025	0.019	0.023	0.02	0.022	0.015
12						
SLS	0.003	0.002	-	-	-	-
ULS	0.014	0.013	0.011	0.01	0.012	0.011
CPLS	0.02	0.019	0.016	0.021	0.019	0.018
18						
SLS	-	-	-	-	-	-
ULS	0.005	0.004	0.002	0.007	0.004	0.006
CPLS	0.013	0.01	0.008	0.013	0.013	0.012

Table 4-15 – Interstorey drift at the 3 performance levels of the structures subjected to Vrancea 1977, INCERC station.

	6 storey		12 storey		18 storey	
VR77INC	Rigid	Pinned	Rigid	Pinned	Rigid	Pinned
SLS	0.00505	0.00538	0.00640	0.01000	0.05500	0.00680
SLU	0.01265	0.01840	0.01500	0.01900	0.01220	0.01240
CPLS	0.02208	0.03100	0.02100	0.02460	0.01800	0.01780

Table 4-16 – Interstorey drift at the 3 performance levels of the structures subjected to Vrancea 1986, EREN station.

	6 storey		12 storey		18 storey	
VR86ERE	Rigid	Pinned	Rigid	Pinned	Rigid	Pinned
SLS	0.0045	0.0465	0.0060	0.0093	0.0052	0.0068
SLU	0.0112	0.0120	0.0140	0.0179	0.0110	0.0178
CPLS	0.0202	0.0226	0.0240	0.0240	0.0190	0.0240

Table 4-17 – Interstorey drift at the 3 performance levels of the structures subjected to Vrancea 1986, Magurele station.

	6 storey		12 storey		18 storey	
VR86MAG	Rigid	Pinned	Rigid	Pinned	Rigid	Pinned
SLS	0.0052	0.0056	0.0075	0.0080	0.0043	0.0048
SLU	0.0163	0.0140	0.0160	0.0150	0.0100	0.0100
CPLS	0.0230	0.0270	0.0234	0.0215	0.0150	0.0152

Table 4-18 – Interstorey drift at the 3 performance levels of the structures subjected to Vrancea 1990, Armeana station.

	6 storey		12 storey		18 storey	
VR90ARM	Rigid	Pinned	Rigid	Pinned	Rigid	Pinned
SLS	0.0035	0.0042	0.0650	0.0065	0.0053	0.0074
SLU	0.0105	0.0127	0.0142	0.0156	0.0146	0.0141
CPLS	0.0223	0.0228	0.0242	0.0253	0.0210	0.0203

Table 4-19 – Interstorey drift at the 3 performance levels of the structures subjected to Vrancea 1990, INCERC station.

	6 storey		12 storey		18 storey	
VR90INC	Rigid	Pinned	Rigid	Pinned	Rigid	Pinned
SLS	0.0058	0.0061	0.0075	0.0078	0.0060	0.0063
SLU	0.0143	0.0156	0.0162	0.0170	0.0146	0.0110
CPLS	0.0237	0.0256	0.0234	0.0230	0.0210	0.0196

Table 4-20 – Interstorey drift at the 3 performance levels of the structures subjected to Vrancea 1990, Magurele station.

	6 storey		12 storey		18 storey	
VR90MAG	Rigid	Pinned	Rigid	Pinned	Rigid	Pinned
SLS	0.0040	0.0043	0.0062	0.0078	0.0070	0.0071
SLU	0.0152	0.0130	0.0147	0.0230	0.0128	0.0133
CPLS	0.0201	0.0210	0.0222	0.0280	0.0186	0.0191

4.6.3. q factor evaluation

The European code seismic code [40], gives just a generic estimate of the q-factor, generally related to the typology of the structure (moment frames, braced frames, etc.) and minimum ductility requirements for elements and connections. If present, vertical irregularity leads to a reduction of this factor. This generic q-factor is not capable of representing in detail the real structural response and completely disregards important aspects such as, the duration of the ground motion, the number of cycles and their amplitude.
In order to develop simple design rules for steel buildings in seismic zones, it is important to characterize the behavior of steel members and beam-to-column joints under cyclic reversal loading, and in particular to focus on the damage caused by plastic deformations (low-cycle fatigue).
Current seismic codes are based on the force-controlled design, by using the base shear approach. The parameter related to the degradation of the structure is the behavior factor q, based on the maximum capacity of the structure to dissipate energy in the ultimate limit state (ULS).
In the study, the *q* factor was defined as the ratio of the peak ground acceleration producing local or global collapse of the structure (a_{gu}) to peak ground acceleration producing the first yielding in the structure:

$$q = \frac{a_{gu}}{a_{gy}} \tag{4.15}$$

where:
- a_{gu} is the peak ground acceleration leading to collapse
- a_{gy} is the peak ground acceleration corresponding to first yielding.

The value a_{gu} is obtained by scaling the peak ground acceleration value (PGA) from λ=0.2 ($\times$ PGA) upwards until the near-collapse criterion is met. According to P100/2006, the PGA is 0.24g corresponding to an acceleration multiplier of λ=1. The peak ground acceleration corresponding to yielding of the frame was taken as the acceleration when the tension strips present first plastic deformation.
Table 4-21 and Table 4-22 show the values of *q* for 6, 12 and 18 storey structure with rigid and pinned beam to column connections. As it can be seen form the tables, the type of ground motion affects the behavior factor q_{μ}. The mean value of the *q* factor is 5.7 for the 6 storey rigid structure while for 12 and 18 storey the *q* factor amounts 6.3. The pinned structures present an average q factor of 5.8 for the 6 storey structure, 6.5 for 12 storey structure and 6.4 for 18 storey structure.

Table 4-21 – q factors for rigid connection structures

earthquake	Storey	Accelera-tion		q	Storey	Accelera-tion		q	Storey	Accelera-tion		q
		a_{gy}	a_{gu}			a_{gy}	a_{gu}			a_{gy}	a_{gu}	
VR77INC		0.10	0.58	6.0		0.10	0.53	5.5		0.10	0.48	5.0
VR86ERE		0.12	0.62	5.2		0.10	0.58	6.0		0.10	0.77	8.0
VR86MAG	6	0.10	0.58	6.0	12	0.10	0.72	7.5	18	0.13	0.67	5.1
VR90ARM		0.12	0.72	6.0		0.10	0.62	6.5		0.10	0.72	7.5
VR90INC		0.10	0.58	6.0		0.10	0.53	5.5		0.10	0.53	5.5
VR90MAG		0.12	0.62	5.2		0.10	0.62	6.5		0.10	0.67	7.0
AVERAGE				**5.7**				**6.3**				**6.3**

Table 4-22 – q factors for pinned connection structures

Quake	Storey	Accelera-tion		q	Storey	Accelera-tion		q	Storey	Accelera-tion		q
		a_{gy}	a_{gu}			a_{gy}	a_{gu}			a_{gy}	a_{gu}	
VR77INC		0.10	0.58	6.0		0.10	0.53	5.5		0.10	0.48	5.0
VR86ERE		0.12	0.62	5.2		0.10	0.62	6.5		0.10	0.77	8.0
VR86MAG	6	0.10	0.53	5.5	12	0.10	0.72	7.5	18	0.12	0.67	5.6
VR90ARM		0.12	0.77	6.4		0.10	0.72	7.5		0.10	0.72	7.5
VR90INC		0.10	0.58	6.0		0.10	0.58	6.0		0.10	0.53	5.5
VR90MAG		0.12	0.67	5.6		0.10	0.62	6.5		0.10	0.67	7.0
AVERAGE				**5.8**				**6.5**				**6.4**

4.7. Conclusions

In total, 6 structures were analyzed in order to asses the global behavior of SPSW structures. The main parameters were the beam to column connection in the SPSW area and height of the structures. The nonlinear static and dynamic analysis have shown that this type of structures posses a good initial stiffness and excellent ductility. This fact categories this type of structures as high dissipative structures, similar with moment resisting frames (MRF), eccentrically braced frames (EBF) and frames with buckling restrained braces (BRB). The type of connection between HBE and VBE affects the ultimate strength of the system but has no major effect on the initial stiffness.

The q factor, obtained as the ratio between the acceleration leading to collapse and the acceleration at the first yielding, increases by 10% from the 6 storey structure to the 12 storey structure, but then remains constant if the number of storeys increases. The structures with pinned connections show a slightly higher behavior factor compared to structures with rigid connections, due to the lower onset of yielding. The mean behavior factor q for all cases amounts 6 and confirms the findings in the experimental program.

5. Design approach for multi-storey frames of dissipative steel shear walls

5.1. Introduction

Results of the numerical study presented in chapter 4 shown that strip model can adequately represent the behavior of non-compact SPSW. However, there are some limitations when one applies this model in the nonlinear analysis. Past research (Rezai, 1999 [15]) shows that modeling of SPSW with strips is reasonably accurate if panel aspect ratio L/h exceeds 0.8. Additional horizontal intermediate boundary elements could be introduced in SPSW to modify the L/h of panels having an aspect ratio less than 0.8, even in practical application this is rarely the case. No theoretical upper bound exists on L/h (provided sufficiently stiff HBE can be provided), but a maximum value of 2.5 is specified on the basis that most research has not investigated the seismic behavior of SPSW having L/h greater than 2.0. Excessive flexibility of HBE is of concern for L/h ratios beyond the specified limit. Again, applications of SPSW with aspect ratio L/h exceeding 2.5 are seldom used. For conditions beyond the specified limits, other analysis methods (eg. finite element method FEM) shall be used.

However, for preliminary analysis, the strip model may be replaced by an equivalent braced frame. The resulting area of the diagonal can be further used to estimate the thickness of the infill plates. Other members of the structural system may be also sized. Caution must be paid for boundary HBE and VBE members that require additional checking.

5.2. Design methodology

5.2.1. Pre-design of an equivalent diagonal braced frame

A number of analytical approaches are possible to achieve capacity design and determine the same forces acting on the vertical boundary elements. One of these methods is the preliminary proportioning of infill plates and boundary elements HBE, VBE. SPSW may be approximated by a vertical truss with tension diagonals. Each web is represented by a single diagonal tension brace within the storey (Figure 5-1). For seismic combinations, if modal spectral analysis is employed, the design response spectrum is reduced from the elastic one with the behavior factor q. The q factor is composed of the ductility q factor (q_μ) and the overstrenght q factor (q_s). The ductility q factor can be taken between 5 and 6 (according to experimental and numeric analysis). By analogy with this type of structure, EN1998-1 [40] defines the overstrength of these structures due manly to their statically redundancy, taken between 1.1 - 1.3. So, the final value ranges between 6 and 8 as in the case of highly ductile moment resisting frames MRF. In this case is recomanded to take in consideretation a maximum value of 6.5 for q factor.

Equivalent braces

- For gravity load combinations (non-seismic), diagonal braces need to be removed from the analysis.
- SLS (0.005He) and ULS (appropriate strength) requirements are used to size the equivalent braces.
Additionally, capacity design rules (see EN1998-1 [40], P100-1/2006 [47]) should be used for designing the boundary elements.

Beams

- It should be verified that the full plastic moment of resistance and rotation capacity are not decreased by compression and shear forces
- Sections belong to cross-sectional classes 1 (for DCH) and 1 or 2 (for DCM)
- If a dual system with coupling beams is used (see Figure 5-1.b), conditions for coupling beams shall refer also to seismic links, according to the type of plastic mechanism developed: short links, which dissipate energy by yielding essentially in shear; long links, which dissipate energy by yielding essentially in bending; intermediate links, in which the plastic mechanism involves bending and shear. In practical applications, the void (between two infill plates) is designated for access to corridors, offices, elevators, and therefore the resulted beam link is medium or long.

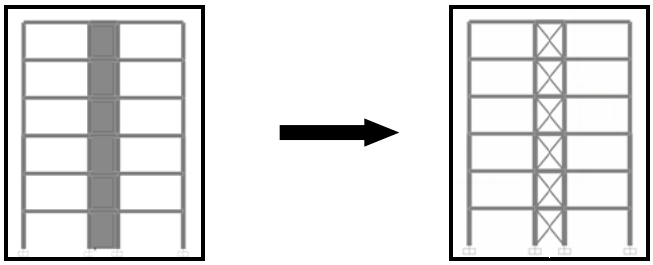

a)

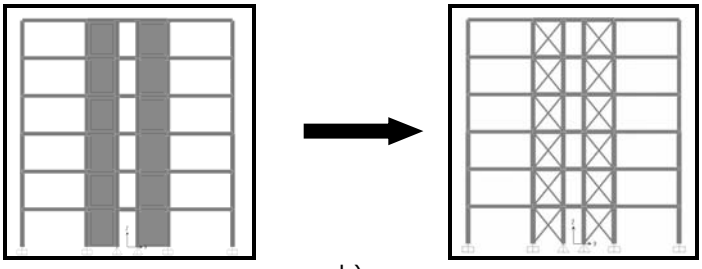

b)

Figure 5-1 – Vertical truss with diagonals: single system; system with coupling beams

Columns

- The columns shall be taken as class 1, 2 or 3.
- They MRF columns shall be verified considering the most unfavorable combination of the axial force, shear force and bending moments (see clause 6.6 from [43]),

where the overstrength factor $1.1\gamma_{ov}\Omega$ can be taken as 2.

$$\begin{aligned} N_{Ed} &= N_{Ed,G} + 1.1\gamma_{ov}\Omega N_{Ed,E} \\ M_{Ed} &= M_{Ed,G} + 1.1\gamma_{ov}\Omega M_{Ed,E} \\ V_{Ed} &= V_{Ed,G} + 1.1\gamma_{ov}\Omega V_{Ed,E} \end{aligned} \quad (5.1)$$

- The CBF columns shall be verified in compression considering the most unfavorable combination of the axial force and bending moments (see clause 6.7 from [43]),

$$N_{pl,Rd}(M_{Ed}) \geq N_{Ed,G} + 1.1\gamma_{ov}\Omega N_{Ed,E} \quad (5.2)$$

Beam to column connections (EN1993-1-8 [47]; EN1998-1 [40], clauses 6.5.5, 6.6.4 from [43]):
- If dissipative zones are located in the structural members, the connections of the dissipative parts to the rest of the structure shall have sufficient overstrength to allow the development of cyclic yielding in the dissipative parts.
- When dissipative zones are located in the connections, the connected members shall have sufficient overstrength to allow the development of cyclic yielding in the connections.
- For boundary beam HBE to boundary column VBE connections, when partial strength connections are used, the capacity of the connection should be larger than 50% of the connected beam or column, whichever is less. Simple connections may be used, also.

5.2.2. Design of Shear Wall

The plastic shear strength of a SPSW is obtained with relationship (5.3). The formula is based on the assumption that each web may be modeled by a series of inclined pin-ended strips, oriented at angle α:

$$V_n = 0.42F_y t_w L_{cf} \sin 2\alpha \quad (5.3)$$

where:
F_y is yield strength
t_w is thickness
of the plate, see (5.3)
L_{cf} is clear distance between VBE flanges
α is angle of the tension field, as measured relative to the vertical

Based on the equivalent tension brace obtained in previous paragraph and using an assumed angle of inclination α, the thickness of the steel plates t_w in formula (5.3) can be calculated using the following equation,.

$$t_w = \frac{2A\Omega_s \sin\phi}{L \sin 2\alpha} \quad (5.4)$$

where:

A is area of the equivalent tension brace;
θ is angle between the vertical and the longitudinal axis of the equivalent diagonal brace (Figure 5-2);
L is the distance between VBE centerlines;
α is the assumed angle of inclination of the tension field measured from the vertical (optimum tension field inclination 45º);
Ω is the system overstrength factor, as defined by FEMA 356 [43], and taken as 1.2 for SPSW (Berman and Bruneau, 2003 [21] or NBCC 2005 [31]). This factor is equivalent to q_{Ω}, see 3.6.3 and 4.6.3.

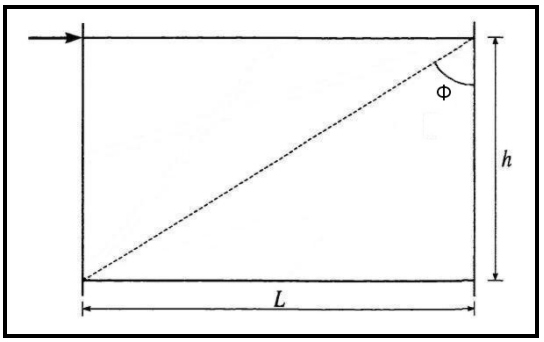

Figure 5-2 – Angle between the vertical and the longitudinal axis of the equivalent diagonal brace

Depending on the slenderness of shear walls, they can be categorized as Compact, Non-compact and Slender as shown in Figure 5-3:

- Category 1, where the slenderness of the wall defined by L_{cf}/t_w is less than $1.1\sqrt{k_v E / F_{yw}}$. Steel shear walls in this category are denoted as "compact". It is expected that under applied shear, as shown in Figure 5.3, the steel plate will yield in shear before buckling occurs.
- Category 2, where the slenderness ratio L_{cf}/t_w is larger than $1.1\sqrt{k_v E / F_{yw}}$ but smaller than $1.37\sqrt{k_v E / F_{yw}}$. This category is denoted "non-compact". It is expected that walls that fall in this category are expected to buckle while some shear yielding has already taken place. In this case, the storey shear is resisted by the horizontal components of the tension and compression diagonal forces as shown in Figure 5-4.
- Category 3, where the wall is very slender and its L_{cf}/t_w is greater than $1.37\sqrt{k_v E / F_{yw}}$. Shear walls in this category can be called "slender" and are expected to buckle while almost elastic.

k_v is the plate buckling coefficient given by relationship (5.5). Where a/h is greater than 3 or $[260/(h/t_w)]^2$, k_v should be taken as 5.0.

$$k_v = 5 + \frac{5}{\left(H/L_{cf}\right)^2} \tag{5.5}$$

where

L_{cf} is defined above
H is the storey height
Although no theoretical bounds exist on the ratio L_{cf}/t_w, drift limits will indirectly constrain the upper bound, while the requirement that webs to be non-compact governs the lower bound ratio.

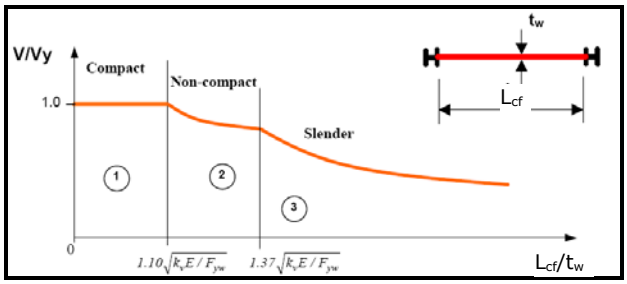

Figure 5-3 – The regions of behavior of steel plate walls

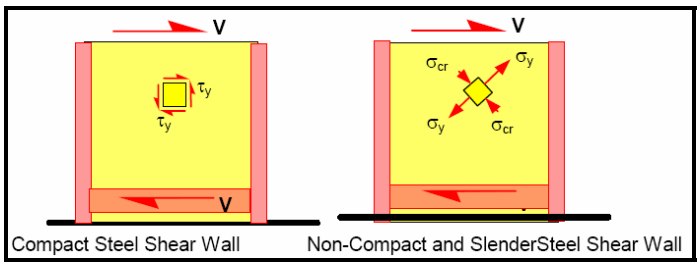

Figure 5-4 – SPW resisting shear in "shear yield" and tension field action

5.2.3. Checking of HBE, VBE and HBE to VBE connection

According to AISC 2005 [5], VBE and HBE are to remain essentially elastic under forces generated by fully yielded plates, but flexural hinges are allowed at the ends of HBE elements.
The required strength of HBE shall be the greater of the forces corresponding to the expected yield strength, in tension, of the web calculated at an angle α or that determined from the load combinations assuming the web provides no support for gravity loads. The size of the HBE is checked if its plastic modulus is at least equal to (and without developing mid-span hinges):

$$W_{pl(beam)} \geq \frac{f_{yw} t_w \cos^2 \alpha L^2}{4 f_{ym}} \tag{5.6}$$

The required strength of VBE shall be based upon the forces corresponding to the expected yield strength, in tension, of the web calculated at an angle α. In order to prevent excessive deformations leading to premature buckling under the pulling action of the plates, the minimum moment of inertia of the columns shall be verified using the following equation (5.7). If different sections are used for boundary elements, then the average values of moment of inertia and area can be used in

calculation.

$$I_c \geq \frac{0.00307 t_w h^4}{L} \tag{5.7}$$

5.2.4. Design of infill plate to boundary elements connection

The required strength of web connections to the surrounding HBE and VBE shall equal the expected yield strength, in tension, of the web. Net sections must be also providing this strength for the case of bolted connections. Two typical details of connections of steel plate shear wall to boundary beams and columns are shown in Figure 5-5. The welded connection should be designed such that the connection plates (fin plates) and welds develop the "expected shear yield" strength of the wall. If field-bolted connections are used, the bolts should be slip-resistant and able to develop the "expected shear strength" of the wall. Even if bolts are slip-resistant, it is expected that during the cyclic loading of the wall, the bolts slip before the tension field yields. Therefore, the design shear resistance and the design bearing resistance should be also verified (EN1993-1-8 [40] clause 3.4).
In the tests done by the author, the 8.8 grade bolts were preloaded according to EN1993-1-8 [40] provisions. Observations during and after the tests revealed no important slippage occurred both for monotonic and cyclic tests, even for large storey drifts and considerably plastic deformations.

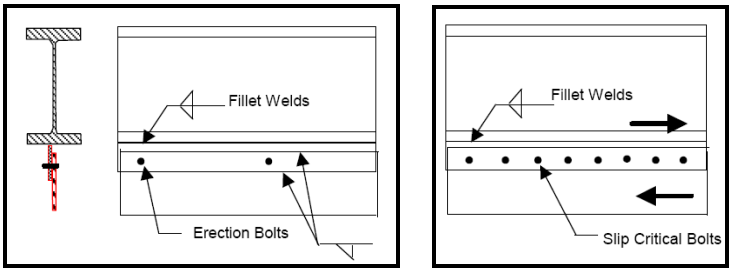

(a) (b)

Figure 5-5 – Connection of the steel plate shear wall to boundary beams and columns: a) Welded connection; b) Bolted connection

(a) (b)

Figure 5-6 – Views after the test: a) monotonic test; b) cyclic test

Connections between HBE and VBE shall satisfy the requirements of section 5.2.1.

In addition, the required shear strength of a full strength HBE-to-VBE connection shall not be less than the shear corresponding to moments at each end equal to (5.8), together with the shear resulting from the expected yield strength in tension of the webs yielding at an angle α. For partial strength connections, the same requirement applies but (5.8) is replaced by the maximum end moment that the connection is capable of resisting.

$$1.1\gamma_{ov}R_{fy} \tag{5.8}$$

5.3. Performance base seismic evaluation

The *first* step in PBSE is to establish performance objectives described as the combination of an expected performance level with expected levels of hazard (e.g. ground motion). A performance level is an expression of the maximum desired extent of damage to a building.
The *second* aspect to PBSE is the definition of the expected hazard level that may occur at the given site. The performance objectives for a structure are the coupling of expected performance level with expected hazard.
The *third* and final ingredient necessary for PBSE is a mean to verify that the design is meeting the performance objectives. In this step, nonlinear static or nonlinear dynamic (time-history) analysis can be employed in order to check if the acceptance criteria at the performance levels are fulfilled.
Influence of higher mode of vibrations modifies the behavior of the structures and consequently dynamic nonlinear analysis must be used. In the 2005 NBCC [31], dynamic analysis is mandatory for the following classifications of buildings:
(i) regular structures that are 60 m or taller or have fundamental period greater than or equal to 2.0 s and are located in areas of high seismicity with:

$$I_E F_a S_a(0.2) \geq 0.35 \tag{5.9}$$

where:
I_E is the moment of inertia;
F_a is an acceleration-based site coefficient;
Sa(0.2) is the spectral response acceleration for a period of 0.2 s;

(ii) irregular buildings that are 20 m or taller or have a fundamental period of 0.5 s or longer and are located in areas of high seismicity with (5.9)
(iii) all buildings that have rigid diaphragms and are torsionally sensitive.

An option of this analysis can be the incremental dynamic analysis (IDA) (see paragraph 4.5.2.6). With respect to seismological intensity measures (IM), such as peak ground acceleration, engineers can estimate principal response quantities in terms of governing engineering demand parameters (EDP), such as the maximum deflection or drift of the structure. The IDA approach involves performing nonlinear dynamic analyses of a structural system under a selection of ground motion records, each scaled to several IM levels designed to force the structure all the way from elastic response to final global dynamic instability (collapse).
Depending on the steel plate shear wall being "compact", "non-compact" or

"slender" and depending on the capabilities of the analysis software to handle with plate buckling, shear walls can be modeled for nonlinear analysis in several ways. In the following, different modeling techniques for compact and non-compact/slender shear walls are briefly summarized.

In compact shear walls, the steel plate is expected to yield in shear before buckling. Therefore in the analysis, the compact shear walls can be modeled using full shell elements and isotropic material. It is suggested that the wall panel be modeled using at least 16 shell elements (4x4 mesh) per panel. The shear force V acting on the cross section of the wall can be calculated by adding up the shear in the elements. This applied shear force represents the demand on the wall and should be less than or equal to shear capacity of the wall established in this chapter.

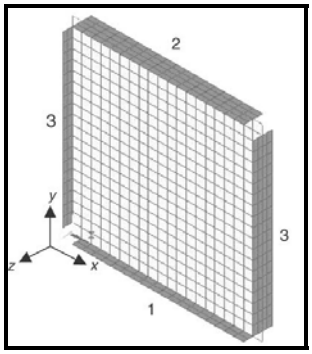

Figure 5-7 – Compact steel plate shear wall modeling

In slender shear walls, steel plates are expected to buckle along compressive diagonals under relatively small shear forces. After buckling, the tension field action of the tension diagonal becomes the primary mechanism to resist shear force in the wall. In this case the steel plate can be modeled also with shell elements having anisotropic or orthotropic capabilities. But, if the analysis software does not have anisotropic or at least orthotropic shell elements, one can replace the steel plates with a series of truss members (strips) along the tension field. Results depend on the inclination of tension field, and therefore it is necessary to evaluate this angle:

$$\tan^4 \alpha = \frac{1+\frac{t_w L}{2A_c}}{1+t_w H\left(\frac{1}{A_b}+\frac{H^3}{360 I_c L}\right)} \tag{5.10}$$

where:

H is the distance between HBE centerlines;

A_b is cross-section area of HBE;

A_c is cross-section area of VBE ;

I_c is moment of inertia of VBE taken perpendicular to the direction of the plate line;

L is the distance between VBE centerlines.

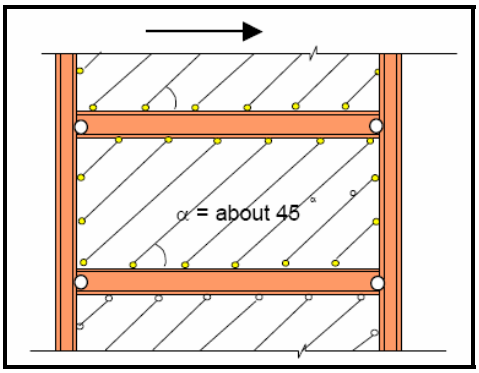

Figure 5-8 – Non-compact or slender steel plate shear wall modeling

5.4. Flowchart for Design and PBSE

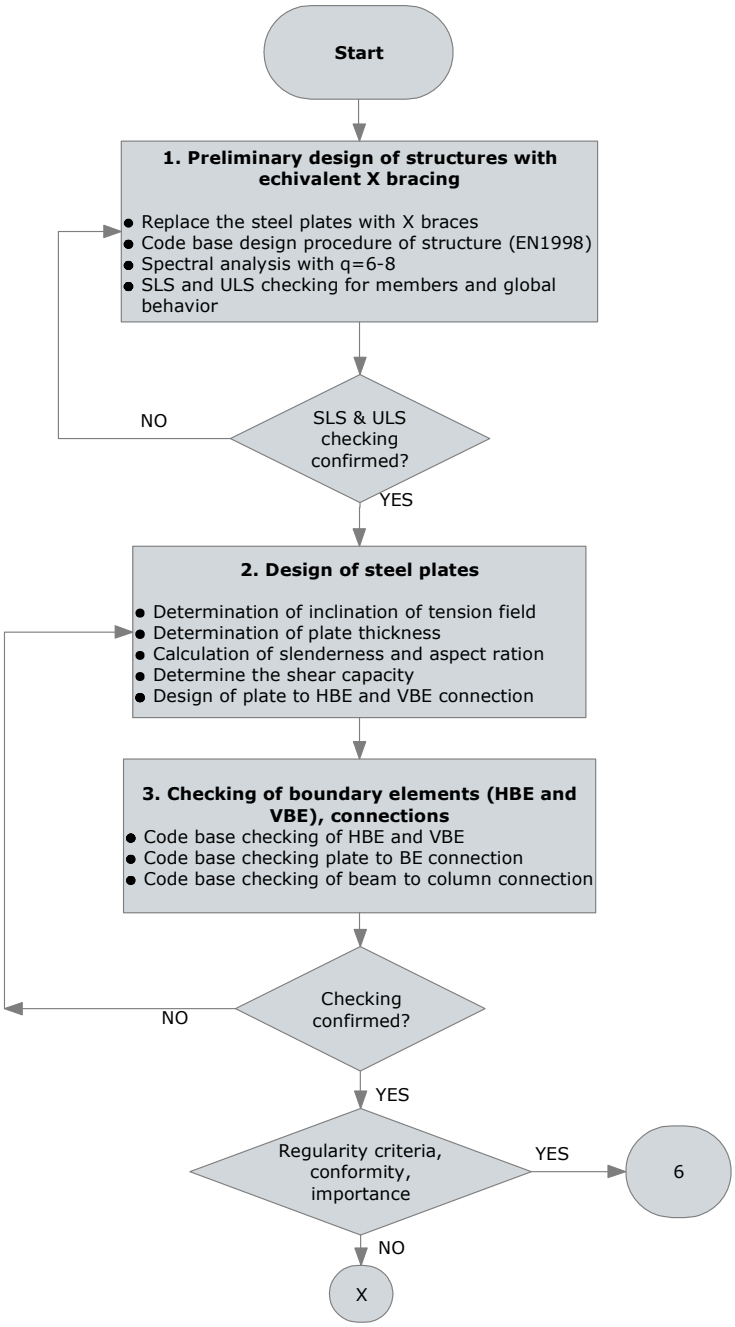

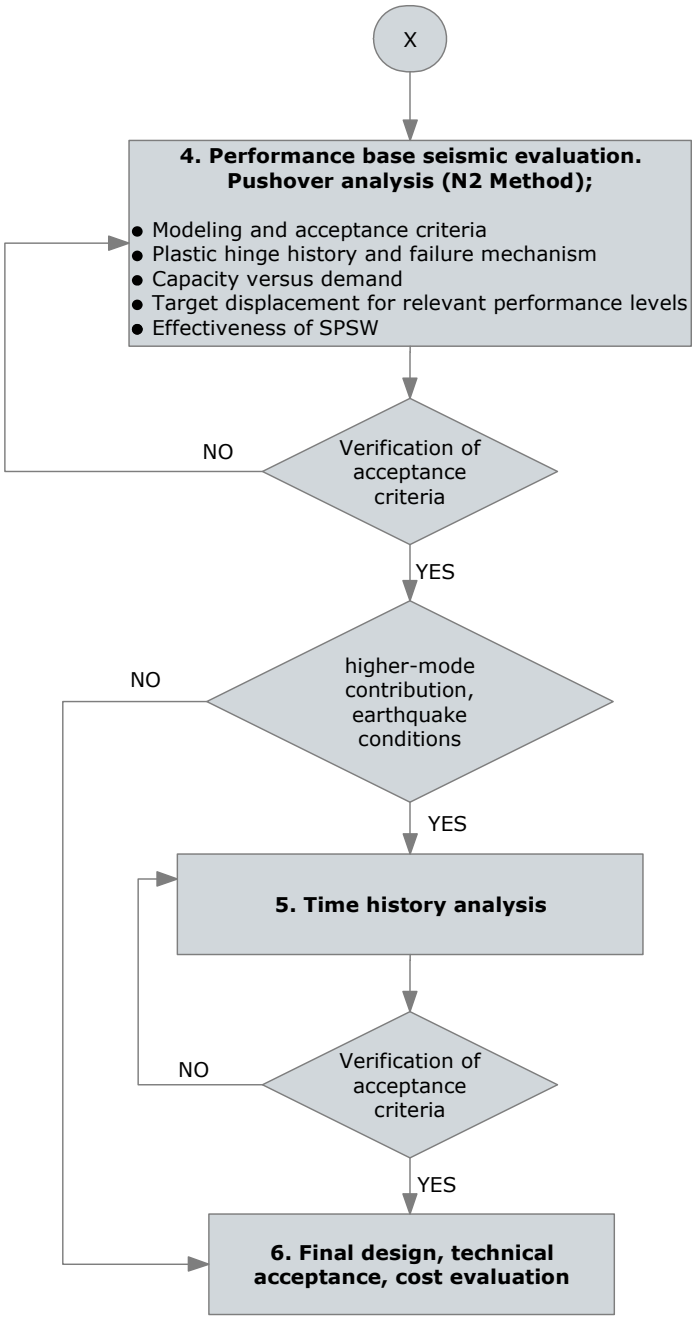
X
4. Performance base seismic evaluation. Pushover analysis (N2 Method);
Modeling and acceptance criteria
Plastic hinge history and failure mechanism
Capacity versus demand
Target displacement for relevant performance levels
Effectiveness of SPSW
Verification of acceptance criteria
NO
YES
higher-mode contribution, earthquake conditions
NO
YES
5. Time history analysis
Verification of acceptance criteria
NO
YES
6. Final design, technical acceptance, cost evaluation

6. Final conclusions, contribution of the author, dissemination of results

6.1. Final conclusions

The paper investigated the performances of dual SPSW structures. Due to the limitations of the testing capacity, the models were half-scaled. A total of 4 specimens were designed and fabricated, which included specimens with semi-rigid and rigid connections. Specimens were tested monotonically and cyclically.

In order to evaluate the influence of beam-to-column connections on the response of the structure, two connection typologies were used, i.e. flush end plate bolted connections (semi-rigid) and extended end plate bolted connections (rigid). Rigid joints increased the "yield resistance" and the ultimate capacity of the structures. The initial stiffness was also improved when rigid beam-to-column connections are used. They reduce the pinching effect occurred at the load reversal and this contributes to the reduction of the intersorey drifts. In case of the semi-rigid connections, the degradation of the system due to repeated cycles is more important. Behavior factor q (considering the contribution of the ductility, only), was evaluated based on the results of the cyclic tests. It was found a value of approximately 5, similar with the value offered by the Canadian standard NBCC 2005 [31].

The initial imperfections of the infill plates, especially where the thickness is very small, need be very avoided or reduced. They can be caused by fabrication, welding or assembling processes. These imperfections have significant influence on the elastic limit, while the strength of the system does not depends on it.

In order to strengthen the findings of the experimental program, a numerical study was employed on different typologies of structures. The main parameters of the analyzed structures were the type of beam to column connection (rigid and pinned) and the height of the structure (6, 12 and 18 storey).

The strip model was used for the nonlinear static and dynamic analysis of the models. Based on the experimental results, this model was modified by calibrating the plastic hinge used for the tension only strip elements.

The dynamic analysis using 6 sets of ground motion records have shown that the q factor is sensitive to the type of ground motion input. The height of the structure affects, also, the behavior factor q. A value of 5.7 and 5.8 was obtained for the 6 storey structures having rigid and pinned joints. The 12 and 18 storey structure presented a q factor of approximately 6.3 for the rigid connection and 6.4 for the pinned connection, respectively.

Results obtained have shown that these systems are a very god option for lateral resisting systems. The behavior of the systems manifested through the behavior factor q is very close to the behavior resulted in the experimental program.

The value of the q factor, around 6, obtained in the numerical analysis is in good agreement with the values obtained in the experimental program. These values indicate SPSW structures exhibit a good dissipative behavior, similar to other dissipative structures, like for example moment resisting frames or buckling restrained braces and reflect the provisions from design codes where this system is included (eg. AISC 2005 [5], NBCC 2005 [31]).

6.2. Contribution of the author

The main contributions of the author within present work can be summarized as follows:

1. The experimental program, developed on scaled models (1/2) which correspond to real building frames designed according to code provisions. Two different frame units of 2 storeys and 2 bays each and having rigid and semirigid beam to column joints have been tested. In these units, plates of 2 and 3 mm have been infilled using bolted connections. The models have been tested under monotonic and cyclic loading on the purpose to observe the global behavior of such type of system, to capture and characterize the relevant parameters and, at the end, to be able to evaluate experimentally the behavior factor q.

It has to be underlined that according to our knowledge and based on the review of existing literature, such type of test devoted to the study of framed equipped with dissipative steel plates has not been yet tested. Also, one considers this is a first attempt to evaluate experimentally the behavior factor q for such systems.

2. Numerical program devoted to studying the behavior of MRF with SPSW, in order to observe the response of such type of structure under high demanding seismic motions (Vrancea source) and obtaining the necessary results for characterizing these structures by means of behavior factor q.

Three different frames have been numerically tested: 6, 12 and 18 storeys, respectively. Pushover and IDA analysis have been applied.

In order to model the infill plates, the model proposed by Thorburn et all. has been modified and adapted based on the observation from experimental tests. The modification refers to calibration of the tension only hinge according to the specific behavior of the specimen resulted from the monotonic test.

It also represents a specific contribution of the thesis.

The values obtained by processing the results of IDA analysis on the purpose of evaluation refer mainly to ductility contribution. These values which are around 6 are consistent with what has been obtained by tests. Since the studied structures are MRF and SPSW are practically working as centrically braced bays within these structures, one considers in such a case that we have in fact dual frames.

By analogy with this type of structure, as they are presented in Chapter 6 of P100-1/2006 (or in EN1998-1), one appreciates the overstrength of these structures is due manly to their statically redundancy (α factor in codes) and it can be taken 1.1 - 1.3. So, if one considers the global q factor is obtained by multiplying the ductility q factor (q_μ) and overstrength q factor (q_s), the final value ranges between 6 and 8 as in the case of highly ductile MRF. These values are supported by comparison with AISC 2005 code, in which the reduction factor R is taken equal for both special MRF and SPSW.

This study is the first one developed in Europe on the purpose to evaluate the behavior factor q for such a type of structure and the obtained values are, according to the author' opinion, relevant and reliable, so they can be used in design.

3. A general scheme including a flowchart and description of component steps of the methodology to apply for designing MRF of SPSW.

It was stated in the introduction of the thesis the fact that in Europe this type of structures is not yet applied in real applications due to the lack of specific provisions in the relevant design codes. By integrating the results of the present research

within the proposed design methodology, the structural engineers have now the necessary information for designing such a type of structures.

6.3. Dissemination of results

The results of the research have been presented during national and international conferences and have been submitted to journals and technical papers. A list of most important reports and papers is presented below.

Conferences

- C. Neagu, F. Dinu, D. Dubina: Seismic performance of ductile shear wall frame systems, 11th WSEAS Int. Conference on Sustainability in Science Engineering (SSE '09), Timisoara, Romania, 27-29.05.2009, ISBN 978-960-474-080-2, (ISI).
- C. Neagu, F. Dinu, D. Dubină: Performanta seismica a structurilor in cadre multietajate echipate cu panouri disipative din hotel, Simpozionul „Comportarea Structurilor Metalice La Actiuni Extreme", in cadrul celei de-a XI-a editii a Zilelor Academice Timisene, 29.05.2009.
- F. Dinu, D. Dubina, C. Neagu: A comparative analysis of performances of high strength steel dual frames of buckling restrained braces vs. dissipative shear walls, Philadelphia, 16-20 aug. 2009, International Conference, STESSA 2009, Behavior of Steel Structures in Seismic Areas, CRC Press 2009, Ed. F.M. Mazzolani, J.M. Ricles, R. Sause, ISBN: 978-0-415-56326-0 (BDI).
- F. Dinu, D. Dubina C. Neagu: Performance criteria for dissipative steel plate shear walls structures, Proc. Conferinţa internaţionala 14th European Conference on Earthquake Engineering ECEE 2010, Aug. 30 – Sept. 3 2010, Ohrid, Republic of Macedonia, ISBN 978-608-65185-1-6, pe CD-ROM.
- C. Neagu, F. Dinu, D. Dubina: Design of steel frames of dissipative shear walls, Proc. of SDSS'Rio 2010, International Colloquium Stability and Ductility of Steel Structures, 08-10 Sept. 2010, Rio de Janeiro, Brazil, Ed. E. Batista, P. Vellasco, L. de Lima, ISBN 978-85-285-0137-7, pg. 401-408.
- F. Dinu, D. Dubina, C. Neagu: Experimental evaluation of q factor for dual steel frames with dissipative shear walls, COST Action Final Conference – Urban Habitat Constructions under Catastrophic Events, CRC Press, A Balkema Book, 16-18 September 2010, Naples, Italy, Ed. F. Mazzolani, ISBN 978-0-415-60685-1, pg. 975-980.
- C. Neagu, F. Dinu, D. Dubină: Criterii de performanţă pentru structuri cu panouri disipative din oţel, a 12-a Conferinta Nationala de Constructii Metalice, 26-27 noiembrie 2010, Timisoara, Romania, pg. 323 – 332, ISBN 978-973-638-464-6.
- C. Neagu, F. Dinu, D. Dubina: Global performance of multistorey frames of steel shear walls, EUROSTEEL, The 6th European Conference on Steel and Composite Structures, 5-7 September, 2011, Budapest, Hungary.

Journals

- D. Dubina, A. Stratan, F. Dinu, S. Bordea, C. Neagu, A. Ioan: Sisteme structurale cu elemente metalice disipative demontabile pentru clădiri multietajate în zone seismice, Revista AICPS Nr. 2-3 / 2010, pg. 106-113.

- C. Neagu, F. Dinu, D. Dubina: Criterii de performanţă pentru structuri cu panouri disipative din oţel, Revista AICPS Nr. X-x/2011, pg. X-x (in printing).
- C. Neagu, F. Dinu, D. Dubina: Seismic performances of steel plate shear wall structures, An International Journal for Engineering and Information Sciences "Pollack Periodica", DOI: 10.1556/Pollack.6.2011.1.x Vol. 6, No. 1, (acceptad for publishing), ISI.
- D. Dubina, F. Dinu, C. Neagu: Calibration of seismic behavior factors for steel frames of dissipative shear walls Earthquake Engineering and Structural Dynamics, Jhon Wiley, 2011, ISSN: 0098-8847 (sent for publication), ISI.

Research programs

- FP6 PROHITECH INCO-CT-2004-509119/2004 „Earthquake Protection of Historical Buildings by Reversible Mixted Technologies – member in the research team.
- RFCS: proiect RFSR-PR-2009-00024 HSS-SERF: High Strength Steel in Seismic Resistant Building Frame.
- PN–II–RU–TD–2008–3, „Proiecte de Cercetare pentru tineri Doctoranzi "
- COST C26 – COST Action C26 – Urban Habitat Constructions under Catastrophic, 2006 - 2010.

Technical committees

- TC13 – Seismic Resistant Structures, Comitetul Tehnic al Conventiei Europene de Construcţii Metalice ECCS.

References

[1] Wagner, H., 1931, "Flat Sheet Metal Girders with Very Thin Webs, Part I – General Theories and Assumptions." Technical Memo No. 604, National Advisory Committee for Aeronautics, Washington, D.C.

[2] Kuhn, P., Peterson, J.P., and Levin, L.R., 1952,"A Summary of Diagonal Tension, Part I – Methods of Analysis." Technical Note 2661, National Advisory Committee for Aeronautics, Washington, DC.

[3] Basler, K., 1961, "Strength of Plate Girders in Shear." Journal of Structural Division, ASCE, Vol. 87, No. ST7, October, pp. 151-180.

[4] Canadian Standards Association, CSA 2000, "Limit states design of steel structures." CAN/CSA S16-01, Willowdale, Ontario, Canada, 2000.

[5] American Institute of Steel Construction Inc 2005, Seismic Provisions for Structural Steel Buildings, Chicago, 2005.

[6] Takahashi, Y., Takemoto, Y., Takeda, T., and Takagi, M., 1973, "Experimental Study on Thin Steel Shear Walls and Particular Bracings Under Alternative Horizontal Load." Prelim. Rep., IABSE Symp. on Resistance and Ultimate Deformability of Structures Acted on by Well-defined Repeated Loads, Lisbon, Portugal, pp. 185-191.

[7] Thorburn, L.J., Kulak, G.L., and Montgomery, C.J., 1983, "Analysis of Steel Plate Shear Walls", Structural Engineering Report No. 107, Department of Civil Engineering, University of Alberta, Edmonton, Canada.

[8] Timler, P.A., Kulak, G.L., 1983, "Experimental Study of Steel Plate Shear Walls", Structural Engineering Report No. 114, Department of Civil Engineering, University of Alberta, Edmonton, Canada.

[9] Xue, M., and Lu, L.-W., 1994, "Interaction of Infilled Steel Shear Wall Panels With Surrounding Frame Members", Proceedings, Structural Stability Research Council Annual Technical Session, Bethlehem, PA, pp. 339–354.

[10] Driver, R.G., Kulak, G.L., Kennedy, D.J.L., and Elwi, A.E., 1997, "Seismic Behavior of Steel Plate Shear Walls", Structural Engineering Report No. 215, Department of Civil and Environmental Engineering, University of Alberta, Edmonton, Canada.

[11] Driver, R.G., Kulak, G.L., Kennedy, D.J.L, Elwi, A.E., 1998a, "Cyclic Test of a Four–Storey Steel Plate Shear Wall", ASCE Journal of Structural Engineering, Vol. 124, No. 2, pp. 112–120.

[12] ATC 24. Guidelines for Seismic Testing of Components of Steel Structures, Applied Technology Council, Report 24, 1992.

[13] Driver, R.G., Kulak, G.L., Elwi, A.E., Kennedy, D.J.L, 1998b, "FE and Simplified Models of Steel Plate Shear Wall", ASCE Journal of Structural Engineering, Vol. 124, No. 2, pp. 121–130.

[14] Driver RG, Kulak GL, Kennedy DJL, Elwi AE. Cyclic test of four-story steel plate shear wall, Journal of Structural Engineering, ASCE, 124(1998) 112-30.

[15] Rezai, M., 1999, "Seismic Behavior of Steel Plate Shear Walls by Shake Table Testing", PhD Dissertation, Department of Civil Engineering, University of British Columbia, Vancouver, BC, Canada.

[16] Tromposch EW, Kulak GL. Cyclic and static behavior of thin steel plate shear walls. Structural Engineering Report No. 145, University of Alberta, Edmonton, Canada, 1987.

[17] Caccese, V., Elgaaly, M. and Chen, R., 1993, "Experimental Study of Thin Steel Plate Shear Walls Under Cyclic Load," ASCE Journal of Structural Engineering, 119 (2), pp. 573-587.

[18] Lubell, A.S., 1997, "Performance of Unstiffened Steel Plate Shear Walls Under Cyclic Quasi-Static Loading", M.A.Sc. Thesis, Department of Civil Engineering, University of British Columbia, Vancouver, BC, Canada.

[19] Abolhassan Astaneh-Asl, 2001, Seismic Behavior and Design of Steel Shear Walls, 2001 SEOANC Seminar, Structural Engineers Assoc. of Northern California, November 7, 2001, San Francisco.

[20] Behbahanifard, Grondin and Elwi, 2003, Experimental and numerical investigation of steel plate shear wall, Department of Civil and Environmental Engineering University of Alberta Edmonton, Alberta, Canada, Structural Engineering Report No. 254, 2003.

[21] Berman, J. W., and Bruneau, M. (2003b), "Plastic Analysis and Design of Steel Plate Shear Walls", Journal of Structural Engineering, ASCE, Vol. 129, No. 11, pp1448-1456, 2003.

[22] D. Vian, and M. Bruneau, 2004 "Testing of Special LYS steel plate shear walls," 13th World Conference on Earthquake Engineering, Vancouver, B.C., Canada, August 1-6, 2004, Paper No. 978, 2004.

[23] Shishkin, Driver and Grondin, 2005, Analysis of steel plate shear walls using the modified strip model, Department of Civil and Environmental Engineering University of Alberta Edmonton, Alberta, Canada, Structural Engineering Report No. 261, 2005.

[24] M.M. Alinia, M. Dastfan (2006), Behavior of thin steel plate shear walls regarding frame members, Journal of Constructional Steel Research 62 (2006) 730–738.

[25] Chih-Han Lin 1, Keh-Chyuan Tsai 2, Ying-Cheng Lin 3, Kung-Juin Wang 4, Wang-Da Hsieh 5, Yuan-Tao Weng 4, Bing Qu 6 and Michel Bruneau 7, 4th

International Conference on Earthquake En gineering Taipei, Taiwan, October 12-13, 2006, Paper No. 155.

[26] C.H. Lin, K.C. Tsai, Y.C. Lin, K.J. Wang, B. Qu and M. Bruneau, Full scale steel plate shear wall: NCREE/MCEER phase I tests, Ninth Canadian Conference on Earthquake Engineering, Ottawa, Ontario, Canada, 26-29 June 2007.

[27] Jeffrey W. Berman, Laura N. Lowes, Taichiro Okazaki, Michel Bruneau, Keh-Chyuan Tsai, Robert G. Driver, Rafael Sabelli, (2008), Research Needs and Future Directions for Steel Plate Shear Walls, Structures 2008: Crossing Borders, 2008 ASCE.

[28] Mehdi H.K. Kharrazi, Helmut G.L. Prion, Carlos E. Ventura (2008), Implementation of M-PFI method in design of steel plate walls, Journal of Constructional Steel Research 64 (2008) 465–479

[29] S. Sabouri-Ghomi and M. Gholhaki (2008), Ductility of thin steel plate shear walls, Asian Journal of Civil Engineering (Building and Housing), Vol. 9, No. 2 (2008), pg. 153-166.

[30] A. K. Bhowmick, R. G. Driver, G. Y. Grondin, 2009, Seismic analysis of steel plate shear walls considering strain rate and P- delta effects, Journal of Constructional Steel Research 65, 1149-1159, 2009

[31] National Research Council of Canada, 2005. "National Building Code of Canada". National Research Council of Canada, Ottawa, ON, 2005.

[32] H.R. Habashi, M.M. Alinia, Characteristics of the wall_frame interaction in steel plate shear walls, Journal of Constructional Steel Research 66 (2010) 150_158.

[33] Troy, R.G., and Richard, R. M. (1988). " Steel Pate Sear Wall Design." Struct. Engrg. Review, 1(1), 1988.

[34] Celebi, M. (1997). "Response of Olive View Hospital to Northridge and Whittier Earthquakes", J. of Structural Engineering, ASCE, . v. 123 Apr. 97, p. 389-96, 1997.

[35] Fujitani, H., Yamanouchi, H., Okawa, I. Sawai, N., Uchida, N. and Matsutani, T. (1996). "Damage and performance of tall buildings in the 1995 Hyogoken Nanbu earthquake". Proceedings. The 67th Regional Conference, Council on Tall Building and Urban Habitat, Chicago, 103-125, 1996.

[36] Yamaguchi, T., et al., (1998). Seismic Control Devices Using Low-yield-point Steel. Nippon Steel Technical Report No. 77. Pp.65-72, 1998.

[37] Wang D. et al. (2008), "The Structural design of Jinta Tower", The proceedings of the 16th national high rise structural design technical exchange conference, Dalian China 2008.

[38] Mathias N., Sarkisian M., Long E. and Huang Z. (2008), "Steel Plate Shear Walls: Efficient Structural Solution for Slender High-Rise in China", Seismic Engineering International Conference, Reggio Calabria, July 2008.

[39] FEMA450. NEHRP Recommended Provisions For Seismic Regulations For New Buildings And Other Structures – Part1: Provisions, Building Seismic Safety Council for the Federal Emergency Management Agency, June 6, 2006.

[40] EN 1998-1: Design provisions for earthquake resistance of structures - 1-1: General rules - Seismic actions and general requirements for structures, CEN, EN1998-1-1, October 1994.

[41] ASCE 7-05. Minimum Design Loads for Buildings and Other Structures, American Society of Civil Engineers / 01-Jan-2006 / 424 pages, ISBN: 0784408092, 2006.

[42] FEMA273, NEHRP Guidelines for seismic rehabilitation of buildings, Building Seismic Safety Council for the Federal Emergency Management Agency, October , 1997.

[43] FEMA 356, Prestandard and Commentary for the Seismic Rehabilitation of Buildings, Building Seismic Safety Council for the Federal Emergency Management Agency, Washington D.C., 2000.

[44] ASCE 41-06. Seismic Rehabilitation of Existing Buildings , Edition: 1st American Society of Civil Engineers / 15-May-2007 / 423 pages, ISBN: 9780784408841, 2007.

[45] ECCS (1985). Recommended Testing Procedures for Assessing the Behaviour of Structural Elements under Cyclic Loads. European Convention for Constructional Steelwork. Technical Committee 1, TWG 1.3 – Seismic Design, No.45, 1985.

[46] FEMA 461 Interim Testing Protocols for Determining the Seismic Performance Characteristics of Structural and Nonstructural Components / June 2007.

[47] EN1993-1-8: Design of Steel Structures. Part 1-8: Design of joints, CEN, Brussels, 2003.

[48] P100-1 (2006). Cod de proiectare seismică P100: Partea I, P100-1/2006: Prevederi de proiectare pentru clădiri (in Romanian), 2006.

[49] EN1991. "Actions on structures", CEN – European Committee for Standardization, 2001.

[50] American Institute of Steel Construction Inc., 1999, "Load and Resistance Factor Design Specification," American Institute of Steel Construction Inc., Chicago, 1999.

[51] Montgomery, C.J., and Medhekar, M., 2001, "Discussion of Unstiffened Steel Plate Shear Wall Performance Under Cyclic Loading by Lubell, A.S., Prion,

H.G.L., Ventura, C.E., and Rezai, M." Journal of Structural Engineering, ASCE, Vol. 127, No. 8, August, pp. 973, 2001.

[52] CSI, 2000, "SAP2000, Version, 7.44, Three Dimensional Static and Dynamic Finite Element Analyses of the Structures", Computers and Structures Inc., Berkeley, CA, 2000.

[53] EN ISO 6892-1. Metallic materials – Tensile testing – Part 1: Method of test a room temperature, 2009.

[54] EN1993-1-5. "Design of steel structures. Part 1-5: Plated structural elements". CEN – European Committee for Standardization, 2004.

[55] Newmark, N.M. and Hall, W.J., 1982, Earthquake Spectra and Design. Earthquake Engineering Research Institute, Berkeley, California, pp. 29-37, 1982.

[56] Bing Qu and M. Bruneau. Experimental investigation of full scale two-storey steel plate shear wall, 2006.

[57] EN1993-1-1. "Design of steel structures. Part 1-1: General Rules and Rules for Buildings". CEN - European Committee for Standardization, 2003.

[58] SEAOC, 1999, "Recommended Lateral Force Requirements and Commentary," Seventh Ed., Structural Engineers Association of California, Sacramento, CA, 1999.

[59] ATC-40, 1996, "Seissmic Evaluation and Retrofit of Concrete Buildings, Vol I., by Applied Technology Council 555 Twin Dolphin Drive, Suite 550, Redwood City, Californai 94065, funded by Seismic Safety Commission State of Californaia, Report No. SSC 96-01, 1996.

[60] P100-3 (2006). Cod de proiectare seismică P100: Partea 3, P100-3/2006: Lucrari de consolidare a cladiri existente, vulnerabile seismic, Vol. 1 - Evaluare, 2005.

[61] D. Lungu, A. Aldea, S. Demetriu and C. Arion, "Zonation of seismic hazards for the city of Bucharest", Tehnical Report prepared for Association Francaise du Genie Parasismique, 59p, 2000.

[62] D. Lungu, A. Aldea, A.Zaicenco, T. Cornea. "Hazardul seismic din sursa sub-crustala Vrancea. Macrozonare si microzonare sismica ". Conferinta: Siguranta constructiilor in conditiile de teren si seismicitate specifice Romaniei si Republici Moldova, 27-28 octombrie, 1999, Chisinau, edit. UTCB p.1-24, 1999.

[63] Gasparini, D., and Vanmarcke, E. H. 1976. SIMQKE: A Program for Artificial Motion Generation, Department of Civil Engineering, Massachusetts Institute of Technology, Cambridge, MA, 1976.

[64] FEMA302. NEHRP Recommended Provisions For Seismic Regulations For New Buildings And Other Structures, Building Seismic Safety Council for the Federal Emergency Management Agency, 1997.

[65] Fajfar, P. (2000). "A nonlinear analysis method for performance-based seismic design". Earthquake Spectra, 16(3): 573-92, 2000.

[66] Vamvatsikos, D. and Cornell, C.A. (2002). "Incremental Dynamic Analysis". Earthquake Engineering and Structural Dynamics, 31(3): 491–514. 2002.

[67] F. Dinu, D. Dubina, C. Neagu: A comparative analysis of performances of high strength steel dual frames of buckling restrained braces vs. dissipative shear walls, Philadelphia, 16-20 aug. 2009, International Conference, STESSA 2009, Behavior of Steel Structures in Seismic Areas, CRC Press 2009, Ed. F.M. Mazzolani, J.M. Ricles, R. Sause, ISBN: 978-0-415-56326-0 (BDI), 2009.

Appendix A

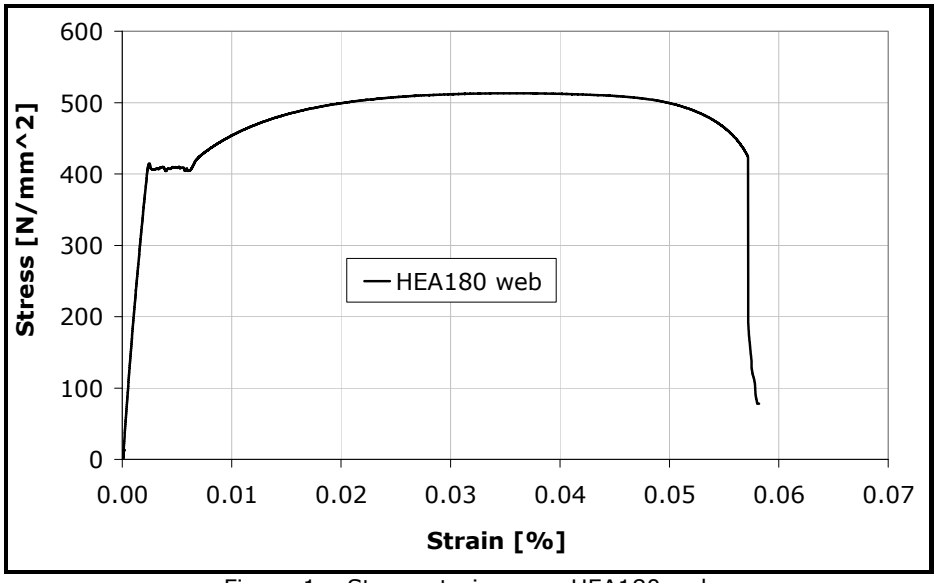

Figure 1 – Stress-strain curve HEA180 web

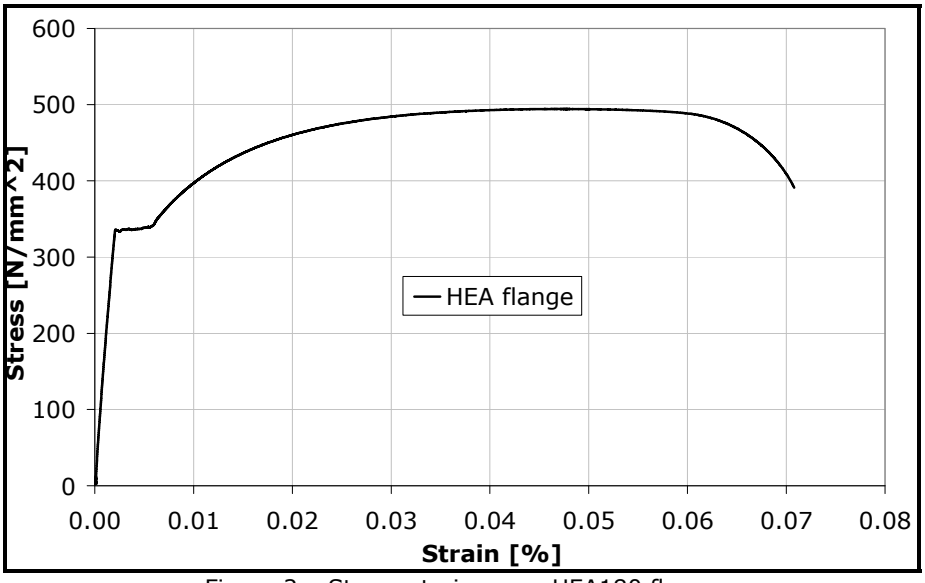

Figure 2 – Stress-strain curve HEA180 flange

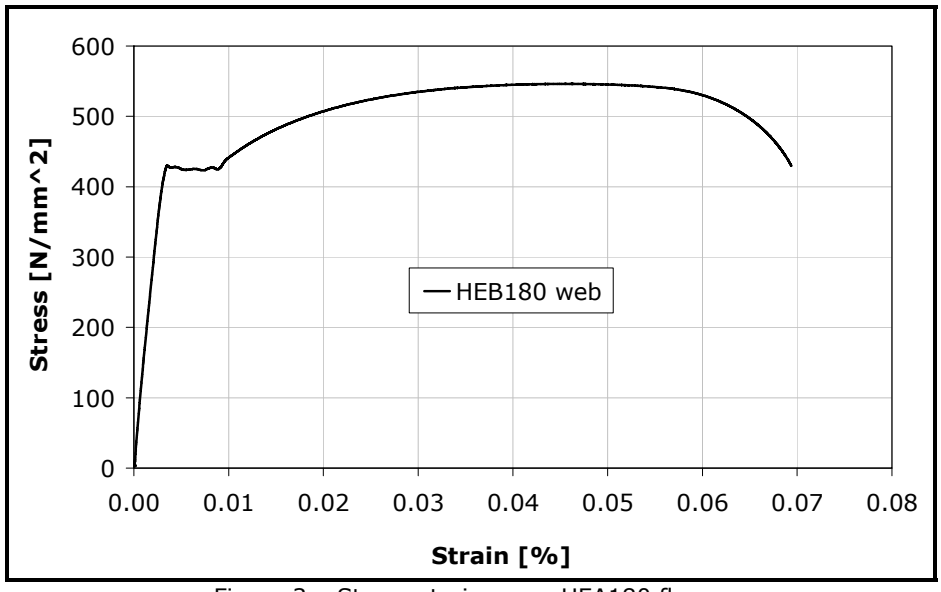

Figure 3 – Stress-strain curve HEA180 flange

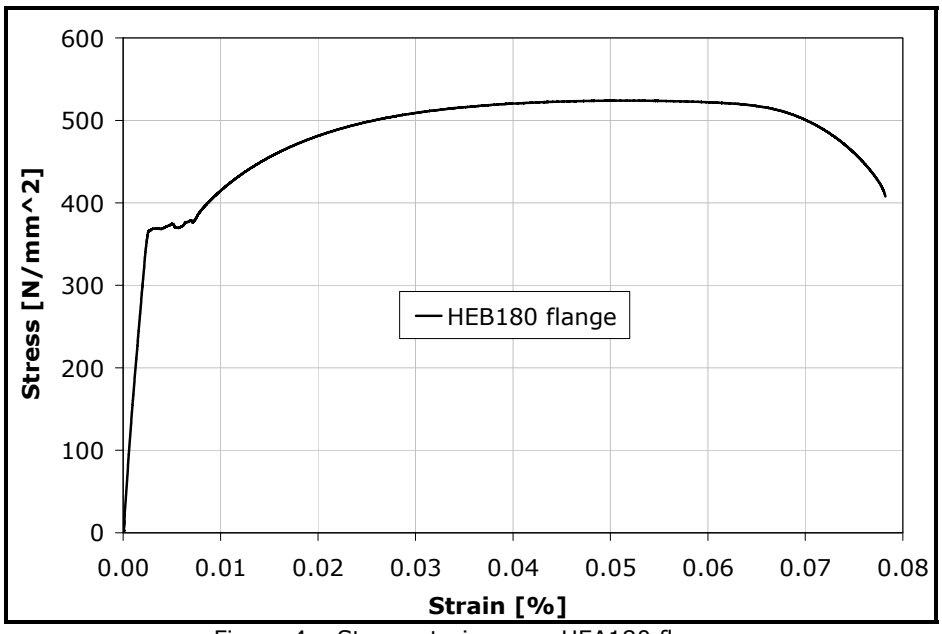

Figure 4 – Stress-strain curve HEA180 flange

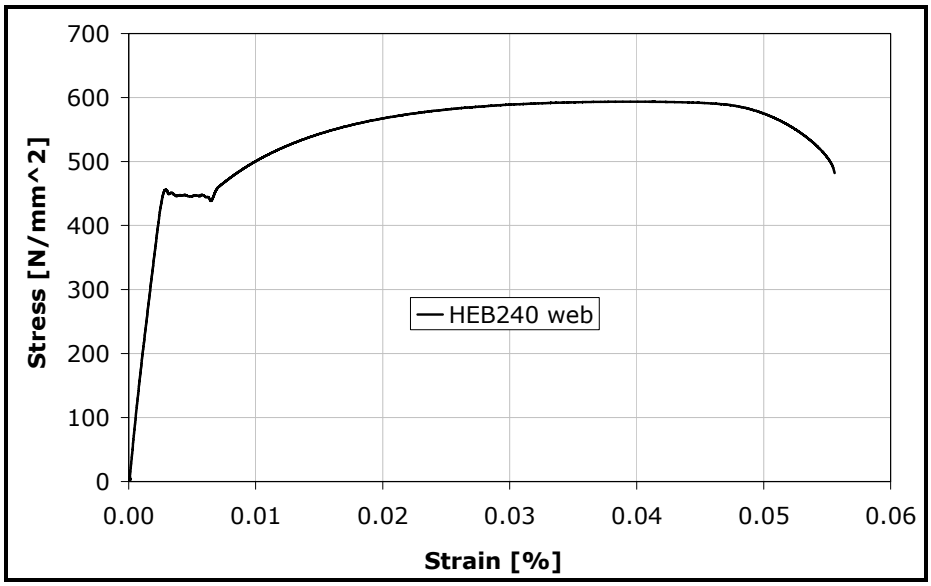

Figure 5 – Stress-strain curve HEA180 flange

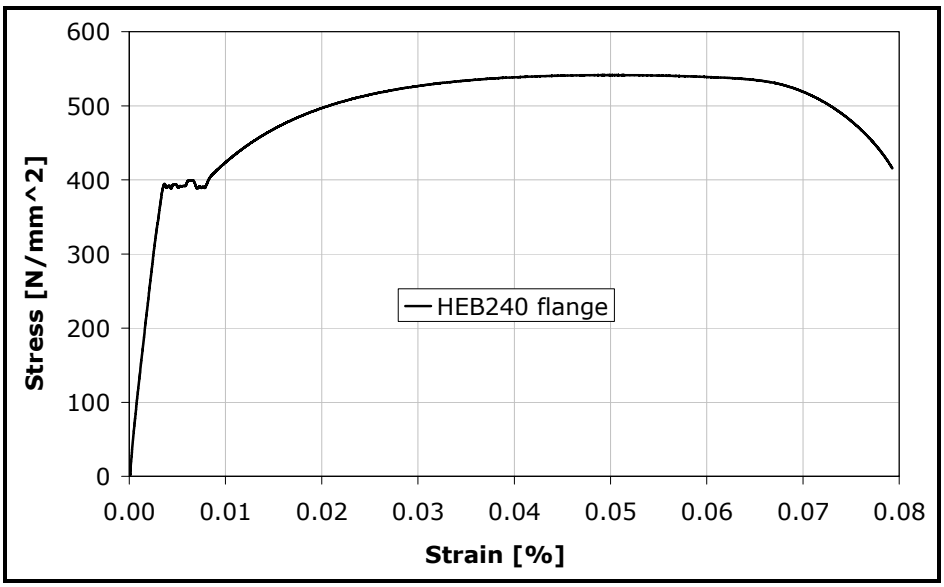

Figure 6 – Stress-strain curve HEA180 flange

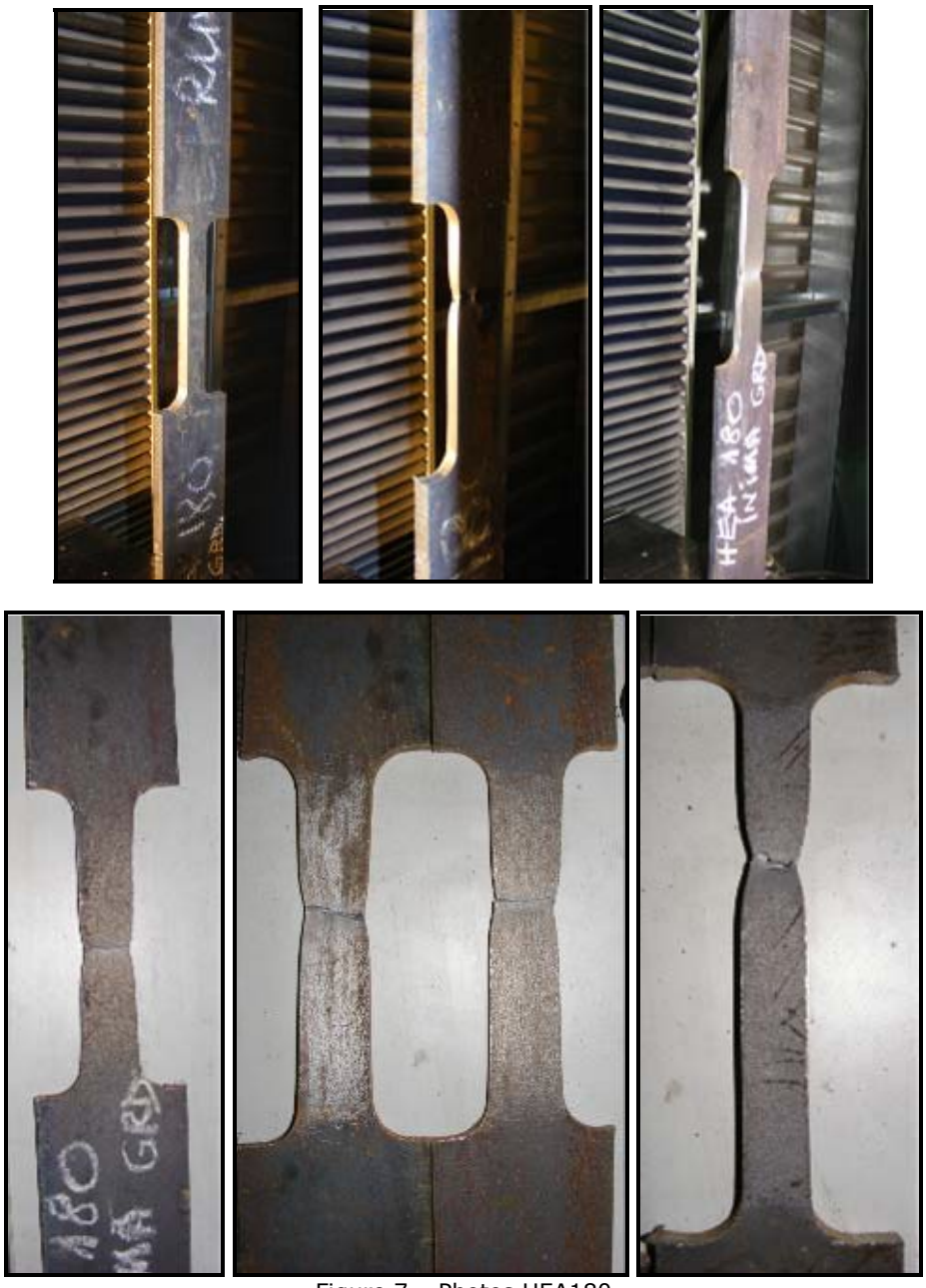

Figure 7 – Photos HEA180

Figure 8 – First storey mounting

Figure 9 – Base connection to reaction beam tightening

Figure 10 – Measuring devices support welding

Figure 11 – Frame without infill plates

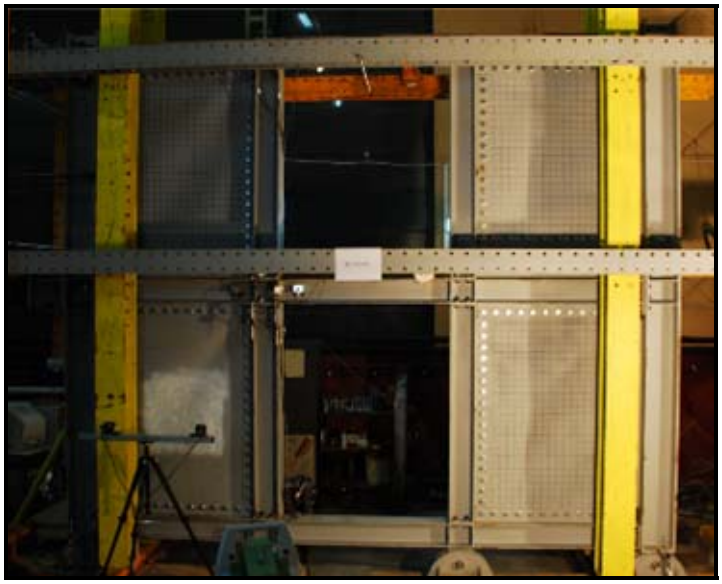

Figure 12 – Base shear force of 0 KN (initial stage)

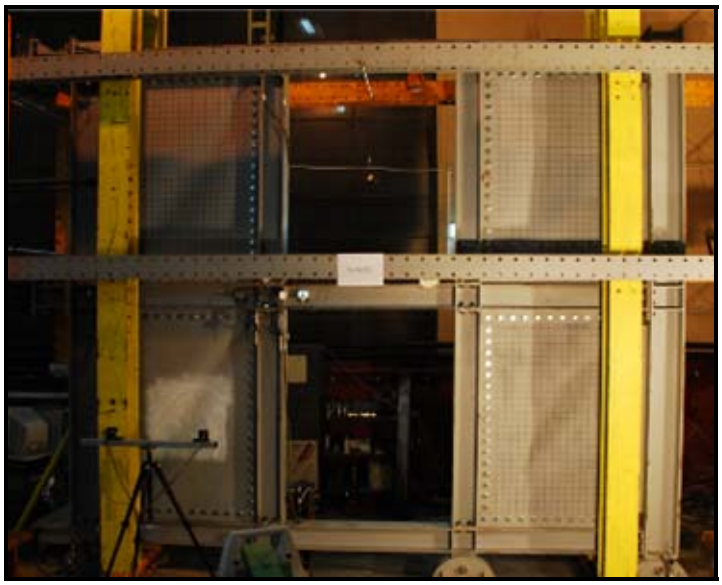

Figure 13 – Base shear force of 300 KN

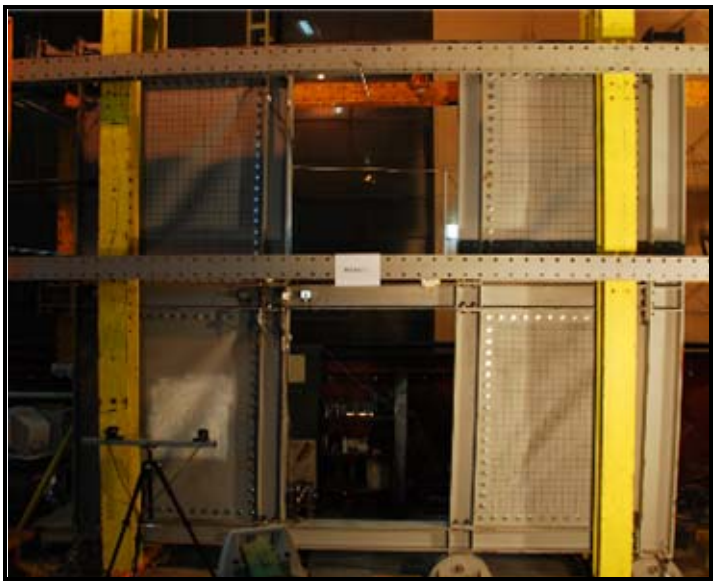

Figure 14 - Base shear force of 600 KN (yielding stage)

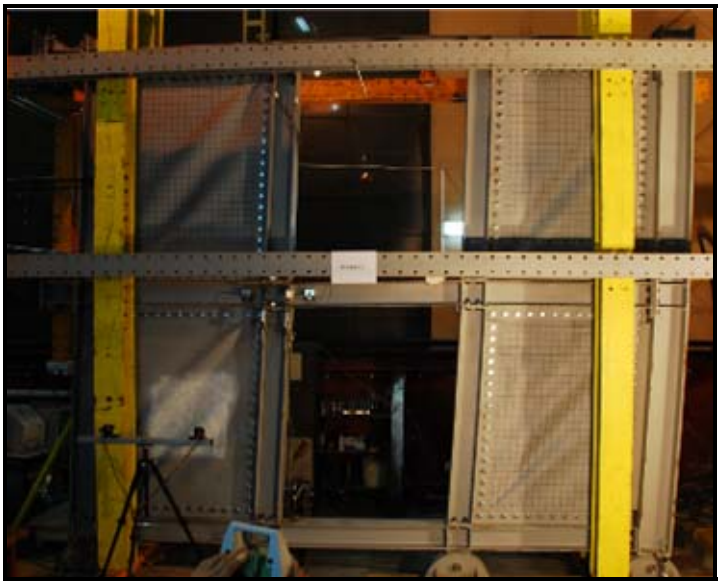

Figure 15 - Base shear force of 900 KN

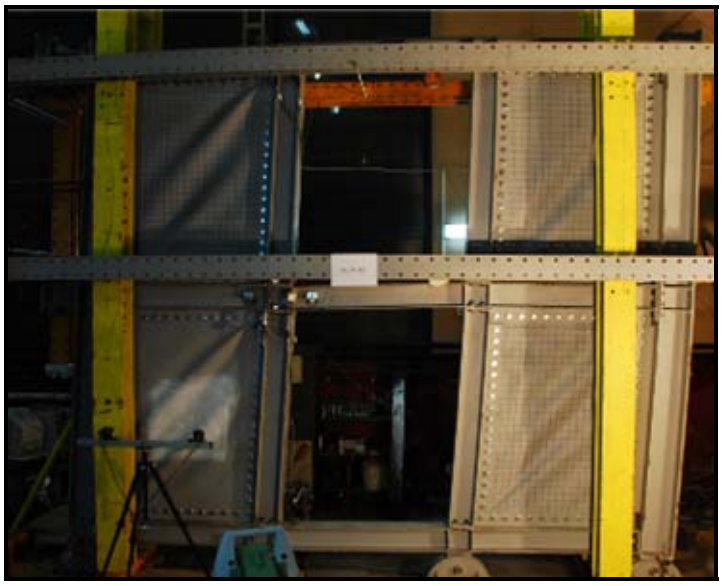

Figure 16 - Base shear force of 1150 KN (peak capacity)

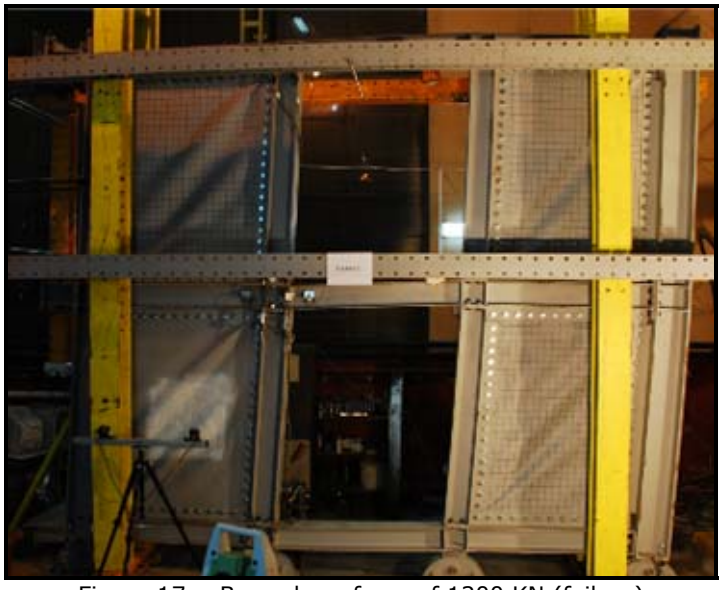

Figure 17 - Base shear force of 1200 KN (failure)

Figure 18 - Tested R-M-T2 specimen

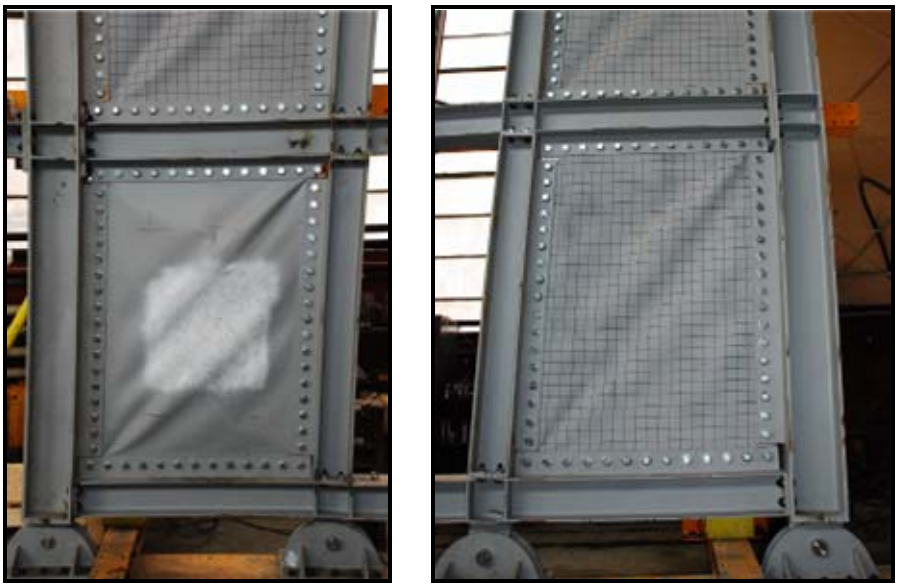

Figure 19 - Details of left and right side

Figure 20 - Details of joints

Figure 21 - Infill plate corner tearing

The following figures show the maximum of each cycle for R-C-T2 specimen: D_y, $2xD_y$, $4xD_y$ and $6xD_y$.

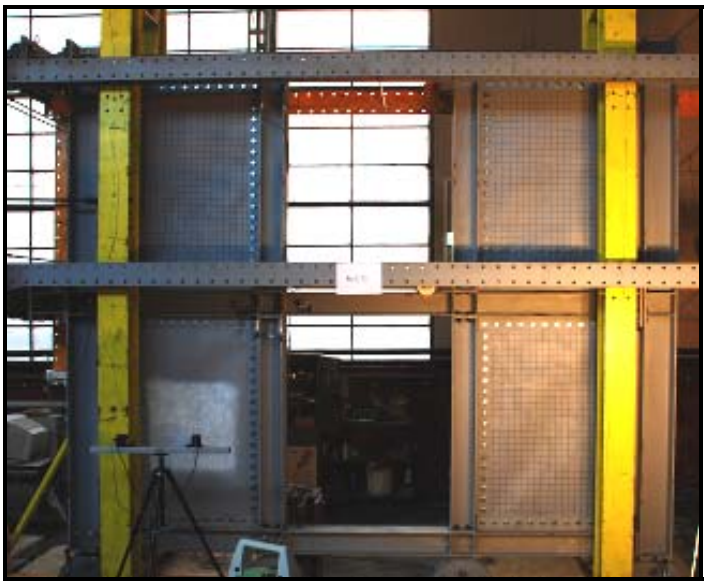

Figure 22 - D_y cycle

Figure 23 - 2xD_y cycle

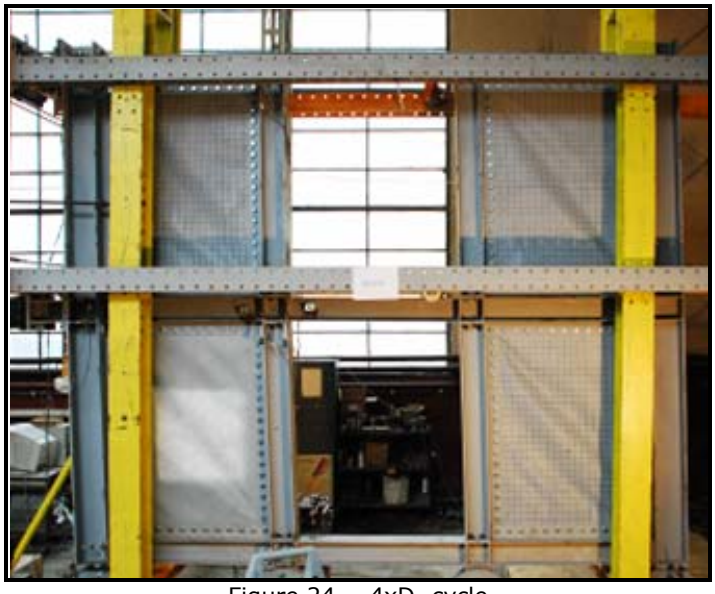

Figure 24 - 4xD_y cycle

Figure 25 - 6xDy cycle

Figure 26 - Tested specimen

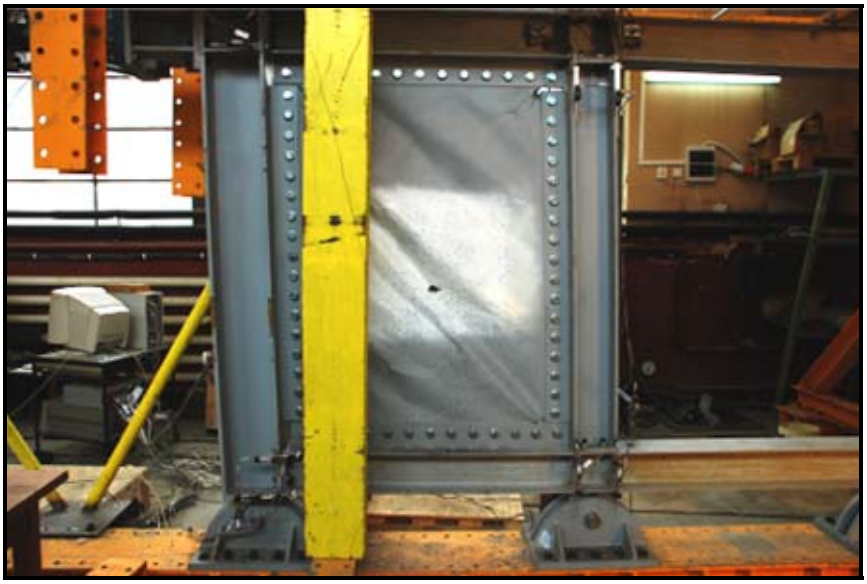

Figure 27 -Detail of left-lower infill plate

Figure 28 - Final stage of plate (both sides)

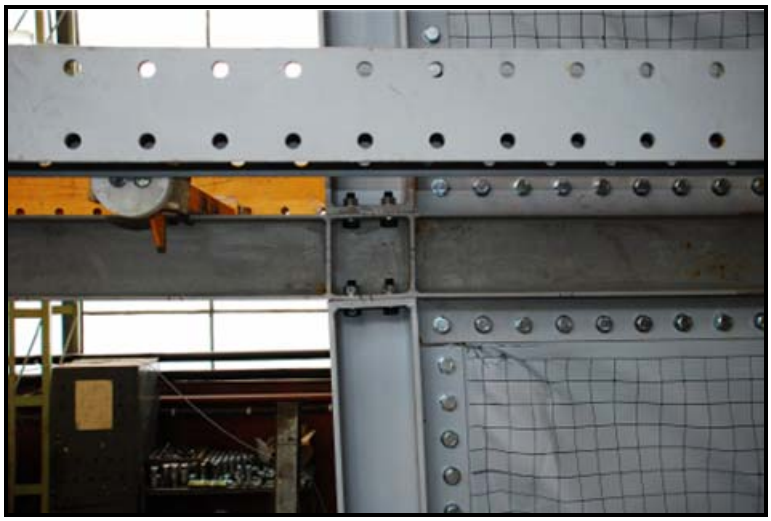

Figure 29 - Interior joint detail

Figure 30 - Plate tearing

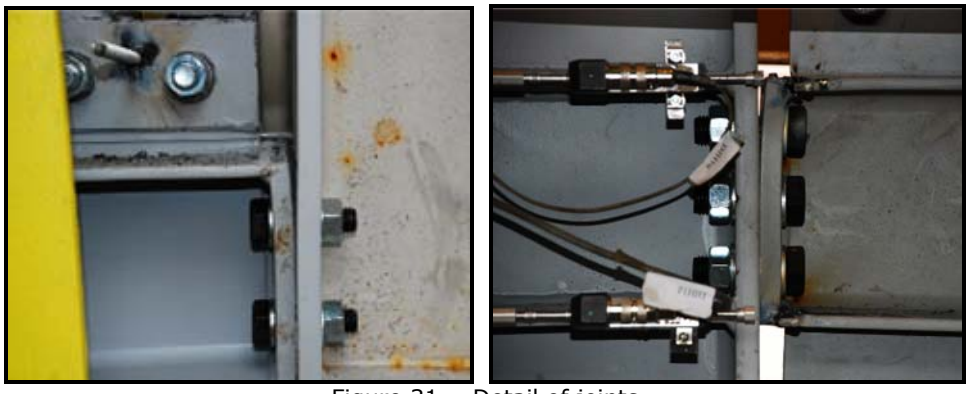

Figure 31 - Detail of joints

Figure 32 - Tested specimen

Figure 33 - Frontal view of infill plate

Figure 34 - Details of joints

Figure 35 - Details of infill plates corners

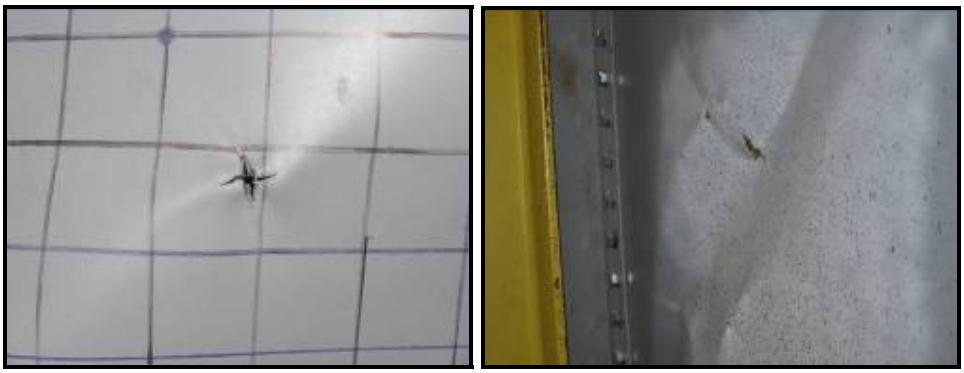

Figure 36 - Tearing of the plate in the midle

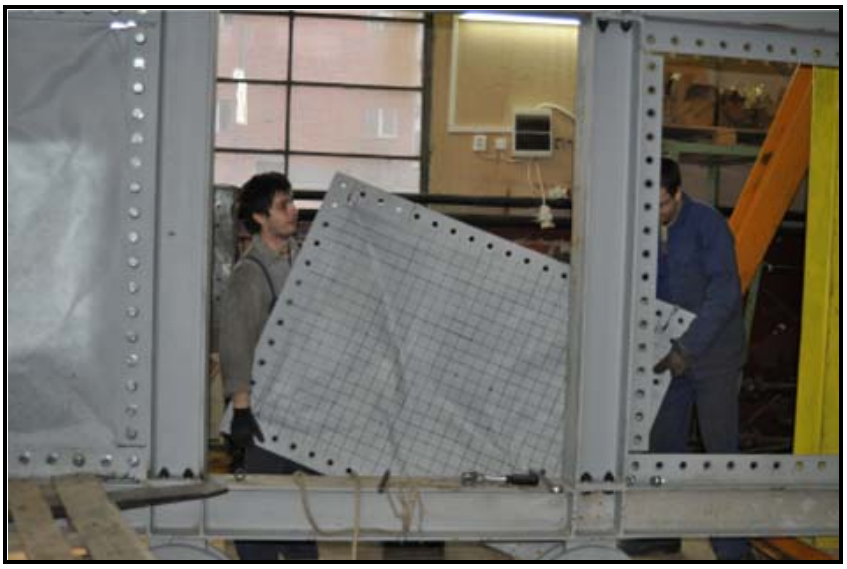

Figure 37 - Infill plate dismantling

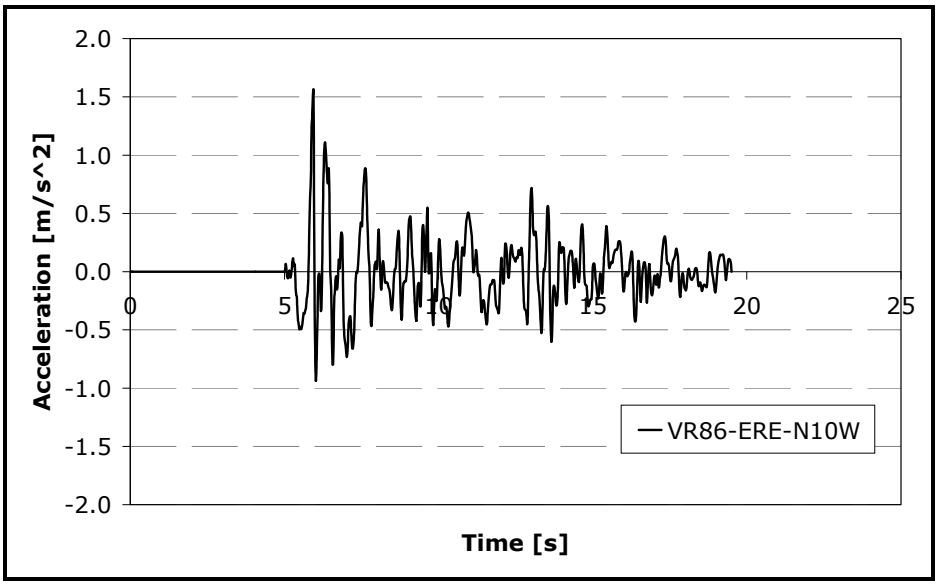

Figure 38 - Original Vrancea 1986 record, EREN recording station, N10W component

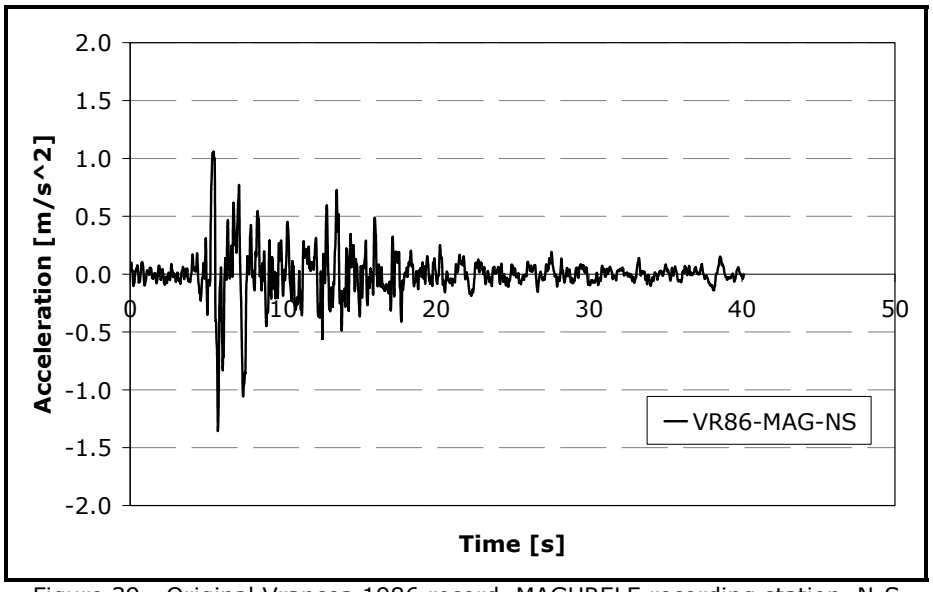

Figure 39 - Original Vrancea 1986 record, MAGURELE recording station, N-S component

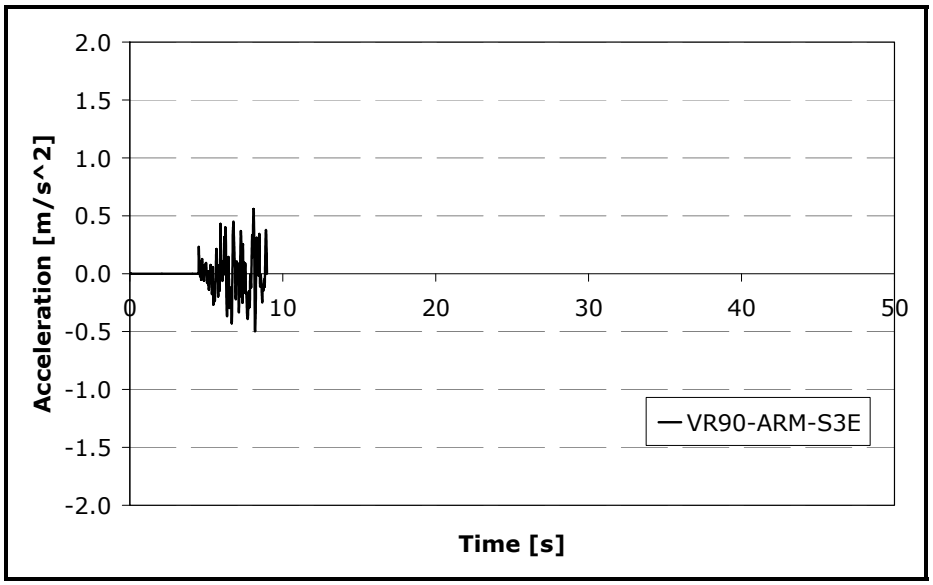

Figure 40 - Original Vrancea 1986 record, ARMENEASCA recording station, S3E component

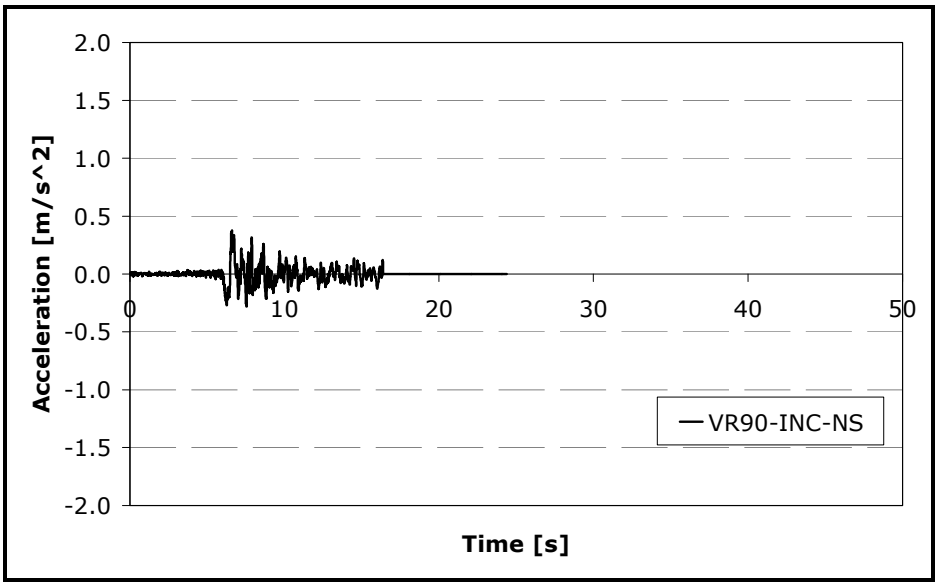

Figure 41 - Original Vrancea 1986 record, INCERC recording station, N-S component

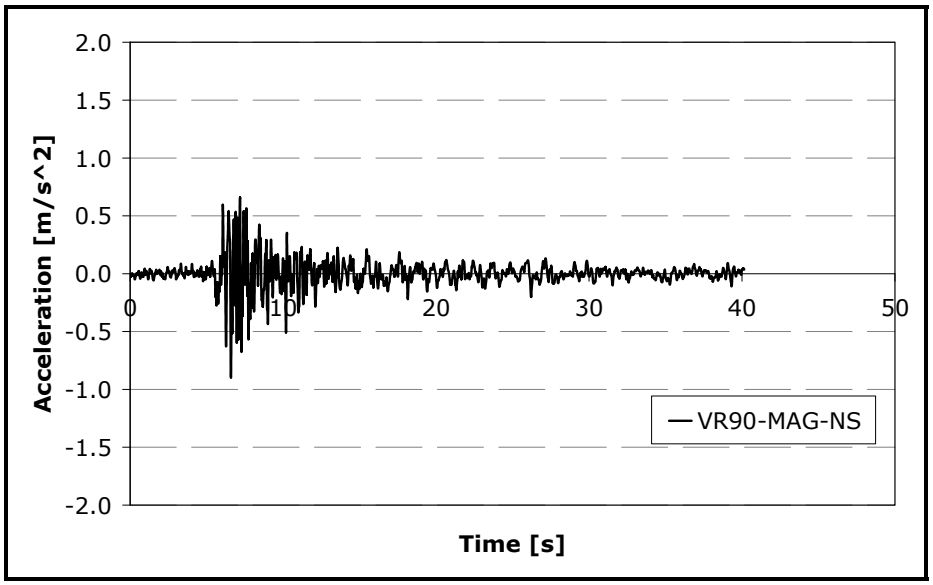

Figure 42 - Original Vrancea 1986 record, MAGURELE recording station, NS component

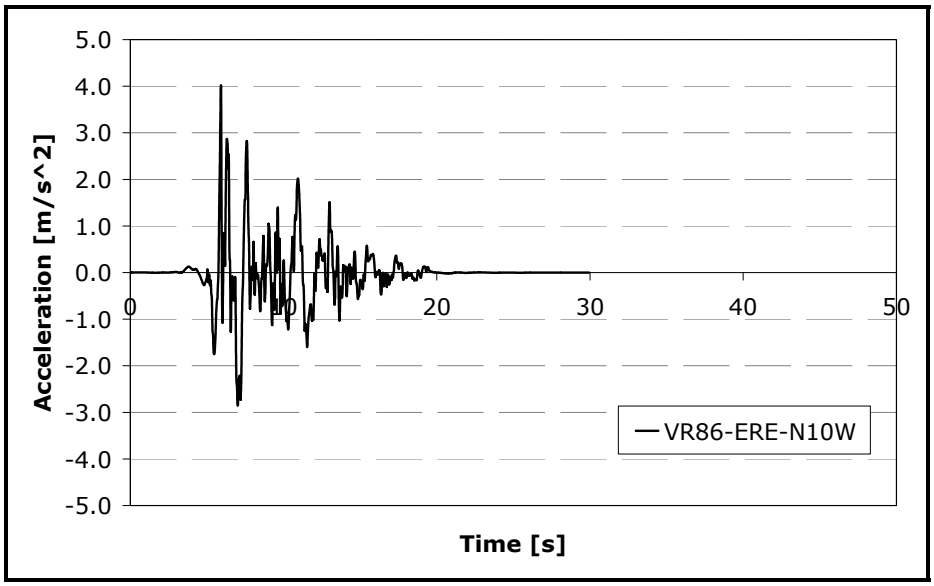

Figure 43 - Scaled record of Vrancea 1986, EREN recording station, N10W component

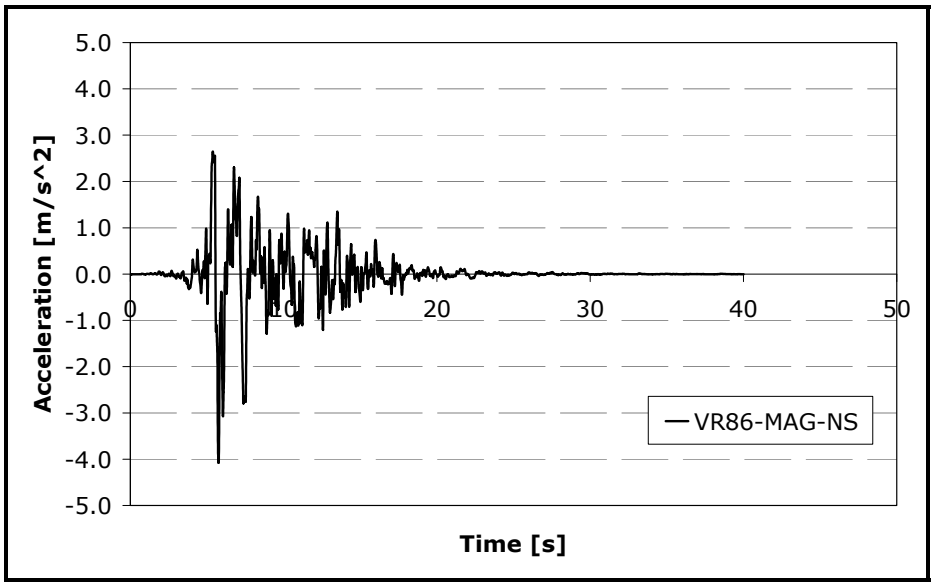

Figure 44 - Scaled record of Vrancea 1986, MAGURELE recording station, N-S component

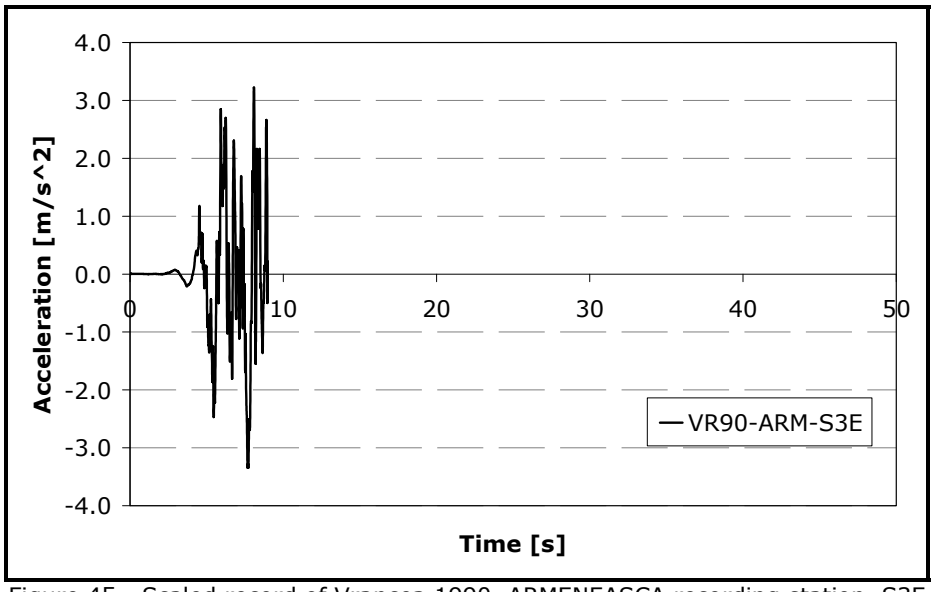

Figure 45 - Scaled record of Vrancea 1990, ARMENEASCA recording station, S3E component

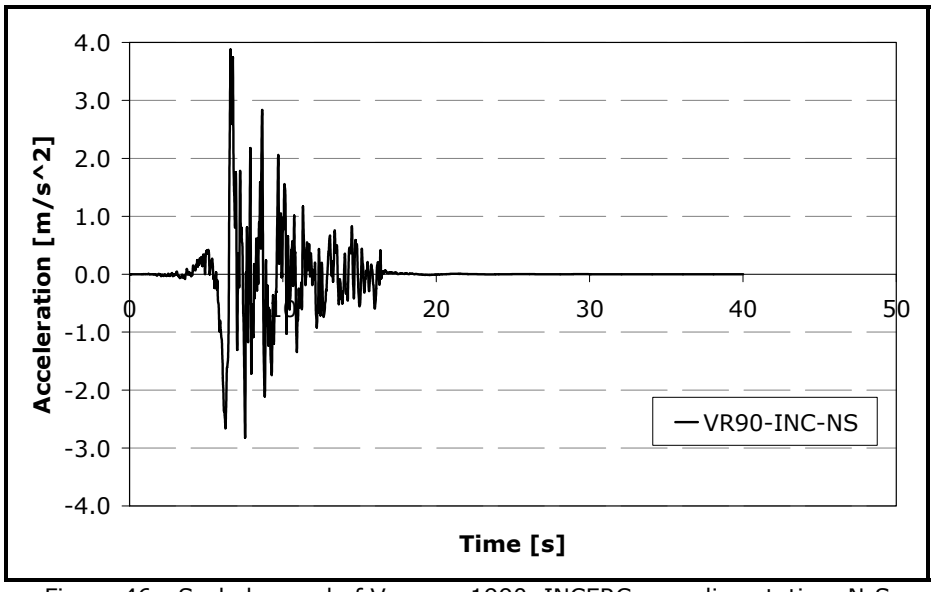

Figure 46 - Scaled record of Vrancea 1990, INCERC recording station, N-S component

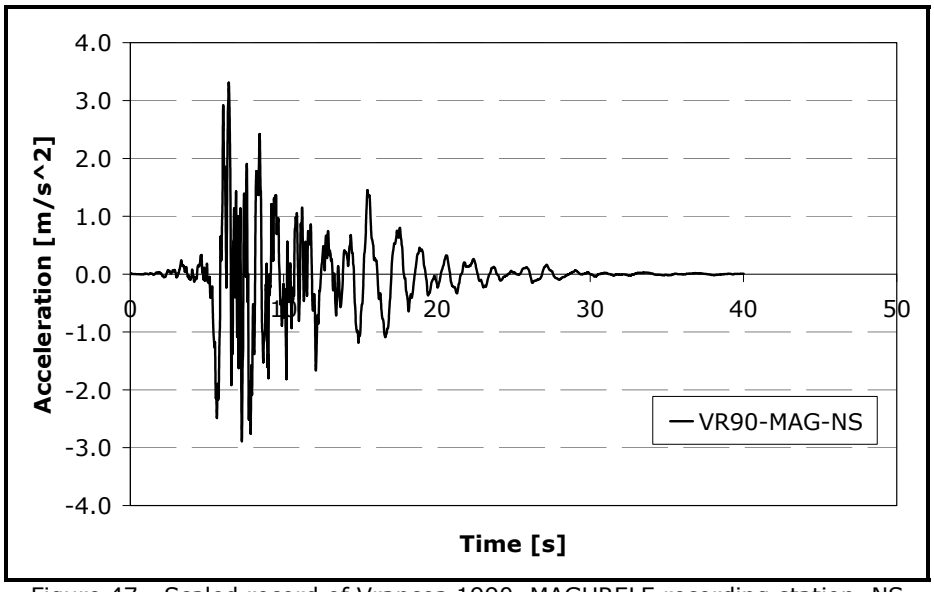

Figure 47 - Scaled record of Vrancea 1990, MAGURELE recording station, NS component

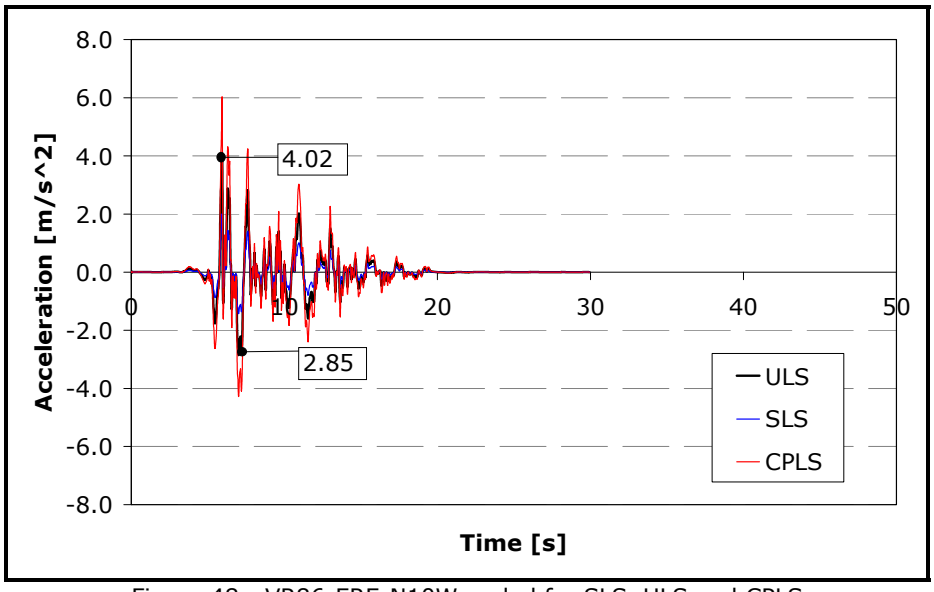

Figure 48 - VR86-ERE-N10W scaled for SLS, ULS and CPLS

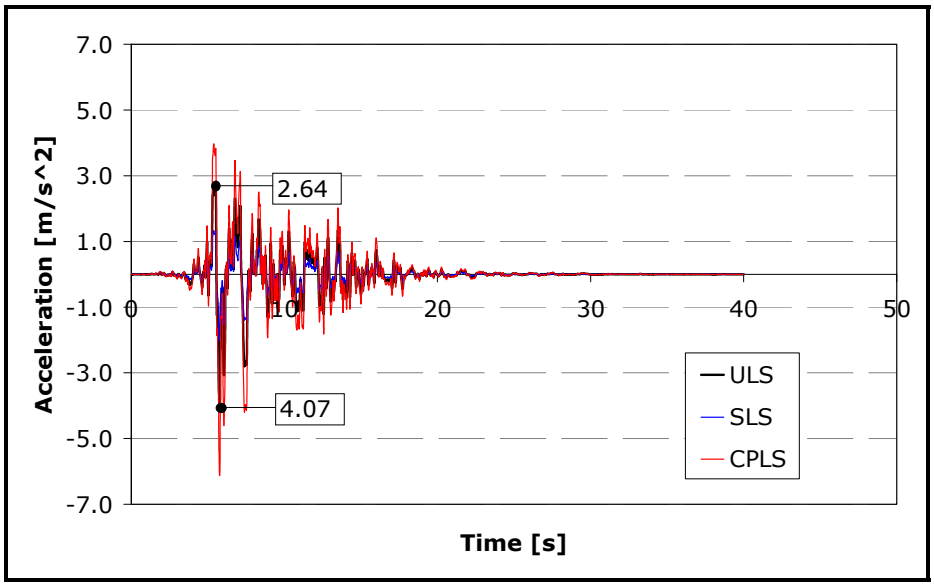

Figure 49 - VR86-MAG-NS scaled for SLS, ULS and CPLS

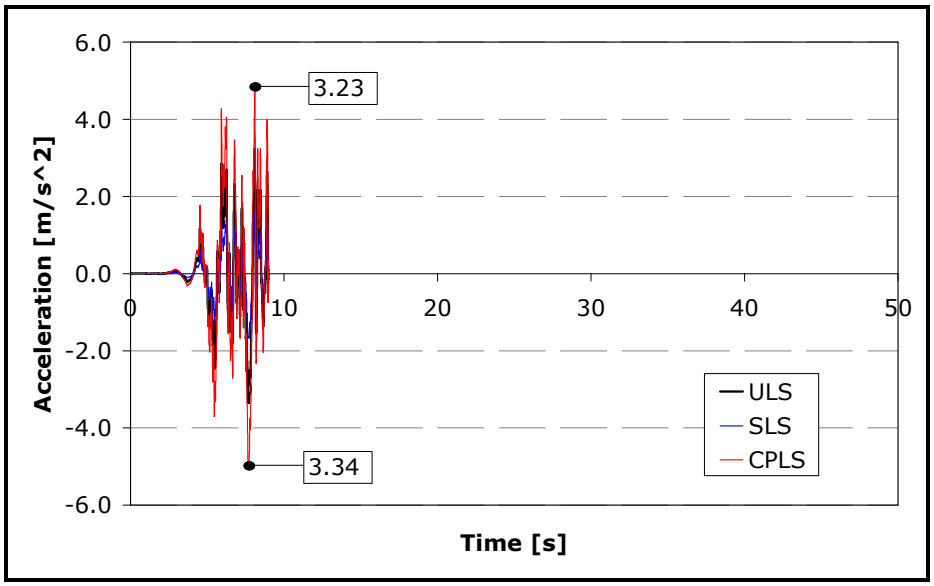

Figure 50 - VR90-ARM-NS scaled for SLS, ULS and CPLS

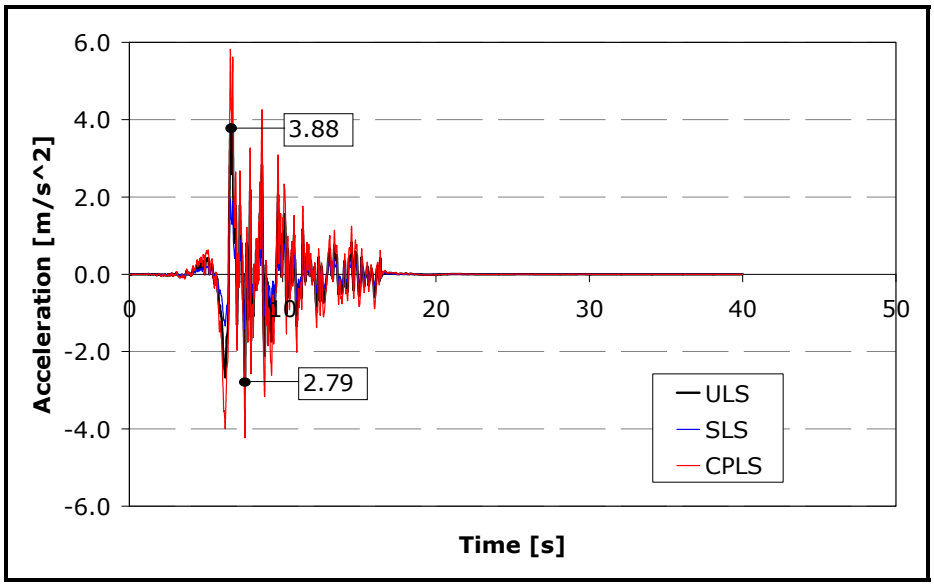

Figure 51 - VR90-INC-NS scaled for SLS, ULS and CPLS

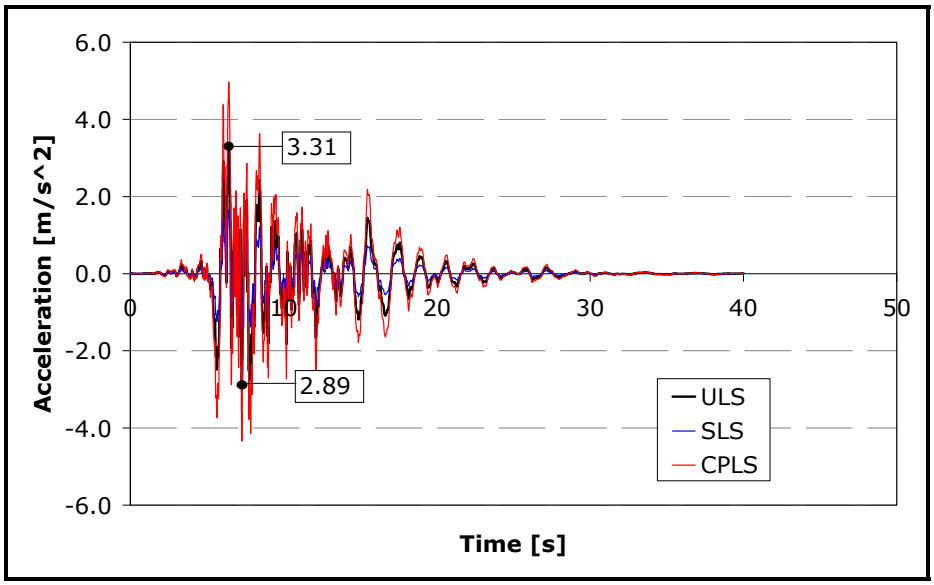

Figure 52 - VR90-MAG-NS scaled for SLS, ULS and CPLS

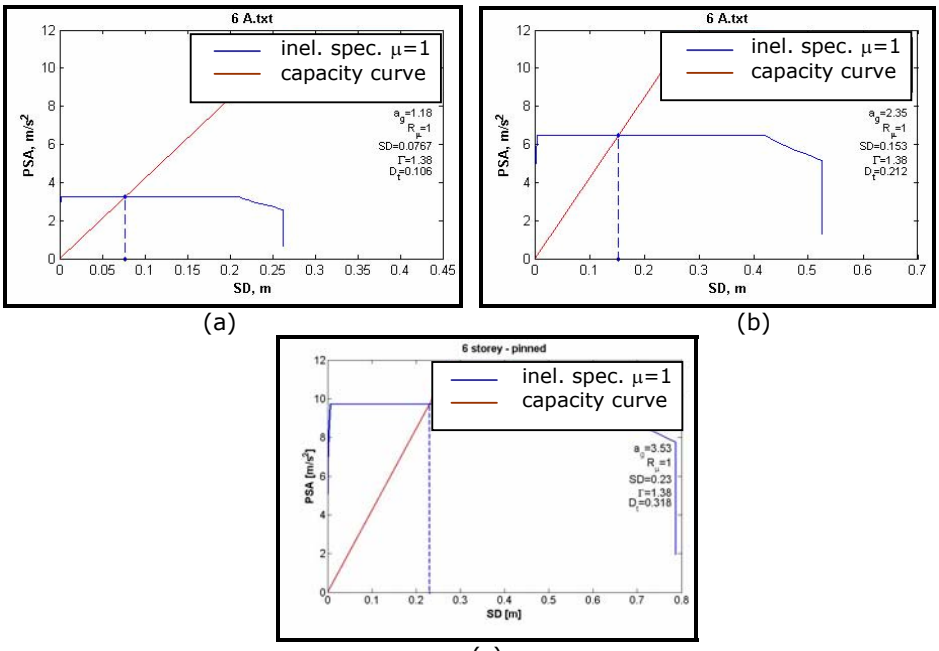

Figure 53 - D_t for 6 storey structure, pinned joint: a) SLS; b) ULS; c) CPLS

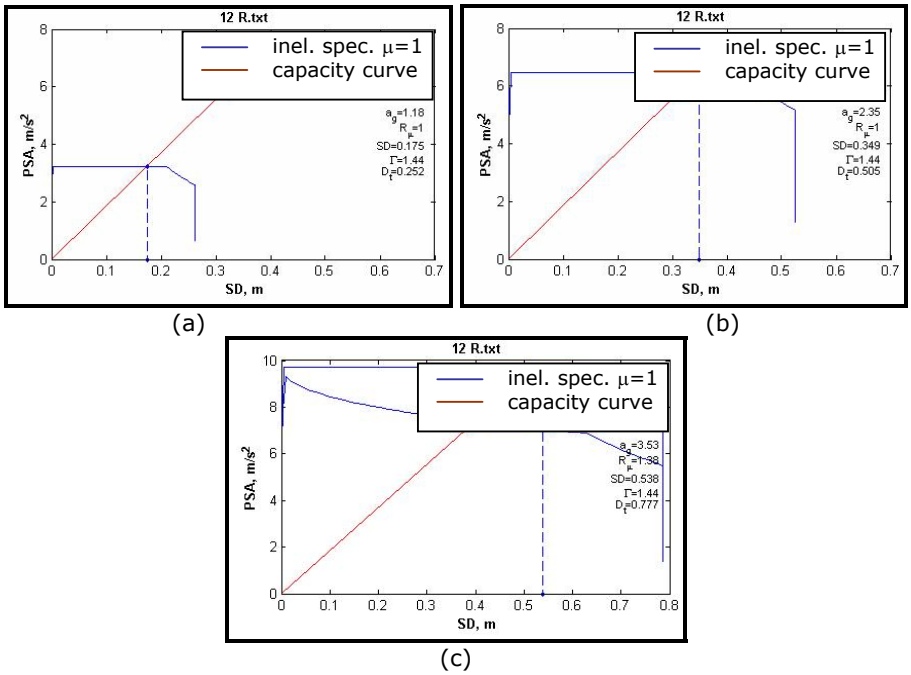

Figure 54 - D_t for 12 storey structure, rigid joint: a) SLS; b) ULS; c) CPLS

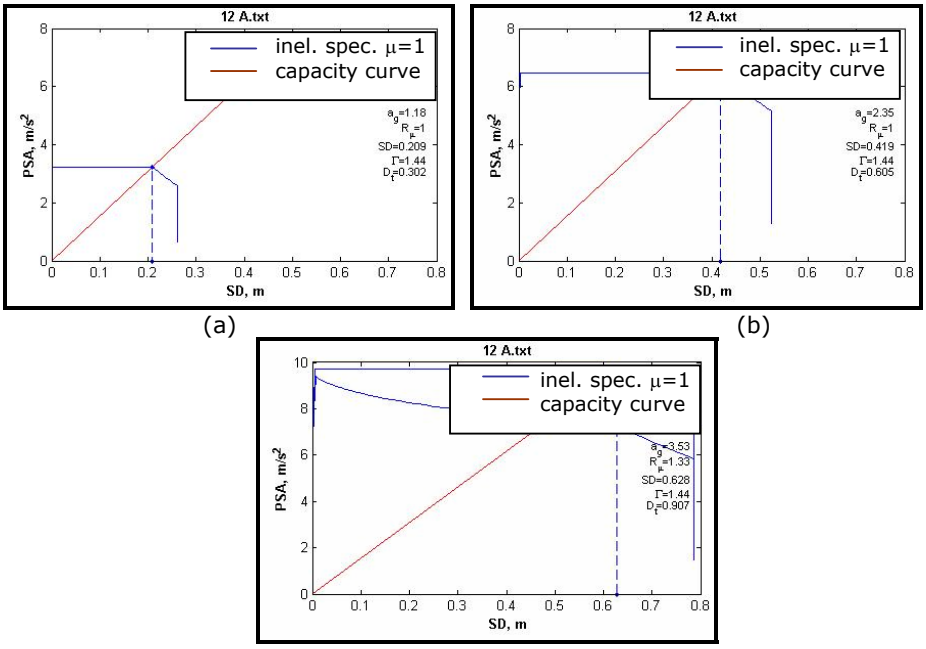

Figure 55 - D_t for 12 storey structure, pinned joint: a) SLS; b) ULS; c) CPLS

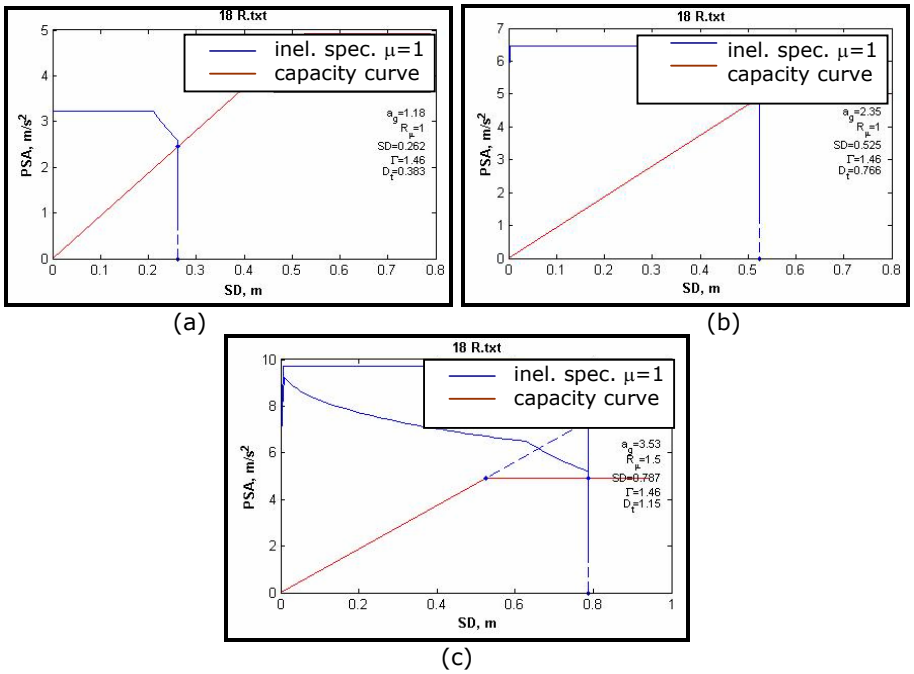

Figure 56 - D_t for 18 storey structure, rigid joint: a) SLS; b) ULS; c) CPLS